Exploring the Functional Roles of π-helices and Flavin-Induced Oligomeric State Changes in Flavin Reductases of Two-Component Monooxygenase Systems

by

Jonathan Makau Musila

A dissertation submitted to the Graduate Faculty of
Auburn University
in partial fulfillment of the
requirements for the Degree of
Doctor of Philosophy

Auburn, Alabama
May 6, 2017

Keywords: Oligomerization, kinetics, desulfonation, π-helix, dis(asso)ciation

Approved by

Holly R. Ellis, Chair, Professor of Chemistry and Biochemistry
Douglas C. Goodwin, Associate Professor of Chemistry and Biochemistry
Evert C. Duin, Associate Professor of Chemistry and Biochemistry
Steven Mansoorabadi, Assistant Professor of Chemistry and Biochemistry

Abstract

Sulfur-containing biomolecules participate in various chemical and structural functions in enzymes. When sulfate is limiting, bacteria upregulate *ssi* enzymes to utilize organosulfonates as an alternative source. The alkanesulfonate monooxygenase enzymes mitigate sulfur scarcity through desulfonation of various alkanesulfonates releasing sulfite which is incorporated into sulfur-containing biomolecules. This two-component monooxygenase system utilizes flavin as a substrate with the SsuE enzyme supplying reduced flavin to SsuD. It is unclear what structural properties of flavin reductases of two-component systems dictate catalysis. The SsuE enzyme undergoes a tetramer to dimer oligomeric switch in the presence of FMN. Oligomeric state changes are common in flavin reductases but the roles and regulation of the quaternary structural changes have not been evaluated. Intriguingly, the flavin reductases of two-component systems contain π-helices located at the tetramer interface. π-Helices are generated by a single amino acid insertion in an established α-helix to confer an evolutionary advantage.

Substitution of the π-helix insertional residue in SsuE (Tyr118) generated FMN-bound Y118A and Y118S SsuE variants, unlike the wild-type enzyme which is flavin-free. Structural and kinetic analyses were performed on these canonical flavoprotein variants and on the flavin-free variants (Y118F and ΔY118 SsuE) to understand the roles of π-helix in SsuE. We further investigated the structural effects of perturbing the π-helix in SsuE by solving the three-dimensional structures of Y118A SsuE in the oxidized form, when reduced, and in the apo form. Our findings show the π-helix is vital in the functioning of SsuE as a flavin reductases of two-

component systems. In combination, the studies suggested the π-helix in SsuE promotes structural stability through hydrogen bonding and π-stacking interactions, and facilitates the transfer of reduced flavin to SsuD through protein-protein interactions. The π-helix may regulate the oligomeric changes in SsuE upon flavin binding and could be vital in controlling dioxygen reactivity. We also report herein that reduced flavin transfer from SsuE to SsuD occurs through a channeling mechanism facilitated by conformational changes in the flexible loop of SsuD. Overall, these studies unravel the evolutionary role of the π-helices in defining oligomeric state changes and in the transfer of reduced flavin in two-component monooxygenase systems.

Acknowledgments

A time has come for me to wind up my graduate studies and unfold a new chapter of my life. This journey would not have been a success without a team's effort. I am sincerely indebted to Prof. Holly R. Ellis for the opportunity to do research in her lab, coupled with her mentorship throughout my graduate studies here in Auburn University. I am particularly grateful for her scientific and research input, and for providing the resources which made this research a success. I also appreciate collective and individual contributions of Dr. Douglas C. Goodwin, Dr. Evert C. Duin, and Dr. Steven Mansoorabadi for ensuring that I remained on track during my graduate studies and research, for advising constructively, and for allowing me access to the instrumentation in their respective labs. In addition, I highly appreciate the role played by Dr. Floyd Woods as the University Reader. I also recognize former and current lab mates among them Dr. Catherine Njeri, Paritosh Dayal, Dianna Forbes, Claire Graham, Katie Stanford, and Richard Hagen for open discussions and scientific opinions during my stay in CB351. I also express my gratitude to the Department of Chemistry and Biochemistry Auburn University for offering me with the opportunity to advance my academic career, and the National Science Foundation for financing this research project. Finally, words cannot express enough the appreciation I have for the sacrifice, the background perseverance, physical, and emotional support invested by my lovely wife Naomi Makau, and our adventurous boys Wesley Makau and Johnstone Makau. Indeed, your investment was not in vain! This dissertation work is dedicated to my dad, John Musila who has sacrificed his entire life to see me this far! Long live Auburn University! War Eagle!

Table of Content

List of Tables

List of Schemes

List of Figures

CHAPTER ONE

LITERATURE REVIEW

1.1 Sulfur Metabolism in Bacteria

1.1.1 General Introduction to Sulfur Metabolism

Sulfur is a ubiquitous element with a relative abundance of ~1.9% that exists in different forms and is vital in living organisms. As the sixth most abundant element on Earth, sulfur is found in the Earth's mantle as sulfide minerals and in crustal rocks as sulfide or sulfate minerals. Native sulfur is found in both active and dormant volcanoes. Sulfur also exists as a trace gas in the atmosphere and as dissolved sulfate and dimethyl sulfide in the ocean.[1, 2] Sulfur occurs in rocks and sediments as pyrite (FeS_2) and gypsum ($CaSO_4$), and as sulfate in seawater. Microorganisms are crucial in the sulfur cycle from which they also benefit.[3]

Sulfur is a constituent of amino acids methionine and cysteine the only sulfur containing canonical amino acids. The other amino acids contain only CHON atoms. Cysteine readily forms intra- and interchain disulfide bonds with other cysteine residues in protein structures, which provides protein structural stabilization. Cysteine is also a crucial amino acid in oxidoreductases (such as thioredoxins, cytochromes, and Fe-S proteins) as it mediates electron transfer.[4, 5] Methionine is a hydrophobic amino acid and tends to be located in the hydrophobic core of globular proteins and interacts with the lipid bilayer in membrane-spanning protein domains. In the synthesis of eukaryotic proteins, methionine is the initiating amino acid; but in prokaryotes, the initiating amino acid is *N*-formyl methionine. After initiation of translation, the methionine residues may be removed, and therefore may not contribute to protein structure.[4]

Sulfur participates in unique chemistry and constitutes cofactors (biotin, CoA, glutathione, CoM, thiamine, and thiocyanate), hormones (insulin, vasopressin), penicillin and sulfa drugs (also known as sulfonamide drugs). It is also vital in sulfur-based photosynthesis. Sulfur can serve as a source of energy (through sulfate reduction or sulfide oxidation) and energy storage in the form of adenosine 5'-phosphosulfate (APS) and 3'-phosphoadenosine 5'-phosphosulfate (PAPS).[22] Sulfur is a constituent of Fe-S clusters in enzymes. The formation of Fe-S cluster involves sulfur transfer from L-cysteine, a reaction catalyzed by cysteine desulfurases (IscS or SufSE).[6, 7] Owing to the importance of sulfur in living organisms, sulfur was potentially involved in the development of early life.[1] Studies on Archaean rocks suggest that microorganisms with sulfur-based metabolism existed 3.5 billion years ago.[8-13]

The cycling of sulfur involves chemical and biological transformations that occur through different oxidation states (from –2 to +6).[3] The ability to exist in multiple valence states enables sulfur to be involved in various geochemical and biochemical processes.[1] The sulfur cycle is complex and augments other elemental cycles such as carbon and nitrogen.[3] Sulfur is assimilated in bacteria from inorganic and organic sources. In aerobic soils, sulfur predominantly exists in the form of ester-sulfur and sulfonates (95% of the total sulfur). In the lab setting, bacteria are usually supplied with inorganic sulfur (sulfate) and therefore optimal sulfur conditions are met.[14] The sulfur cycle entails a cohort of successive reactions in which sulfur transits through different oxidation states. The main oxidation states of sulfur are -2 for thiol and thiolate (such as cysteine and hydrogen sulfide), 0 for elemental sulfur, and +6 for sulfate. Microorganisms are crucial in the transformation of both inorganic and organic sulfur.[15] Assimilation of organosulfur is vital for symbiotic relationships in bacteria, nitrogen fixation, and other metabolic processes requisite for

survival, pathogenicity, and adaptation. Unfortunately, a detailed understanding of the mechanism and regulation of sulfonate metabolism is lacking.[16, 17]

1.1.2 Sulfur Assimilation Pathway in Bacteria

Sulfate compounds are central in sulfur assimilation in bacteria. The sulfate compounds cross the cell membrane through ABC-like transporter proteins, and then undergo enzymatic transformations inside the cell.[3] The sulfur assimilation process in bacteria commences with the activation of sulfate (SO_4^{2-}) through the adenylation of sulfate (**Figure 1**). This ATP consuming reaction, catalyzed by ATP sulfurylase (ATPS), generates adenosine 5′-phosphosulfate (APS).[18, 19] The APS is phosphorylated by APS kinase to 3′-phosphoadenosine 5′-phosphosulfate (PAPS), a potential sulfate donor. PAPS is usually reduced to sulfite (SO_3^{2-}), which is further reduced to bisulfide (HS^-). Bisulfide and *O*-acetylserine are utilized in the biosynthesis of cysteine and other sulfur-containing biomolecules.[17, 20, 21] Bacteria can also hydrolyze APS without the formation of PAPS to release sulfite (APS reductase pathway). The bacterial APS and PAPS reductases exhibit a high sequence similarity. Plants can only utilize the APS reductase pathway (**Figure 1.1**).[17]

Sulfur-containing biomolecules are requisite in bacteria for survival and pathogenicity, and hence, disruption of different enzymes in the pathway affects overall metabolic processes.[17] Inhibition of sulfate assimilation steps disrupts sulfur-based redox processes, a concept that can be harnessed in drug development against pathogenic bacteria.[22] APS reductase catalyzes the first committed step in sulfate reduction.[17, 23] Inhibitors targeting APS reductase in *M. tuberculosis* resulted in decreased cellular levels of sulfur-containing metabolites.[17] In *E. coli*, the presence of APS signals sulfate excess resulting in the upregulation of sulfate assimilation genes. In addition, the use of organosulfur compounds in bacteria as a source of sulfur is repressed by high levels of

sulfate. Therefore, cellular APS levels helps bacteria distinguish when to utilize inorganic and organic sulfur sources.[24]

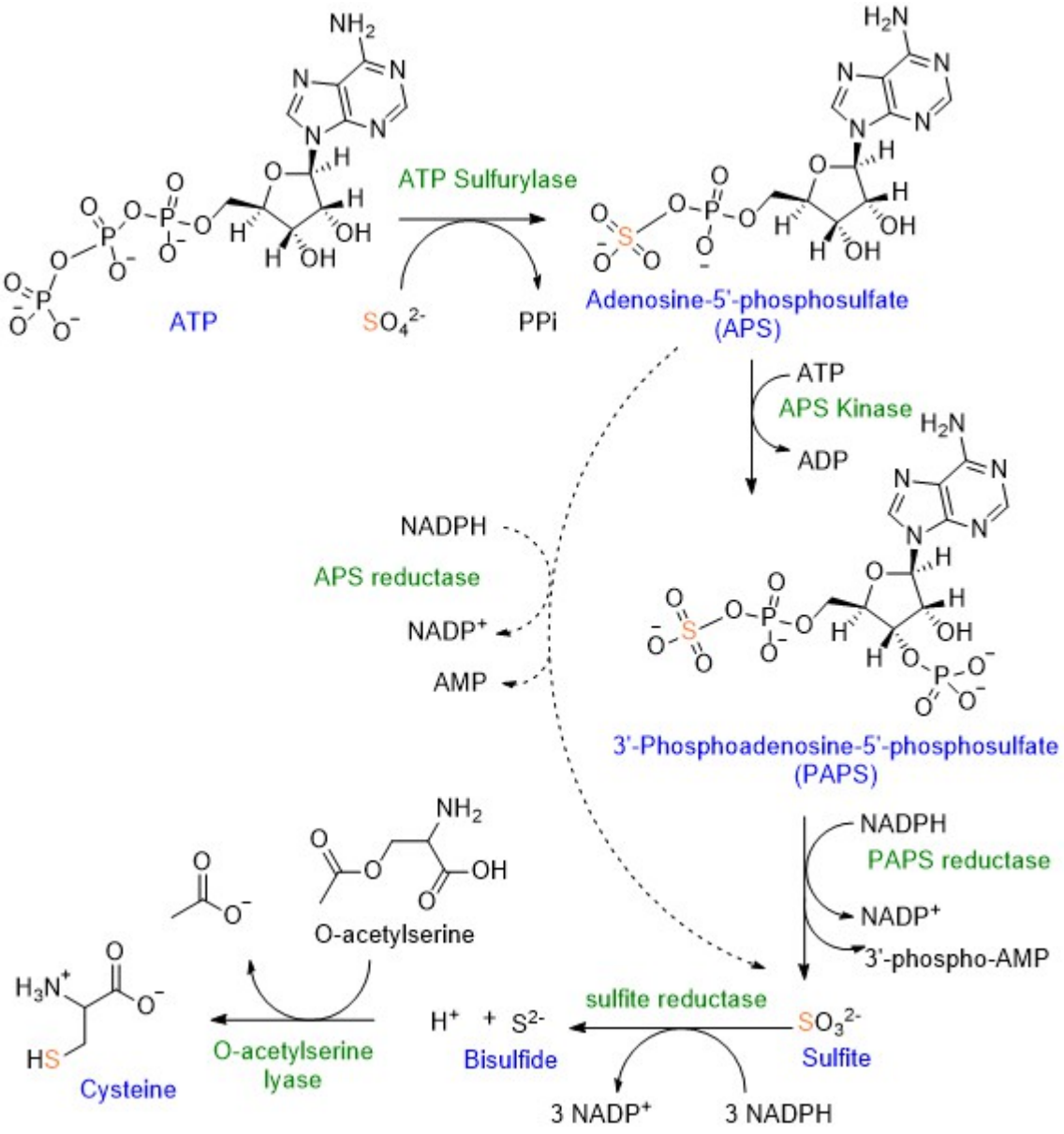

Figure 1.1: Proposed sulfur assimilation pathway and cysteine biosynthesis in bacteria. Bacteria can follow either the APS reductase pathway or the PAPS reductase pathway. Plants utilize the APS reductase pathway only. (Adapted from [17, 19]).

1.1.3 Persulfides in Trafficking of Sulfur in Biosynthetic Pathways

Numerous studies to elucidate the functional roles of sulfur in cofactors and biomolecules, and their involvement in diverse metabolic processes have been evaluated. However, the trafficking of sulfur for incorporation in cofactors and nucleosides is vaguely understood. The persulfide group (R–S–SH) is the predominant sulfur donor for sulfur incorporation in biomolecules.[25] The persulfide form of sulfur delivers the sulfur to acceptor molecules.[25] Bisulfide is utilized *in vitro* in the enzymatic and non-enzymatic synthesis of sulfur-containing cofactors and nucleosides. Bisulfide reacts with a free active cysteine to form an enzyme persulfide intermediate which ensures safe trafficking and delivery of bisulfide.[25] The interaction of bisulfide with oxidized thiols generate persulfides which enhances the reactivity of bisulfide.[26] The persulfide group is chemically rich because each sulfur can exist in three different oxidation states; sulfane (S^0), persulfide (S^{1-}) or sulfide (HS^-). Sulfane sulfur is an electrophile and can transfer electrons to a range of nucleophiles.[27] The sulfur atoms in persulfides can be attacked to release the second sulfur as a bisulfide (HS^-) or thiol (**Figure 1.2**a and **Figure 1.2**b). The exterior sulfur in the persulfide can act as a nucleophile, generating a disulfide bond (R–S–S–R) (**Figure 1.2**c). This versatility makes persulfide groups suitable for the incorporation of sulfur in several metabolic pathways.[28]

The amino acid cysteine participates in the biosynthesis of most sulfur containing cofactors in bacteria and eukaryotes.[29, 30] Cysteine desulfurases and rhodanese homology domain proteins play a crucial role in thiol transfer and incorporation. Cysteine desulfurases forms a protein persulfide on an active cysteine with a free L-cysteine converting the L-cysteine to L-alanine (Figure **1.3**a).[28] Examples of cysteine desulfurases include NifS/IscS enzymes which are found in all bacteria and eukaryotes and in some Archaea species.[31-33] Cysteine desulfurases are pyridoxal

a.

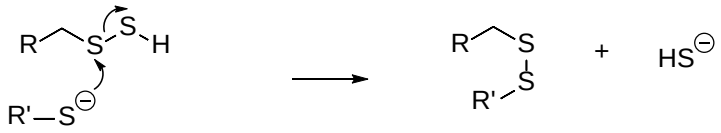

The bridging sulfur as an electrophile

b.

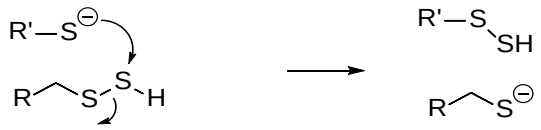

The terminal sulfur as an electrophile

c.

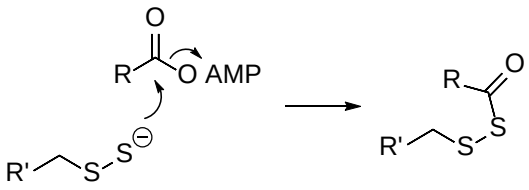

The terminal sulfur as a nucleophile to attack an activated carboxylate to form a thiocarboxylate (at the carboxylic end of sulfur carrier proteins involved in the biosynthesis of thiamin and molybdopterin).

Figure 1.2: Role of persulfide in trafficking sulfur. A persulfide is formed on a cysteine residue for safe trafficking and delivery of bisulfide. (Adapted from [25]).

5′-phosphate (PLP) -dependent and utilizes PLP to cleave of the C–S bond of L-cysteine after the formation of a persulfide enzyme intermediate.[34]

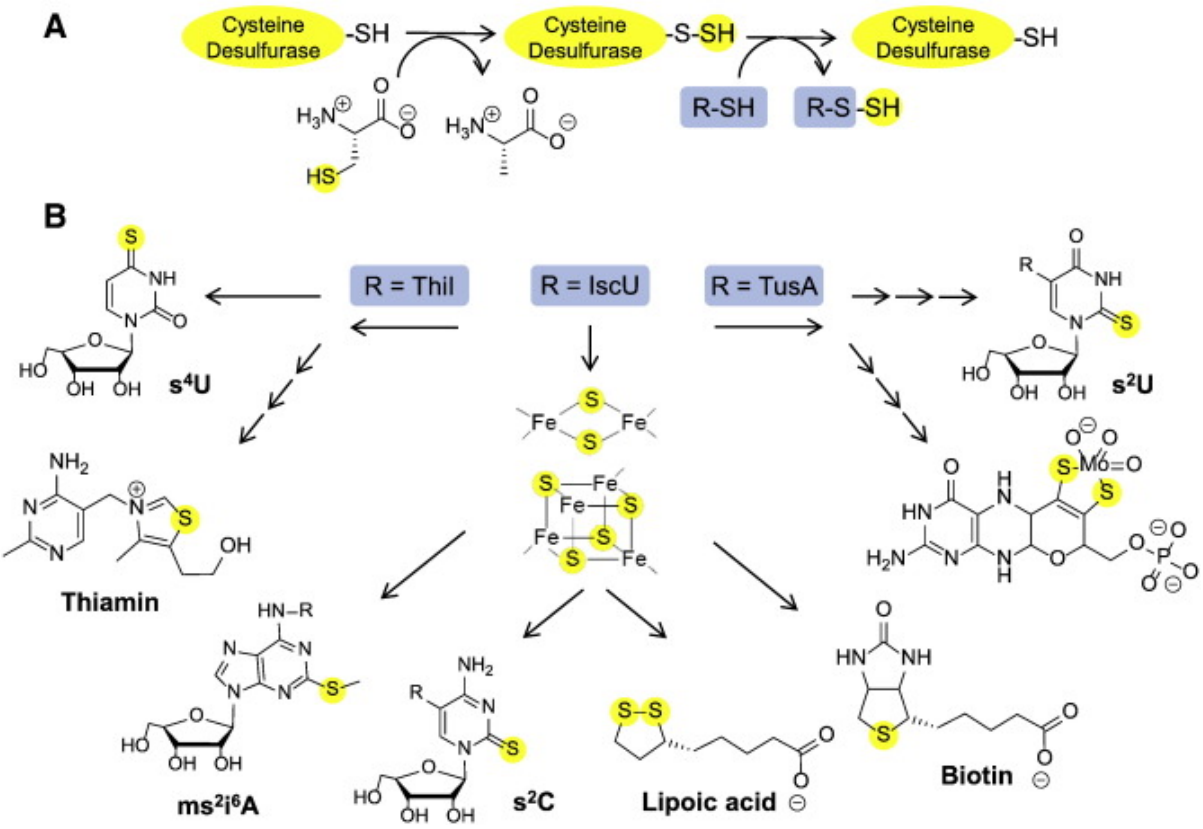

Figure 1.3: Biosynthetic pathways generating sulfur-containing cofactors in *E. coli* which involve IscS. (Adapted from [34]). Copyright © 2014 Elsevier B.V. All rights reserved.

There are three distinct cysteine desulfurases found in *E. coli* which are homologous to NifS. These are IscS, CsdA also known as CSD, and SufS also known as CsdB.[35-38] NifS is cysteine desulfurase involved in the biosynthesis of nitrogenase Fe–S clusters.[39] Although IscS participates in the mobilization of sulfur for Fe–S cluster biosynthesis, it is not restricted to sulfur fixation.[37] IscS is involved in thionucleosides and thiamin/biotin biosynthesis and in the incorporation of

selenium into selenoproteins and selenouridine residues.[35, 40, 41] Different sulfur acceptors (shown in blue in **Figure 1.3**) mediate the transfer of sulfur from IscS persulfide to different sulfur containing cofactors.[34]

Rhodaneses are thiosulfate sulfur transferases found in all three domains of life, which transfer the thiosulfate sulfur to other enzymes involved in sulfur metabolism.[42, 43] The mechanism of rhodaneses involve an active site cysteine of rhodanese enzyme accepting sulfane sulfur from thiosulfate, and transferring it to a sulfur acceptor.[25] Thil is a rhodanese which participates in thiamin and 4-thiouridine biosynthesis.[25, 34] Rhodanese also transfers the thiosulfate sulfur to cyanide (**Figure 1.4**).[42, 43] Rhodanese, in the course of sulfur trafficking helps downregulate bacterial cyanide toxicity. Cyanide is produced in bacteria as a defensive metabolite or for invasive purposes. Cyanide forms stable complexes with transition metals and hence it is highly toxic in most living organisms.[44, 45]

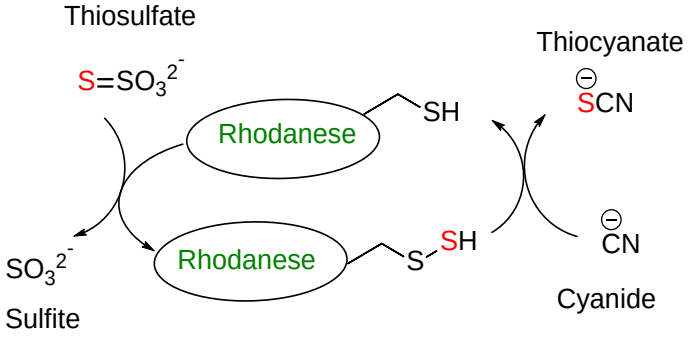

Figure 1.4: The active site cysteine of rhodanese accepts sulfane sulfur from thiosulfate and transfers it to cyanide. (Adapted from [25]).

Endogenous production of H_2S by pathogenic bacteria such as *Staphylococcus aureus* and *Clostridium difficile* enhances their pathogenicity and survival.[46] However, a high cellular bisulfide level is toxic requiring regulation of intracellular H_2S concentrations or a safe sulfur

delivery strategy in the biosynthetic pathways.[25] In *Staphylococcus aureus*, H_2S is converted bisulfide in the cytoplasm. The bisulfide is bound to sulfide:quinone oxidoreductase (SQR) to form SQR-bound persulfide (**Figure 1.5**). The bisulfide is passed to reduced cellular LMW thiols (LMW-SH) through a reaction that forms LMW persulfides (LMW-SSH). CstBPDO uses O_2 to oxidize LMW persulfides to either LMW thiol-S-sulfonate or CstB-S-sulfonate (shown as R-S-SO_3^-). The thiosulfate (TS) is generated by CstBRhod (or other cellular rhodanese proteins) through persulfide transferase activity, or directly via LMW persulfide reacting with LMW thiol-S-sulfonate or CstB-S-sulfonate (**Figure 1.5**). The thiosulfate is processed by CstBRhod, CstARhod, or other cellular rhodanese proteins (thiosulfate sulfurtransferases) to SO_3^{2-} and sulfane sulfur (S^0). The SO_3^{2-} is transported out of the cell by TauE while sulfane sulfur may be assimilated.[47] Similar rhodanese sets have been identified in human pathogenic bacteria, *Enterococcus facaelis* and *Bacillus anthracis* and are thought to regulate intracellular bisulfide concentrations.[47]

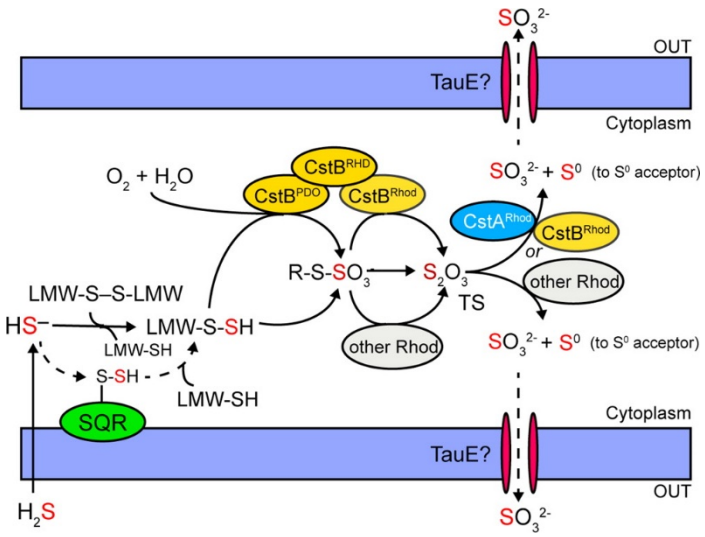

Figure 1.5: Proposed H_2S detoxification by cst operon enzymes in *Staphylococcus aureus.* (Adapted with permission from [47]). Copyright (2015) American Chemical Society.

1.1.4 Sulfur Incorporation and Occurrence in Biomolecules

Sulfur is found in a variety of biological compounds such as cofactors and thionucleosides (**Figure 1.6**). Various biomolecules contain sulfur since sulfur has a wide range of chemical and structural properties.[25] The thiol (–SH) group of cysteine functions as an acid or a base, and forms a disulfide (R–S–S–R) bond that participates in protein-stabilization. The thiol group can also participate in hydrogen bond interactions (donor or acceptor), is a potential catalytic nucleophile, and can bind a metal ligand.[25]

The sulfur atom in thiamin (vitamin B1) bears a partial positive charge which stabilizes the carbanionic form involved in the transketolation of sugars and α-keto acid decarboxylation.[48] Examples of such decarboxylations are reactions catalyzed by pyruvate and α-ketoglutarate dehydrogenase enzymes. These enzymes also utilize lipoic acid which bears two sulfur atoms that cycles between the reduced dithiol and oxidized cyclic disulfide form during catalysis (**Figure 1.6**).[25] The molybdenum cofactor (**Figure 1.6**) also contains two sulfur atoms which serve as the metal binding site of the molybdopterin ligand and sustains the redox potential of molybdenum during catalysis in enzymes such as sulfite oxidase, xanthine dehydrogenase, and aldehyde oxidase.[49] The sulfur atom in biotin (**Figure 1.6**) contributes to an essential ring structure that generate the stable carboxylate form of biotin.[25, 50, 51] Coenzyme A functions as the main acyl group carrier in all cells in carbohydrates, amino acids, fatty acids and ketone body metabolism. It forms an energy-rich thioester bond with the acyl moiety for example in acetyl-CoA.[52, 53] Numerous sulfur-containing nucleobases in tRNA function as recognition centers in enzymes that assign amino acids to tRNA during translation (**Figure 1.6**).[25]

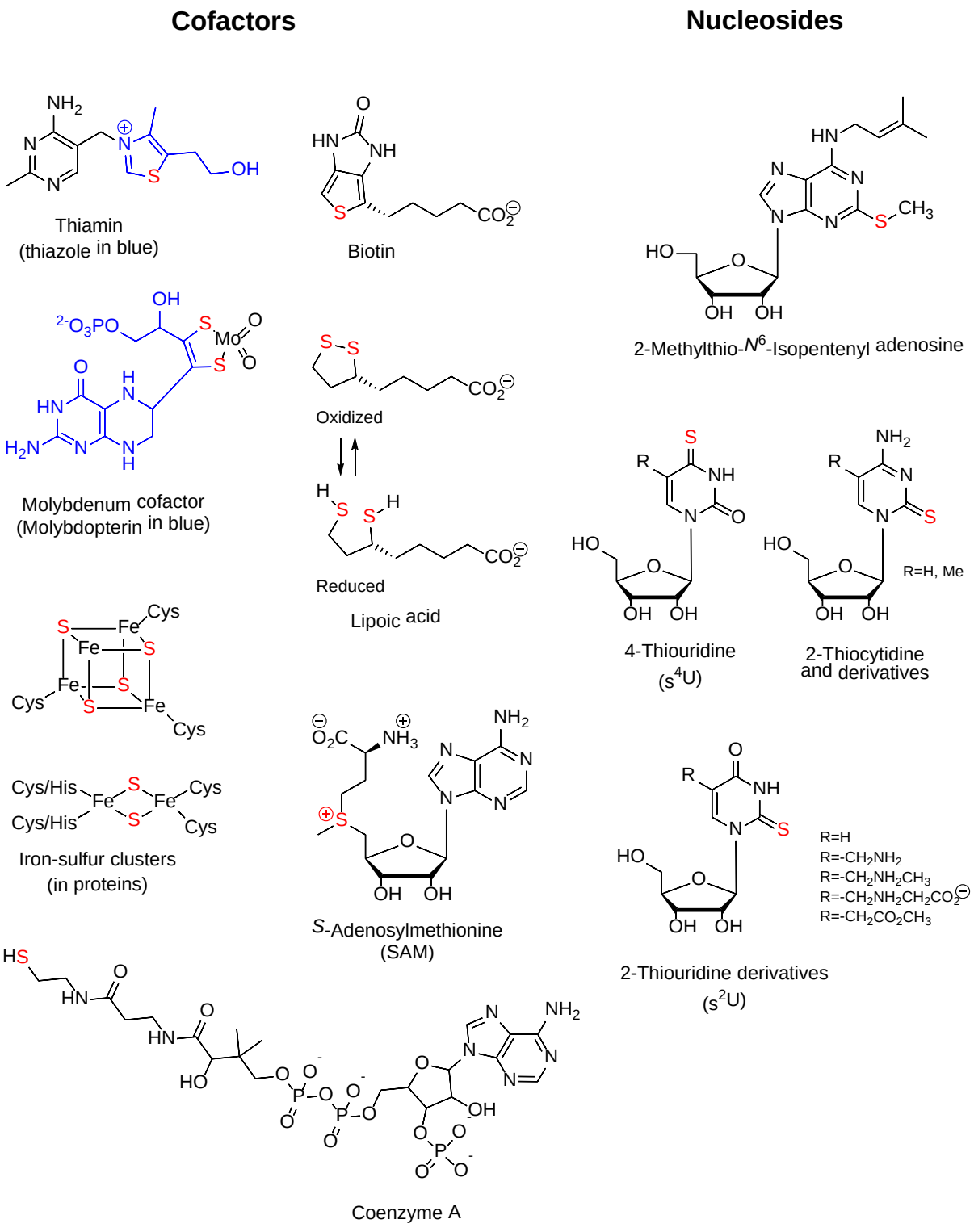

Figure 1.6: Sulfur-containing cofactors and RNA nucleosides. (Adapted from [25]).

The side chain of methionine contains a thioether group (R–S–R) which is hydrophobic. The thioether group of methionine has a lone pair of electrons on the sulfur atom and hence can function as a metal ligand.[54] This lone pair of electrons of methionine makes a nucleophilic attack on ATP in the generation of S-adenosylmethionine (SAM) (**Figure 1.7**, reaction A).[54] SAM has a

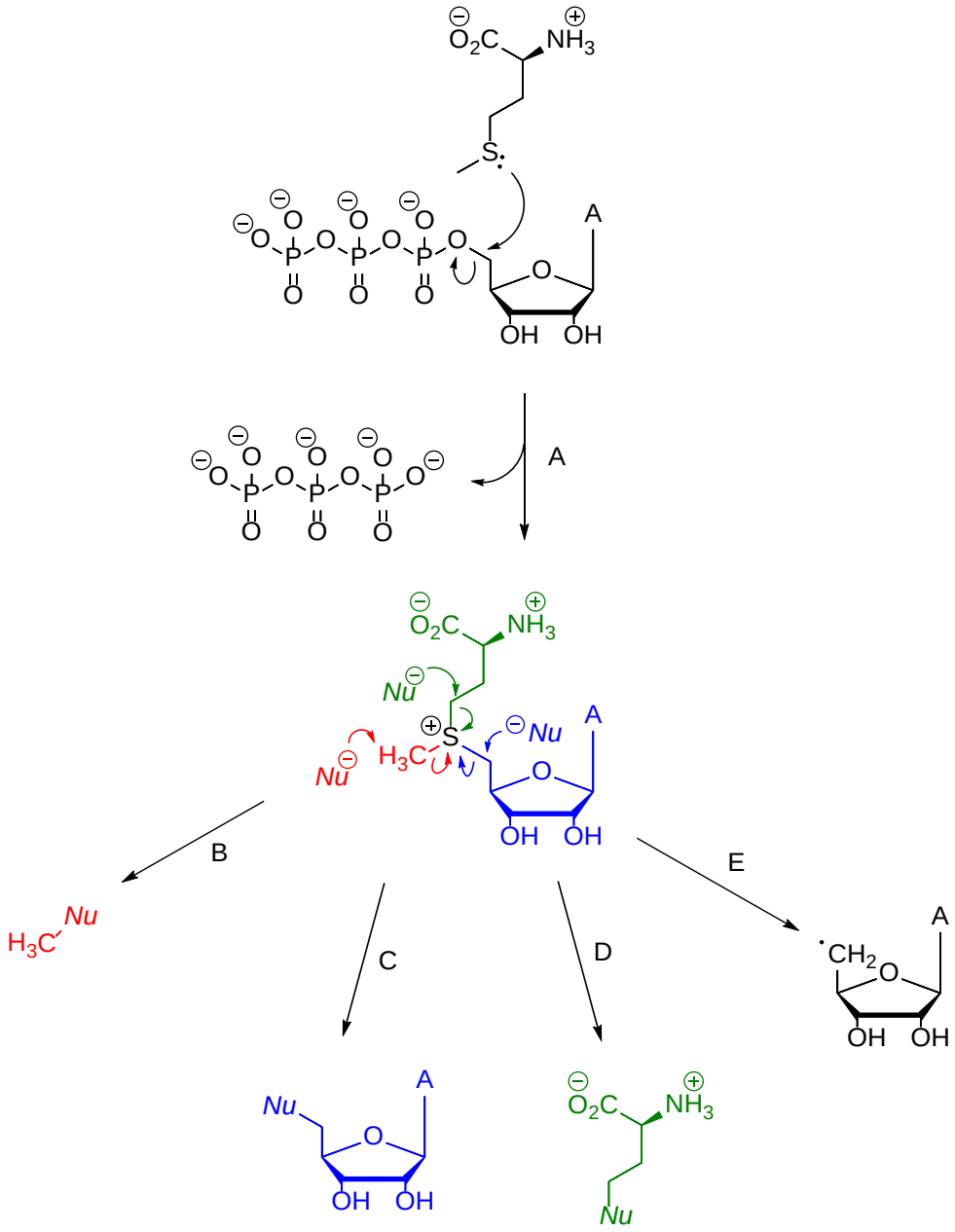

Figure 1.7: Generation of SAM and its reactions. (Adapted from [25]).

cationic sulfur (sulfonium) which allows it to participate in diverse reactions. The sulfonium group can leave as a neutral thioether enabling SAM to perform methylation reaction. The SAM cofactor is crucial in the transfer of ribosyl and aminoalkyl groups (**Figure 1.7**, reactions B–D). The sulfonium group endows SAM with the ability to generate 5′-deoxyadenosyl radicals (**Figure 1.7**, reaction E). These SAM utilizing reactions involve iron-sulfur clusters and other cofactors that are redox centers.[25]

1.1.5 Scavenging Sulfur during Sulfur Starvation Conditions

Sulfur-containing biomolecules participate in various enzymatic chemical and structural functions.[25] The primary source of sulfur in bacterial systems is inorganic sulfates. Bacteria are usually supplied with sufficient inorganic sulfates in the laboratory.[14] However, bacteria often find themselves in environments with low sulfate availability and utilize organosulfonates as an alternative source of sulfur through desulfonation. The organosulfonates exist as natural products of low and high molecular weight most of which can be desulfonated. The process of desulfonation entails cleavage of the C-S bond of organosulfonates by desulfonation enzymes; taurine dioxygenase and alkanesulfonate monooxygenase enzymes releasing sulfite. The desulfonation enzymes are induced when sulfonate serves as a carbon and energy source, or by sulfate-starvation-induced *(ssi)* stimulon when organosulfonates serve as a sulfur source in bacteria.[55]

Sulfonates are widely available and are utilized by aerobic bacteria as an alternate source of sulfur during sulfate limitation.[56] The desulfonation of these organosulfonates is catalyzed by desulfonation enzymes which are expressed when sulfate is limiting in bacteria and include the α-ketoglutarate-dependent dioxygenase (TauD) and alkanesulfonate monooxygenase (SsuD). The *ssi* enzymes are encoded by the *tauABCD* and *ssuEADCB* genes respectively (**Figure 1.8**), and are repressed by the presence of sulfate.[57]

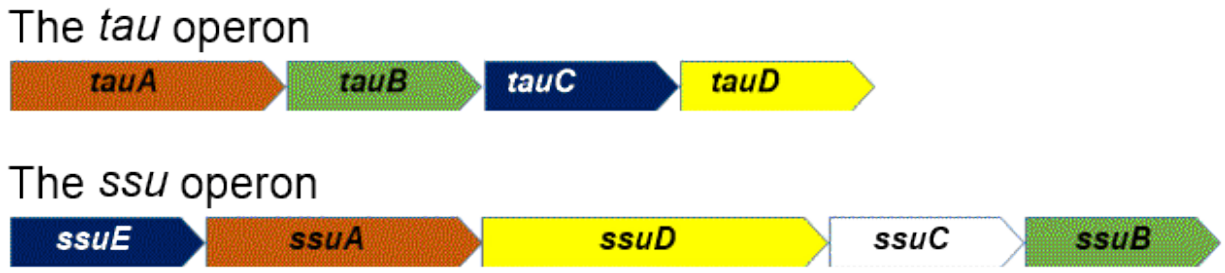

Figure 1.8: The *tau* and *ssu* operons are induced during sulfur starvation. The *ssu* operon encodes for a flavin reductase (SsuE) and alkanesulfonates monooxygenase (SsuD), while *tau* operon codes for taurine dioxygenase. Both operons encode for ABC-like organosulfonates transporter proteins. (Adapted from [58]).

The taurine dioxygenase (TauD) enzyme desulfonates taurine (2-aminoethanesulfonate) releasing sulfite and aminoacetaldehyde. TauD belongs to the non-heme Fe(II) oxygenase family. TauD also converts α-ketoglutarate to succinate with the release of a CO_2 molecule **(Figure 1.9)**.[59]

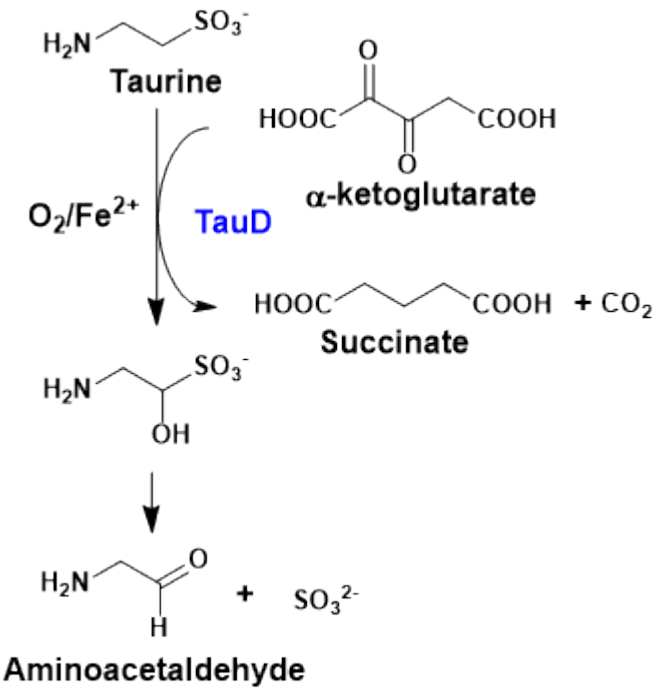

Figure 1.9: Desulfonation of taurine (2-aminoethanesulfonate) by TauD. TauD desulfonates taurine releasing sulfite and aminoacetaldehyde. (Adapted from [59]).

The alkanesulfonate monooxygenase system catalyzes the desulfonation of alkanesulfonates as an alternative pathway for sulfur acquisition when sulfur is limiting in various bacteria. These enzymes are expressed under regulation of the sulfate-starvation utilization *(ssu)* operon commonly made up of five cistrons (*ssuEADCB)* (**Figure 1.8**).[60] The alkanesulfonate monooxygenase system is a two-component system comprised of a NAD(P)H:FMN reductase (SsuE) that reduces flavin and delivers the reduced flavin to the monooxygenase enzyme (SsuD). The SsuD enzyme catalyzes the $FMNH_2$-dependent desulfonation of alkanesulfonates generating sulfite, FMN, a molecule of water, and the corresponding aldehyde (**Figure 1.10**). The sulfite produced is incorporated into sulfur-containing biomolecules (**Figure 1.6**).[57, 60]

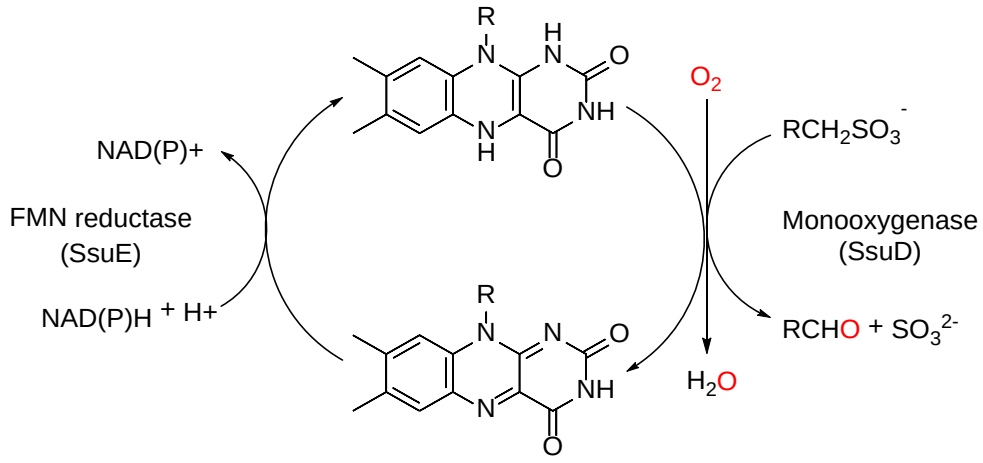

Figure 1.10: Desulfonation of alkanesulfonates by *ssu* enzymes. The desulfonation reaction is catalyzed by SsuD and utilizes reduced flavin supplied by SsuE. (Adapted from [61]).

The SsuD enzyme is able to desulfonate diverse organosulfonates including C-2 to C-10 alkanesulfonates, 1,3-dioxo-2-isoindolineethanesulfonate, 2-(4-pyridyl)ethanesulfonate, and sulfonated buffers, and is found in a range of bacterial genera.[57, 62-64] The alkanesulfonate

monooxygenase system in different bacterial systems resemble that of *E. coli* and is usually comprised of both SsuE/SsuD. In most cases, the *SsuE* gene is located in an operon that contains a SsuD homolog. The order of the *ssu* genes varies in different bacterial organisms. They usually contain an ABC-type transporter, a monooxygenase (SsuD), and a flavin reductase (SsuE). The flavin reductases are close homologs with >60% sequence identity.[63] In some bacteria such as in *Bacillus subtilis*, *Burkholderia cenocepacia*, and *Corynebacterium glutamicum*, the operon contains a SsuD homolog but lacks an SsuE-like reductase.[65-67] Although the *ssu* operon in *Bacillus subtilis* does not have the *ssuE* gene, a flavin reductase is encoded on a separate operon.[68, 69] The SsuD in the organisms lacking *ssuE* gene may not require a specific flavin reductase. Unrelated flavin reductases have been successfully utilized in some two-component oxygenase systems to supply unrelated oxygenase enzymes with reduced flavin.[70, 71] The *ssu* genes are thought to have been acquired through horizontal gene transfer among bacterial systems.[72]

Pseudomonas putida has the unique ability to desulfonate methanesulfonate, dimethyl sulfonate (DMSO), dimethyl sulfide, and arylsulfonates. The operon of *Pseudomonas spp*. contains an extra gene *ssuF* whose role has not been firmly established. The SsuF protein is thought to be either a transporter protein or a molybdopterin-binding protein. The ability of *Pseudomonas spp*. to desulfonate arylsulfonates has been attributed to the presence of SsuF.[63] *Pseudomonas aeruginosa* was initially thought to have two sets of *ssu* operons (*ssuEADCBF* and *ssuEDC*), but the *ssuEDC* operon has been revised to the *msuEDC* annotation identified as the MsuE/D system.[68, 73] However, two gene clusters similar to *E. coli ssuEADCB* were identified in *Bradyrhizobium japonicum*.[16] In addition to processing organic sulfonates in *B. japonicum*, the genes were shown to express sulfonate monooxygenases and sulfatases in soybean nodules, linking organosulfur utilization to nitrogen fixation and nodulation.[16]

1.1.6 The Alkanesulfonates Transport System

Expression of ABC-like transporter proteins is requisite for the uptake of organosulfonates utilized by the *tau* and *ssu* systems.[59, 60] The two-component alkanesulfonate monooxygenase system relies on an ATP-binding cassette (ABC)-type aliphatic sulfonate (SsuABC or on TauABC) transporter (**Figure 1.11**).[57, 63] The ABC transporters generally bind and hydrolyze ATP to transport diverse substrates across membranes, bringing nutrients and other molecules into the cell or removing unwanted cellular molecules across the membrane. The ABC transporters are found in the three domains of life (bacteria, archaea and eukaryota). They exhibit two transmembrane regions and two soluble nucleotide binding domains.[74, 75] The nucleotide binding domains of ABC proteins are highly conserved in both sequence and structure.[75] The organosulfonates cross the cell membrane to serve as a sulfur and carbon source.

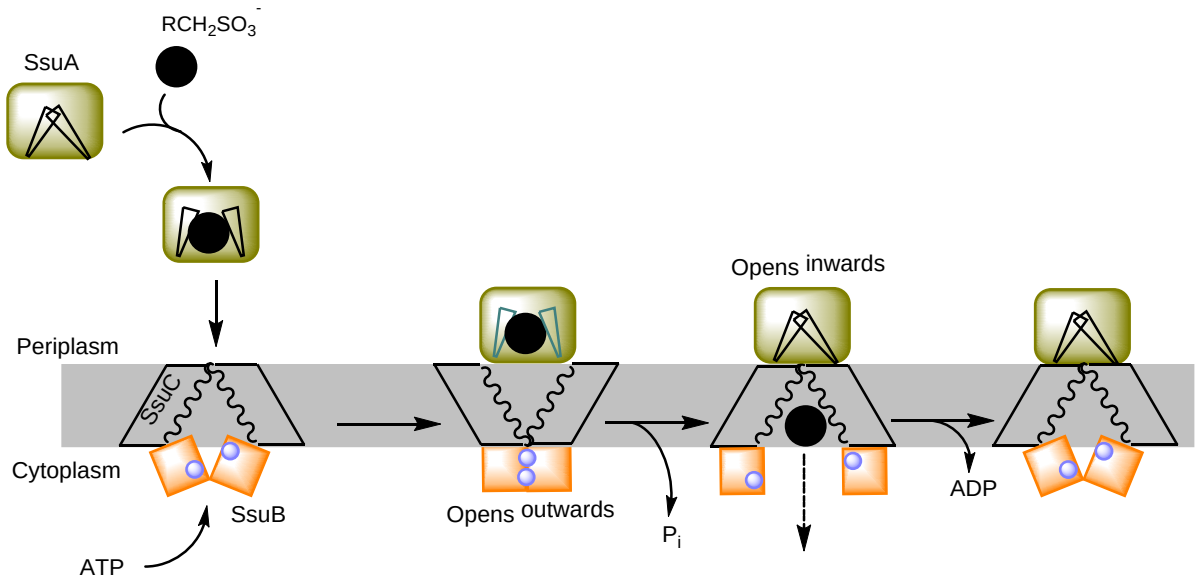

Figure 1.11: The alkanesulfonate monooxygenase system transporter proteins.

Although organosulfonates require transport systems across the cell membrane, little mechanistic knowledge is available on their transport. Sequences of some transporter genes have been identified.[55] SsuA constitutes the periplasmic alkanesulfonate binding protein, SsuC is a membrane permease protein, and SsuB is an ATP-binding protein.[60] The synergistic effort of sulfonate transporter proteins provides alkanesulfonates for the cytoplasmic proteins SsuE and SsuD to process (**Figure 1.12**).[60] Three-dimensional studies on SsuA from *X. citri* shows a large binding pocket which should support binding of various alkanesulfonates.[72] The alkanesulfonate uptake and *ssu* expression were shown to increase in uropathogenic *E. coli* (UPEC) during human urinary tract infections (UTI) and suggests the transporter system may be a potential therapeutic target against pathogenic bacteria.[76] The transport of taurine into bacterial cell is exclusively dependent on the TauABC transporter proteins. The TauABC transporter proteins can also transport some alkanesulfonates into the cell.[58] Although SsuD cannot desulfonate taurine, some alkanesulfonates can be desulfonated by the TauD enzyme. Therefore, taurine desulfonation is exclusively dependent on TauD.[58]

1.1.7 Regulation of the *ssi* Operons

The alkanesulfonate monooxygenase enzymes are expressed under the regulation of the *ssuEADCB* operon. In *E. coli*, the expression of the *ssuEADCB* genes is regulated by Cbl, a transcriptional activator which binds to the Cbl-binding site located upstream of the promoter at the -35 region. The Cbl protein binds at the upstream regions of the *ssuEADCB* and *tauABCD* operons during sulfate starvation conditions to activate their transcription.[24, 77] The expression of the *cbl* gene is controlled by the transcriptional activator CysB that binds at the CysB-binding site.[60] CysB upregulates the transcription of the *ssu* operon. The expression of the *tau* operon is also regulated by Cbl whose expression is activated by CysB in the *tau* system.[78]

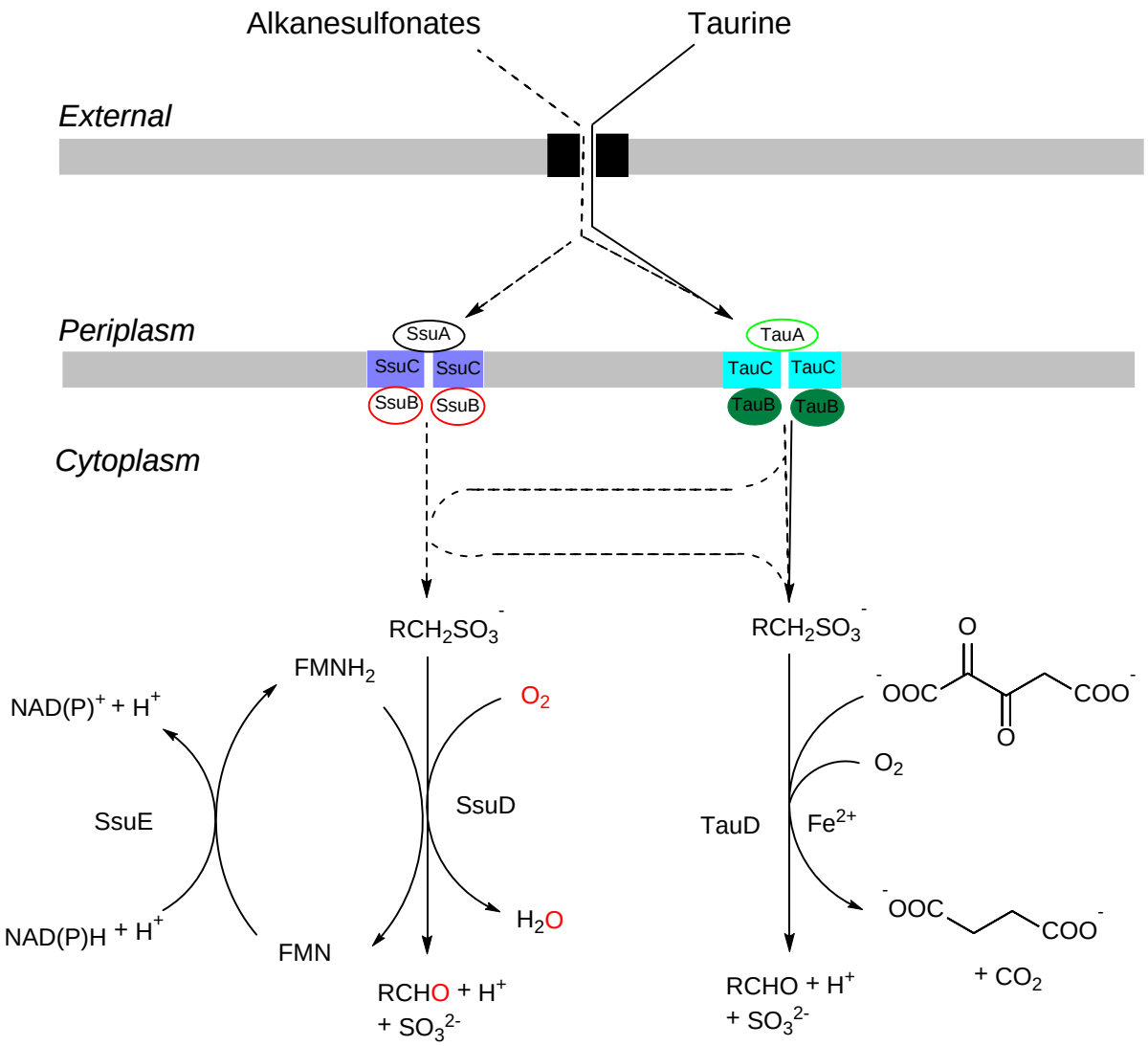

Figure 1.12: Sulfonate uptake and desulfonation in *E. coli*. The alkanesulfonates enter the cell through ssuABC system and some can be transported via TauABC system (dashed lines). Taurine is transported into the cell only through TauABC (solid lines). It is not known how the alkanesulfonates and taurine cross the outer membrane. (Adapted from [58]).

Studies on the regulation of *ssi* gene expression in *E. coli* shows that the CysB protein (a LysR-family transcriptional regulator) is key in regulating the expression of cysteine biosynthetic and *ssi* genes.[79] The CysB protein upregulates the expression of *cbl* which encodes a LysR-family transcriptional regulator.[78] During sulfate-rich conditions, adenosine-5-phosphosulfate (a cysteine biosynthetic intermediate) represses *cbl*, consequently suppressing the expression of both the *ssu* and *tau* operons.[80]

Recent studies of the *E. coli* transcription regulatory network identified fumarate and nitrate regulatory protein (FRN), and Cbl are positive regulators of Ssu enzymes.[81] The FNR is a transcriptional regulator of a several genes involved in respiratory pathways. It is responsive to oxygen levels and its transcriptional activity requires an iron–sulfur cofactor.[82, 83] CysB was identified as a negative regulator, while integration host factor (IHF) can be a negative or positive regulator for the *ssu* operon.[81] IHF is a global regulator of many DNA functions in prokaryotes including replication and transcription, hence housekeeping levels are always maintained.[84, 85] The CysB regulator is also involved in the assimilation of organosulfur in *Pseudomonas spp.*[63, 86-88] The regulation of *ssi* genes in *Pseudomonas spp.* could be different from that of *E. coli* because there is no *cbl* gene or its equivalent identified in *P. aeruginosa* and *P. putida* genomes.[89, 90] Although some transcriptional regulators have been reported, the regulation of organosulfur assimilation in *pseudomonads* during sulfur starvation conditions is not well known.[63, 91-94]

1.2 Flavoproteins in Enzymology

1.2.1 Flavin

Flavin-dependent proteins are versatile and participate in different functions. The flavin cofactors are involved in various fundamental enzymatic redox reactions.[95, 96] The term flavin encapsulates a group of molecules whose structure contains a heterocyclic isoalloxazine ring (7,8-dimethylisoalloxazine) which is the business-end of the flavin molecule (**Figure 1.13**). Naturally occurring flavins include lumiflavin, riboflavin, flavin mononucleotide (FMN), and flavin adenine dinucleotide (FAD) (**Figure 1.14**). These flavins all have an isoalloxazine ring but have different R-groups.[97]

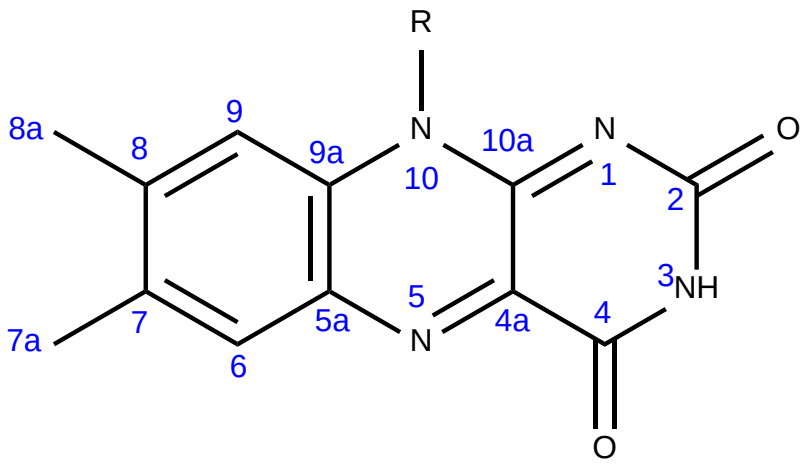

Figure 1.13: The isoalloxazine ring of flavins.

Lumiflavin has a methyl group attached to the isoalloxazine ring at position N-10 and riboflavin has a ribityl sugar side chain attached at the same position (**Figure 1.14**). FMN has an additional phosphate group at the end of the ribityl sugar side chain, while FAD has an adenine dinucleotide group attached to the phosphate group of the FMN constituents. A natural riboflavin

analog called roseoflavin (**Figure 1.14**) produced by *Streptomyces davawensis* and *Streptomyces cinnabarinus* manifests antibiotic activity through the targeting of flavoenzymes and flavoswitches.[98, 99] The isoalloxazine ring is not synthesized in mammals and is supplemented in the diet as riboflavin (vitamin B2). Riboflavin, the precursor in the synthesis of other flavin cofactors is typically converted to FMN and FAD in mammals to sustain physiological functions. Ariboflavinosis (riboflavin deficiency) in man and experimental animals has been linked to neuromuscular disorders, neurological disorders, cardiovascular diseases, and cancer.[100-102] This is because riboflavin is used to synthesize cofactors FMN and FAD, which are crucial in diverse functions including energetic metabolism, maintenance of redox homeostasis, and protein folding and function.[97, 103-105]

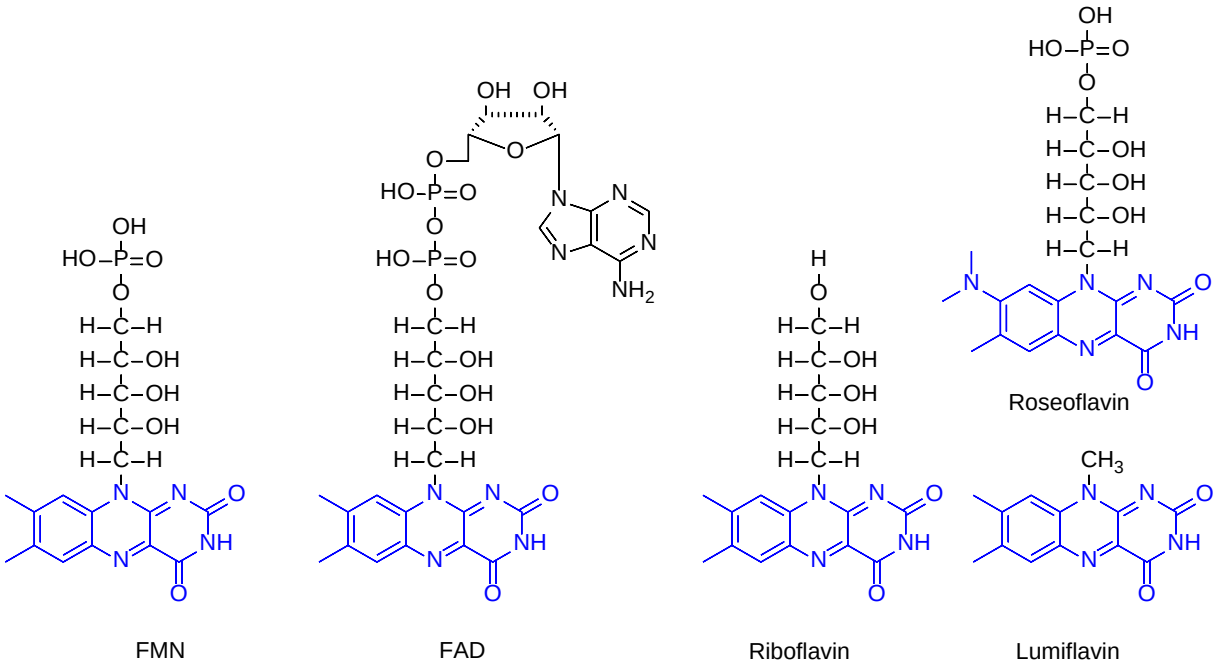

Figure 1.14: Structures of naturally occurring flavin.

1.2.2 Biosynthesis of Flavins in Bacteria

Many bacteria and plants synthesize riboflavin (constituted of ribityl side chain attached to the N10 of the isoalloxazine ring).[106, 107] The biosynthesis of the isoalloxazine moiety of riboflavin is the most complex and its detailed biosynthetic pathway is largely unknown. Studies have shown that some reactions in the artificial synthesis (nonenzymatic) of isoalloxazine do not require catalysts suggesting that the initial flavin synthesis may have occurred spontaneously before the evolution of enzymatic macromolecules.[107-109] The biosynthesis of flavin utilizes GTP (1) which is converted (through several intermediate steps) to 5-amino-6-ribitylamino-2,4(1H,3H)-pyrimidinedione (6) (**Figure 1.15**). The 5-amino-6-ribitylamino-2,4(1H,3H)-pyrimidinedione intermediate is formed from different precursors in different organisms. In fungi and Archaea, the 2,5-diamino-6-ribosylamino-4(3H)-pyrimidinone 5'-phosphate (2) (the first committed pathway intermediate) is reduced and deaminated.[110, 111] In eubacteria and plants, the reduction of the side chain of 2,5-diamino-6-ribosylamino-4(3H)-pyrimidinone 5'-phosphate occurs before the deamination step.[112-115] The 5-amino-6-ribitylamino-2,4(1H,3H)-pyrimidinedione 5'-phosphate (5) is dephosphorylated to generate 5-amino-6-ribitylamino-2,4(1H,3H)-pyrimidinedione (6) through an unknown mechanism. The dephosphorylation of 5- amino-6-ribitylamino-2,4(1H,3H)-pyrimidinedione 5'-phosphate (5) is required because a phosphate ester is not a possible substrate for the condensation of 5-amino-6-ribitylamino-2,4(1H,3H)-pyrimidinedione (6) with 3,4-dihydroxy-2-butanone 4-phosphate (8) catalyzed by 6,7-dimethyl-8-ribityllumazine synthase (VIII). The 3,4-dihydroxy-2-butanone 4-phosphate (8) is obtained from ribulose 5-phosphate (7) through a series of rearrangements and elimination.[107]

The final two steps in the synthesis of FMN and FAD (**Figure 1.15**) are catalyzed by an ATP-dependent riboflavin kinase (generating FMN and ADP), and an ATP-dependent FMN

adenylyltransferase (generating FAD and ADP).[116] The phosphorylation of riboflavin and subsequent adenylation steps in eukaryotic organisms are catalyzed by two separate enzymes.[117, 118] In most prokaryotes, a single bifunctional enzyme (FAD synthetase) functions as both a riboflavin kinase and FMN adenylyltransferase to phosphorylate the ribityl end of riboflavin to form FMN, and further adenylate the FMN to FAD in a two ATP-dependent reaction.[119-123]

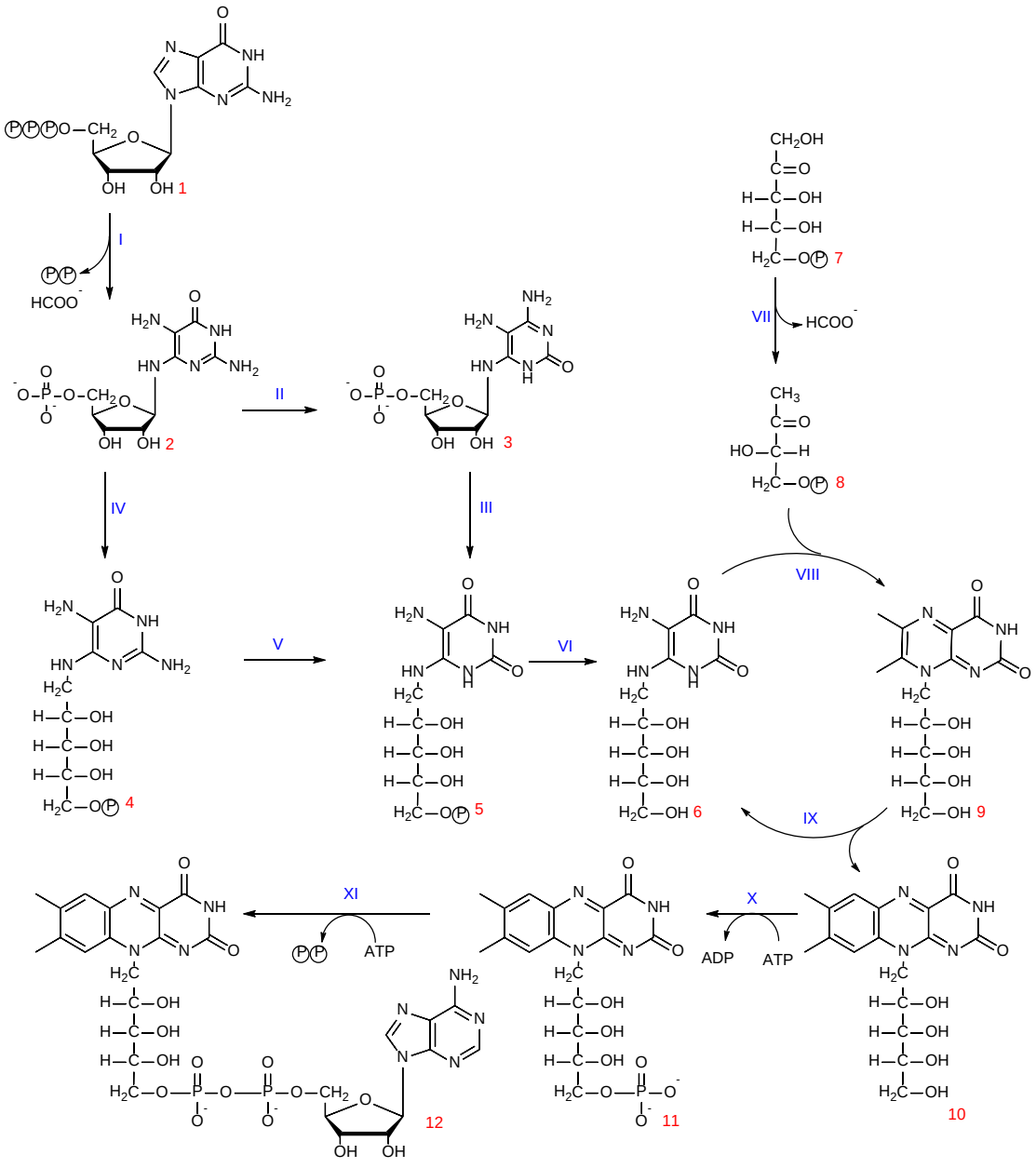

Figure 1.15: Biosynthetic pathway of flavin. (Adapted from [107]).

Table 1.1: *Organic intermediates and enzymes involved in flavin biosynthesis*

Organic molecules/Intermediates	Enzymes involved in flavin synthesis steps
1. GTP	I. GTP cyclohydrolase II
2. 2,5-diamino-6-ribosylamino-4(3*H*)-pyrimidinone 5′-phosphate	II. 2,5-diamino-6-ribosylamino-4(3*H*)-pyrimidinone 5′-phosphate deaminase
3. 5-amino-6-ribosylamino-2,4(1*H*,3*H*)-pyrimidinedione 5′-phosphate	III. 5-amino-6-ribosylamino-2,4(1*H*,3*H*)-pyrimidinedione 5′-phosphate reductase
4. 2,5-diamino-6-ribitylamino-4(3*H*)-pyrimidinone 5′-phosphate	IV. 2,5-diamino-6-ribosylamino-4(3*H*)-pyrimidinone 5′-phosphate reductase
5. 5-amino-6-ribitylamino-2,4(1*H*,3*H*)-pyrimidinedione 5′-phosphate	V. 2,5-diamino-6-ribitylamino-4(3*H*)-pyrimidinone 5′-phosphate deaminase
6. 5-amino-6-ribitylamino-2,4(1*H*,3*H*)-pyrimidinedione	VI. Hypothetical phosphatase
7. ribulose 5′-phosphate	VII. 3,4-dihydroxy-2-butanone 4-phosphate synthase
8. 3,4-dihydroxy-2-butanone 4-phosphate	VIII. 6,7-dimethyl-8-ribityllumazine synthase
9. 6,7-dimethyl-8-ribityllumazine	IX. Riboflavin synthase
10. Riboflavin	X. Riboflavin kinase
11. FMN	XI. FAD synthetase
12. FAD	

1.2.3 Spectral Properties of Flavin at Different Oxidation States

Flavin and flavoproteins exhibit various spectroscopic properties which facilitates their spectroscopic characterization in redox reactions involving different flavin intermediates.[97, 124, 125] Flavoproteins can carry out one- and two-electron transfers depending on the flavin environment.[126-128] The generation of the hydroquinone form of the flavin can occur when flavin is reduced by a two electron transfer, or by a two-single electron transfer through a semiquinone intermediate. The different spectral properties of flavin are based on the oxidation state of the isoalloxazine ring.[129] An absorption spectrum with a peak at ~450 nm is usually observed with oxidized flavin (both free and bound) (**Figure 1.16**). The oxidized flavin also has fluorescence properties with maximum emission wavelengths of around 520 nm.[130]

A single electron transfer to oxidized flavin generates a neutral semiquinone (red in color with a broad absorbance between 500-650 nm with maxima at 580 nm) or an anionic semiquinone (light blue in color, has an absorbance peak at 370 nm but weakly absorbs beyond 550 nm) (**Figure 1.16**).[124, 125] The semiquinone flavin portrays a weak absorbance at 450 nm but has a strong peak at ~370 nm (**Figure 1.16**). Although free semiquinone flavin shows no fluorescent properties, the flavin semiquinone can exhibit fluorescent properties when bound to enzymes.[130] The fully reduced flavin (hydroquinone form) is colorless, has no absorbance peak at 450 nm (**Figure 1.16**), and is assumed to be nonfluorescent, although some fluorescence has been observed with some flavoenzymes at specific excitation wavelengths. The fluorescence properties of reduced flavin is generally dependent on the buffer pH, viscosity, the active site environment, and substitutions on the isoalloxazine ring.[125, 131]

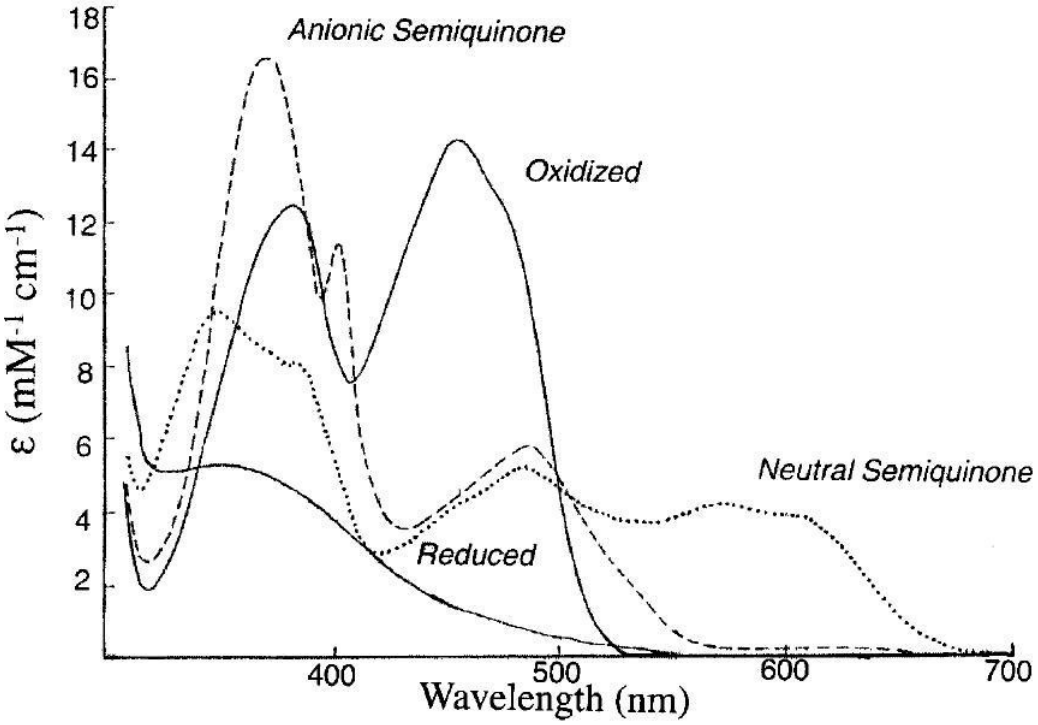

Figure 1.16: The spectral properties exhibited by flavins corresponds to the different oxidation states. (Adapted from [97]). Copyright © 2000 The Biochemical Society/Portland Press.

The flavin semiquinone can be generated when free fully-oxidized flavin is mixed with free fully-reduced flavin in solution.[97] At least, 5% of the semiquinone portrayed stability at pH 7 even when not bound to protein.[97] The equilibrium shifted towards semiquinone formation when protein was flavin-bound.[97, 124] The N1 of the isoalloxazine ring can be protonated or deprotonated resulting in different redox states and different ionic flavin species. Generally, the neutral and anionic forms of flavin are considered physiologically relevant (**Figure 1.17**). The cationic forms of flavin can only be observed at extremely low pH values.[132] Flavin can exist in other electronic states (charge-transfer states) in which there is a partial charge transition between

the three redox states (**Figure 1.17**).[132] The unique and resolute spectral properties of the different forms of flavin allows one to trace the flavin oxidation states in catalytic events and in evaluation of the step-wise mechanisms exhibited by flavoproteins.

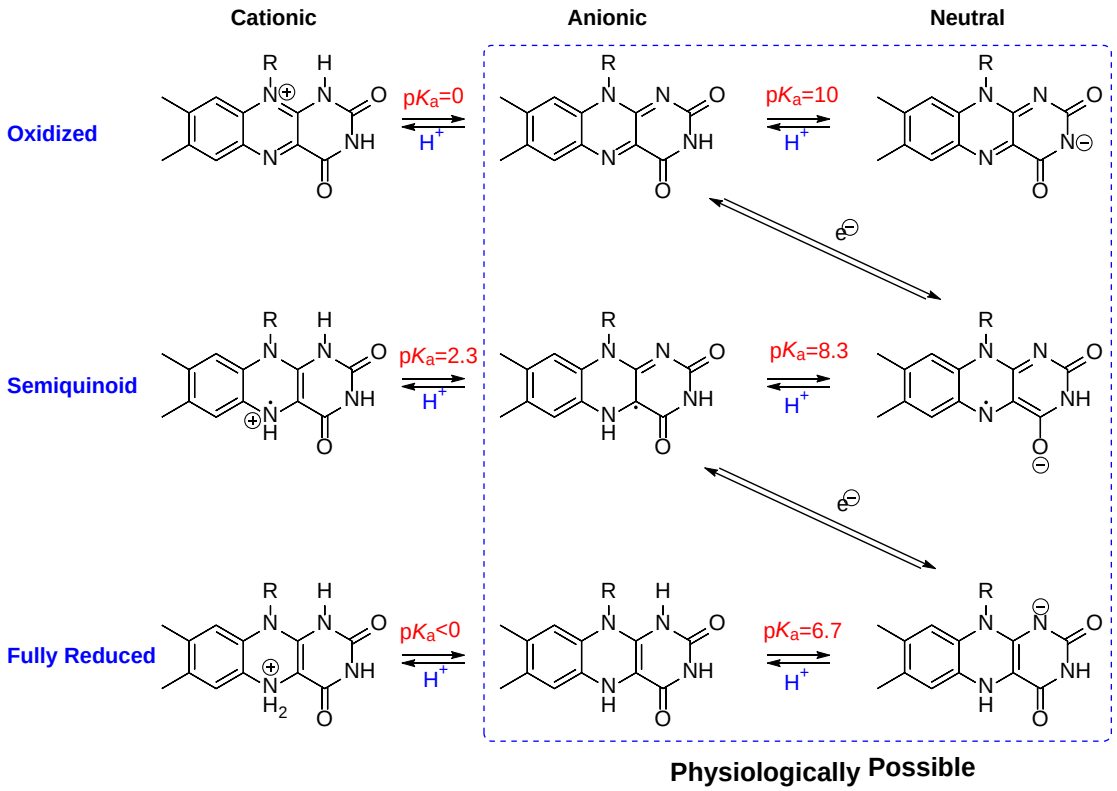

Figure 1.17: Flavin can exist in different redox and ionic states. Generally, the neutral and anionic forms of flavin are considered physiologically relevant. The cationic forms of flavin can only be realized at extremely low pH. (Adapted from [132]).

1.2.4 Flavoproteins

Flavoproteins refers to the proteins whose execution of biological functions is dependent on the flavin cofactor. The seminal flavoprotein was characterized through structural determination and chemical synthesis in the Richard Kuhn (Heidelberg) and Paul Karrer (Zurich) labs as old yellow enzyme in the 1930's. The compound was named "riboflavin" after the ribityl side chain attached at the N(10) position (**Figure 1.13**) and word "flavus" (Latin for yellow) based on its color. Flavin cofactors have a characteristic yellow color and possess a heterocyclic alloxazine chromophore.[133, 134] In 1879, Blyth identified a yellow compound isolated in cows' milk and reported it as lactochrome.[135] Prior to the identification of lactochrome, bioluminescence by luciferase had been reported in non-scientific descriptions.[136] It was later determined that many biologically relevant flavin compounds were FMN and FAD both of which are synthesized from riboflavin (**Figure 1.15**).[97, 106, 107]

Flavoproteins can be classified based on the substrate they utilize, the number of electrons per catalytic cycle, electron acceptors, and structural and physicochemical properties.[132] Flavoproteins perform different functions and have been extensively explored. The flavin cofactors are involved in various fundamental enzymatic redox reactions involving one- and two-electron transfer reactions.[95, 97, 105, 137-156] The chemical versatility of flavoproteins is based on the flavin environment (usually the enzyme active site).[128] Canonical flavoproteins are flavin-bound with the flavin being either tightly or covalently bound. The flavin-free flavoproteins however, are typically supplied with free flavin.[95, 96] The covalently bound flavoproteins have the flavin attached to the protein through either the 8α-methyl group or through the C6 of the flavin isoalloxazine ring. The residues that form covalent bonds at the 8α-methyl group are Cys, Tyr, and

His. Cys is the only amino acid that forms a covalent bond through the C6 position of the isoalloxazine ring.[155]

Flavoproteins are commonly categorized into oxidases, reductases, dehydrogenases, and monooxygenases. Flavin dehydrogenases (which include acyl-CoA, succinate, and alcohol dehydrogenase) do not use O_2 in the transfer of two electrons and a proton (**Figure 1.20**).[150] Flavin oxidases use dioxygen to oxidize the substrate, and generate H_2O_2 (**Figure 1.20**). They first get reduced by the substrate before substrate oxidation. The reduced flavin is stabilized before reacting with dioxygen.[97] Examples of enzymes that are flavin oxidases include glucose, glycine, and amine oxidase.[139-141] Flavin monooxygenases insert oxygen atom(s) in diverse substrates releasing the other oxygen atom as water. They form and utilize peroxyflavin intermediates to insert an oxygen atom in the substrate they catalyze (**Figure 1.20**).[157-159] Some flavoproteins are involved in electron transport.[137, 149-152] While some flavoproteins form reactive oxygen species contributing to oxidative stress, others counter oxidative stress by decreasing hydroperoxide levels.[128]

1.2.5 Reactivity of Flavin with Molecular Oxygen

Flavoproteins display remarkable differences on how they react with molecular oxygen, but there is no common explanation for the differential reactivity.[156, 160] The ability of the reduced flavin to react differently with dioxygen has been linked to the chemical versatility of flavoproteins.[161] Oxygen is not always the intended electron acceptor for flavoproteins, hence flavin-dependent redox reactions can occur under low oxygen levels. Some flavoproteins (oxidases or monooxygenases) utilize oxygen as a substrate. Suppression of dioxygen reactivity is favored by the flavoproteins involved in the redox reactions that do not need oxygen, minimizing reactive oxygen species formation.[160] Several factors including charge distribution, protein dynamics,

ligand binding, and solvation effects have been proposed to regulate oxygen reactivity with flavoproteins.[156, 160]

The fully reduced hydroquinone flavin can undergo non-enzymatic oxidation in the presence of molecular oxygen (**Scheme 1.1**).[97] The oxidation of reduced flavin occurs through electron transfer from a singlet reduced flavin to triplet O_2 to form a caged radical pair.[154] Collapse of the radical pair, followed by spin inversion generates the flavin hydroperoxide which can dissociate yielding H_2O_2 and oxidized flavin (**Scheme 1.1**).[97, 154]

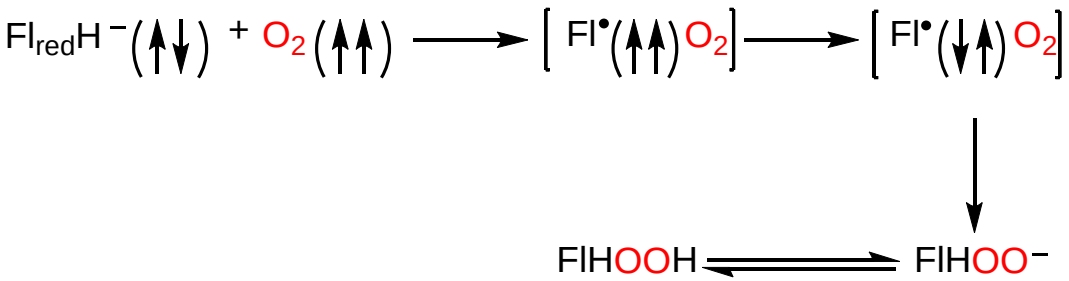

Scheme 1.1: Activation process of oxygen by reduced flavin. (Adapted from [97]).

Flavin monooxygenases form peroxyflavin intermediates which they utilize to insert an oxygen atom in the substrate in the reactions they catalyze.[157-159] The flavin monooxygenases can be flavin-containing or be a part of a two-component flavin-dependent monooxygenase system. The flavin-containing monooxygenases are reduced using pyrimidic substrates (NADH and/or NADPH) whereas the two-component monooxygenase enzymes are supplied with reduced flavin by a flavin reductase (which catalyzes the transfer of reducing equivalents from NAD(P)H (**Figure 1.18**). These flavoproteins accepts a hydride from NAD(P)H, and can donate one or two electrons

to an acceptor. NADPH varies from NADH by an extra phosphate group attached at one of the sugars in NADPH (**Figure 1.18**). The isoalloxazine end of flavin becomes reduced (**Figure 1.19**a), while the nicotinamide end of pyrimidic substrates becomes oxidized (**Figure 1.19**b). The $NADP^+$

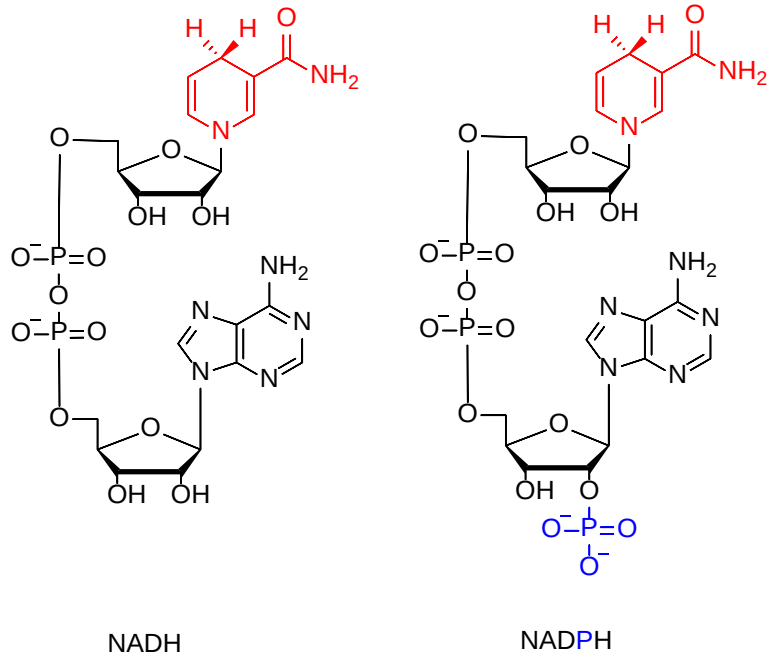

Figure 1.19: The structures of reduced pyridine nucleotides.

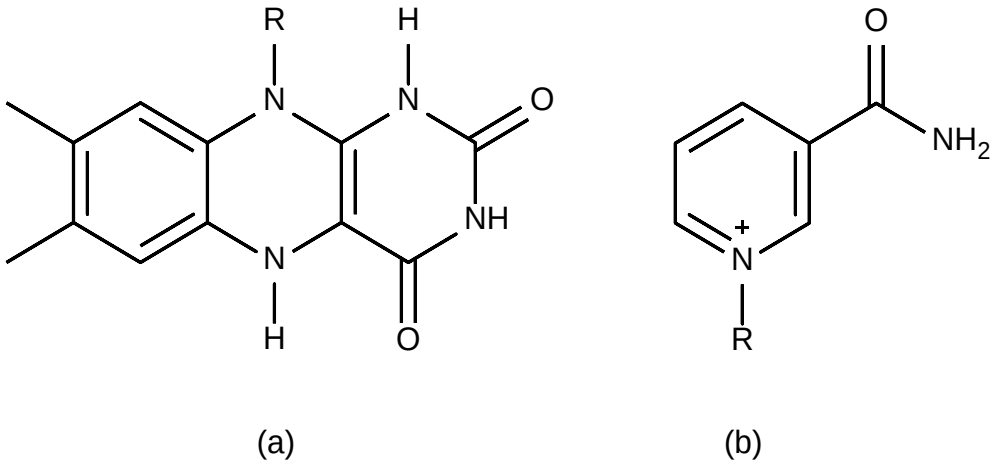

Figure 1.18: Structure of reduced isoalloxazine-end of flavin (a) and the oxidized nicotinamide moiety of pyridine nucleotides (b).

and NAD^+ participate in anabolic redox processes and catabolic metabolism, respectively. The extra phosphate in NADPH is far from the business-end of $NADP^+$ and typically has no influence on electron transfer.[162]

Once the reduced flavin is bound to the monoxygenase enzyme, the flavoprotein uses the reduced flavin to activate O_2 forming the reactive peroxyflavin (Fl-OO^-) or hydroperoxyflavin (Fl-OOH) intermediates (**Figure 1.20**). Flavin monooxygenases have a unique ability to form and stabilize peroxyflavin (Fl-OO^-) or hydroperoxyflavin (Fl-OOH) intermediates depending on the type of reaction they catalyze (**Figure 1.20**). The C4a-hydroperoxyflavin (the oxygenating intermediate) act as an electrophile or nucleophile to insert one oxygen atom into a substrate (**Figure 1.20**).[97, 163] The other atom of the dioxygen is incorporated into water in these flavin-dependent monooxygenase catalyzed reactions.[158] They stabilize C4a-hydroperoxyflavin intermediate and out-competes possible side-reactions which eliminates the wasteful production of reactive oxygen species and minimizes the NAD(P)H oxidase activity.[158]

Flavin monooxygenases forms a quasi-stable C4a(hydro)peroxyflavin, which is considered the activated form of oxygen. The C4a(hydro)peroxyflavin incorporates a single oxygen atom into organic substrates (**Figure 1.20**). The reactions catalyzed by flavin monooxygenases exhibit regio-, chemo-, and stereospecificity which facilitates the synthesis of different compounds.[104, 164-166] Flavin monooxygenases stabilize the C4a-(hydro)peroxyflavin adduct unlike most oxidases which produce hydrogen peroxide without the formation of detectable stable intermediates. Such oxidases would either form an unstable C4a-hydroperoxyflavin forms which rapidly decays, or accepts a second electron (**Figure 1.20**). Structural characterization of monooxygenases and oxidases capable of stabilizing the C4a-hydroperoxyflavin shows that a hydrogen bonding of C4a-(hydro)peroxyflavin at the N5 position is crucial for stabilization.[156] The C4a-(hydro)-

peroxyflavin intermediate in SsuD and in bacterial luciferase have been shown to be stabilized by a conserved cysteine residue.[167-169] In addition, the presence of Arg226 at the active site of SsuD is important in stabilizing the C4a-(hydro)-peroxyflavin intermediate.[170]

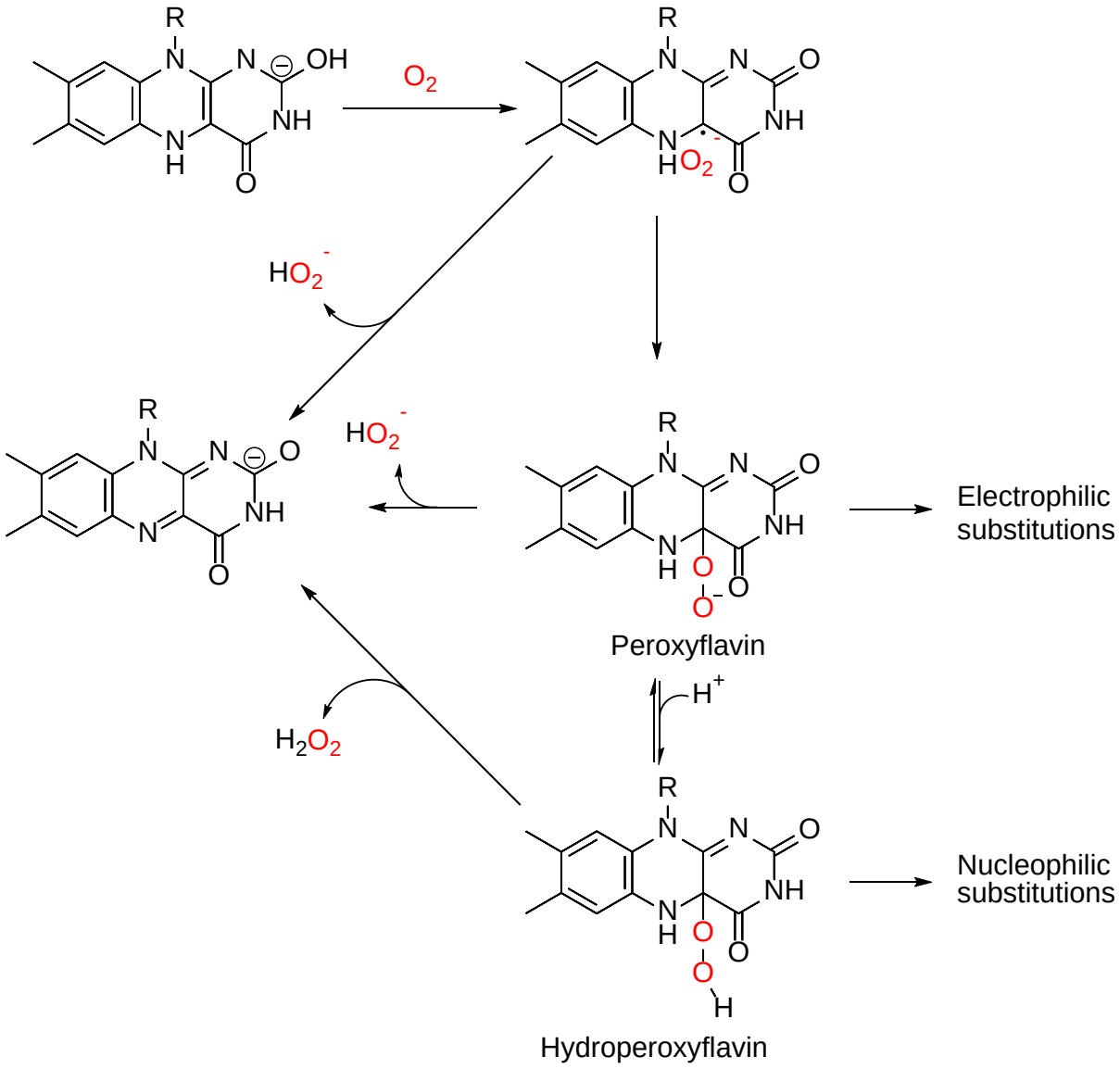

Figure 1.20: Activation of molecular oxygen by reduced flavin. (Adapted from [97, 163]).

1.3 Two-Component Flavin-Dependent Systems

1.3.1 Examples of Two-Component Flavin-Dependent Systems

Flavin-dependent monooxygenases can have flavin bound or utilize flavin as a substrate. The two-component flavin-dependent monooxygenase systems are a group of flavin-dependent enzymes made up of a flavin-reductase (that reduces flavin) and a monooxygenase enzyme, that utilizes the reduced flavin to activate dioxygen and insert an oxygen atom into the substrate(s). The NAD(P)H:flavin reductases are usually smaller in size than the monooxygenases they supply with reduced flavin. The genes coding for both the NAD(P)H:flavin reductase and monooxygenase of two-components system are often located on the same operon. The reductive and oxidative half-reactions are catalyzed by separate enzymes in two-component flavin-dependent monooxygenase systems. The two-component flavin-dependent enzymes catalyze diverse reactions that include the oxidation of environmental aromatic and polycyclic compounds for use as carbon sources, the biosynthesis of antibiotics, bioluminescence, the oxidation of long-chain alkanes, and the desulfurization of sulfonated compounds (**Figure 1.21**).[171] In two-component flavin-dependent monooxygenase systems, the flavin reductase and the monooxygenase enzymes usually have a higher affinity for oxidized flavin and for reduced flavin respectively.[171, 172]

The first two-component flavin-dependent monooxygenase system to be identified was bacterial luciferase.[173-176] Bacterial luciferase uses $FMNH_2$ and oxygen as co-substrates to catalyze the oxidation of a long-chain aldehyde producing a carboxylic acid resulting in the emittance of visible light (**Figure 1.21**). Bacterial luciferase has been utilized in a wide range of applications as a bioreporter and a gene reporter in mammalian cells.[177, 178] Several other two-component monooxygenase systems have since been identified, which catalyze a diverse range of reactions (**Figure 1.21**).

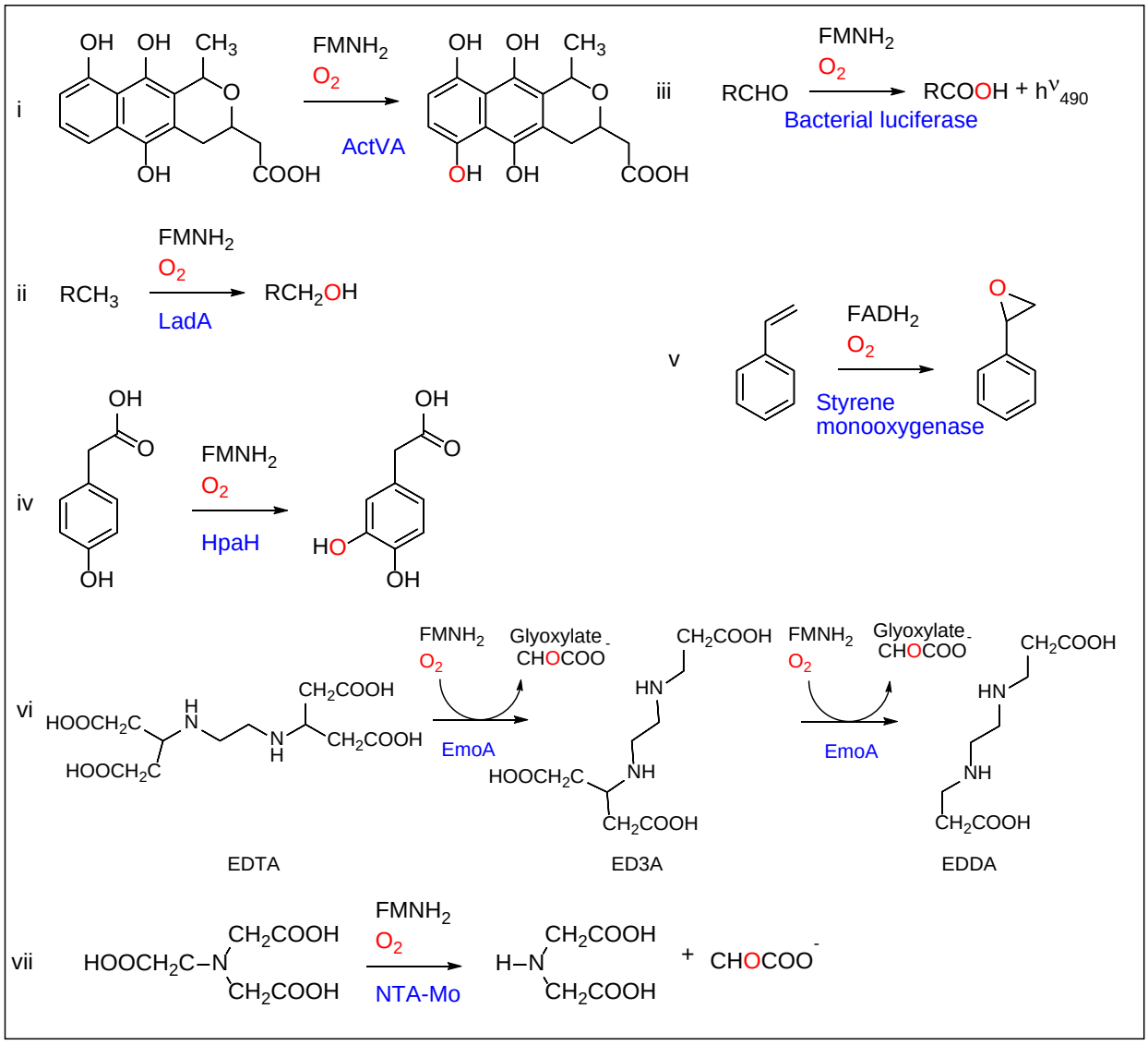

Figure 1.21: Examples of two-component flavin-dependent monooxygenase systems. (Adapted from [171]).

The monooxygenase enzymes utilize reduced FAD or FMN (supplied by flavin reductase) to insert an oxygen into their respective substrates.[171] The nitrilotriacetate (NTA) monooxygenase (NTA-Mo) oxidatively cleaves nitrilotriacetate using reduced flavin supplied by the associated flavin reductase (component B). The NTA-Mo hydroxylates an α-carbon which spontaneously collapses to form iminodiacetate (IDA) and glyoxylate (**Figure 1.21**).[179,180] The ethylene-diamine-

tetra-acetic acid (EDTA) degrading monooxygenase system present in *Mesorhizobium* species catalyzes the $FMNH_2$ dependent oxidation of EDTA to form ethylenediaminetriacetate (ED3A) and glyoxylate. This is followed by further oxidation of ED3A to ethylenediaminediacetate (**Figure 1.21**). The EDTA monooxygenase enzyme (EmoA) can also oxidize NTA and diethylenetriaminepentaacetate (DTPA). EmoA is supplied with reduced $FMNH_2$ by EmoB, the associated flavin reductase.[181, 182]

Several two-component systems involved in bacterial sulfur acquisition have been identified. The two-component alkanesulfonate monooxygenase system catalyzes the $FMNH_2$-dependent oxygenolytic cleavage of C-S bond of various alkanesulfonates into sulfite and the corresponding aldehydes during sulfur scarcity conditions in bacteria (**Figure 1.22**).[57] The

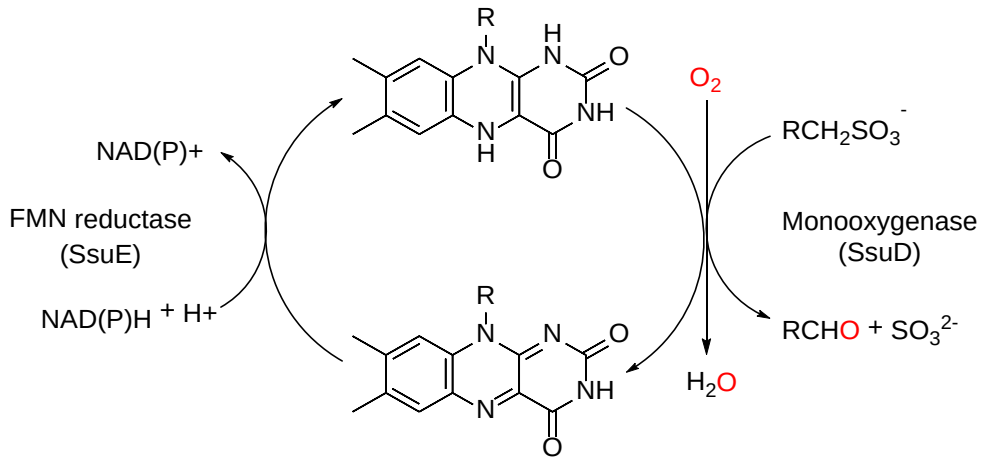

Figure 1.22: The two-component $FMNH_2$-dependent alkanesulfonate monooxygenase system. (Adapted from [61]).

biocatalytic desulfurization of petroleum through 4S-pathway in *Rhodococcus erythropolis* utilizes four enzymes; DszA, DszB, DszC, and DszD, which desulfurizes organosulfur compounds (**Figure 1.23**). The DszD (NADH:FMN oxidoreductase) supplies monooxygenases DszC and

DszA with $FMNH_2$. DszC converts DBT to DBT sulfone while the DBT sulfone is converted into 2'-hydroxybiphenyl-2-sulfinite by DszA. The DszB enzyme catalyzes the final step in desulfurization of DBT by cleaving the C-S bond of 2'-hydroxybiphenyl-2-sulfinate releasing 2-hydroxybiphenyl and sulfite but does not use flavin cofactor.[183-186] The *Rhodococcus erythropolis* strain IGTS8 utilizes alkylated dibenzothiophenes (DBTs) in crude oil as a source of sulfur without degrading the fuel value of the product through the 4S-pathway.[187] Dibenzothiophenes are the largest group of sulfur-containing compounds found in petroleum derivatives underlining the importance of the Dsz system.[188]

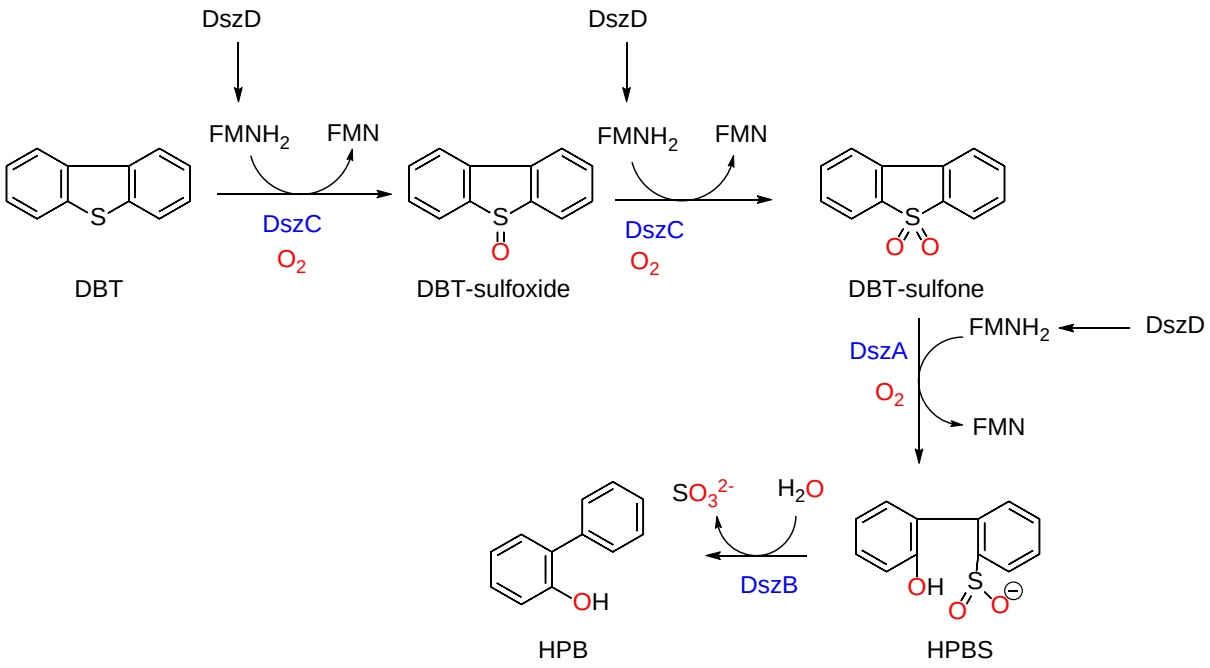

Figure 1.23: The biodesulfurization 4S pathway. DszC and DszD convert DBT to DBT-sulfoxide and then to DBT-sulfone. The conversion of $DBTO_2$ to HBPS is catalyzed by both DszA and DszD. The DszB catalyzes the last step, the conversion of HBPS to HBP. (Revised based on [186]).

Another crucial two-component $FMNH_2$-dependent monooxygenase biocatalytic desulfurization system is found in *P. putida* DS1 which desulfurizes dimethyl sulfide (DMS). The DMS is converted to sulfite through dimethyl sulfoxide (DMSO), dimethyl sulfone ($DMSO_2$), and methanesulfonate (MSA) intermediates (Figure **1.24**). The DMS is oxidized in two successive steps into DMSO and dimethyl sulfone ($DMSO_2$). The $DMSO_2$ is further converted by SfnG ($FMNH_2$-dependent monooxygenase) to methanesulfinate and a molecule of formaldehyde. The methanesulfinate is converted to methanesulfonate (MSA) by a $FMNH_2$-dependent monooxygenase (MsuC). The MSA is desulfonated by MsuD ($FMNH_2$-dependent monooxygenase) releasing sulfite and a molecule of formaldehyde. The $FMNH_2$ for SfnG enzyme is provided by SfnE while for the MsuC and MsuD steps, the $FMNH_2$ is supplied by MsuE (**Figure 1.24**).[163] The unique desulfurization of $DMSO_2$ by the Sfn enzymes is dependent on a transcriptional regulator SfnR.[163]

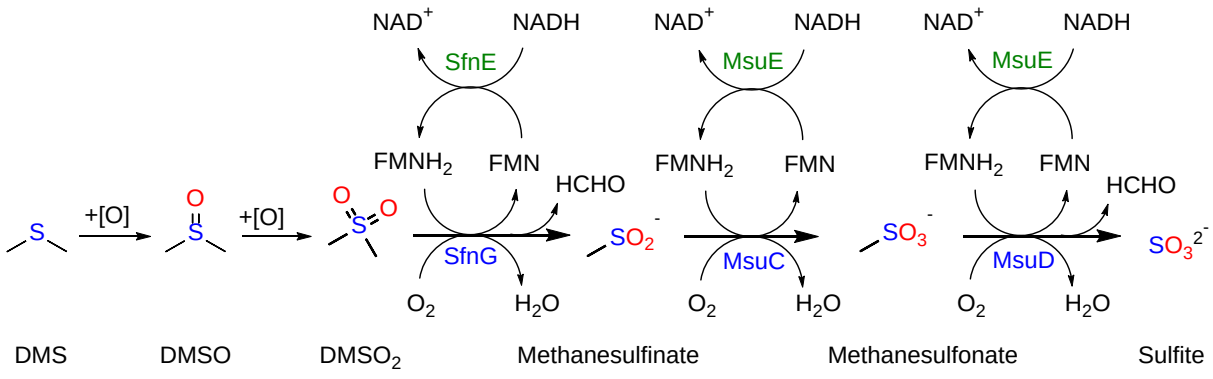

Figure 1.24: Desulfurization pathway of dimethyl sulfide (DMS) in the *Pseudomonas spp*. (that utilize DMS). (Proposed based on information obtained from [91, 163, 189] and Wicht, D.K (personal communication).

1.3.2 Kinetic Analysis of the Flavin Reductases and Monooxygenase of Two-Component Monooxygenase Systems

1.3.2.1 Flavin Reductases of Two-Component Monooxygenase Systems

The flavin reductase enzymes of two-component systems utilize reducing equivalents from pyridine nucleotides to catalyze the reduction of flavin. They have a substrate specificity for either FAD or FMN, and can have a preference for NADH and NADPH, or can utilize both NADH and NADPH with similar efficiencies.[190] Because the flavin reductases of two-component systems supply the associated monooxygenase with reduced flavin, the flavin preference is observed in both the flavin reductase and monooxygenase enzymes. Flavin reductases either have oxidized flavin tightly bound and manifest a signature spectrum for oxidized flavin or are flavin-free as purified and utilize flavin as a substrate during catalysis.[2, 57, 171] Despite the numerous structural studies and biochemical analyses on flavodoxin and flavodoxin-like domains, the chemistry behind flavin binding and the process of electron transfer remains unclear.[191]

The mechanism of two-component flavin reductases vary depending on whether flavin is tightly bound or utilized as a substrate. Some flavin reductases with a tightly bound flavin follow a ping-pong mechanism during flavin reduction (**Figure 1.25**). The bound flavin is reduced by NAD(P)H followed by the release of oxidized pyridine nucleotide. A second free flavin docks and is reduced by the primary reduced bound flavin.[172, 192] The flavin reductases with no bound flavin follow an ordered-sequential kinetic mechanism in which either the flavin or pyridine nucleotide binds first to the flavin reductase (**Figure 1.26**). In an ordered sequential mechanism, a ternary complex must be formed for the flavin reduction to occur. After flavin reduction, the oxidized $NAD(P)^+$ or the reduced flavin is released and the other product follows.[57, 192, 193]

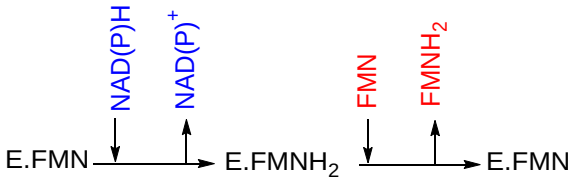

Figure 1.25: Flavin reductases with tightly bound flavin tend to follow a ping-pong kinetic mechanism. (Adapted from [171])

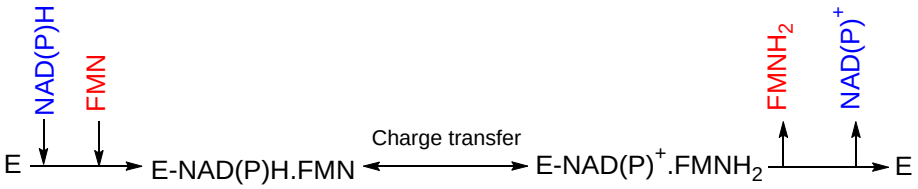

Figure 1.26: Flavin reductases with no bound flavin utilize flavin as substrate and follows an ordered sequential kinetic mechanism. SsuE uses FMN as a substrate and follows an ordered sequential kinetic mechanism. (Adapted from [171]).

The kinetic mechanisms followed by flavin reductases of two-component systems can vary depending on flavin concentration and the availability of the monooxygenase enzyme.[62] The SsuE enzyme has no flavin bound as purified, and utilizes flavin as a substrate. The SsuE enzyme had a higher catalytic efficiency with FMN compared to FAD suggesting it has a preference for FMN as a substrate but can use either NADH or NADPH as the reductant.[2, 57, 171] The SsuE enzyme also has a tighter binding affinity (1000-fold) for oxidized FMN over the reduced flavin which facilitates product release.[2, 61] The reduction of FMN by SsuE is achieved through an ordered

sequential kinetic mechanism in which NADPH binds first, followed by FMN resulting in the formation of a ternary complex. Following charge transfer, product release also occurs sequentially with $NAD(P)^+$ being the last to be released. The rate-determining step (hydride transfer from NAD(P)H to FMN) occurs after the ternary complex is formed.[2]

The SsuE enzyme is tasked with supplying SsuD with $FMNH_2$, for SsuD to cleave the C-S bond in various alkanesulfonates yielding sulfite.[57] When SsuD was included in SsuE flavin reductase assays, the steady-state kinetic parameters did not change.[2] The kinetic parameters for SsuE changed in the presence of both SsuD and octanesulfonate, adopting an equilibrium-ordered kinetic mechanism. The results from these studies suggested that substrate NAD(P)H, and product $NAD(P)^+$ were in equilibrium with the free SsuE enzyme. As such, the flavin reduction by SsuE was independent of NADPH and the equilibrium was oriented to the formation ternary complex. The K_m value for SsuE in single-enzyme assays was comparable to the K_d value in flavin titrations with SsuE implying that the K_m value for FMN by SsuE represented the dissociation constant. The inclusion of SsuD and octanesulfonate in the SsuE flavin reductase assay resulted in a 10-fold increase in K_m value for FMN which suggested a decrease in FMN binding affinity by SsuE in presence of SsuD.[2, 194] The weak FMN binding in the presence of SsuD would be strategic in ensuring productive flavin transfer from SsuE to SsuD once flavin reduction takes place. The mechanistic change to a rapid equilibrium mechanism by SsuE orients the reaction to form the ternary complex and ultimately facilitates flavin transfer. The observed kinetic mechanistic behavior coupled with an increase in the K_m value for FMN by SsuE (in the presence of SsuD and alkanesulfonates) facilitates flavin exchange between SsuE and SsuD.[2, 194]

A charge-transfer complex between the pyridine nucleotide and the flavin is characterized spectrally by a broad peak from 550 and 800 nm.[195-198] Such a peak is also observed in flavin

reductases that utilize flavins as substrate.[199] Rapid reaction kinetic studies of flavin reduction by SsuE at 450 and 550 nm showed three phases associated with distinct steps involved in flavin reduction.[200] After substrate binding, the initial phase occurs which involves the generation of the initial charge-transfer complex (CT-1) between FMN and NADPH with a rate constant (k_1) of 241 s^{-1} (**Scheme 1.2**). The second phase leads to the charge-transfer complex (CT-2) between reduced flavin and the $NADP^+$ with a rate constant (k_2) of 11 s^{-1}. The transition step of CT-1 to CT-2 is associated with a hydride transfer from NADPH to FMN. The final phase in flavin reduction entails the conversion of CT-2 to the Michaelis complex (MC-2) of SsuE (which contains bound products) with a rate constant (k_3) of 19 s^{-1}. Hydride transfer to FMN from NADPH is the rate-limiting step in flavin reduction as supported by isotope studies with [4(R)-^{2}H] NADPH.[200]

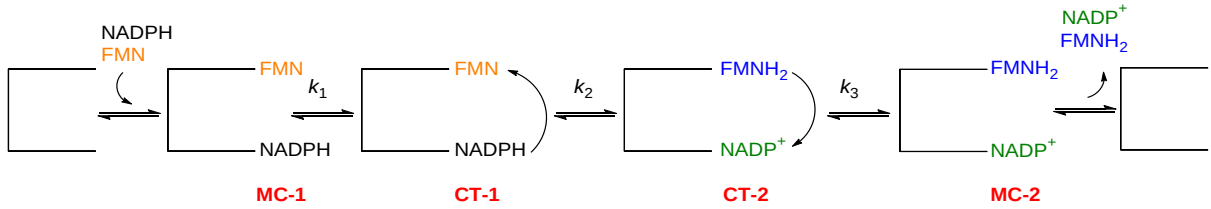

Scheme 1.2 Formation of charge–transfer complex in FMN reduction by SsuE. (Adapted from [200]).

At elevated flavin concentrations, hydride transfer was inhibited with SsuE suggesting the step was rate-limiting. The charge-transfer complex observed in SsuE was weaker than that of flavin reductases with tightly bound flavin. This correlates with weak flavin binding at the active site of flavin-free flavin reductases. An effective flavin reductase in a two-component system should catalyze flavin reduction while promoting subsequent transfer. A flavin reductase with tightly bound flavin would hinder effective flavin transfer.[194] The sequential-ordered kinetic

mechanism by SsuE changed to a rapid equilibrium-ordered mechanism when SsuD and octanesulfonate are included, suggesting that protein-protein association between SsuE and SsuD alters the kinetics of SsuE.[2]

The kinetic mechanism of flavin reductases might alternate between sequential and ping-pong depending on flavin concentration and availability of the intended monooxygenase enzyme.[62] A general kinetic mechanism was proposed for flavin reductases in the flavodoxin-like superfamily based on experimental data and three-dimensional studies on SsuE, EmoB and other NAD(P)H:FMN reductases (**Figure 1.27**).[62] For flavin-free flavin reductases which follow a ping-pong mechanism, one FMN binds tightly and acts as a prosthetic group (**Figure 1.27** reaction 1). The bound flavin is reduced (**Figure 1.27** steps 2) and a second FMN binds weakly, and is reduced by the primary reduced flavin (**Figure 1.27** step 3) followed by product release. The flavin-free flavin reductases which follow sequential-ordered kinetic mechanism binds FMN follows steps 1, 2, and then 4. Flavin reductases with tightly bound flavin usually follows a ping-pong kinetic mechanism involving steps 2 and 3. The kinetic mechanism followed by NADPH-dependent FMN reductases in the flavodoxin-like superfamily may also vary depending on cellular flavin concentrations.[62]

FMN reductases can be classified into ferredoxin reductases, nitroreductases and flavodoxin-like superfamilies based on the SCOP database.[62] The flavin reductases of ferredoxin reductase and nitroreductase superfamilies follow a similar catalytic mechanism.[62, 171] Of the FMN reductases in the flavodoxin-like superfamily, only SsuE and EmoB have been characterized, both of which portray distinct kinetic mechanisms.[62, 171] The NADH:flavin reductase (EmoB) follows a ping-pong kinetic mechanism although it is flavin-free as purified (**Figure 1.25**).[172] EmoB is the FMN reductase of a two-component system (associated with EmoA) involved in EDTA

degradation. The three-dimensional structure of EmoB has two-stacked FMN molecules. One FMN is tightly bound to EmoB and acts as a cofactor, while the second FMN binds loosely and NADH reduces it. The EmoB redox processes occur on the second loosely stacked FMN.[62, 172] Recent studies suggested the tightly bound $FMNH_2$ in EmoB could be transferred to EmoA through direct channeling involving protein–protein interactions.[201]

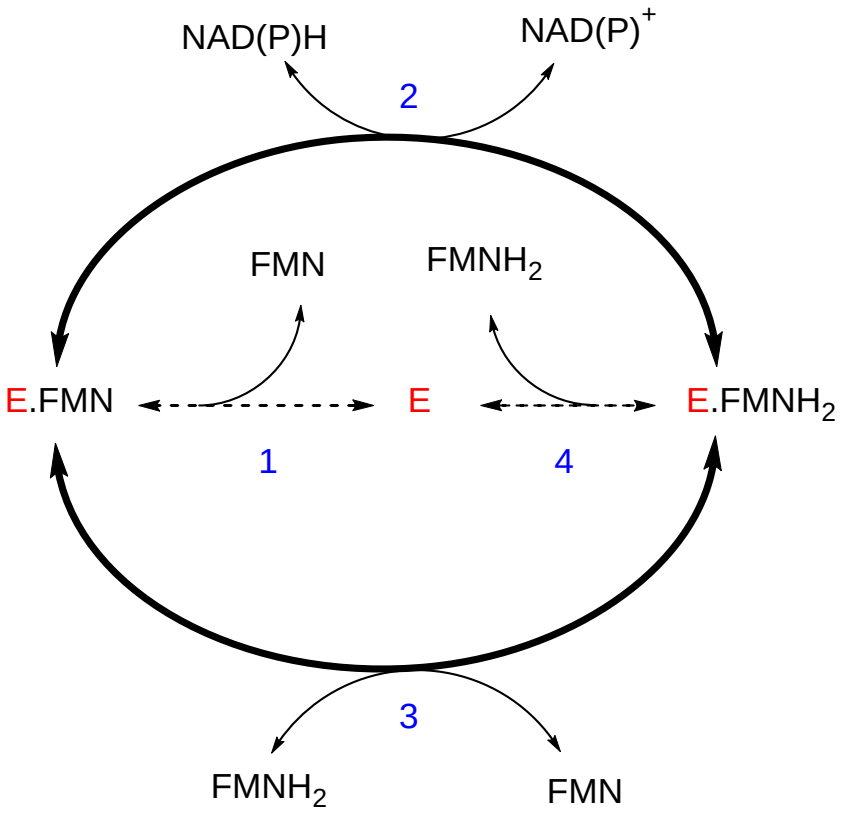

Figure 1.27: Proposed kinetic mechanism for flavin reductases in the flavodoxin-like superfamily. Replace FMN with FAD for flavin reductases that utilize FAD as substrate. (Adapted from [62]).

1.3.2.2 Monooxygenase of Two-Component Monooxygenase Systems

Flavin-dependent monooxygenases of two-component monooxygenase systems catalyze a range of reactions which entails oxidation of the corresponding substrates.[171] In the alkanesulfonate monooxygenase system, the SsuD enzyme catalyzes the $FMNH_2$-dependent oxygenolytic cleavage of the C-S bond of various alkanesulfonates as an alternative sulfur source during sulfur limiting conditions (**Figure 1.10**).[57] The SsuD enzyme binds reduced flavin supplied by SsuE, and activates dioxygen to form the C4a-(hydro)peroxyflavin intermediate that cleaves alkanesulfonates releasing a molecule of sulfite, the corresponding aldehyde, FMN, and water.[57, 170, 194]

The desulfonation reaction by SsuD could occur either through the formation of a C4a-peroxyflavin (Fl-OO^-), or through a C4a-hydroperoxyflavin (Fl-OOH) intermediate. In the C4a-peroxyflavin (Fl-OO^-) mechanism (**Figure 1.28**, peroxyflavin intermediate route I through V), the reduced flavin activates O_2 to form a peroxyflavin intermediate. The peroxyflavin intermediate attacks the sulfur atom of the alkanesulfonate generating a peroxyflavin-organosulfonate adduct (**Figure 1.28**, peroxyflavin intermediate route step III). The peroxyflavin-organosulfonate adduct undergoes a Baeyer–Villiger rearrangement releasing sulfite and a peroxyalkane intermediate. An abstraction of a proton by an active site base from the C1 of the alkane side of the adduct results in heterolytic cleavage of the O-O bond of the alkane-flavin adduct, to release the corresponding aldehyde, and the C4a-hydroxyflavin (**Figure 1.28**, hydroperoxyflavin intermediate route step IV).[194]In the mechanism involving C4a-hydroperoxyflavin (Fl-OOH) intermediate, the reduced flavin activates O_2 to form a C4a-hydroperoxyflavin intermediate. An abstraction of a proton from C1 of the alkanesulfonate by an active site base generates a carbanion intermediate, which carries

a nucleophile attack on the hydroperoxyflavin resulting to an unstable 1-hydroxyalkanesulfonate. The 1-hydroxyalkanesulfonate then collapses producing the corresponding aldehyde and sulfite (**Figure 1.28**, hydroperoxyflavin intermediate route I through IV).[194] The sulfite product of desulfonation by SsuD is incorporated into sulfur-containing biomolecules alleviating the sulfur scarcity in bacterial systems.[57, 170, 194] The other products of the desulfonation reaction are the

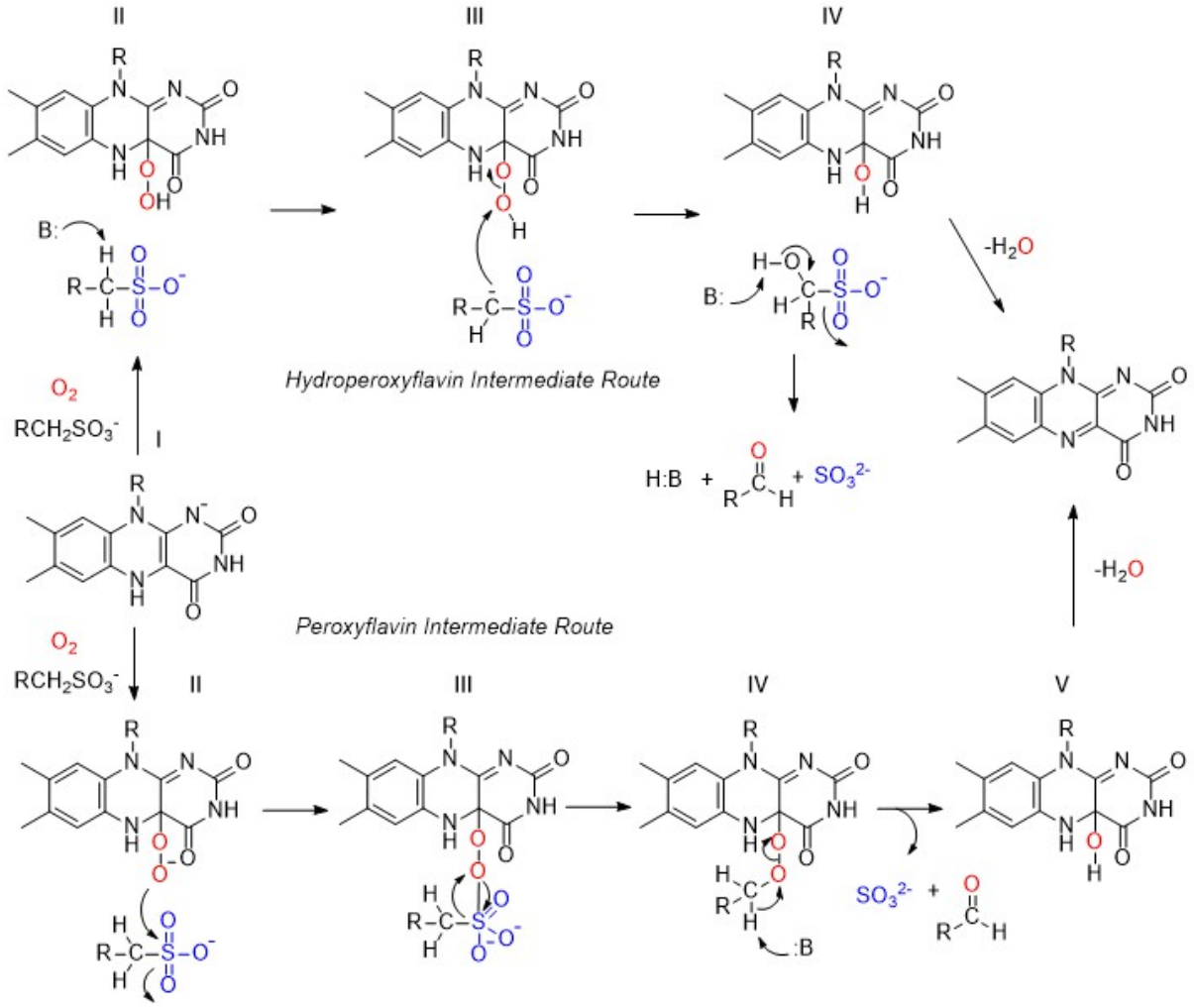

Figure 1.28: Proposed mechanism of alkanesulfonate desulfonation by SsuD. The desulfonation reaction by SsuD could occur through the formation of a C4a-peroxyflavin (Fl-OO) or C4a-hydroperoxyflavin (Fl-OOH) intermediate. (Adapted from [189, 194]).

corresponding aldehydes, FMN, and water.[57, 170, 194] Accumulation of aldehydes in bacteria may result in cellular toxicity. The aldehyde product can be metabolized as a source of carbon and energy, or be utilized in the synthesis of biomolecules, alcohol and fatty acids.[55, 202, 203]

1.3.3 Structural Properties of the Two-Component Flavin-Dependent Enzymes

1.3.3.1 Structural Properties of the NAD(P)H:FMN Reductases of Two-Component Flavin Monooxygenase Systems

The structure of the NAD(P)H:FMN reductases of two-component flavin monooxygenase systems have a flavodoxin fold. The flavodoxin fold is composed of five parallel, centrally located β-strands flanked by α-helices (**Figure 1.29**). The flavin reductases of two-component

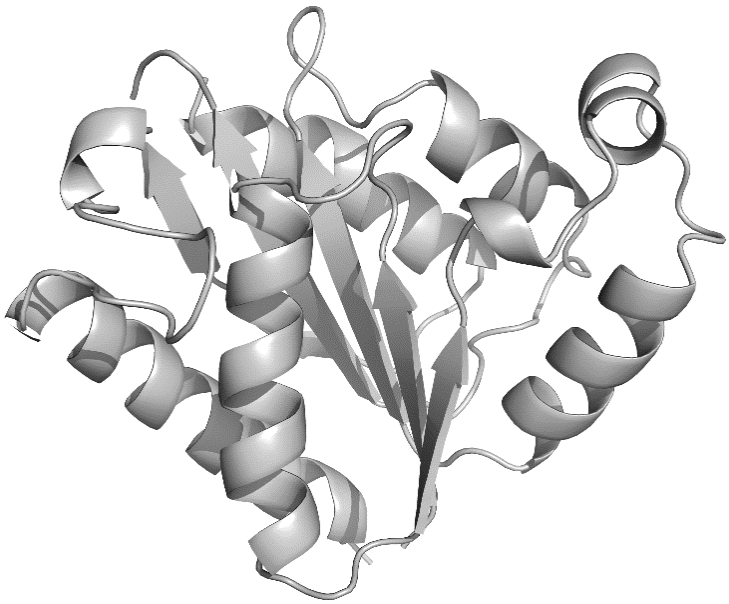

Figure 1.29: The NAD(P)H:FMN reductases of two-component flavin monooxygenase systems have a flavodoxin fold. SsuE has the β-strands arranged in the order 21345 and flanked by α-helices. The α2A and α2B helices occur between β1 and β2.

monooxygenase systems are members of the NAD(P)H:flavin reductase family which have the conserved classical flavodoxin sequence (T/S)XRXXSX(T/S). This motif facilitates FMN binding through hydrogen bond formation with the phosphate group of FMN.[62, 204, 205] The SsuE enzyme belongs to the flavodoxin-like superfamily and has a flavodoxin motif (SPRFPSRS) from residue 8 to 15, while EmoB has a corresponding amino acid sequence (SPSRNSTT) from residue 11 to 18.[172] Interestingly, the SsuE enzyme being a sulfur scavenging flavin reductase contains no cysteine residues and has only one methionine (**Figure 1.30**). Protein evolutionary studies between the flavodoxin-like folds and the $(\beta\alpha)_8$-barrel suggests that these two folds might have originated from a common ancestor.[206] This could help trace the evolutionary development of two-component flavin monooxygenase systems. The structural properties of flavin reductases of two-component flavin monooxygenase systems remain largely underexplored. Only a few three-dimensional structures of flavin reductases of two-component monooxygenase systems have been resolved which include EmoB, MsuE, 3k1y and SsuE.

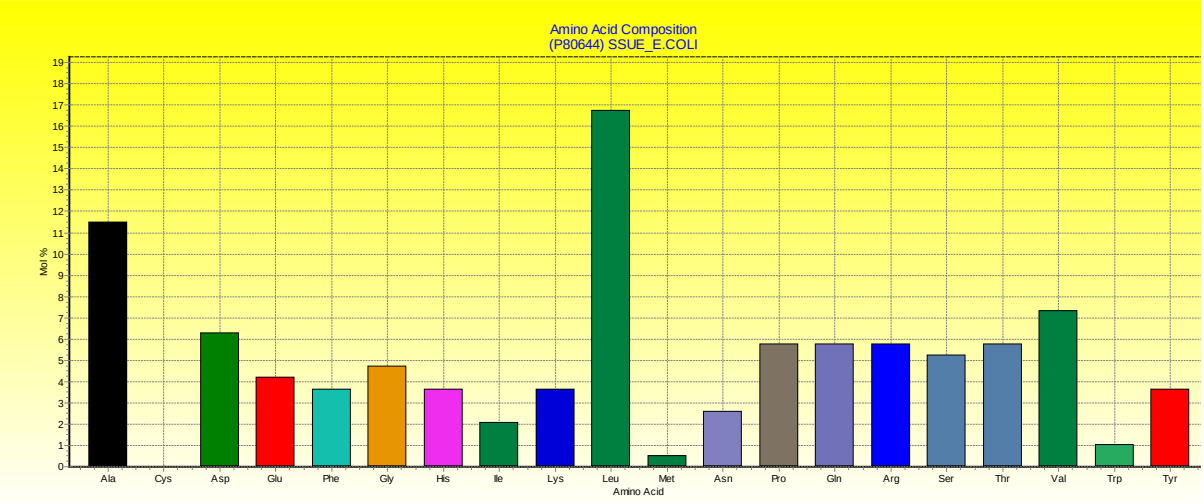

Figure 1.30: Amino acid composition of SsuE (P80644) from *E. coli* (191 amino acids and Molecular Weight, 21252.13 Daltons).

The three-dimensional structure of SsuE was solved by molecular replacement of the EmoB crystal structure which has 37% sequence similarity to SsuE. The three-dimensional structure of apo-SsuE, FMN-bound SsuE, and $FMNH_2$-bound SsuE are tetramers with a 222 symmetry.[62] The SsuE enzyme has the β-strands arranged in the order 21345 and are flanked by α-helices (**Figure 1.30**). The α2A and α2B helices occur between β1 and β2.[62] The overall structure was described using the FMN-bound form of SsuE which had a resolution of 1.9Å. The tetramer of SsuE is a dimer of dimers (**Figure 1.31**) chain A through D. It shows one well-ordered bound FMN in each monomer which is located in a similar position to the FMN in other flavodoxins. Chains B and D have a second bound FMN, which is less ordered.[62] Several residues position the FMN in the active site of SsuE (**Figure 1.32**). The Ser residues 8, 13, and 15 and Arg10 coordinates the phosphate group of FMN in the three-dimensional structure of SsuE (**Figure 1.32**).[62, 204]

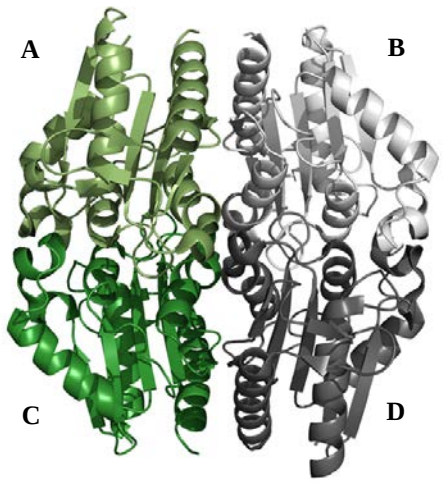

SsuE Tetramer

Figure 1.31: The tetramer of SsuE (dimer of dimers).

Conformational changes of SsuE based on different oxidation states of flavin ($FMNH_2$ and FMN) were investigated. The crystals of SsuE showed a weaker electron density for the bound $FMNH_2$ (product) as compared to FMN (substrate).[62] Previous results have shown that SsuE has 1000-fold higher affinity for FMN compared to SsuD. The affinity is reduced 10-fold when FAD is utilized with SsuE.[2] The reduction of FMN weakens SsuE FMN binding because the $FMNH_2$ SsuE would be in the product release mode. The reduction of the FMN-bound SsuE resulted in

one flavin bound to chains A, C, and D, with chain B having no $FMNH_2$ bound. The $FMNH_2$ are weakly bound culminating in a conformational shift in Arg10.[62]

The three-dimensional studies which showed SsuE existed as a tetramer contradicts with the initial characterization in which SsuE was reported as a dimer.[12, 75] The three-dimensional structure of flavin-bound SsuE was obtained by soaking preset SsuE crystals (tetramer) in flavin

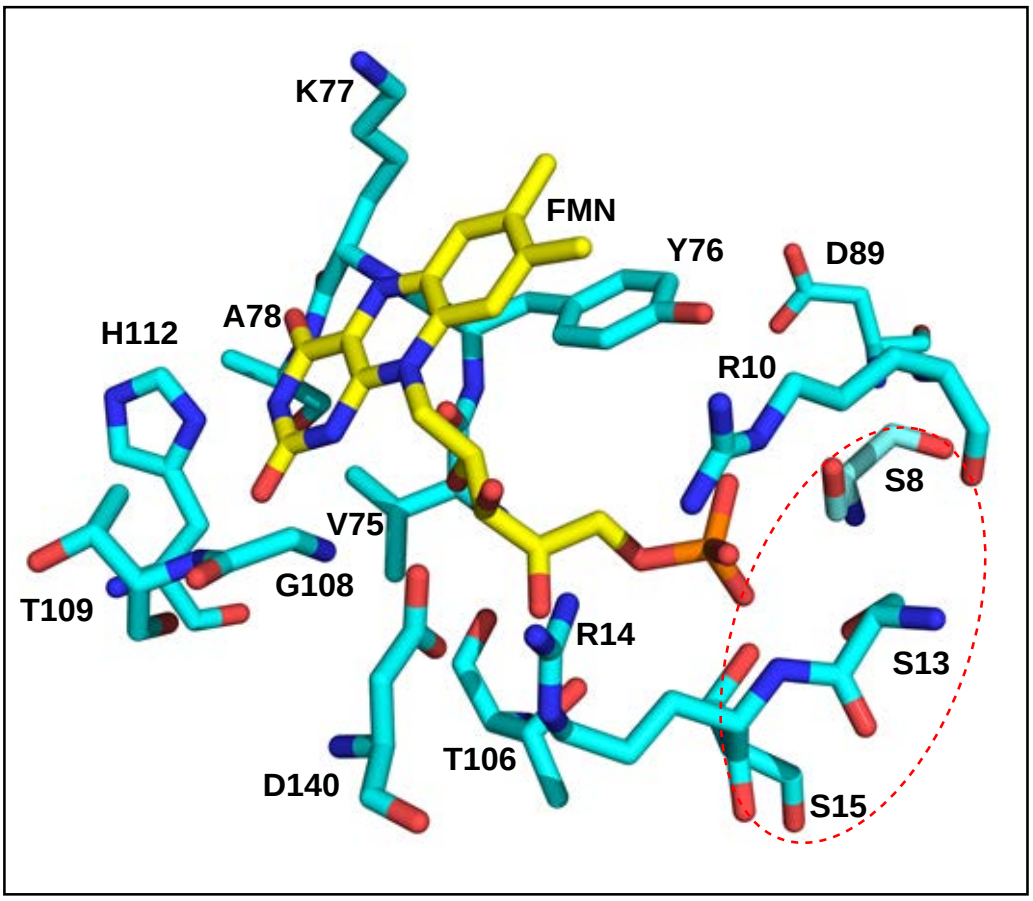

Figure 1.32: Active site of SsuE showing residues that position FMN in the active site. The Ser residues 8, 13, and 15 (highlighted in red) and Arg10 coordinates the phosphate group of FMN in three-dimensional structure in SsuE.

which is thought to have forced the oligomeric state of FMN-bound SsuE to be a tetramer. In addition, previous studies also showed that SsuE binds one FMN per monomer but some monomers had of SsuE had two FMN bound in the three-dimensional structure. However, the flavin bound SsuE structure was solved using two-fold stoichiometric levels of flavin.[57, 62] This could be the reason that two FMN were bound in some monomers of SsuE. In addition, preformed crystals of SsuE were soaked in FMN solution. High concentrations of FMN usually leads to SsuE inhibition. Because contradicting oligomeric states were reported with SsuE, sedimentation velocity studies were performed to investigate the oligomeric form of SsuE in solution in the presence and absence of FMN. The apo-SsuE was shown to exist as a tetramer while the FMN-bound SsuE was a dimer suggesting that a tetramer-dimer equilibrium may exist with SsuE that is flavin-dependent.[62]

Comparative studies show that the flavin reductases of two-component monooxygenase systems (EmoB, SsuE, 3k1y) have a π-helix centrally located at the tetramer interface (**Figure 1.33**).[62] π-Helices result from mutations that insert a single residue in an established α-helix to create 5 amino acids per turn (rather than 4 amino acids per turn) and a bulge at the point of insertion. The presence of π-helices is the result of protein evolution and is associated with a gain or enhancement of function. The π-helices are generally conserved within functionally-related proteins and can be used as markers for evaluating evolutionary relationships as well as identifying unique functions associated with protein families.[207, 208]

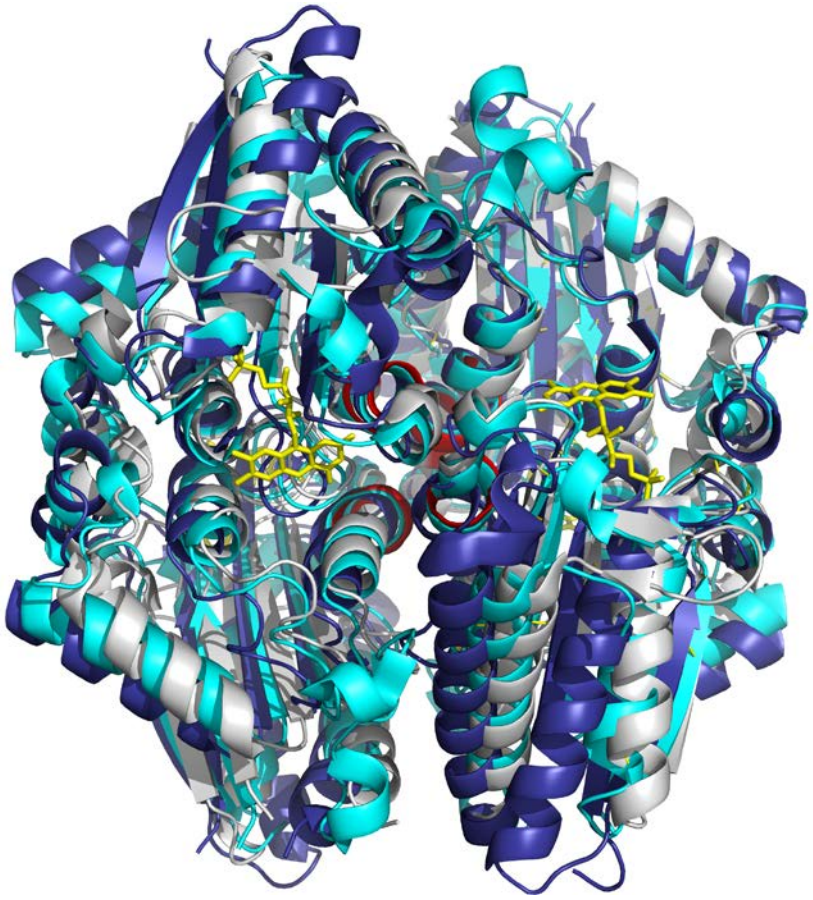

Figure 1.33: Structural alignment of the flavin reductases of two-component monooxygenase systems that contain π-helices. EmoB (Cyan), SsuE (Grey), and 3k1y (Blue) have the π-helix centrally located at the tetramer interface, and is highlighted in red for SsuE.

1.3.3.2 Structure of Monooxygenase Enzymes of the Bacterial Luciferase Family

Some of the two-component flavin monooxygenase enzymes belong to the bacterial luciferase family. Enzymes within this family have a triosephosphate isomerase (TIM)-barrel fold, which have a characteristic eight alternate α-helices and eight parallel β-strands that fold to form a doughnut-like protein fold (**Figure 1.34**). TIM-barrel proteins also have the active site residues positioned at the C-terminal end of the β-barrel.[209-213] None of the monooxygenases in the luciferase family have reduced flavin-bound in the resolved three-dimensional structures. Substrate binding has been shown to induce conformational changes in both bacterial luciferase and SsuD. This poses a challenge in understanding the catalytic events in these monooxygenases,

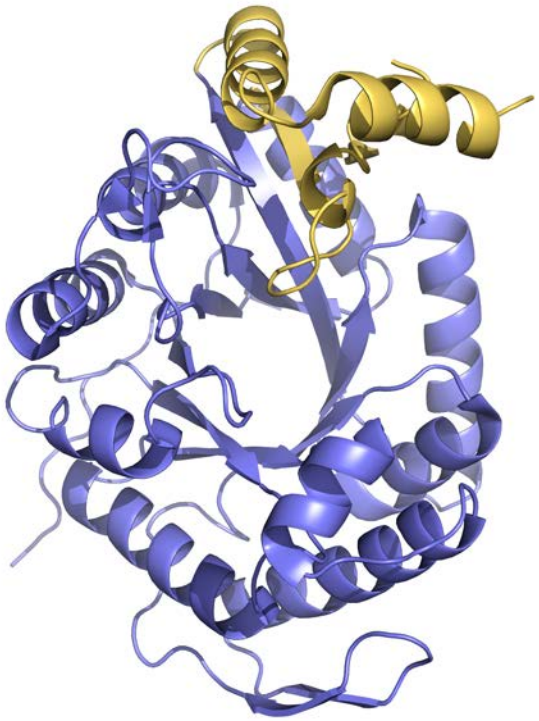

Figure 1.34: TIM-Barrel fold in SsuD, characterized by eight alternate α-helices and eight parallel β-strands that fold to form a doughnut-like protein fold. The unresolved loop in SsuD is part of the insertion region from Glu233 to Asp307 (highlighted in brown).

because the spatial arrangement of active site residues may be different during catalysis from those shown in the flavin-bound three-dimensional structures. LuxAB and LadA are the only members with oxidized FMN bound in the three-dimensional structure.[2, 61, 167, 170, 171, 209, 214-217] The SsuD enzymes belong to the bacterial luciferase family but diverges from the classical TIM-barrel structure by the presence of several discrete insertion regions. One such insertion at the putative active site of SsuD is largely unresolved in the three-dimensional structure, and has been associated with conformational changes in this region.[211, 218] This disordered loop region is conserved in all SsuD homologs, and has been proposed to close over the active site.[61, 218] Flexible loops in TIM-barrel proteins contribute to the dynamics of the enzyme active site and in substrate binding. During catalysis, loop closure over the active site protects the substrate and intermediates from bulk solvent.[219-221]

Several approaches have been employed to unravel the role of the flexible loop in SsuD. The Arg297 residue located in the loop region of SsuD is highly conserved and contributes to catalysis. Generation of R297C and R297A SsuD variants showed no desulfonation activity, but the R297K SsuD had a 4-fold decrease in the k_{cat}/K_m value compared to wild type SsuD.[216] Molecular simulations on the loop region in SsuD (residues 250–282) showed the loop region to be highly mobile when both C(4a)-peroxyflavin intermediate ($FMNOO^-$) and octanesulfonate were bound to SsuD.[222] This mobile loop was suggested to facilitate the transfer of reduced flavin from SsuE to SsuD.[61, 220, 222] Partial deletions of the loop region in SsuD did not affect the binding affinity for reduced flavin or result in overall changes to the protein secondary structure.[218] However, the resultant SsuD variants were unable to desulfonate alkanesulfonates suggesting that a lid-gating conformational change could not be achieved for catalysis.[218] Unproductive oxidation of reduced flavin was observed with the SsuD deletion variants suggesting the flexible loop

protects reduced flavin from unproductive oxidation. The studies on SsuD also associated the flexible loop to assisting in the transfer of reduced flavin from SsuE to SsuD.[218]

Although the monooxygenases of the luciferase family are structural homologs, they share low sequence identity. They have several conserved amino acid residues that are vital for enzymatic activity.[57, 209-212, 214, 223-227] For instance, SsuD from *E. coli* shares 15% and 16% sequence identity with *V. harveyi* LuxAB and *Geobacillus thermodenitrificans* LadA respectively, although their active sites have conserved amino acid residues that are responsible for flavin binding and catalysis.[57, 210, 211] Several catalytically relevant amino acid residues have been

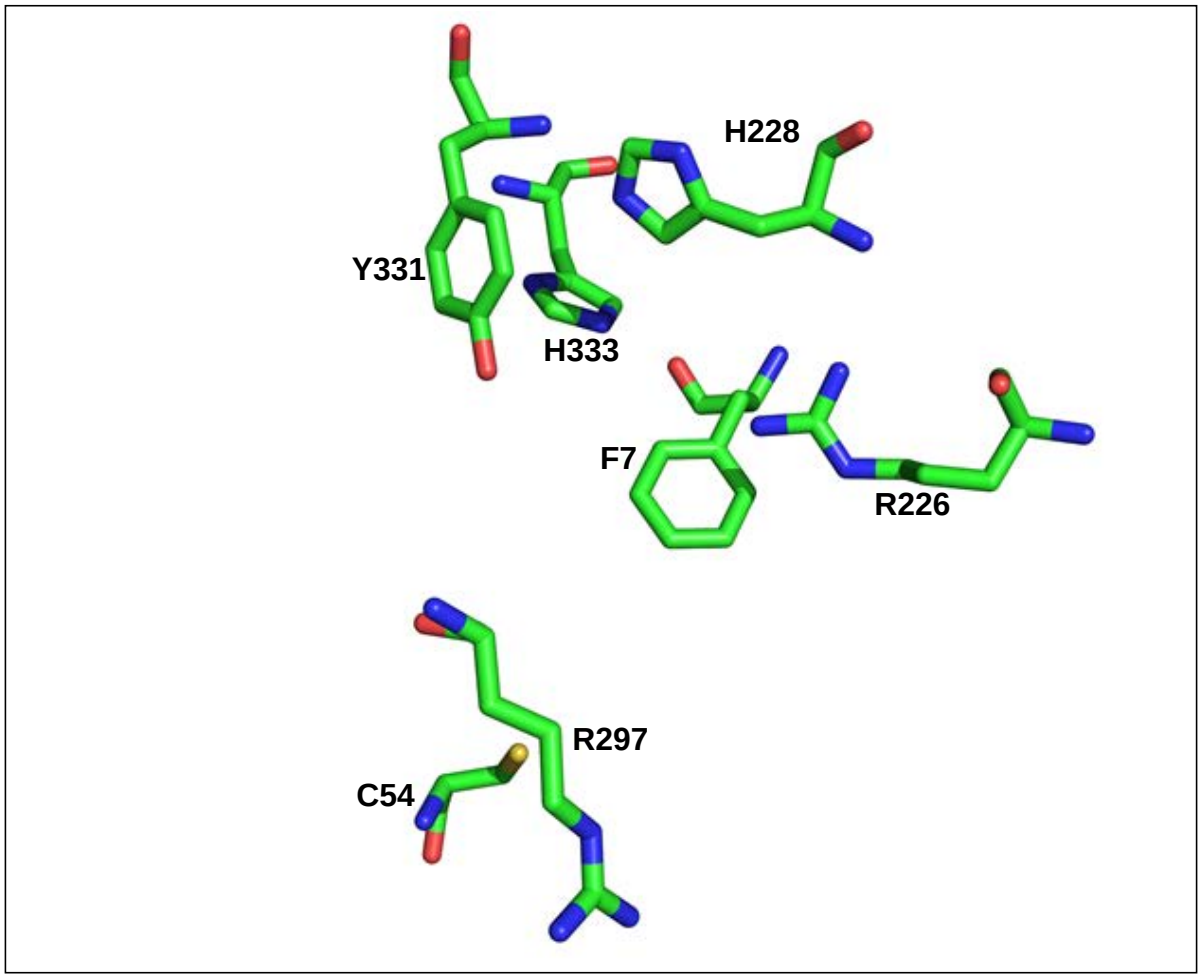

Figure 1.35: The active site residues in SsuD.

identified in the active site of SsuD which include Cys54, Arg226, His228 and His333, all of which are conserved in the bacterial luciferase family (**Figure 1.35**).[2, 61, 167, 170, 171, 215-217]

1.3.3.3 Mechanism of Reduced Flavin Transfer in Two-Component Flavin-Dependent Monooxygenase Systems

The flavin reduction step is vital in a two-component system, and the subsequent reduced flavin transfer step is essential for the monooxygenase-catalyzed reaction to occur. Reduced flavin is highly unstable and is oxidized when exposed to dioxygen forming reactive oxygen species (mainly hydrogen peroxide and superoxide radicals). Understanding how two-component system enzymes counters the unstable nature of reduced flavin preventing non-enzymatic oxidation is rather critical. Free diffusion, direct channeling mechanisms, or both mechanism have been proposed as the modes of reduced flavin transfer from flavin reductases to the oxygenases in two-component systems (**Figure 1.36**). In free diffusion, the flavin reductase does not come into contact with the monooxygenase during flavin transfer, and the reduced flavin reaches the monooxygenase by diffusing through bulk solution (**Figure 1.36**a).[157, 228, 229] Free diffusion is non-specific, energetically expensive (because any potential recipient can bind the reduced flavin), and may undergo autoxidation generating reactive oxygen species. In the two-component system involved in EDTA degradation in *Mesorhizobium* sp. BNC1, initial studies suggested reduced flavin diffuses from EmoB to the associated monooxygenase, EmoA (**Figure 1.36**a). Although EmoB is flavin free, the three-dimensional structure shows one tightly bound FMN, and a second FMN bound that is loosely stacked on the tightly bound flavin. The loosely bound flavin diffuses to EmoB (in *Mesorhizobium* sp. BNC1) upon reduction.[62, 172] However, protein-protein interactions were recently identified between EmoB and EmoA (in *Chelativorans* sp. BNC1) through isothermal titration calorimetry, molecular docking, and kinetic assays suggesting that

a) Reduced flavin transfer by free diffusion (dissociative mechanism)

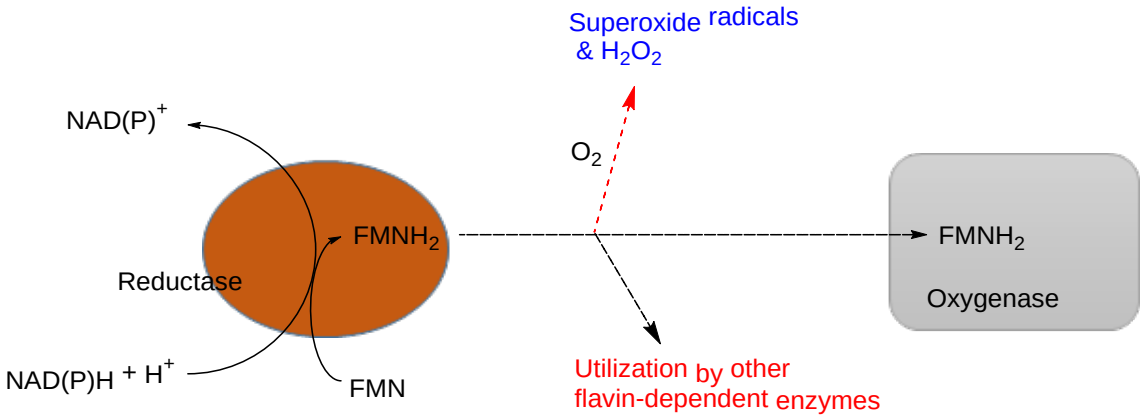

b) Direct transfer of reduced flavin involves SsuE-SsuD interaction (channeling mechanism)

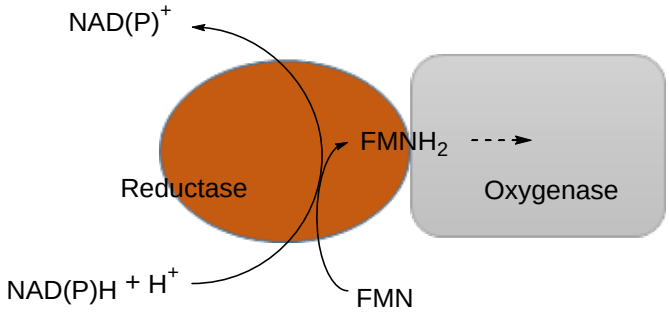

Figure 1.36: Mechanisms of reduced flavin transfer in two-component monooxygenase enzyme systems.

channeling of reduced flavin from EmoB to EmoA was the likely mode of flavin transfer.[201] Reduced flavin was transferred from EmoB to EmoA through diffusion when a membrane that impeded physical interaction between EmoA and EmoB was utilized resulted into slow rate of EDTA monooxygenation. However, the EmoA had a faster turnover when in physical contact with EmoB suggesting a channeling mechanism of reduced flavin transfer was more favorable in the EDTA degradation system.[201] For channeling of reduced flavin to occur, the flavin reductase has to interact with the monooxygenase enzyme in the right orientation (**Figure 1.36**b). Specific protein-protein interaction regions must be available for the two enzymes to associate. A direct channeling mechanism is energetically inexpensive and prevents the formation of reactive oxygen species.[215, 229]

Several studies support direct channeling in the transfer of reduced flavin in several two-component monooxygenase systems which involves protein-protein interaction. Protein-protein interactions were observed between SsuE and SsuD through pull-down assay indicating a possible channeling mechanism for reduced flavin transfer from SsuE to SsuD.[215] Further investigations were conducted to identify the interaction sites and relate protein-protein interaction with flavin transfer events in SsuE/D system (**Figure 1.37**). Studies involving hydrogen deuterium exchange showed remarkable differences in solvent accessibility for SsuE and SsuD upon complexation. Regions 78−89 (KAAYSGALKTLL) and 118−124 (YALKPVL) in SsuE and regions 251−261 (DDETIAKAQAA) and 285−295 (EISPNLWAGVG) in SsuD showed a decrease in deuterium exchange upon SsuE−SsuD complexation (**Figure 1.37**A). These protected sites are the regions involved in protein-protein interactions. In SsuE, the protected sites are located on two different α-helical regions one of which contains the π-helix in SsuE (**Figure 1.37**B). The protected sites in SsuD are in the flexible loop region over the active site (**Figure 1.37**B).[62, 229]

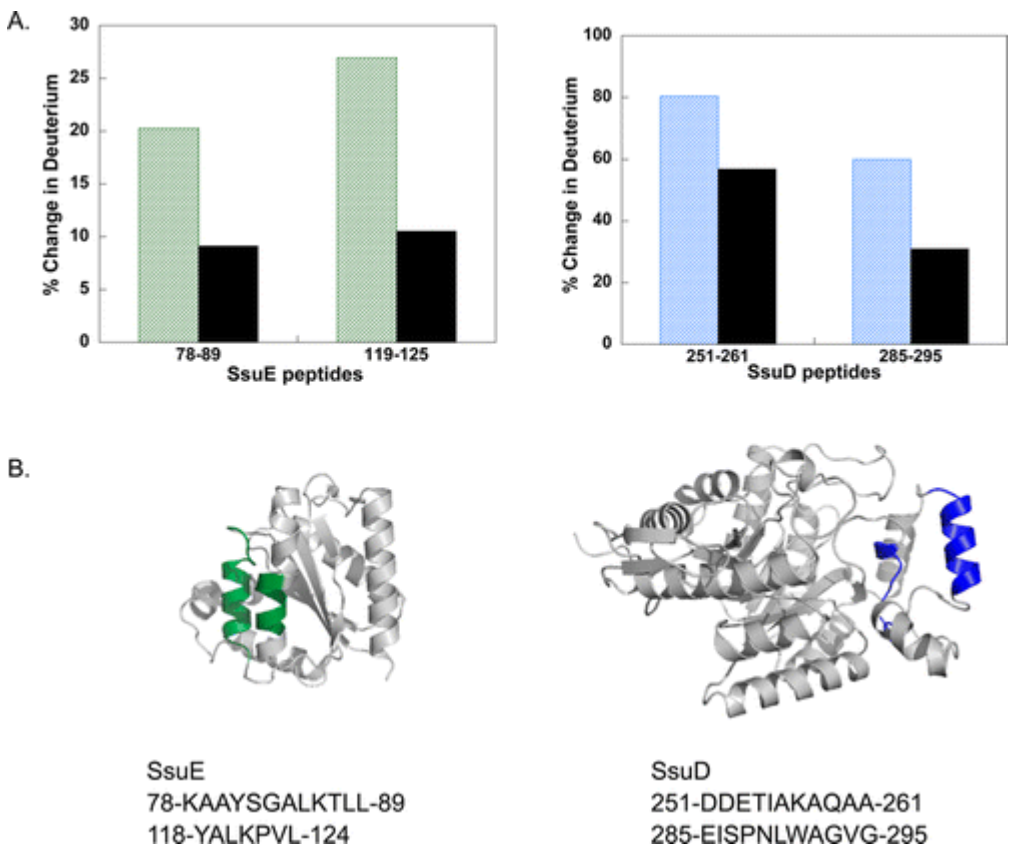

Figure 1.37: Identification of protein-protein interaction sites between SsuE and SsuD. Solvent-protected sites in SsuE and SsuD were identified through HDX-MS. Part of the π-helix in SsuE is involved in protein-protein interaction. (Adapted with permission from [229]). Copyright (2015) American Chemical Society.

Interruption of the interaction sites in SsuD led to diminished reduced flavin transfer from SsuE to SsuD resulting to no observable sulfite production. Protein-protein interactions between SsuE and the SsuD variants were adversely affected as supported by pulldown assays and fluorimetric titration studies.[229] The results suggested that the primary mode of reduced flavin

transfer from SsuE to SsuD was by direct channeling and involved the interaction of SsuE and SsuD enzymes. Protein-protein interactions would bring the active sites of SsuE and SsuD into proximity facilitating reduced flavin transfer. Increasing the supply of reduced flavin by elevating the concentrations of SsuE and its substrates (NAD(P)H and FMN) recovered some desulfonation activity by SsuD despite having the interaction sites disrupted, indicating that reduced flavin transfer from SsuE to SsuD could be achieved by diffusion under specified conditions.[229] The higher affinity characteristic of SsuD for reduced flavin relative to SsuE ensures simultaneous well-coordinated capture and utilization of reduced flavin by SsuD, and reduces non-enzymatic oxidation.[61] Such increased affinity for reduced flavin is common in monooxygenases of two-component monooxygenase systems and augments reduced flavin transfer in both diffusion mediated and protein-protein interaction transfer mechanisms.[171]

1.4 π-helices in Proteins

1.4.1 Introduction to Helical Structures in Proteins

The chief secondary structures in protein architecture are α-helices and β-sheets.[208] The stability of protein helical structures is determined by recurring hydrogen bonds between the backbone carbonyl oxygen (C=O) and amide hydrogen (NH). Helical structures constitute majority of secondary structures in most proteins and are classified into 3_{10}-helices, α-helices, and π-helices based on the backbone hydrogen bonding pattern. The 3_{10}-helices exhibit ($i \leftarrow i + 3$), α-helices have ($i \leftarrow i + 4$), and π-helices ($i \leftarrow i + 5$) hydrogen bond repeats (**Figure 1.38**).[208] Approximately 31% of amino acids in proteins participate in α-helices which qualifies α-helices to be the most abundant type of secondary structures. The 3_{10}-helix have been identified in approximately 4% of secondary structures.[231, 232]

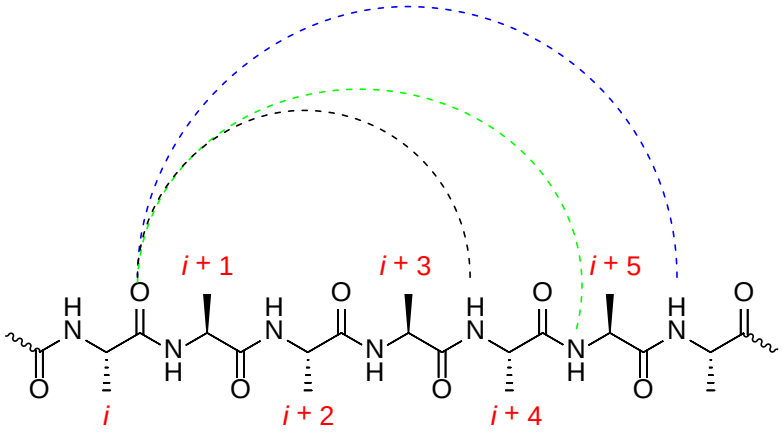

Figure 1.38: Assignment of helical structures in proteins. The helical structures are assigned based on H-bonds between backbone carbonyl oxygen (C=O) of residue i and amide hydrogen (NH) of residue i + n. The helical protein structures are classified into 3_{10}-helix, α-helix, and π-helix with corresponding i←i + 3 (black), i←i + 4 (green), and i←i + 5 (blue) respectively. (Adapted from [230]).

The π-helices in enzymes were thought to be rare, but recent studies suggest that they are more common. π-Helices result from mutations that insert a single residue in an established α-helix to create 5 amino acids per turn (rather than 4 amino acids per turn) and a bulge at the point of insertion.[207, 208] Recent analysis of helical structures show π-helices to be the same as α-bulges, α-aneurisms, π-bulges, as well as looping outs.[207] Natural π-helices typically have 7 residues that have 2 π-type H-bonds.[208] The diameter of a π-helix exceeds that of an average α-helix by ~1 Å (**Figure 1.39** and **Figure 1.40**).[233] They have large radii implying backbone chain atoms are not in van der Waals contact along the helix axis.[234] The formation of π-helices requires an alignment of five amino acid residues to allow ($i \leftarrow i + 5$) hydrogen bond which is energetically expensive

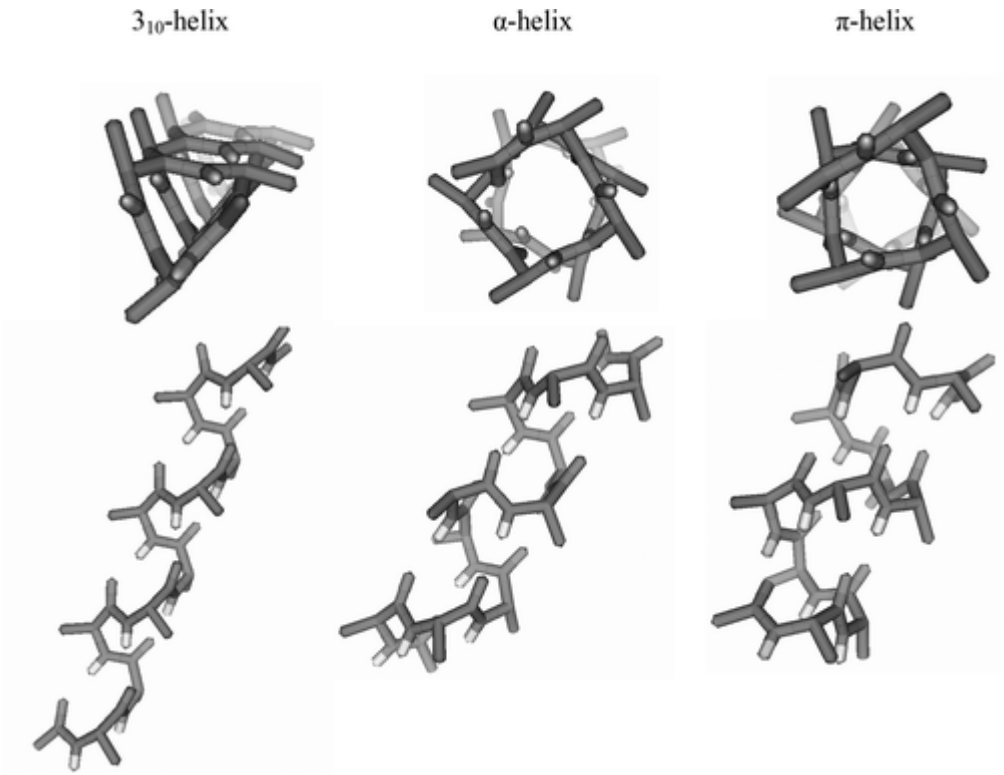

Figure 1.39: Top view and side view of α-helix, 3_{10}-helix and π-helix in alanine deca-peptide. (Adapted with permission from [235]). Copyright (2011) American Chemical Society.

and requires a large entropic energy.[236] The π-helices tend to be unstable because the dihedral angles (ϕ and Ψ) are at the edge of the allowed minimum energy region in the Ramachandran plot.[237]

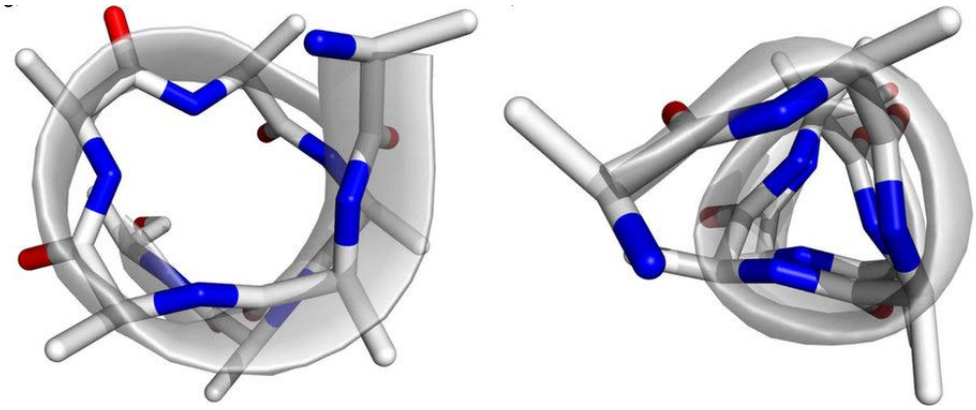

Figure 1.40: Top view of π-helix (left) and 3_{10}-helix (right). (Adapted from [91, 163, 233]). Copyright © 2016, Rights Managed by Nature Publishing Group.

Although π-helices are rarely reported, it is estimated that 10-15% of all known proteins have π-helices.[207, 208] However, recent studies suggest that π-helices could be common.[207, 208, 238, 239] The evolutionary origin of π-helices provides insights into why they are cryptic, rarely assigned, and unrecognized.[207] The highest number of π-helices in a single protein chain is eight (Protein Data Bank entry 2a65).[207, 240] Although there are no extended π-helices in proteins, short π-helices do exist.[241] Transformation from α-helices to 3_{10} or π-helices can also occur during catalysis.[233] Protein simulations have also shown the formation of π-helical conformations during catalysis.[242-244] It is unclear if such conformations reflect the true occurrence of π-helices.[245] Through molecular dynamics simulations of peptides, π-helix formation has been observed.[246-248] The transition of α-

helices to π-helical structures during catalysis has also been reported through molecular dynamics simulation.[249, 250] In addition, site-directed spin-labeling (SDSL) and ^{2}H-isotopic labeling has been utilized to distinguish helical structures in protein. SDSL involves the ^{2}H-labelling of the amino acid side chain *i* and the introduction of a cysteine at *i* + 1, *i* + 2…… *i* + 4, for nitroxide spin-labeling. Electron spin echo envelope modulation (ESEEM) spectroscopic studies (which uses SDSL and deuteration) can then be used to monitor changes in ^{2}H-ESEEM patterns.[251] Although secondary structure and protein folding are usually studied using circular dichroism, the difference between a π-helix and an α-helix are usually not distinguishable by this method.[252-254]

1.4.2 Generation of π-Helices in Protein

Environmental conditions trigger mutations in living organisms resulting in proteins acquiring novel functionalities.[255-257] A knowledge gap exists on how the first protein folds occurred and how protein secondary structure and folds have evolved over time.[207] Francois Jacob in 1970 lays a strong argument for protein evolution which maintains that evolution modifies what already exists culminating into new or advanced functions.[258] The π-helices are evolutionary products linked to the introduction of a single amino acid residue into α-helices resulting in a bulge conformation.[207, 208] The π-helices are thought to have evolved from proteins containing α-helices. They are found in sub-branches of larger protein superfamilies, are highly conserved, and augment functional sites in proteins.[207, 239, 259] The presence of π-helices is the result of protein evolution and is associated with a gain or enhancement of a function. They are conserved in functionally-related proteins, although such proteins may have low sequence identity. For example, the chelatase family of proteins (with less than 12% overall sequence identity), possess a π-helix at the active site and catalyze the insertion of metals into various proteins.[208, 260-263]

The π-helices are informative markers of evolution and have functional implications. They provide insight into the origin and evolution of proteins, and on the diversification of protein functions. [185, 186] Creation of π-helices is energetically unfavorable. After the π-helix has been developed and accommodated in a protein, its removal becomes even more energetically unfavorable. Deletion of the inserted residue in the π-helix of heat shock transcription factor created an α-helix but resulted in an unstable protein.[264] The interconversion of α- and π-helices during evolution is bidirectional but is skewed towards π-helix formation. The gain and loss of π-helices correlate temporally (during evolutionary over long time) and spatially (structurally at specific sites) resulting in modified functionality.[207] Mutational insertions resulting in π-helices is a phenomenon in protein evolution and is significant in solving the evolutionary route of many protein families.[208] The mutation leading to a π-helix could be directly adaptive or originate from a genetic drift in a stable protein culminating in a non-adaptive change that can further advance to adaptive mutations.[255, 256]

The flavin reductases of the NAD(P)H:FMN reductase family have a π-helix centrally located at the dimer of dimers interface.[62] For the flavin reductases initially evaluated, the π-helix emanates from an insertional mutation involving a tyrosine residue. The Tyr118 residue insertion generated the π-helix in SsuE enzyme and was the candidate insertional residue in EmoB from *Mesorhizobium* sp. BNC1, and in an uncharacterized oxidoreductase (3k1y) found in *Corynebacterium dipththeriae* (37% and 29% structural similarity respectively).[62, 172] All of these flavin reductases belong to two-component monooxygenase systems.[62] The insertional tyrosine residue is absent in other members of the NAD(P)H:FMN reductase family which do not have an associated monooxygenase (**Scheme 1.3**).[62] Therefore, the π-helices in SsuE-like flavin reductases may have developed to provide a distinct function in two-component monooxygenase systems.

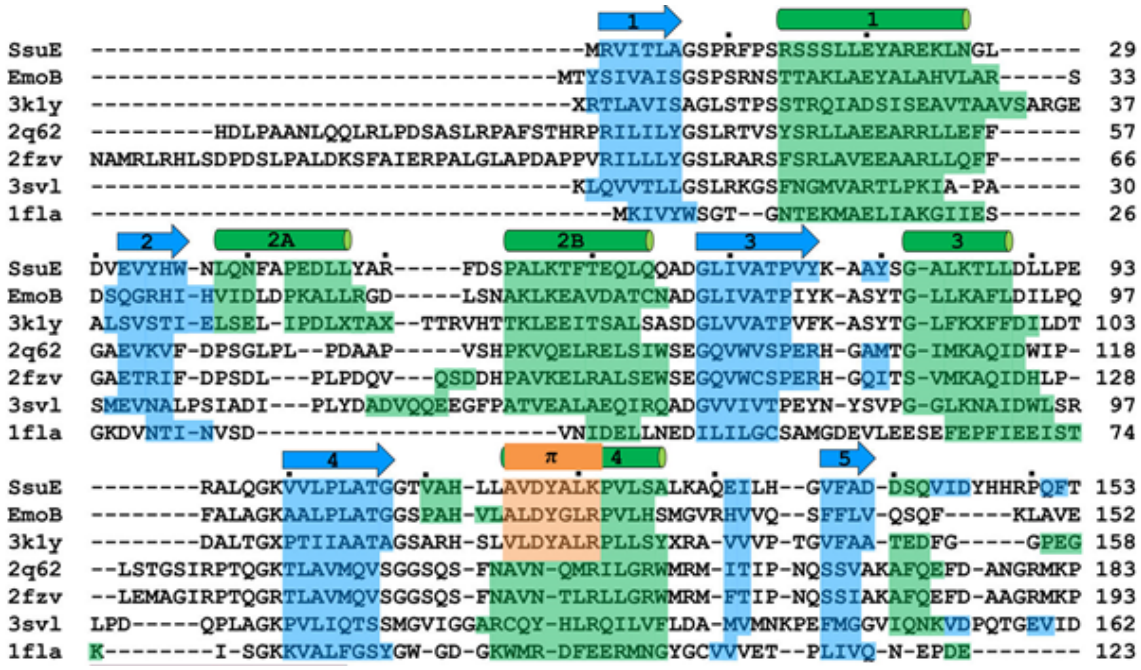

Scheme 1.3: Tyr insertions in flavin reductases of two-component monooxygenase systems. (Adapted with permission from [62]). Copyright (2014) American Chemical Society.

1.4.3 π-helices Augment Function in Proteins

The π-helices in proteins tend to be less favored unless they confer a functional advantage. The π-helices augment functional sites in proteins and are highly conserved in sub-branches of protein superfamilies.[207, 239, 259] The phosphorylase descendant of the UDP:glycosyl transferases has a π-helix resulting from a Trp residue insertion at the pyridoxal phosphate binding site.[265] This conversion of an α- to a π-helix is responsible for their deviation from UDP-glucose to pyridoxal phosphate-dependent.[207] A tyrosine insertion transforms an α-helix to a π-helix in mercuric ion reductases ("ancient" members of the pyridine nucleotide-disulfide reductases). The inserted Tyr is a catalytic residue at the mercury binding site.[207, 266] In acetylcholine esterase (a subgroup of the

α/β hydrolase superfamily), an α-helix to π-helix transformation introduces a bend that alters the shape of the active site pocket which positions the glutamate of the Glu-His-Ser catalytic triad. The π-helices are also conserved in protein families in heat shock transcription factors (a subgroup of peroxidredoxins), and in halo- and bacteriorhodopsin.[207, 264, 267-269] The π-helix in M1 (a subunit of a transmembrane domain) is involved in the activation of endplate-receptor and in muscle nicotinic acetylcholine receptors (AChR) desensitization. This π-helix regulates ion conductance and the binding of agonists through gating.[270] π-Helices are prevalent in ferrochelatases in which they aid in metal binding.[271] A surface exposed π-helix in soybean lipoxygenase is located at the mobile loop region. The π-helix is highly dynamic and participates in substrate recognition (**Figure 1.41**).[272] The π-helices in heme-copper oxidases differs in length and are involved in inter-helical interactions.[273] The π-helices enhance protein structure by facilitating protein folding and by changing the orientation of the protein chains.[238]

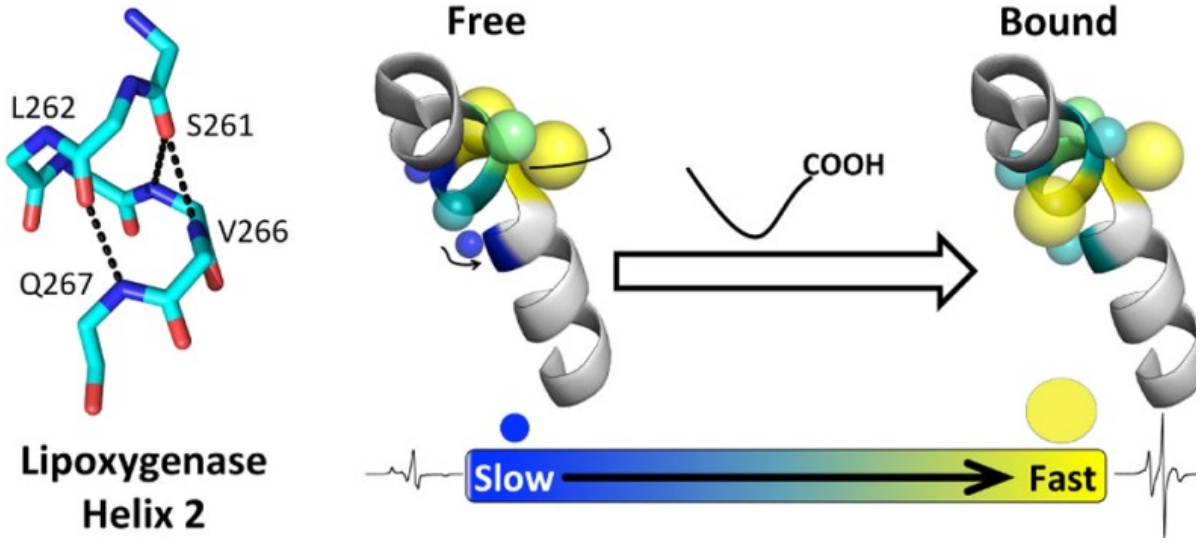

Figure 1.41: Lipoxygenase π-helix flexibility increases with substrate binding. (Adapted with permission from [272]). Copyright © 2014 American Chemical Society. Further permission requests should be directed to the ACS).

Unique structural dynamics associated with π-helices augment protein function. The soluble methane monooxygenase (MMOH) has a hydroxylase component which contains an active site π-helix. This enzyme belongs to the bacterial multicomponent monooxygenases (BMM). Upon binding of a product analog, the π-helix in MMOH was initially reported to elongate.[274] Thorough scrutiny of this π-helical segment disproved the elongation of a single long π-helix, and showed that the structural behavior was a result of two overlapping π-helices (πB and πD). The πD is reported to shift in an esophageal peristaltic-like manner during substrate binding.[207] Such peristaltic shifts of π-helices was revealed in toluene-4-monooxygenase hydroxylase (related to MMOH).[207, 275] Ligand binding at the regulatory subunit results in a peristaltic-like shift of the active site π-helices in all BMMs.[207] The buried active site cavity enlarges for substrate binding.[207] The π-helical shift phenomena explains the activation of BMMs by their regulatory subunits.[276] In toluene-4-monooxygenase, π-helical shifts at the active site coordinates with a shift in a nearby π-helix (πE-helix). Upon ligand binding, the πE-helix (conserved in BMM enzymes) undergoes conformational changes which influence the regulatory subunit. The coordinated movement of π-helices influence the buried active sites in BMM enzymes and shows how π-helices removed from the active site can influence the active site.[207]

π-Helical structures have been identified in various flavin reductases based on three-dimensional structures. The π-helices identified so far are highly conserved in a sub-branch of NADPH:flavin reductases (**Figure 1.42**), suggesting that the π-helices enable a common functionality.[62] The flavin reductases bearing π-helices are members of two-component monooxygenase systems but the role of the π-helices in these enzymes is not known.[62] The flavin reductases bearing π-helices exist as tetramers and the π-helices are located at the tetramer

interface. The π-helical structure could be a norm in some flavin reductases associated with two-component monooxygenase systems, which suggests a common evolutionary path.

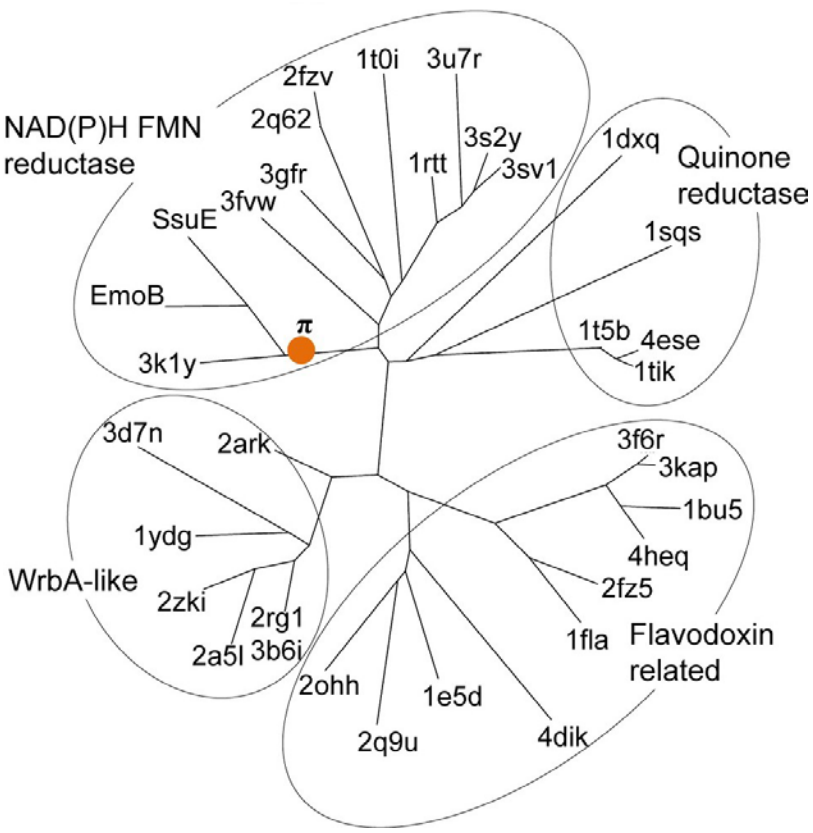

Figure 1.42: Phylogenic tree of the flavodoxin superfamily. Among the NAD(P)H:FMN reductases, only the SsuE sub-branch have a π-helix shows (highlighted in orange). (Adapted with permission from [62]). Copyright (2014) American Chemical Society.

1.4.4 π-helices show Preference for Certain Amino Acids

The occurrence of amino acids within different types of secondary structures has been under scrutiny to reveal the sequences that are preferred for certain secondary structures. The amino acid residues tend to be located at specific positions within secondary structures.[277] Aromatic and large aliphatic amino acids (Ile, Leu, Tyr, Trp, Phe, His and Asn) are more prevalent

in π-helices than small amino acids residues (Ala, Gly and Pro).[208] Hydrophobic and aromatic residues are commonly found in π-helices suggesting that hydrophobic and aromatic interactions involving side chains help stabilize π-helices.[238] Residue preference can be position specific with large amino acids (Phe, Trp, Tyr, Ile, Leu and Met) located at the start and end of the π-helix. The bulkiness of these residues provides favorable van der Waals interactions at the side chains which stabilizes the π-helices. Polar residues (Asn, Glu, Thr and Ser) are preferred at other positions within the π-helix, while Asn had a high propensity to be positioned at the middle of the π-helix.[208]

The amino acid residues immediately preceding and after the π-helices show no sequence preferences except at the +1 position. A Pro residue has a high propensity to be located at the +1 position (the first residue after the π-helix).[208] Although Pro is associated with breakage of at least two adjacent hydrogen bonds, the Pro at the +1 position (in a 7 residue π-helix for example) would form a hydrogen bond with the residue at position π3.[208, 278] The π-helices tend to have a Pro residue at the point where the helix shifts to an α-helix.[207, 208, 259] The pyrrolidine ring in Pro shifts the carboxyl group of the amino acid at π4 away from the helical axis resulting in another non-hydrogen bonding carboxyl group.[208] Although Pro enhances a π-turn formation, it could also limit the size of π-helices.[208, 279] The high probability of Pro at the +1 position and low propensity to be within the π-helices implicate Pro as a π-helix terminator.[208]

Comprehensive analysis of structural properties of π-helices and the preferences for certain amino acid sequences is requisite in understanding the forces that stabilize π-helices.[208] The interactions between side chains of residues in a π-helix (van der Waals, aromatic ring stacking, and a few electrostatic interactions) are a stabilizing factor, illuminating why aromatic and bulky aliphatic amino acids are likely to be located at the start and end of π-helices. Alignment of π-helix residues may generate shorter and even stronger hydrogen bonds.[208] Steric repulsion in the residues

could contribute to the instability of π-helices limiting their occurrence in protein structures.[208, 280] Although experimental studies imply that π-helices are unstable, molecular dynamics simulation suggest π-helices could be more stable than α-helical conformations.[207, 208, 237] Stability of protein secondary structures is also dependent on entropic effects. When the volume and surface area of a π-helix were compared to those of an α-helix, the π-helix had 10% less volume and surface area, suggesting that solvent entropic effect for π-helices are more favorable.[281] This compensates the required entropic effect to the alignment of residues in a π-helix.[208]

1.4.5 Assignment of π-helices in Secondary Structures of Proteins

Several algorithms have been developed to assign secondary structure in proteins based on three-dimensional coordinates. **D**ictionary of **S**econdary **S**tructure of **P**roteins (DSSP) and **STR**uctural **IDE**ntification (STRIDE) are the commonly used algorithms to assign protein secondary structure using three-dimensional coordinates.[283, 284] The STRIDE algorithm capitalizes on main chain dihedral angles and hydrogen bond energy in the assignment of protein secondary

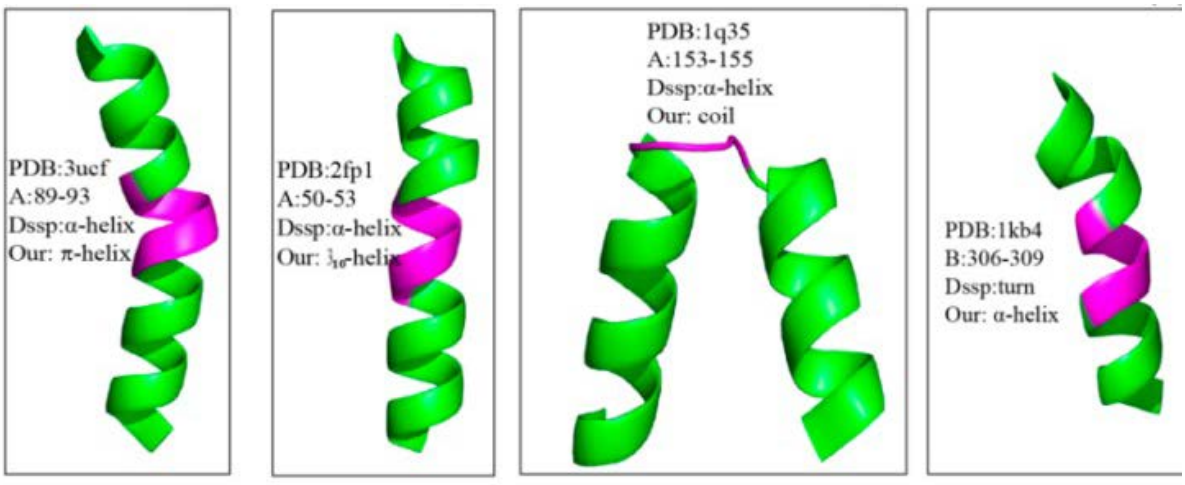

Figure 1.43: SACF and DSSP algorithms assigning helical structures. The algorithms showed different results for the same protein strand. (Adapted with permission from [282]). Copyright © 2016 by [282]; licensee MDPI, Basel, Switzerland.

structure. DSSP assigns secondary structure based solely on hydrogen bond energy. The DSSP algorithm utilizes ($i \leftarrow i + n$) hydrogen bond repeats to assign helices. The DSSP-based n value for an α-helix, 3_{10}-helix, and π-helix are 3, 4 and 5 respectively. STRIDE utilizes both hydrogen bonds and backbone chain dihedral angles to assign the secondary structures.[283-288]

Although secondary structures in majority of proteins have been assigned based on DSSP and STRIDE, these algorithms can have limitations. Assignment of secondary structures in 6,000 proteins using DSSP identified only nine π-helices.[239] Both STRIDE and DSSP were unable to identify π-helices that had been identified using graphical analysis of three-dimensional structures.[260, 289] For precise assignment of π-helices in proteins, modification of the existing helix identification algorithms is needed.[208] The π-helices are cryptic and tend to escape the angular restrictions and stringent H-bonding allocation standards of DSSP.[207] Using different algorithms in protein structure assignments often show observable disagreements. For instance, SACF and DSSP assign a different helical structure to the same strand (**Figure 1.43**).[282] The increasing use of modified π-helix definition algorithms reveal that π-helices are more prevalent than initially reported.[208] A recently coined algorithm **A**ssignment of **S**econdary **S**tructure in **P**roteins (ASSP) shows improved functionality.[230] The π-HUNT script identified π-helices in the flavin reductases of two-component monooxygenase systems including SsuE.[207]

1.5 Protein Oligomerization

1.5.1 Importance of Protein Oligomerization

Oligomerization is a form of protein self-association involving two or more monomers. It is an interactome of tertiary structures resulting in high-order oligomers. Oligomerization allows a relatively short single gene to encode for a large protein. Two or more peptide sequences encoded

by specific gene(s) interact to form a multimeric protein. Through oligomerization, the effective concentration is increased and the resultant protein is more stable (**Figure 1.44**a). Although oligomerization may not be a requirement for activity, the active sites of some oligomeric enzymes are found in the oligomeric interfaces.[290, 291] As few as two residues may be required for oligomerization and mutations at the oligomeric interface may lead to a loss of enzymatic activity.[292] Surfaces between oligomers could be allosteric sites for cofactor or substrate binding and can cooperatively trigger conformational changes in the other oligomers (**Figure 1.44**b).[291]

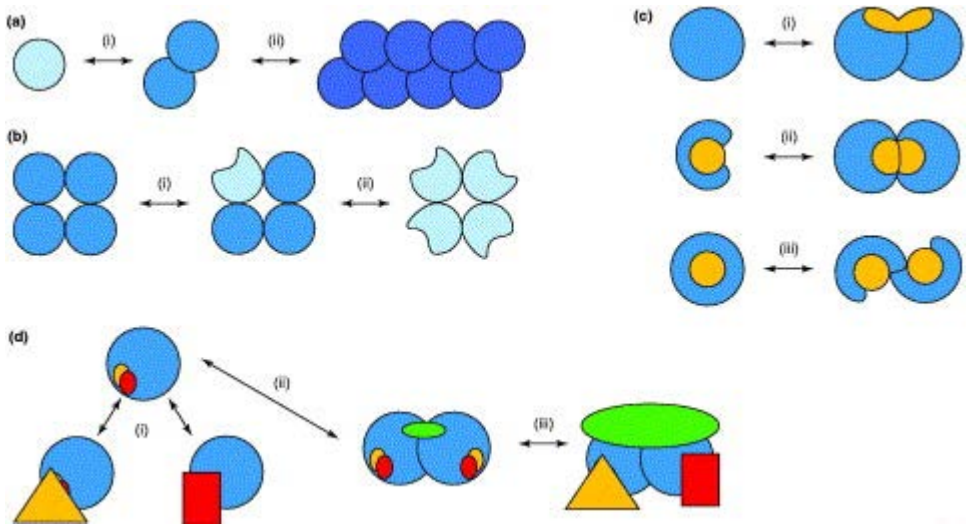

Figure 1.44: Oligomerization and enzyme activity. Oligomerization can optimize enzyme activity through enhancement of concentration and stability through oligomeric assemblage (a). Oligomerization can trigger cooperativity (b), conceal or reveal active sites based on the need for enzymatic activity (c), or even create new binding sites (d). (Adapted with permission from [291]). Copyright © 2004 Elsevier Ltd.

Oligomerization and oligomeric state changes can create new binding sites at the protein interface and can also conceal or reveal active sites in proteins based on the need for protein activity (**Figure 1.44**c). Oligomerization may create new binding sites and help in regulating protein complexes (**Figure 1.44**d).[291] Oligomerization can therefore be an efficient method for regulating enzymatic activity.

1.5.2 Oligomeric State Changes in Flavin Reductases

Oligomeric state changes have been observed in flavin reductases of two-component systems.[62, 293] The NADPH:FMN reductase from *Vibrio harveyi* associated with the bacterial luciferase system (both apo and native enzymes) exists in a monomer-dimer equilibrium.[293] The half-site activity reported with LuxG, a flavin reductase associated with bacterial luciferase, LuxAB from *Photobacterium leiognathi (TH1)* which exists as a dimer, could be as a result of oligomeric state changes during catalysis.[294] A dimer-tetramer equilibrium that is dependent on enzyme concentration exists with FerB, a NADPH:FMN reductase of *Paracoccus denitrificans*.[295]

The SsuE enzyme was reported to be a dimer in the initial characterization through gel filtration studies, but was shown to be a tetramer in the three-dimensional structure.[57, 62] Because contradicting oligomeric states were reported with SsuE, sedimentation velocity studies were performed to investigate the oligomeric form of SsuE in solution in the presence and absence of FMN. The apo-SsuE was shown to exist as a tetramer while the FMN-bound SsuE was a dimer suggesting the existence of a tetramer-dimer equilibrium that is flavin-dependent.[62] Oligomeric state changes could be a norm within flavin reductases and could have a role in substrate binding and in management of catalytic events. Although the flavin reductases exist in different oligomeric states, it is unclear how these oligomeric states relate to catalysis and how they are regulated. Broad and intense structural pursuits in this group of enzymes therefore becomes imperative. The basis for

the dissociation of the tetramer to dimers in SsuE upon flavin binding has not been established and requires further scrutiny. The oligomeric state changes might help reveal the FMN binding sites which are located at the interface of the tetramer.

In addition to oligomeric state changes in SsuE, a π-helix is centrally located at the tetramer interface. This π-helix abuts the active site of SsuE and may have an indirect role in catalysis through initiating flavin-induced oligomeric changes.[62] The oligomeric state changes observed in flavin reductases of two-component systems could also facilitate coordination of the protein-protein interaction sites. In the three-dimensional structure of SsuE, the hydroxyl group of Tyr118 forms a hydrogen bond with the carbonyl group of Ala78. The N atom of Ala 78 in turn forms a hydrogen bond with FMN. This hydrogen-bond network involving the π-helix in SsuE could be influencing the oligomeric changes from a tetramer to dimer upon FMN binding.[62] In addition, the loop before the π-helix was proposed to be vital in FMN binding through side chains of His112, while the N's of Thr109 and Gly108 forms hydrogen bonds with FMN at N3, O2, and N1.[62] Any conformational changes within the π-helix in SsuE should therefore influence the loop residues affecting substrate binding and catalytic events. In the reverse, flavin binding could trigger conformational changes at the loop region weakening the hydrogen-bonding network at the tetramer interface, culminating into the observed flavin-induced oligomeric state changes.

1.6 Summary

Although sulfur-containing biomolecules are critical in the execution of various chemical and structural functions, sulfur trafficking and incorporation are vaguely understood.[25] Bacteria often find themselves in environments with low sulfate availability and hence utilize organosulfonates as an alternative source of sulfur through desulfonation. The desulfonation of organosulfonates entails the cleavage of the C-S bond of organosulfonates by taurine dioxygenase and the alkanesulfonate monooxygenase system enzymes releasing sulfite. The desulfonation enzymes are usually induced in aerobic bacteria by sulfate-starvation-induced *(ssi)* stimulon when organosulfonates serve as a sulfur source.[55] Several two-component flavin-dependent monooxygenase systems are involved in bacterial sulfur acquisition from alkanesulfonates. The two-component flavin-dependent monooxygenase systems are made up of a flavin reductase and a monooxygenase enzyme, that utilizes the reduced flavin to activate dioxygen and insert an oxygen atom into the substrates. The genes encoding for both NAD(P)H:flavin reductase and monooxygenase are often located in the same operon in a two-component system. The two-component alkanesulfonate monooxygenase system catalyzes the $FMNH_2$-dependent oxygenolytic cleavage of C-S bond of various alkanesulfonates into sulfite and the corresponding aldehydes during sulfur scarcity conditions in bacteria.[57] The alkanesulfonate desulfonation enzymes are expressed under the regulation of the sulfate-starvation utilization *(ssu)* operon commonly made up of five cistrons (*ssuEADCB).*[60]

Many enzymes that comprise flavin-dependent two-component systems utilize flavin as a substrate, but it is not clear what structural properties of the FMN reductase dictate flavin reduction and transfer. The SsuE/SsuD system is comprised of a NAD(P)H:FMN reductase (SsuE) that reduces flavin and delivers the reduced flavin to the monooxygenase enzyme (SsuD). The SsuD

enzymes catalyzes the $FMNH_2$-dependent desulfonation of alkanesulfonates generating sulfite, FMN, a molecule of water, and aldehyde.[57] Reduced flavin is highly labile in aerobic condition results to formation of reactive oxygen species upon uncoupling. Understanding the structural properties of the NAD(P)H:FMN reductases of two-component flavin monooxygenase systems is imperative because reduced flavin has to be transferred from the reductase to the monooxygenase in the presence of dioxygen.[171] Flavin transfer from SsuE to SsuD involves protein-protein interaction and the interaction sites have been identified.[215, 229] Flavoproteins display remarkable differences in how they react with molecular oxygen, but there is no common explanation for the differential reactivity.[156, 160] The ability of the reduced flavin to react differently with dioxygen has been linked to the chemical versatility observed with flavoproteins.[161] Flavin monooxygenases and some oxidases form a quasi-stable C4a(hydro)peroxyflavin, which then incorporates a single oxygen atom into organic substrates. Structural characterization of monooxygenases and oxidases capable of stabilizing C4a-hydroperoxyflavin shows that a hydrogen bonding of C4a-(hydro)peroxyflavin at the N5 position is crucial for such stabilization.[156]

Distinct structural features enhance catalysis in flavin reductases of two-component monooxygenase systems. The SsuE enzyme alters its oligomeric state from a tetramer to a dimer in the presence of FMN.[62] Oligomeric state changes are a common phenomenon among flavin reductases, but the rationale and regulation of these quaternary structural changes in flavin reductases has not been explored.[62, 293-295,] A π-helix characterized by an insertional mutation of Tyr118 in the α4-helix is located at the tetramer interface of SsuE. Similar π-helical structures were identified at the oligomeric interface of other FMN reductases in the flavodoxin superfamily that were part of two-component systems.[62] Although >80% of π-helices are preponderantly activity-oriented, the roles of the π-helix in SsuE and other flavin reductases of two-component

flavin-dependent monooxygenase systems have not been elucidated. The π-helices often confer a gain or enhancement of a function that provides an evolutionary advantage.[207, 208] The evolutionary roles of the π-helices in flavin reductases of two-component monooxygenase systems have not been reported.

The structural properties of flavin reductases of two-component flavin monooxygenase systems remain largely underexplored. Only a few three-dimensional structures of flavin reductases of two-component monooxygenase systems have been resolved which include EmoB, MsuE, 3k1y and SsuE.[62, 204, 205] The apo-SsuE was shown to exist as a tetramer while the FMN-bound SsuE was a dimer suggesting the existence of a tetramer-dimer equilibrium that is flavin-dependent.[62] Comparative studies showed that the flavin reductases of two-component monooxygenase systems (EmoB, SsuE, 3k1y) have a π-helix centrally located at the tetramer interface.[62] π-Helices result from mutations that insert a single residue in an established α-helix to create 5 amino acids per turn (rather than 4 amino acids per turn) and a bulge at the point of insertion. The presence of π-helices is the result of protein evolution and is associated with a gain of function. The π-helices identified so far are highly conserved in a sub-branch of NADPH:flavin reductases, suggesting that the π-helix enable a common functionality.[62] The flavin reductases bearing π-helices are members of two-component monooxygenase systems but the role of the π-helices in these enzymes is not known.[62] The flavin reductases bearing π-helices exist as tetramers and the π-helices are located at the tetramer interface.[62] The π-helical structure could be a norm in some flavin reductases associated with two-component monooxygenase systems, which suggests a common evolutionary path. Studies on the functional roles of oligomeric state changes in flavin reductases are pivotal for catalysis and for understanding the regulation of enzymatic activity. The π-helix could help regulate the oligomeric state changes observed with SsuE. The different

oligomeric states observed in flavin reductases of two-component monooxygenase systems could be not only vital in flavin reduction but also in the transfer of reduced flavin to SsuD. These studies are globally pivotal in not only understanding the catalytic events in the flavin reductases and monooxygenase of two-component monooxygenase systems but also in comprehending the mechanism of reduced flavin transfer.

CHAPTER TWO

2 Transformation of a Flavin-Free FMN Reductase to a Canonical Flavoprotein through Modification of the π-helix

2.1 Introduction

Sulfur is a critical element in bacteria for effective cellular function and therefore appropriate sulfur levels need to be consistently maintained. Many bacteria are able to utilize alternative sources of sulfur to ensure their survival when sulfur is limiting. The sulfonate-sulfur utilization operon (*ssuEADCB*), expressing SsuD, SsuE, and alkanesulfonate transporter proteins, is upregulated when sulfur is scarce to replenish and maintain adequate sulfur levels in bacterial systems.[60] The SsuD monooxygenase enzyme cleaves the C-S bond of alkanesulfonates resulting in the generation of sulfite and the corresponding aldehyde.[57] Because SsuD is an $FMNH_2$-dependent monooxygenase, reduced flavin has to be provided by the flavin reductase SsuE. The flavin is not tightly bound to SsuE and is utilized as a substrate in the NADPH-dependent FMN reductase reaction.[57] The weaker binding of flavin to SsuE compared to that of canonical flavoproteins promotes the transfer of reduced flavin to SsuD.

There have been several flavin-dependent two-component systems identified in bacteria that catalyzes diverse reactions. The mechanism for reduced flavin transfer in these systems has been proposed to be either a diffusion or channeling mechanism depending on the system under investigation.[171, 296] Although the mechanism of flavin transfer has been investigated in several of these systems, structural information detailing how the flavin reductases utilize flavin as a substrate is limited. Initial characterization of the alkanesulfonate monooxygenase enzymes demonstrated a dimeric quaternary structure for SsuE.[57] The three-dimensional structure of SsuE exists as a dimer of dimers.[62] However, results from sedimentation velocity studies showed that

SsuE undergoes an oligomeric switch from a tetramer to a dimer when FMN is bound.[62] These observed alterations in the quaternary structure indicate that the oligomeric state of SsuE is dynamic and dependent on enzyme and substrate concentrations. It remains unclear how these oligomeric states relate to catalysis and flavin transfer. Interestingly, SsuE has a conserved π-helix at the tetramer interface between the dimer of dimers (**Figure 2.1**).[62]

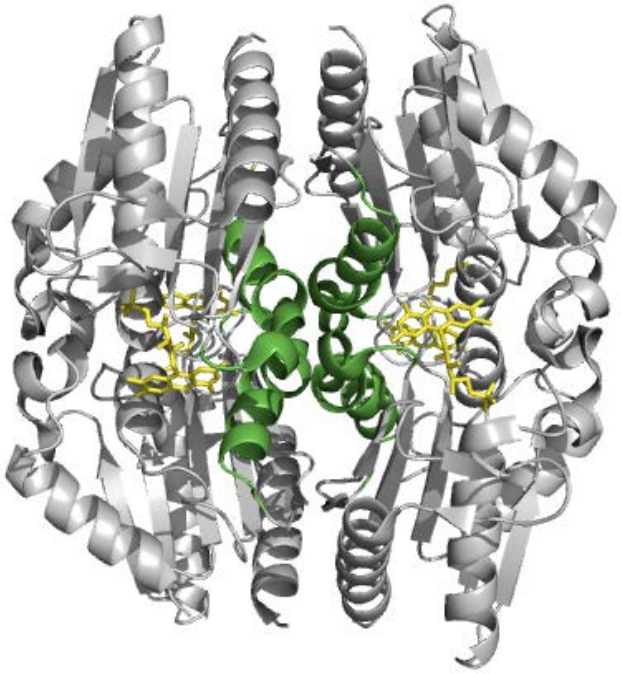

Figure 2.1: The tetrameric structure of SsuE with the π-helix located at the tetramer interface highlighted in green. The structure was rendered with PyMOL using Protein Data Bank entry 4PTZ for SsuE.[62]

Generally, π-helices are characterized by the insertion of a single-residue into α-helices to provide an evolutionary advantage through enhancement or gain of protein function.[207, 208, 297, 298] The identification of π-helices as discrete secondary structural elements is often overlooked in the analysis of protein three-dimensional structures.[207] The π-helix in SsuE is generated by the insertion of Tyr118 into helix α4, and is conserved within a subgroup of the NAD(P)H:FMN

reductase family with known three-dimensional structures (**Figure 2.2**).[62] Members of the subgroup are flavin reductases of two-component monooxygenase systems that are dependent on reduced flavin transfer from the NAD(P)H:FMN reductase to the monooxygenase enzyme.[62]

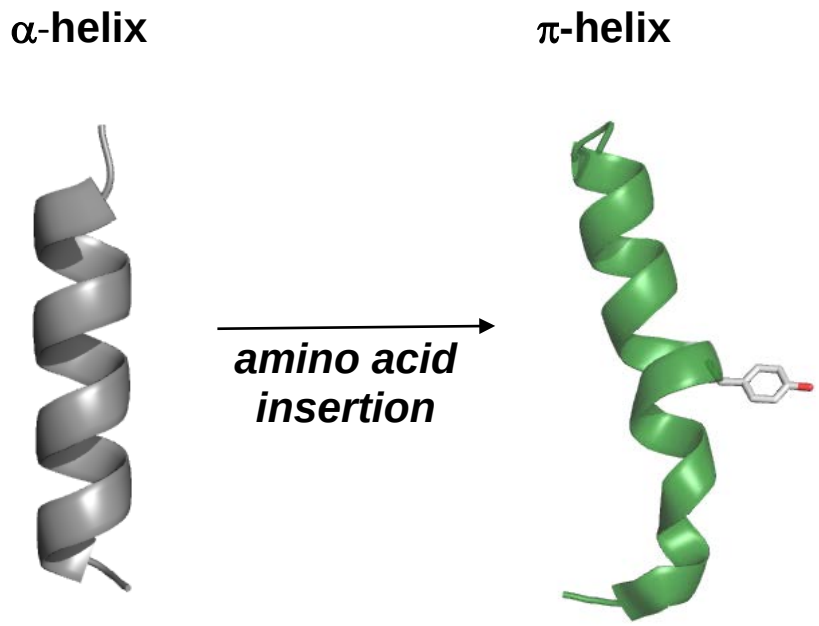

Figure 2.2: Comparison of the helix α4 of *Shigella flexneri* ArsH (gray) from the NAD(P)H:FMN reductase family with the π-helix in SsuE (green). A π-helix is present in a subgroup of the NAD(P)H:FMN reductase family that includes SsuE, generated by the insertion of Tyr118 insertion resulting in a bulge that is not present in the α-helix ArsH. The structures were rendered with PyMOL using Protein Data Bank entries 4PTY (SsuE) and 2fzv (ArsH).[62, 204]

The conserved nature of the π-helix in the two-component NAD(P)H:FMN reductase members suggests that it may play a defined role in mechanistic events.[62, 207] Given the location of the π-helix at the tetramer interface, this structural alteration may impart a distinct functional

role on this subgroup of enzymes within the family. These studies were performed to evaluate the functional role of the π-helix of SsuE. The Tyr118 amino acid insertion was substituted with alanine to evaluate how alteration of the π-helix structural element affects the functionality of SsuE. The Y118A SsuE variant showed striking differences in flavin affinity compared to that of wild-type SsuE, resulting in altered catalytic function. Results from these studies have provided a foundation for further investigations that aim to probe the dynamic structural feature of SsuE that dictates catalysis.

2.2 Experimental Procedures

2.2.1 Materials

All chemicals were purchased from Sigma-Aldrich, Bio-Rad, or Fisher. *Escherichia coli* strain BL21(DE3) was purchased from Stratagene (La Jolla, CA). DNA primers were synthesized by Invitrogen (Carlsbad, CA). The expression and purification of wild-type SsuE and SsuD were performed as previously reported.[2] All UV- vis absorbance spectra were recorded using an Agilent Technologies diode-array spectrophotometer (model HP 8453) equipped with a thermostated water bath.

2.2.2 Construction of Y118A SsuE Variant

The Y118A SsuE variant was generated using the recombinant pET21a plasmid containing the *ssuE* gene. Primers for the Y118A SsuE variant were designed as 27-base oligonucleotides substituting the TAT Tyr codon with the GCG Ala codon. The variant construct was confirmed by DNA sequencing analysis at Davis Sequencing (Davis, CA). The confirmed variant was transformed into *E. coli* BL21(DE3) competent cells for protein expression and stored at -80 ˚C. The Y118A SsuE variant was purified as previously reported.[2] Protein fractions for wild-type SsuE were collected on the basis of sodium dodecyl sulfate-polyacrylamide gel electrophoresis (SDS-

PAGE*)* analysis and UV-visible absorbance at 280 nm. For Y118A SsuE, the protein fractions were collected on the basis of absorbance values at 457 nm and purity on 12% SDS-PAGE. The concentrations of SsuD and SsuE were determined from A_{280} measurements using molar extinction coefficients of 47.9 and 20.3 mM^{-1} cm^{-1}, respectively.[2] A Bradford assay was used to determine the concentration of Y118A SsuE prior to the determination of the molar extinction coefficient. The standard curve used in the Bradford assay was generated with varying bovine serum albumin (BSA) concentrations between 0.2 and 0.8 mg/mL. Following purification, the proteins were frozen and stored at -80 °C.

Circular dichroism (CD) spectra for wild-type and Y118A SsuE were obtained with 1.2 μM of each protein in 10 mM potassium phosphate buffer (pH 7.5) as previously described.[215] Spectra were recorded on a Jasco (Easton, MD) J-810 spectropolarimeter. The experiments were performed at 25 °C using a 0.1 cm path length cuvette. Measurements were taken in 1 nm increments from 300 to 185 nm using a scanning speed of 50 nm/min and a bandwidth of 1 nm. An average of eight scans was performed for each sample. The background correction was achieved using the default parameters of the Jasco J-720 software. Each spectrum is the average of eight accumulated scans.

2.2.3 Preparation and Reconstitution of Apo-Y118A SsuE

Deflavination of Y118A SsuE was performed with the addition of 25 mM potassium phosphate (pH 7.5), 10% glycerol, and 3 M potassium bromide (5 mL) to an equal volume of flavin-bound Y118A SsuE (176 μM) in 25 mM potassium phosphate (pH 7.5), 0.1 M NaCl, and 10% glycerol. A 5 mL saturated acidified ammonium sulfate solution [72% (w/v), pH 2.0] was added to the Y118A SsuE solution. After the mixture had been continuously stirred for 1 min, an additional 20 mL of the saturated acidified ammonium sulfate [72% (w/v), pH 2.0] was added, resulting in

precipitation of the protein. The precipitated protein solution was centrifuged at 12096*g* for 10 min at 4 °C and the protein precipitate redissolved in a 5 mL volume of 25 mM potassium phosphate (pH 7.5), 0.1 M NaCl, and 10% glycerol. The precipitation and dissolution were repeated to remove any residual flavin. After a 30 min incubation at 4 °C, the solution was centrifuged for 5 min at 4424*g* to remove any denatured protein.[299] Deflavinated Y118A SsuE (5 mL) was dialyzed against 1 L of 25 mM potassium phosphate (pH 7.5), 0.1 M NaCl, and 10% glycerol for 3 h followed by a second overnight dialysis, frozen, and stored at −80 °C. The final concentration of deflavinated Y118A SsuE was 123 μM, resulting in a 70% yield. Reconstitution of deflavinated Y118A SsuE was performed by the addition of free FMN to deflavinated Y118A SsuE in a 1:1.2 molar ratio, followed by incubation overnight at 4 °C. Unbound flavin was removed with an Amicon Ultra-4 centrifugation filter (10 kDa molecular weight cutoff). The flow-through was discarded, and the protein sample retained in the filtration device was washed three times with 25 mM potassium phosphate (pH 7.5), 10% glycerol, and 0.1 M NaCl.

2.2.4 Identification of the Flavin Bound to Y118A SsuE

Waters quadruple time-of-flight (Q-TOF) mass spectrometer was used to identify the flavin bound to Y118A SsuE. The Y118A SsuE variant (176 μM) was buffer exchanged with 25 mM potassium phosphate (pH 7.5) to remove glycerol. The flavin cofactor was extracted by heat denaturation at 80 °C for 10 min. The sample was cooled to 25 °C and centrifuged at 12096*g* for 10 min to separate the protein pellet and the flavin-containing supernatant. The mass-to-charge ratio (m/z) of the flavin extract was determined using the Q-TOF mass spectrometer in positive ion mode at room temperature by direct injection.

2.2.5 Kinetic Properties of Y118A SsuE

Steady-state kinetic parameters measuring the oxidase activity of FMN-bound Y118A SsuE (0.04 μM) were obtained with varying concentrations of NADPH (3−60 μM) in 25 mM Tris-HCl (pH 7.5) and 100 mM NaCl at 25 °C. Electron transfer to ferricyanide was performed with FMN-bound Y118A SsuE (0.04 μM), varying concentrations of NADPH (5−50 μM), and 1 mM ferricyanide in 25 mM Tris-HCl (pH 7.5) and 100 mM NaCl at 25 °C. The initial rates for both experiments were obtained by monitoring the decrease in absorbance at 340 nm with the oxidation of the reduced pyridine nucleotide. Coupled assays with deflavinated Y118A and wild-type SsuE monitoring the desulfonation of octanesulfonate were performed as previously described.[61] The reactions were initiated by the addition of 500 μM NADPH to a reaction mixture containing wild-type or Y118A SsuE (0.6 μM), FMN (2 μM), SsuD (0.2 μM), and varying concentrations of octanesulfonate (5−2000 μM) in 25 mM Tris-HCl (pH 7.5) and 0.1 M NaCl at 25 °C. The reaction was quenched after 3 min with 8 M urea, and the sulfite product was quantified as previously described.[61]

Binding of flavin to Y118A and wild-type SsuE was monitored on a Cary Eclipse Agilent (Santa Clara, CA) fluorescence spectrophotometer with an excitation wavelength at 280 nm and emission measurements at 344 nm. A 1.0 mL solution of deflavinated Y118A or wild-type SsuE (0.1 μM) in 25 mM potassium phosphate (pH 7.5) and 0.1 M NaCl was titrated with FMN (from 0.022 to 0.44 μM), and the fluorescence spectrum was recorded following a 2 min incubation after each addition of FMN. The K_d value for FMN binding was determined as previously described.[2] The concentrations of FMN bound to apo Y118A and wild-type SsuE enzymes were computed using **Equation 2.1**, in which [SsuE] is the concentration of SsuE used, I_0 is the fluorescence

intensity of SsuE before FMN titration. I_c represents is the fluorescence intensity of SsuE after each FMN addition while I_f is the fluorescence intensity after the final FMN addition.

$$[FMN]_{bound} = [SsuE]\frac{I_0 - I_c}{I_0 - I_f} \qquad \textbf{Equation 2.1}$$

The concentrations of FMN-bound SsuE (y) was plotted against the total FMN concentration (x), and the dissociation constant (K_d) determined using **Equation 2.2.**

$$y = \frac{(K_d + x + n) - \sqrt{(K_d + x + n)^2 - 4xn}}{2} \qquad \textbf{Equation 2.2}$$

2.2.6 Reductive Titrations of Y118A SsuE

A 1 mL anaerobic solution of Y118A SsuE (40 μM) in 25 mM potassium phosphate (pH 7.5), 100 mM NaCl, and 10% glycerol was prepared by at least 15 cycles of evacuation followed by equilibration with ultra-high-purity argon gas in an airtight vial. An oxygen scavenging system composed of 20 mM glucose and 10 units of glucose oxidase was also included to ensure the solution was kept anaerobic. The anaerobic NADPH solution (1 mM) was prepared separately in 10 mM Tris-HCl (pH 8.5), and the solution was deoxygenated as described for Y118A SsuE before the solution was added to an airtight titrating syringe in an oxygen-free glovebox. The anaerobic cuvette containing deoxygenated Y118A SsuE and the titrating syringe containing NADPH were assembled in the oxygen-free glovebox. The FMN-bound Y118A SsuE (40 μM) anaerobic solution was titrated with NADPH (0−160 μM) at 25 °C, and the enzyme was allowed to reach equilibrium before the spectrum was recorded.

Following the titration, buffer exchange was performed to determine if the reduced flavin remained bound to the Y118A SsuE variant. Buffer exchange was performed with 25 mM potassium phosphate (pH 7.5), 10% glycerol, and 0.1 M NaCl, utilizing a 10000 molecular weight cutoff Amicon Ultra-4 centrifugation filter (Millipore, Billerica, MA). Buffer exchange was

performed three times by centrifugation at 4025*g* in an oxygen-free glovebox. The reduced Y118A SsuE variant was equilibrated with atmospheric oxygen, and a UV−visible absorption spectrum of the oxidized enzyme was recorded.

2.3 Results

2.3.1 Spectroscopic Analysis of Y118A SsuE

The three-dimensional structure and kinetic studies of SsuE provided insight into the flavin reduction mechanism of SsuE.[2, 62, 200] At the tetramer interface of SsuE is a π-helix formed by the insertion of Tyr118 into helix α4.[62] The π-helix is conserved among several flavin reductases that belong to the NAD(P)H:FMN reductase family. The flavin reductases are members of two-component monooxygenase systems, and the π-helix may impart a functional advantage to these flavin reductases.[62] The Y118A SsuE variant was generated to investigate the structural and functional role of the π-helix in SsuE. The purified Y118A SsuE protein exhibited a yellow color with characteristic absorbance peaks at 370 and 457 nm consistent with a flavin-bound protein (**Figure 2.3**). As previously described, recombinant wild-type SsuE does not exhibit a similar spectral signature following purification (**Figure 2.3**).[2, 57]

The CD spectra of wild-type and Y118A SsuE were similar suggesting there were no major changes in the gross secondary structure when a substitution was introduced into the π-helix of SsuE (**Figure 2.4**). Deflavination of Y118A SsuE was achieved by mild acidification followed by salt precipitation and dissolution of the precipitated protein (**Figure 2.3**).[299] The deflavinated Y118A SsuE variant could be reconstituted with flavin to generate the flavin-bound form, and the reconstituted protein had the flavin-bound spectral features restored. The CD spectra of deflavinated Y118A SsuE resembled those of Y118A SsuE prior to deflavination and wild-type

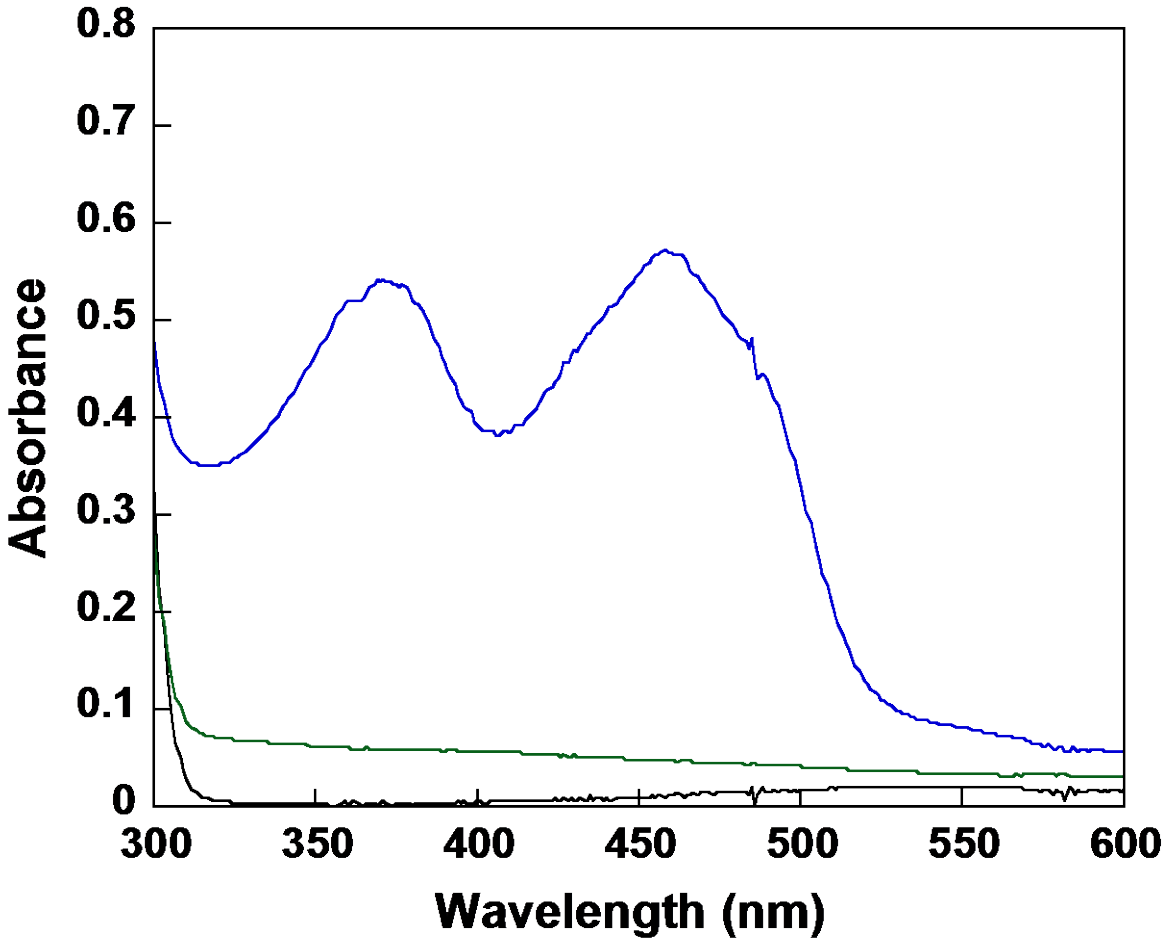

Figure 2.3: The UV-visible absorption spectra of Y118A and wild-type SsuE. The UV-visible absorption spectra of Y118A SsuE (blue), deflavinated Y118A SsuE (green), and wild-type SsuE (black). Purified wild-type SsuE does not contain a bound flavin. The Y118A SsuE variant showed a characteristic oxidized flavin spectrum with peaks at 370 and 457 nm that was no longer present following deflavination.

SsuE, indicating the secondary structure was not compromised during the deflavination procedure (**Figure 2.4**).

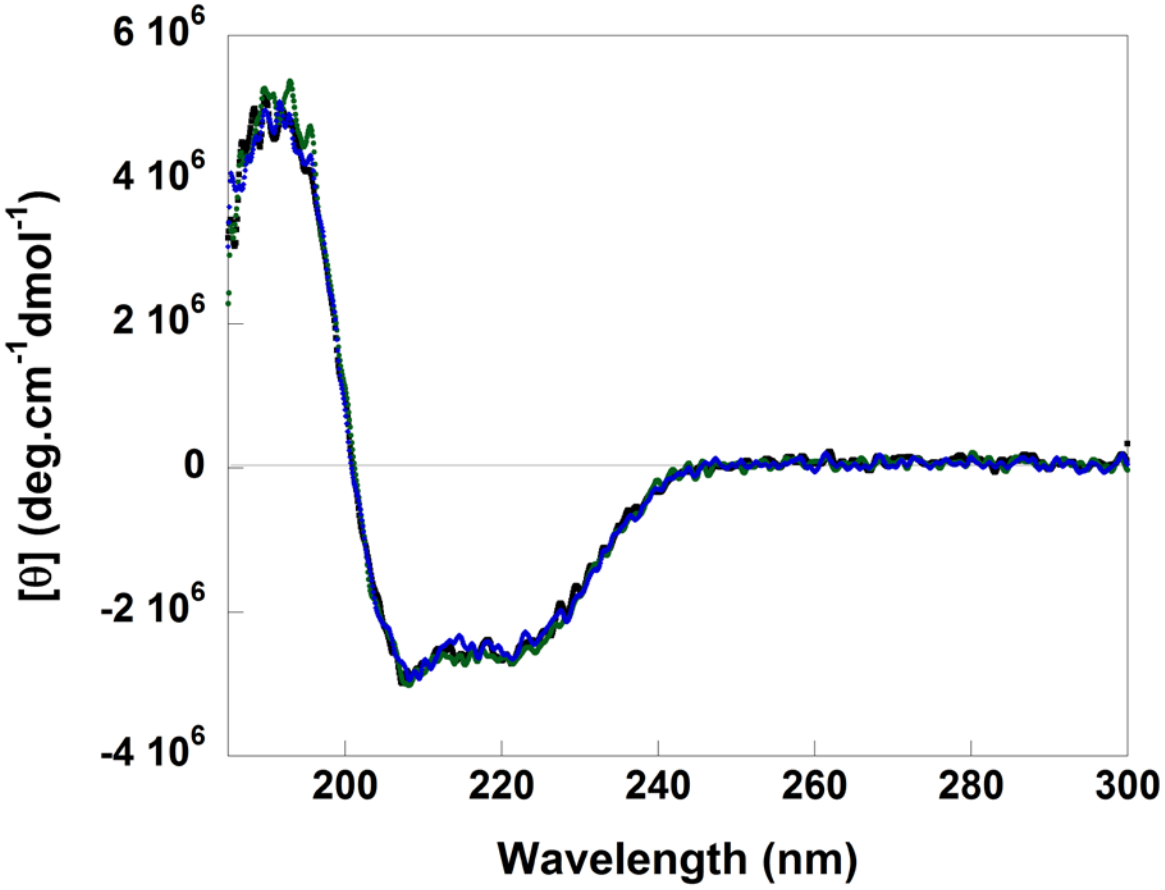

Figure 2.4: The far-UV circular dichroism spectra of flavin-bound Y118A SsuE, deflavinated Y118A SsuE, and wild-type SsuE. Spectra of flavin-bound (blue), deflavinated (green), and wild-type (black) SsuE were obtained with 1.2 µM protein in 10 mM potassium phosphate buffer, pH 7.5, at 25 °C. Measurements were taken in 1 nm increments from 300 nm to 190 nm in a 0.1 cm path length cuvette. Each spectrum is the average of eight accumulated scans.

2.3.2 Identification of the Flavin from Y118A SsuE

Flavin reductases that utilize flavin as a substrate typically have a distinct substrate preference for FMN or FAD.[171] Catalytic investigations have previously identified FMN as the preferred substrate for SsuE over other flavin forms.[57] The Y118A SsuE variant was denatured and the supernatant extracted in an effort to characterize the bound flavin. The flavin was retained in the supernatant suggesting that the cofactor is not covalently bound to Y118A SsuE. The spectral properties of the flavin extract corresponded to that of free FMN (**Figure 2.5**).

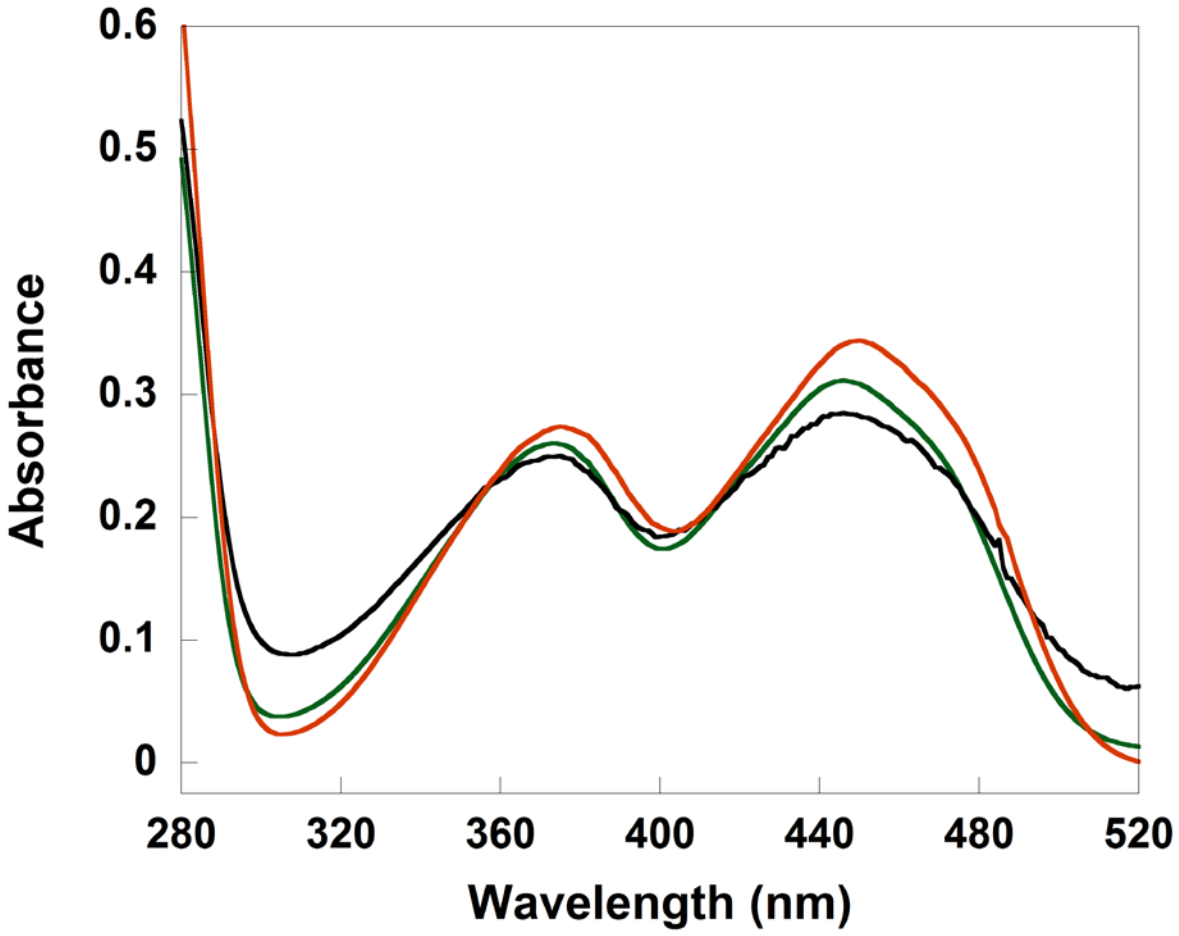

Figure 2.5: Identification of the flavin bound to Y118A SsuE. A. UV-visible absorption spectra of flavin extracted from Y118A SsuE (150 μM) (black), the FMN standard (green), and the FAD standard (orange).

Mass spectrometric analysis was used to identify the flavin based on the mass-to-charge ratio. The noncovalent bound flavin in the Y118A SsuE variant was FMN giving a peak with an *m*/*z* value of 457.11 similar to the calculated molecular weight for FMN (**Figure 2.6**).

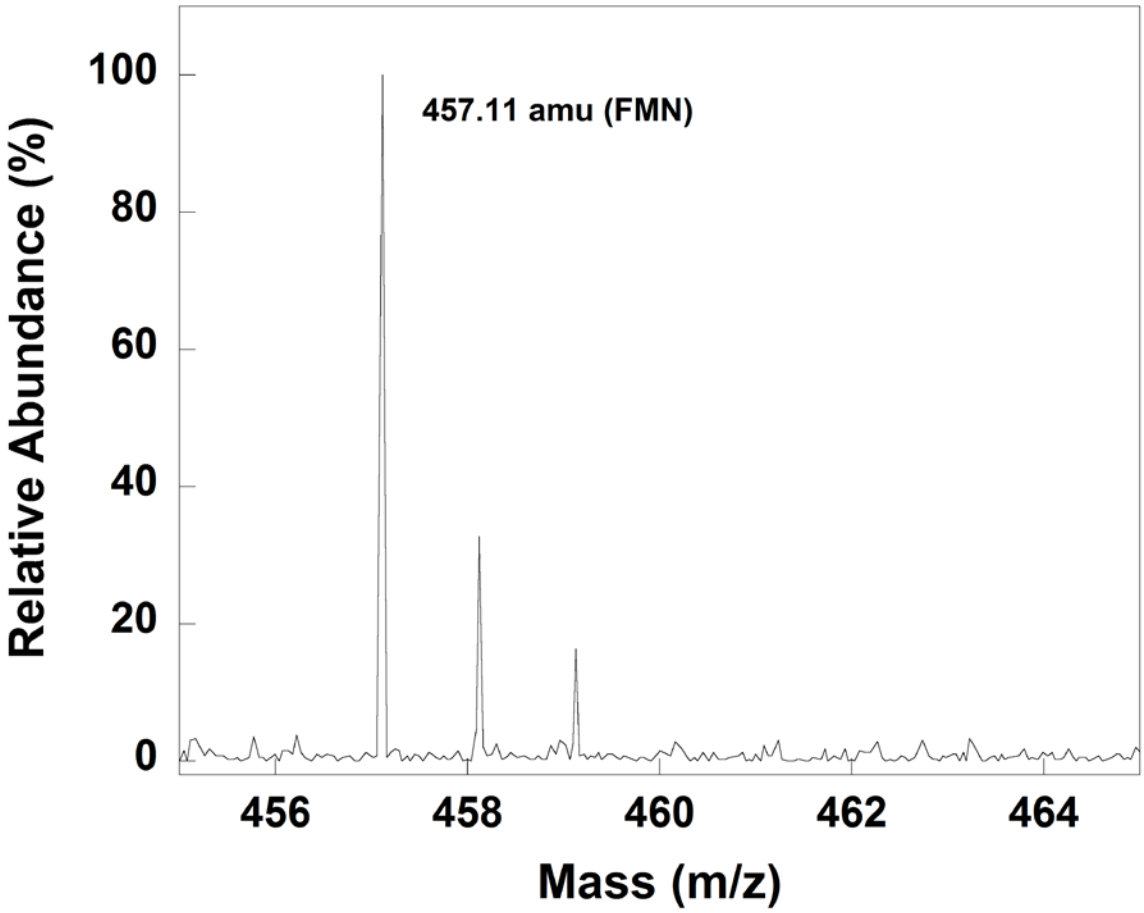

Figure 2.6: Identification of the flavin bound to Y118A SsuE using mass spectrometry. The Y118A SsuE variant was buffer exchanged with 25 mM potassium phosphate (pH 7.5) to remove glycerol. The flavin cofactor was extracted by heat denaturation at 80 ˚C for 10 mins followed by centrifugation. The mass-to-charge ratio *(m/z)* of the flavin extract was determined at room temperature using QTOF-MS in positive ion mode by direct injection.

The molar extinction coefficient of Y118A SsuE was determined by measuring the UV–visible spectroscopic absorbance at 457 nm, before and after denaturation of Y118A SsuE followed by centrifugation to remove precipitated protein. The molar extinction coefficient for Y118A SsuE at 457 nm was 13300 M^{-1} cm^{-1} at pH 7.5.[300] To establish the binding stoichiometry of Y118A SsuE and FMN, both the deflavinated protein and the extracted cofactor were quantified. The concentration of flavin-bound Y118A SsuE was determined using a Bradford assay, and the extracted FMN concentration was calculated using a molar extinction coefficient for FMN at 450 nm of 12500 $cm^{-1}M^{-1}$. A flavin:protein stoichiometry of 0.90 ± 0.06 was calculated from the ratio of the concentration of extracted flavin to monomeric Y118A SsuE. The K_d value for FMN binding to deflavinated Y118A SsuE was 8.2 ± 1 nM, approximately 2-fold lower than that of wild-type SsuE (17 ± 1 nM) (**Figure 2.7**).

2.3.3 Steady-State Kinetic Properties of Y118A SsuE

There were no observable structural perturbations in the Y118A SsuE variant based on results from CD spectroscopy (**Figure 2.4**), but it was not clear if the flavin-bound Y118A SsuE variant could support catalysis. Both flavin reductase and desulfonation assays were performed to evaluate the catalytic activity of Y118A SsuE. The flavin reductase assays measured the kinetic properties of Y118A SsuE only, and the desulfonation activity monitored the ability of the variant to supply reduced flavin to SsuD. A progressive decrease in absorbance at 457 nm was observed upon anaerobic titration of FMN-bound Y118A SsuE with NADPH (**Figure 2.8**). This was coupled with the gradual disappearance of the yellow flavin pigment in the reaction solution, which was slowly restored over approximately 30 min upon exposure of the same solution to oxygen. Full reduction of the bound flavin required approximately one equiv of NADPH (**Figure 2.8** inset).

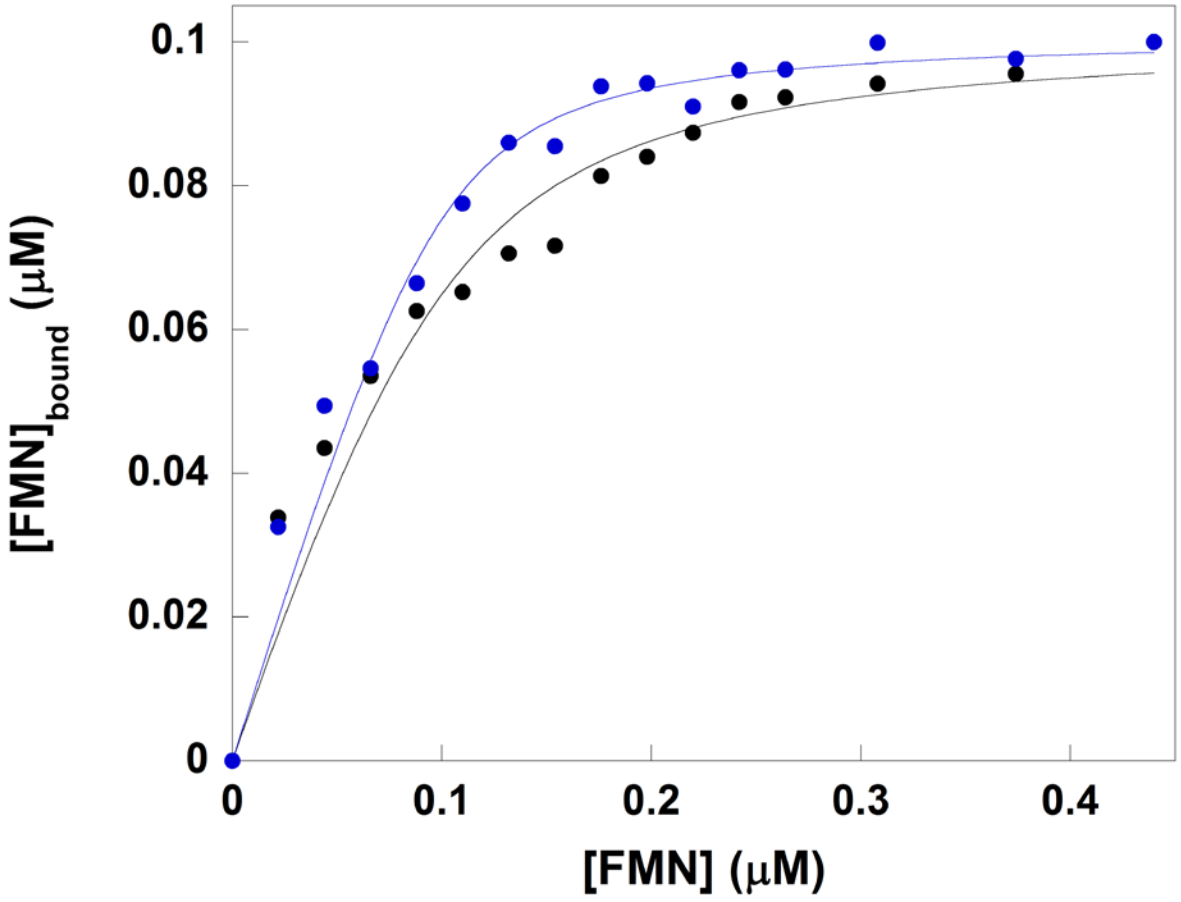

Figure 2.7: Flavin binding to Y118A and wild-type SsuE. A 1.0 mL solution of deflavinated Y118A or wild-type SsuE (0.1 μM) in 25 mM potassium phosphate (pH 7.5) and 0.1 M NaCl was titrated with FMN (0.022 to 0.44 μM), and the fluorescence spectrum recorded following a 2 min incubation after each addition of FMN (at an excitation wavelength of 280 nm and emission wavelength of 344 nm). The K_d value for FMN binding to deflavinated Y118A SsuE was 8.2 ± 1 nM approximately 2-fold lower than wild-type SsuE (17 ± 1 nM).

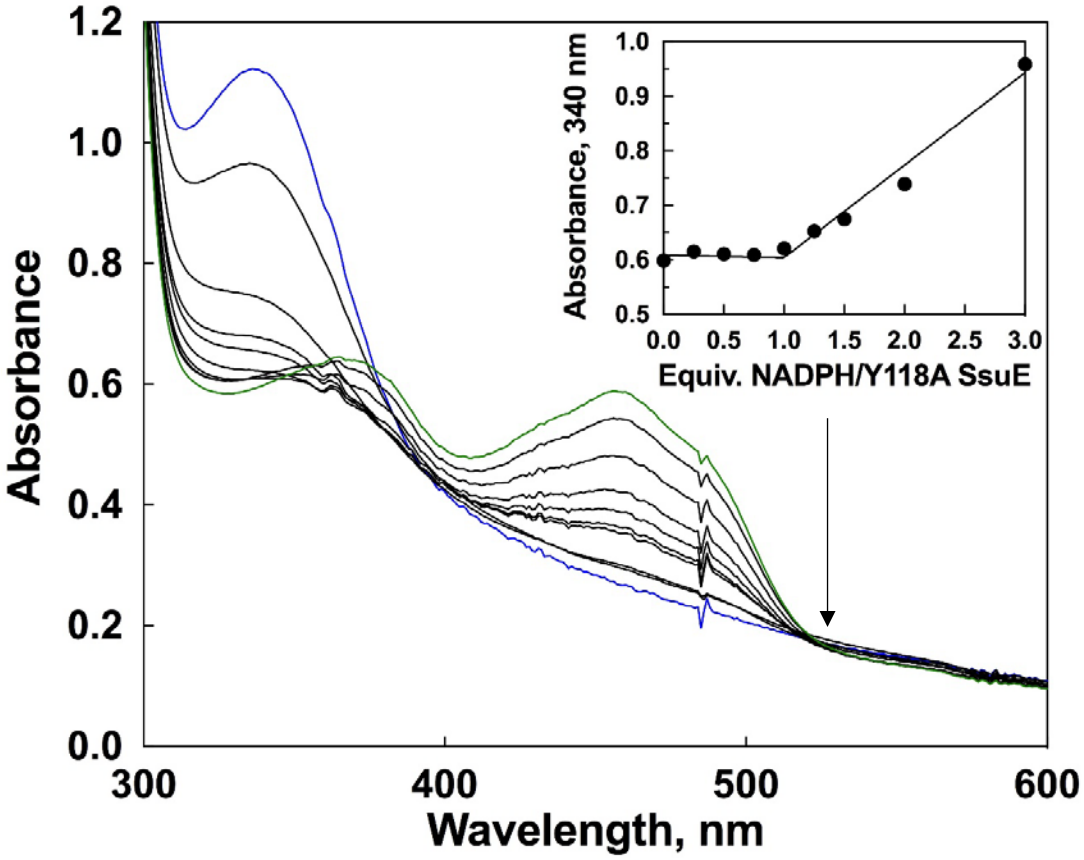

Figure 2.8: Anaerobic NADPH titration of FMN-bound Y118A SsuE. An anaerobic solution of FMN-bound Y118A SsuE (40 µM) in 25 mM potassium phosphate (pH 7.5), 0.1 M NaCl, and 10% glycerol was titrated with a solution of NADPH (1 mM) in 10 mM Tris-HCl (pH 8.5) at 25 ˚C. Spectra were recorded after the addition of 0-4 equiv of NADPH to Y118A SsuE. The arrow indicates the decrease in absorbance at 457 nm with the addition of each aliquot of NADPH. The oxidized FMN-bound Y118A SsuE spectrum is colored in green, and the reduced FMN spectrum after titration with NADPH is colored in blue. The inset shows the absorbance changes at 340 nm (closed circles) were plotted vs the equivalents of NADPH added. Linear regression of the 340 nm plot gave an average of 1.05 ± 0.06 equiv of NADPH oxidized per FMN.

The bound flavin was able to support reduction by NADPH in anaerobic titrations, and >99% of NADPH-reduced flavin remained bound to Y118A SsuE following anaerobic buffer exchange (**Figure 2.9**). Although the flavin was reduced in anaerobic titrations, the Y118A SsuE variant was unable to support NADPH oxidase activity as is typically observed with wild-type SsuE with varying concentrations of NADPH. The absence of NADPH oxidase activity corresponds to the slow reactivity of the flavin observed in the reductive titration with NADPH.

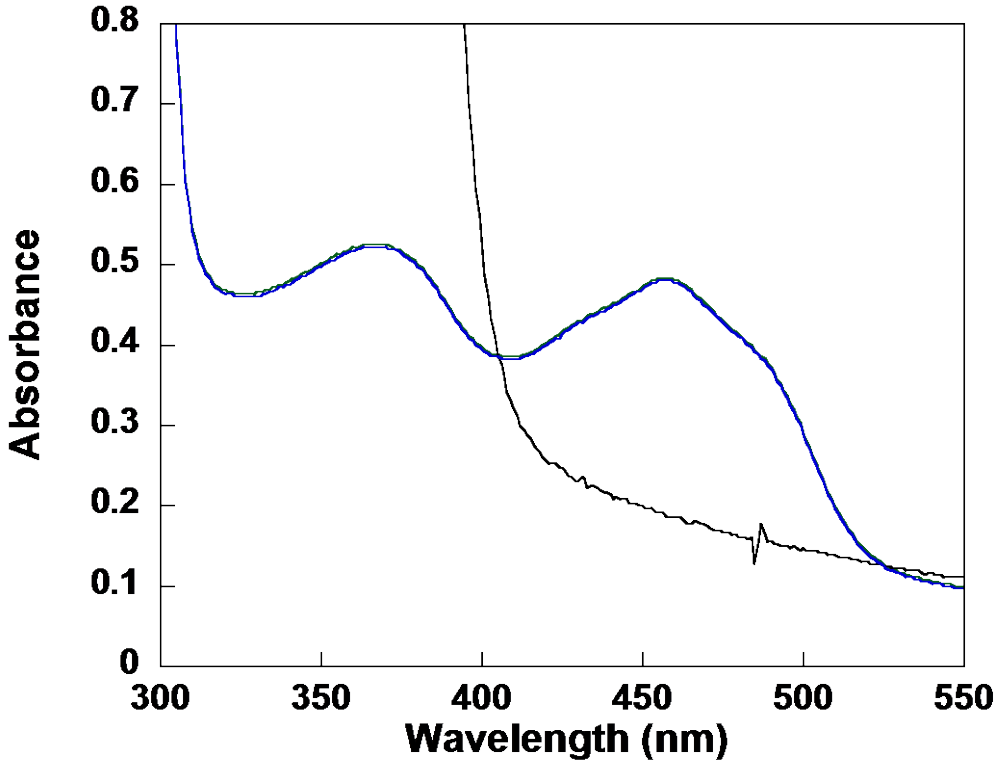

Figure 2.9: Reductive titrations of Y118A SsuE. UV-visible absorbance spectra of Y118A SsuE (green), NADPH reduced Y118A SsuE (black), and oxidized Y118A SsuE following equilibration of the reduced enzyme with atmospheric oxygen (blue). An anaerobic solution of Y118A SsuE (40 μM) was titrated with NADPH (0-160 μM) at 25 ˚C. Reduced Y118A SsuE was buffer washed in a centrifugation filter in an oxygen-free glovebox. Following the buffer wash the sample was allowed to air equilibrate to obtain the oxidized spectrum.

Although Y118A SsuE reacted slowly with oxygen, electron transfer from the reduced flavin to ferricyanide was observed with a k_{cat}/K_m value for NADPH of 10 ± 1 μM^{-1} min^{-1} (**Figure 2.10**). The ferricyanide concentration was saturating to maintain pseudo-first-order kinetic conditions at varying NADPH concentrations (**Figure 2.11**). Comparable experiments with wild-

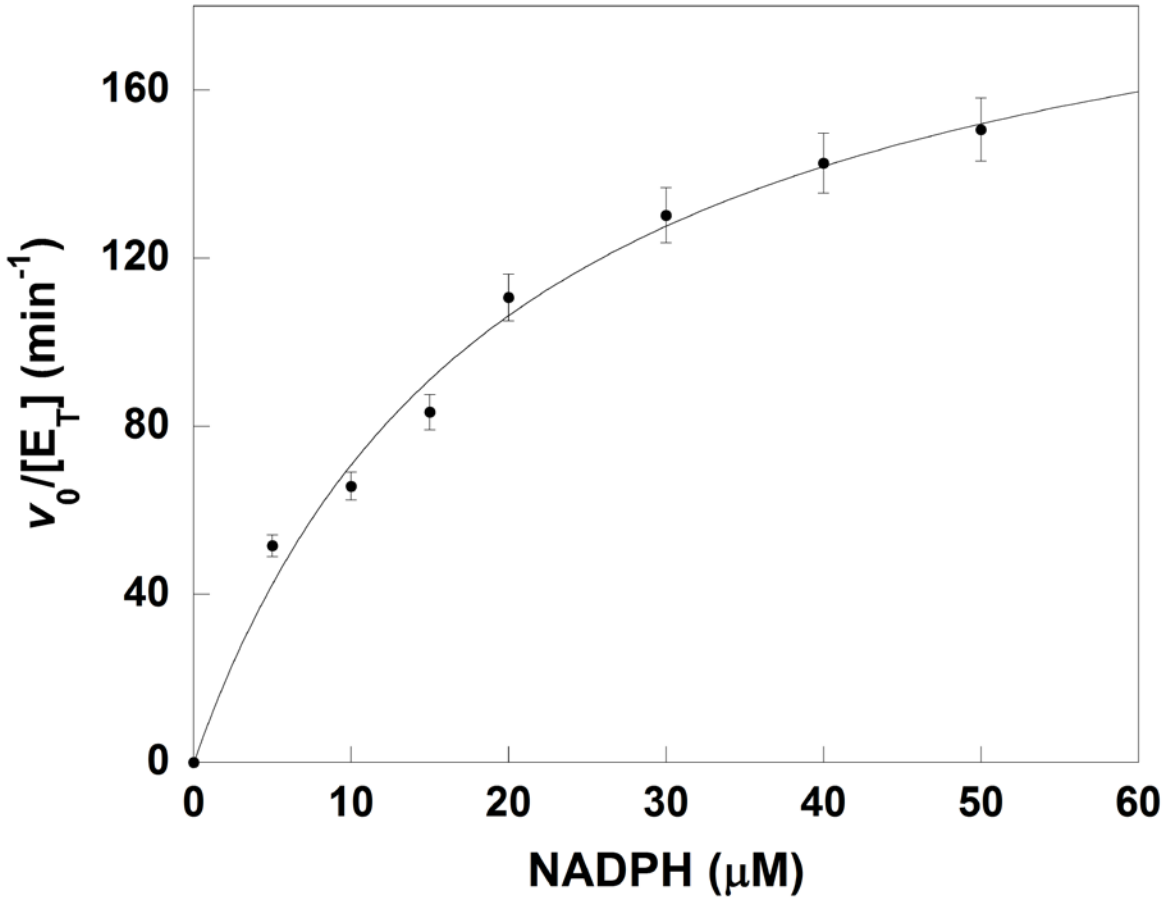

Figure 2.10: Steady-state kinetics of Y118A SsuE with ferricyanide. Initial rates were determined by measuring the decrease in absorbance at 340 nm for Y118A SsuE (0.04 μM) with varying concentrations of NADPH (5 – 50 μM), and ferricyanide (1 mM) in 25 mM Tris-HCl (pH 7.5) and 100 mM NaCl at 25 ˚C. The trace is the average of three separate experiments, and the data were fit to the Michaelis-Menten equation to obtain the steady state kinetic parameters.

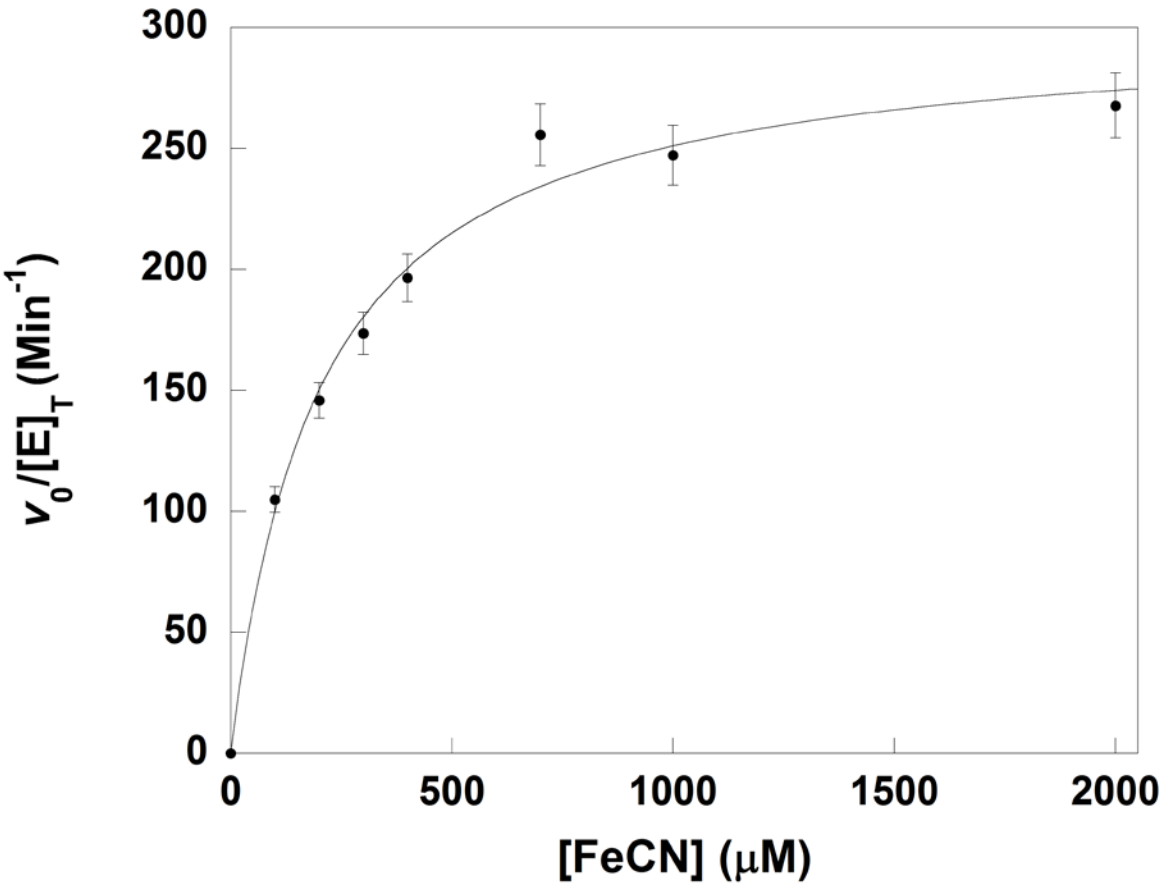

Figure 2.11: Steady-state kinetics of Y118A SsuE with ferricyanide. Steady-state kinetic experiment measuring electron transfer to ferricyanide was performed with FMN-bound Y118A SsuE (0.04 μM) at a constant NADPH concentration (200 μM) with varying concentrations of FeCN (0 - 2000 μM), in 25 mM Tris-HCl (pH 7.5) containing 100 mM NaCl at 25 ˚C. The ferricyanide was saturating at 1 mM in relation to varying concentrations of NADPH.

type SsuE could not be performed because the flavin is released following flavin reduction with wild-type SsuE due to the 1000-fold greater K_d value for reduced flavin relative to the K_d of the

oxidized form.[207, 208] In addition, there was no measurable sulfite generated with Y118A SsuE in the SsuD desulfonation reaction that is dependent on SsuE supplying reduced flavin to SsuD in the assay. Therefore, the Y118A SsuE reduced flavin was not effectively transferred from Y118A SsuE to SsuD to support desulfonation.

2.4 Discussion

The presence of π-helices in proteins has been linked to enhanced function and is generally characterized by intrastrand hydrogen bonding between an amide and carbonyl group five amino acid residues apart resulting in wide turns.[207, 208, 297, 298] These distinct secondary structural elements are often involved in interhelical interactions that play defined roles in protein function. Algorithms used to assign secondary structure often incorrectly annotate the π-helix as α-helices.[207, 208] However, with a growing interest in π-helices, specified functional roles for these secondary structural elements have been experimentally identified in a limited number of proteins. The π-helices generally have distinct amino acid preferences for aromatic and large aliphatic amino acids that are thought to stabilize the secondary structure through van der Waals interactions.[208] The π-helices are conserved within proteins that have related functions and have been used as markers for evaluating evolutionary relationships as well as identifying unique functions associated with protein families.

The single-residue substitution of Tyr118 with Ala in the π-helix of SsuE transforms the FMN-dependent reductase into a canonical flavoprotein retaining the specificity for FMN. There was a 2-fold increase in the affinity of Y118A SsuE for oxidized FMN compared to that of the wild-type enzyme. Although the increase in FMN affinity was minimal, this difference may be enough to

shift the Y118A SsuE variant to a canonical flavoprotein. The Y118A SsuE flavin cofactor was reduced in reductive titrations, and the flavin remained bound to the Y118A SsuE variant following multiple buffer washes in a centrifugal filter under anaerobic conditions. Interestingly, Y118A SsuE was unable to support standard NADPH oxidase and desulfonation activities observed for the wild-type enzyme. Therefore, the flavin is reduced, but the reduced flavin is not released and effectively transferred to SsuD. Structural evaluation of π-helices supports a role for these secondary structures in substrate and cofactor recognition.[207, 208, 297, 298] The π-helix in soybean lipoxygenase is dynamic and participates in the recognition of the fatty acid substrate.[272] Additionally, some metalloproteins utilize π-helical structures for the proper positioning of coordinating metal ligands.[301] Thus, π-helical regions can provide a unique support for aligning critical residues, such that their orientation and separation are optimal for amino acid side chain interactions. In the three-dimensional structure of SsuE, hydrogen bonding occurs between the hydrogen of the hydroxyl group of Tyr118 and the oxygen atom backbone carbonyl of Ala78 across the tetramer interface (**Figure 2.12**). The amide nitrogen of Ala78 hydrogen bonds to the O4 atom of FMN bound to the active site. Substitution of Tyr118 to Ala should disrupt the hydrogen bonding interactions with Ala78 across the tetramer interface (**Figure 2.12**). The preservation of this intricate hydrogen-bond network may be essential in maintaining the functional properties of SsuE. In SsuE, the hydrogen bonding network formed by the π-helix may function in maintaining the structural integrity and requisite flavin contacts crucial for effective transfer.[62] Substitution of Tyr118 with Ala in SsuE likely altered critical contacts made by the π-helix across the tetramer interface leading to an active site environment that supports flavin reduction but not the subsequent transfer to SsuD (**Figure 2.12**).

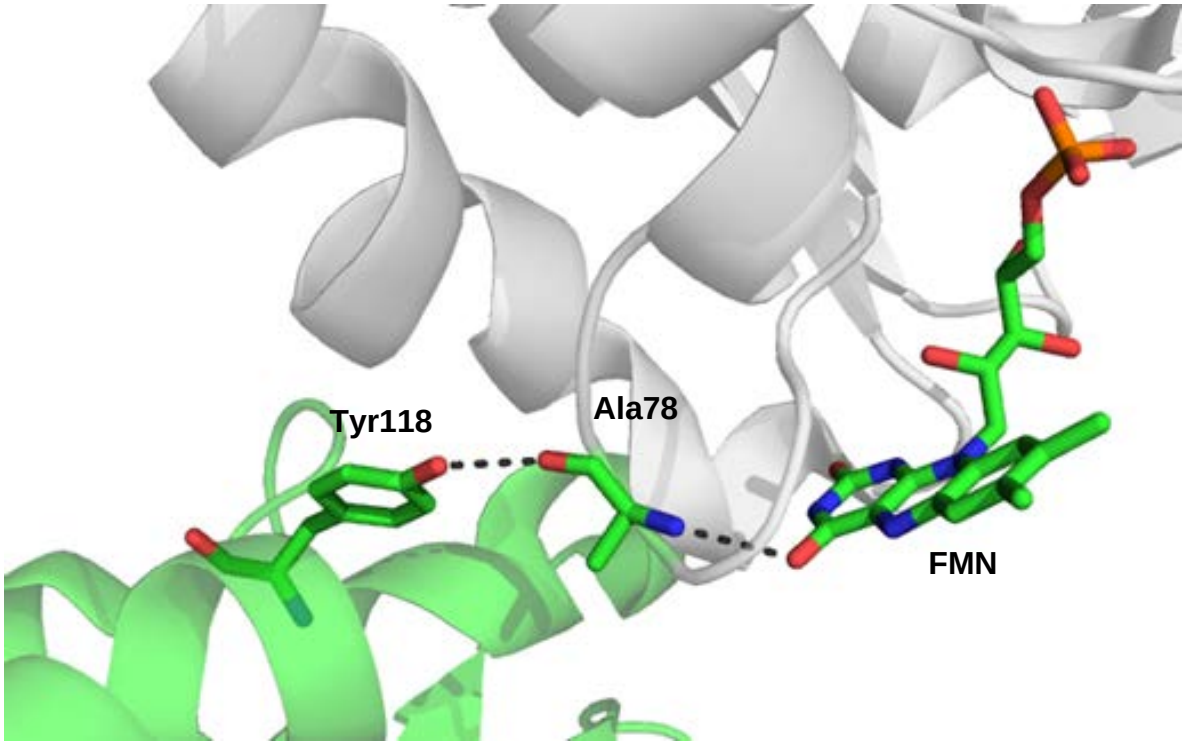

Figure 2.12: Hydrogen bonding interactions of Tyr118 centered in the π-helix of SsuE. A hydrogen bonding network is formed between the dimer interface of SsuE. The Tyr hydroxyl group forms a hydrogen bond with the α-carbonyl group of Ala78 across the tetramer interface. FMN bound to the active site is stabilized through hydrogen bonding of the amide nitrogen of Ala78 to the O4 atom of the flavin. The structure was rendered with PyMOL using Protein Data Bank entry 4PTY for SsuE.

Interestingly, the reduced FMN-bound Y118A SsuE variant showed a relatively slow reactivity with oxygen, but NADPH oxidation by the variant could be monitored with ferricyanide as the electron acceptor. Canonical flavoproteins display marked differences in their reactivity with oxygen, but there are no clearly defined structural features that explain these differences.[160] A combination of charge distribution, dynamics, ligand binding, and solvation effects has been

proposed to play a role in controlling the oxygen reactivity of flavoproteins.[156, 160] However, the distinct structural properties that control oxygen reactivity for two-component flavin reductases have not been fully assessed. The active site of SsuE would need to protect the reduced flavin prior to flavin transfer. The ability of the active site to protect reduced flavin from oxidation in wild-type SsuE is difficult to evaluate because of the immediate release of the flavin following reduction. The structural properties of the active site may slow the reactivity of reduced flavin with molecular oxygen, and may be a mechanistic feature of flavin reductases associated with two-component systems that utilize flavin as a substrate.

The SsuE enzyme was previously classified as a member of the NAD(P)H:FMN reductase family.[5] Members of the NAD(P)H:FMN reductase family all have a flavodoxin fold and exist as dimers or tetramers with similar oligomeric geometries. The enzymes belonging to the NAD(P)H:FMN reductase family are further divided on the basis of the presence or absence of a π-helix. Members of the subgroup of the NAD(P)H:FMN reductase family that contain a π-helix are members of two-component systems, but there are limited structures available for this group. Some members of the NAD(P)H:FMN reductase family are canonical flavin reductases with a bound flavin that contain an α-helix in a position comparable to that of the π-helix due to the absence of the Tyr insertion. Comparison of the helix α4 of the canonical flavoprotein *Shigella flexneri* ArsH (gray) from the NAD(P)H:FMN reductase family with the π-helix in SsuE shows the formation of a distinct bulge in SsuE resulting from the insertion of Tyr118 (**Figure 2.2**).[62, 204] The results described provide compelling evidence of the importance of the π-helix in SsuE and promote a potential role of the π-helix in other FMN-dependent reductases. Studies that aim to identify the role of the π-helix in SsuE provide a tractable system for other flavin reductases that also possess a π-helix within the subgroup of the flavodoxin superfamily. The π-helix appears to

offer an evolutionary advantage to SsuE by promoting flavin transfer, but the rationale for how the π-helix evolved in these systems is not known**.** The results reported herein serve as a foundation for further studies to firmly establish the role and evaluate the evolutionary relationship of the π-helices in SsuE and related flavin reductases. A reasonable explanation for the π-helix in a two-component system would be to provide a structural switch to promote flavin transfer. The coordinated regulation of flavin reduction and transfer is imperative in the alkanesulfonate monooxygenase system given the role of the system in providing an alternative sulfur source when optimal sources of sulfur are limiting. Environmental pressures resulting from sulfur starvation may have led to an autonomous enzyme system in bacteria to provide an alternate mechanism for sulfur acquisition. Independent reductive and oxidative half-reactions would provide a means for these systems to adjust their substrate specificities and independently develop regulatory mechanisms for promoting flavin transfer. However, it is still not certain if FMN-dependent two-component systems represent a more recent model for oxygenase reactions, and if the π-helix in SsuE is coupled to the mechanistic and regulatory strategies of two-component systems. These studies support a model in which the π-helix in SsuE tetramer interface provides the FMN reductase transformative mechanistic properties that allow the enzyme to be a part of the two-component monooxygenase system.

CHAPTER THREE

3 Regulation of Catalytic Activity and Oligomeric State Changes in FMN Reductases of Two-Component Monooxygenase systems

3.1 Introduction

The desulfonation enzymes SsuE and SsuD are upregulated in bacteria during sulfur starvation to cleave the C-S bonds of various alkanesulfonates generating sulfite.[57] The sulfite generated is incorporated into various sulfur containing biomolecules. The SsuD enzyme binds reduced flavin supplied by the SsuE enzyme, then activates dioxygen to form the C4a-(hydro)peroxyflavin intermediate. Following dioxygen activation, the SsuD enzyme utilizes the C4a-(hydro)peroxyflavin intermediate to cleave alkanesulfonates releasing a molecule of sulfite, FMN, water and the corresponding aldehyde.[57] The substrate promiscuity characteristic of SsuD helps mitigate sulfur scarcity when bacteria are in sulfur limiting conditions.[57] For the desulfonation reaction to occur, reduced flavin has to be transferred from SsuE to SsuD. Flavin reductases of two-component monooxygenase systems are able to effectively transfer reduced flavin to the monooxygenase enzymes in the presence of molecular oxygen.[194] However, the structural properties that enable these flavin reductases to traffic the labile reduced flavin product to the oxygenase are not understood.

The structural and conformational changes in enzymes of two-component monooxygenase systems must be synchronized to simultaneously support flavin reduction, reduced flavin transfer, and the oxidation of substrates. The transfer of reduced flavin from SsuE to SsuD was suggested to occur through protein-protein interactions because protein-protein interactions were observed between SsuE and SsuD through affinity chromatography and fluorimetric titrations.[215] Recent hydrogen-deuterium exchange mass spectrometry studies identified the interaction sites in both

SsuE and SsuD.[229] The interaction sites in SsuD are located over the active site of SsuD, at a loop region which was shown to be highly flexible during catalysis.[222, 229, 302] Partial deletion of the interaction region in the loop region of SsuD eradicated the ability of SsuD to interact with SsuE resulting in loss of desulfonation activity.[229] In the SsuE enzyme, the interacting regions include the π-helix located at the tetramer interface of SsuE. This π-helix is associated with a tyrosine residue (Tyr118) inserted at helix α4 resulting to a bulge at the point of insertion.[62] Both the π-helix and the insertional tyrosine residue are highly conserved in flavin reductases of two-component monooxygenase systems.[62, 303]

Results from studies with SsuE suggested the enzyme undergoes substrate-induced oligomeric state changes. The SsuE enzyme is flavin-free as purified, exists as a tetramer, and utilizes flavin as a substrate. When an equimolar concentration of FMN was added, the oligomeric state of SsuE changed to a dimer.[62] Such oligomeric state changes are increasingly being observed in various flavin reductases but the reason for adoption of different oligomeric states has not been evaluated.[293-295] Structural analyses have suggested a potential link between the π-helix of SsuE and the observed flavin-induced oligomeric state changes. The hydroxyl group of Tyr118 residue in SsuE forms a hydrogen bond with the carbonyl group of Ala78, while the N-atom of Ala78 forms a hydrogen bond with the O4 of FMN. In addition, the loop region before the π-helix borders the FMN binding site and facilitate flavin binding through hydrogen bonds with the amide groups of Gly108 and Thr109, and through the side chain of His112. As a result, the loop region and π-helix in SsuE were thought to contribute in the flavin-induced oligomeric shifts.[62]

Perturbation of the π-helix in SsuE through the substitution of Tyr118 with Ala resulted in a FMN-bound SsuE variant.[303] Although the Y118A SsuE variant retained flavin specificity for FMN, the flavin remained bound even when reduced. The reduced Y118A SsuE variant had slow

reactivity in NADPH oxidase assays, but supported electron transfer to ferricyanide. There was no measurable sulfite production by SsuD when coupled with Y118A SsuE, which correlated with the inability of Y118A SsuE to support multiple flavin reduction turnovers.[303]

The identification of π-helices as discrete secondary structures is often overlooked when characterizing three-dimensional structures of proteins.[207, 208] An extensive secondary structural analysis determined ~15% of protein structures contain π-helices. Increasing exploration of π-helices shows they are catalytically relevant in >80% of enzymes containing the π-helical structures.[207, 208] The conserved π-helices in evolutionary-related flavin reductases of two-component systems suggests the π-helices have common functionalities. The characterization and kinetic studies on Y118A SsuE were requisite in determining the roles of π-helix in SsuE, but it was not feasible to make resolute functional conclusions based on the Y118A SsuE variant alone. Additional Tyr118 SsuE variants were generated for structural and functional investigations on the role of the π-helix in flavin reduction and transfer, and in regulating oligomeric state changes in SsuE.

3.2 Materials and methods

3.2.1 Materials

E. coli strains (XL-1 and BL21(DE3)) were purchased from Stratagene (La Jolla, CA). Plasmid vectors and pET21a were obtained from Novagen (Madison, WI). DNA primers were synthesized by Invitrogen (Carlsbad, CA). Ampicillin, streptomycin sulfate, lysozyme, potassium bromide, ammonium sulfate, reduced nicotinamide adenine dinucleotide phosphate (NADPH), flavin adenine dinucleotide (FAD), flavin mononucleotide (FMN), bovine serum albumin (BSA), glycine, lysozyme, ethylenediaminetetraacetic acid (EDTA), potassium phosphate (monobasic anhydrous and dibasic anhydrous), dimethyl sulfoxide (DMSO), 5,5-dithiobis-(2-nitrobenzoic

acid) (DTNB), lysozyme, and urea were from Sigma (St. Louis, MO). Isopropyl-β-D 1-thiogalactoside (IPTG), sodium chloride, and glycerol were obtained from Macron Fine Chemicals (Center Valley, PA). 1-octanesulfonate was purchased from Fluka (Milwaukee, WI).

3.2.2 Site-Directed Mutagenesis and Purification of the Y118 SsuE Variants

Variants of Tyr118 in SsuE were generated to investigate the roles of the π-helix in flavin reduction and transfer to SsuD, and in the regulation of oligomeric state changes. The SsuE primers were designed as 27-base oligonucleotides for the Y118S, Y118F, and ΔY118 SsuE variants. The primers were ordered from Life Technologies by substituting TAT for Tyr with TCT, TTT, and deleting the TAT codon for the Y118S, Y118F, and ΔY118 SsuE variants, respectively. The Qiagen kit plasmid purification protocol was utilized to prepare the SsuE plasmid used for site-directed mutagenesis. Following site-directed mutagenesis, the SsuE variants were confirmed through DNA sequencing analysis (Eurofins/Genomics, Louisville, KY). The previously generated Y118A SsuE variant was also utilized in these studies.[303] The SsuD and SsuE enzymes were expressed and purified from a pET21a expression vector in *E. coli* strain BL21(DE3) as previously described.[2] The protein fractions for the flavin-free SsuE enzymes and SsuD were collected based on the UV-visible absorbance at 280 nm. For the flavin-containing SsuE variants, the fractions were collected based on UV-visible absorbance at 457 nm. The secondary structural analysis on the Y118 SsuE variants was performed using circular dichroism studies from 300 to 185 nm with 1 nm increments as previously outlined.[303]

3.2.3 Kinetic Analysis of the Y118 SsuE Variants

Flavin reductase and desulfonation activity was assessed with the Y118 SsuE variants as previously described.[61, 303] The flavin reductase assays were performed on Y118 SsuE variants (0.04 μM) by varying FMN concentrations (0-1.5 μM) at a fixed NADPH concentration (200 μM),

and monitoring NADPH oxidation through the decrease in UV-visible absorbance at 340 nm. The initial rates were obtained by fitting the linear part of the reaction when <10% of NADPH had been consumed.[193] The steady-state coupled assay with SsuE and SsuD monitoring sulfite production was performed as previously described.[61]

Rapid-reaction kinetic analysis with the Y118 SsuE variants were performed using an Applied Photophysics SX.18 MV stopped-flow spectrophotometer as previously outlined.[218] The single-turnover experiment was performed by mixing wild-type or Tyr118 variants of SsuE (35 μM) with wild-type SsuD (35 μM) and FMN (30 μM) in 50 mM potassium phosphate (pH 7.5), 0.2 M NaCl, and 10% glycerol in one syringe against 250 μM NADPH and 50 μM octanesulfonate in 10 mM Tris–HCl (pH 8.5), 0.1 M NaCl, and 10% glycerol. Similar rapid kinetic experiments were set up in the absence of SsuD and octanesulfonate to monitor the flavin reduction half-reaction and the subsequent non-enzymatic flavin oxidation.[218] The experiments were performed in single-mixing mode by reacting equal volumes of solutions from each syringe. The change in absorbance at 450 nm was monitored over 100 seconds. The kinetic trace was standardized and plotted in Kaleidagraph (Synergy) software.

3.2.4 Fluorimetric Titrations of the Y118 SsuE Variants with SsuD

FMN-bound Y118 SsuE variants (0.4 μM) in 25 mM potassium phosphate (pH 7.5) were titrated with 0.04 - 1.1 μM aliquots of SsuD as previously described.[215] The fluorescence emission at 525 nm was measured (using an excitation wavelength of 450 nm) on a Cary Eclipse Agilent (Santa Clara, CA) fluorescence spectrophotometer with slit widths set at 5 nm. The concentrations of SsuD bound to FMN-bound SsuE variants were calculated using **Equation 3.1**,

$$[SsuD]_{bound} = [SsuE]\frac{I_0 - I_c}{I_0 - I_f} \qquad \textbf{Equation 3.3}$$

in which [SsuE] is the concentration of SsuE used, I_0 is the fluorescence intensity of FMN-bound

SsuE before SsuD titration. I_c represents the fluorescence intensity of SsuE after each SsuD addition while I_f is the fluorescence intensity after the final SsuD addition. The $[SsuD]_{bound}$ (y) was plotted against the total SsuD concentration, and the dissociation constant (K_d) was calculated using **Equation 3.2.**

$$y = \frac{(K_d+x+n)-\sqrt{(K_d+x+n)^2-4xn}}{2} \qquad \textbf{Equation 3.4}$$

3.2.5 Evaluation of the Mechanism of Reduced Flavin Transfer between SsuE and SsuD

To identify the role of protein-protein interactions in reduced flavin transfer, the previously generated inactive Y118A SsuE variant was utilized to compete with SsuE for interaction sites on SsuD in desulfonation assays.[303] The reaction mixture contained SsuE (0.06 µM), FMN (2 µM), SsuD (0.06 µM), octanesulfonate (1 mM), NADPH (0.25 mM), and varying concentrations of Y118A SsuE (0.01-0.3 µM) in 25 mM Tris (pH 7.5), and 0.1 M NaCl in a total volume of 0.5 mL. The endpoint assay was initiated by the addition of NADPH and was incubated for 3 minutes at 25 °C, and quenched with the addition of 8 M urea (167 µL). The sulfite product was measured as previously described.[61] An experiment to evaluate the dependence of desulfonation on the concentration of wild-type SsuE was performed in the absence of Y118A SsuE by varying wild-type SsuE (0.01- 0.12 µM) at constant concentrations of substrates and SsuD as outlined above.

3.2.6 Evaluation of the Oligomeric States of the Y118 SsuE Variants

The molecular weights of the Y118 SsuE variants (50 µM) were determined using Agilent Bio SEC-3, 4.6 x 300 mm, 100 Å column loaded into a 1260 Infinity GPC/SEC chromatograph. The flow rate was 0.2 mL/min and the injection volume was 100 µL. The experiment was run with 150 mM sodium phosphate (pH 7.0), and 100 mM NaCl. A gel filtration standard from Bio-Rad (1.35 to 670 kDa) was used to generate a curve for fitting the molecular weights based on retention

times. The standard curve (Log of molecular weight versus retention time) was generated based on the elution time monitored at 280 nm.

3.2.7 Crystallization of Y118A SsuE.

The Y118A SsuE enzyme for three-dimensional studies was purified as previously outlined.[2, 303] Following purification, the Y118A SsuE enzyme was buffer exchanged with 10 mM HEPES (pH 7.0), and 0.1 M NaCl, and concentrated to 11 mg/mL. Crystal growth was carried out by the hanging drop method at 24 °C. Drops containing 4 μL of purified SsuE Y118A protein at 11 mg/mL were mixed with 2 μL of a reservoir solution of 0.1 M sodium citrate, 12.5% PEG 6000 and small crystals (25 x 25 x 50 μm) formed by 3 – 4 days. For data collection, crystals were soaked in a storage buffer of 0.1 M sodium citrate, 20% PEG 3350 followed by soaking in a cryo solution and serially washed in 0.1 M sodium citrate, 20% PEG 3350 supplemented with 20% (v/v) glycerol as a cryoprotectant for less than 30 s and flash cooled at -160 °C.

3.2.8 Data Collection and Solution of the Three-Dimensional Structure of Y118A SsuE.

Diffraction data (0.25° oscillation images for a total of 180°) were collected at the Stanford Synchrotron Radiation Laboratory (Stanford, CA) beamline 14-1 at a wavelength of 0.9795 Å at 100 K. The exposure time per frame was 9.92 s with a crystal to detector distance of 300.0 mm. The data were indexed and scaled with XDS to 2.12 Å.[304] The crystals were assigned to the space group C2 with unit cell dimensions a = 82.68 Å, b = 41.67 Å, c = 96.04 Å, and β = 101.02° (**Table 3.1**). Molecular replacement calculations were performed using Phaser in the Phenix program suite, using molecule A of 4BTZ as the search model with all ligands including FMN, waters, and alternate conformations removed and all B factors set to 20, yielding a clear solution with a log likelihood gain of 697 with two molecules in the asymmetric unit.[305]

The model was improved with a round of Auto Build in PHENIX. Further model building and refinement were performed using Coot and Phenix Refine.[306] Waters were added automatically in Phenix, and the positions were verified following a cycle of refinement. Molecule A contains residues 1 – 183, and molecule B contains residues 1 – 173. Ramachandran analysis by MolProbity showed good geometry with 98.0% of the residues in the favored region and no residues in the outlier region. The model includes 64 water molecules and no FMN was present in either molecule.[307]

Table 3.1: Data Collection and Refinement Statistics for Y118A SsuE

	Apo Y118A SsuE
Data collection[a]	
Beamline	14-1
Wavelength (Å)	0.9795
Space group	C2
Cell dimensions; *a*, *b*, *c* (Å), β (°)	82.68, 41.67, 96.04, 101.02
Resolution (Å)	37.07 - 2.12 (2.18 - 2.12)
R_{merge}[b]	0.099 (0.604)
Total observations	69578 (5405)
Total unique observations	18557 (1457)
Mean ((*I*) / sd(*I*))	8.4 (2.0)
Completeness (%)	95.8 (88.9)
Redundancy	3.8 (3.7)
Wilson B-factor	24.45
Refinement	
Resolution (Å)	35.57 - 2.117 (2.193 - 2.117)
R_{cryst}[c]	0.1651 (0.1986)
R_{free}	0.2341 (0.2825)
Total unique observations	18540 (1799)
No. of non-hydrogen atoms	
Protein	2796
Water	64
rms deviation bonds (Å)	0.012
rms deviation angles (°)	1.120
Overall mean B-factor (Å^2)	29.56
Ramachandran plot analysis[d]	
Favored region	98.0

Allowed region	2.0
Outlier region	0.00

[a]data indexed and scaled with XDS

[b]$R_{merge} = \Sigma_h|I_h - <I>|/\Sigma_h I_h$, where I_h is the intensity of reflection *h*, and <*I*> is the mean intensity of all symmetry-related reflections

[c]$R_{cryst} = \Sigma||F_o| - |F_c||/\Sigma|F_o|$, F_o and F_c are observed and calculated structure factor amplitudes. Five percent of the relections were reserved for the calculation of R_{free}.

[d]Calculated with MolProbity

3.3 Results

3.3.1 Site-Directed Mutagenesis and Purification of the Y118 SsuE Variants

The conserved π-helix centrally located at the tetramer interface in SsuE is derived from a Tyr118 insertion in helix α4 resulting into a bulge at the insertion point. To investigate the functional and structural roles of the π-helix in SsuE, several variants of Tyr118 were generated. A Tyr118 SsuE deletion variant was generated because the known π-helices in flavin reductases of two-component monooxygenase systems are associated with insertion of a tyrosine at the tetrameric interface position.[62] The Y118S SsuE variant was generated to conserve the hydroxyl group of Tyr118, which is within hydrogen bonding distance to Ala78 across the tetramer interface. In addition, the Y118F SsuE variant was generated to conserve the phenyl group associated with the tyrosine residue.

All the variants including the previously generated Y118A SsuE variant were expressed and purified as previously described.[2, 303] The Y118S SsuE variant was FMN-bound similar to the Y118A SsuE, but the Y118F and ΔY118 SsuE variants were flavin-free similar to wild-type SsuE.[303] The molecular weight of ΔY118 SsuE enzyme was confirmed through mass spectrometry. Interestingly, the Y118S SsuE variant was FMN-bound as was previously observed with Y118A SsuE. There were no significant perturbations in the gross secondary structure of the Y118 SsuE variants compared to the wild-type SsuE based on circular dichroism spectra.

3.3.2 Steady-State Kinetics on Y118 SsuE Variants

Flavin reductase assays were performed with the Y118 SsuE variants to determine if electron transfer was affected by the substitutions at the π-helix. The flavin reductase activity was monitored under steady-state kinetic conditions for the Y118S, Y118F, and ΔY118 SsuE variants monitoring oxidation of NADPH. The Y118S and ΔY118 SsuE variants could not sustain flavin reductase activity. However, the Y118F SsuE variant had a k_{cat}/K_m value of 4000 ± 30 μM^{-1} min^{-1} comparable to the wild-type value of 2300 ± 200 μM^{-1} min^{-1} (**Table 3.2**). The Y118 SsuE variants with an amino acid substitution gave comparable dissociation constants for binding FMN as wild-type SsuE (**Table 3.2**).[303] The ΔY118 SsuE variant had 10-fold lower binding affinity for flavin than wild-type SsuE.

	k_{cat} (min^{-1})	K_m (μM)	k_{cat}/K_m ($\mu M^{-1}min^{-1}$)	K_d (nM)
Wild-type SsuE	255 ± 27	0.11 ± 0.02	2300 ± 200	17
Y118A SsuE[a]	-	-	-	8.2
Y118S SsuE	-	-	-	7
Y118F SsuE	316 ± 2	0.08 ± 0.02	4000 ± 30	50
ΔY118 SsuE	-	-	-	170

Table 3.2: Steady-state kinetic parameters for the Y118 SsuE variants measuring NADPH-dependent FMN reductase activity. The flavin reductase assays were performed with Y118 SsuE (0.04 μM) at varying concentrations of FMN (0−1.5 μM) in 25 mM Tris-HCl (pH 7.5), and 100 mM NaCl, with the NADPH concentration held constant (200 μM). The reaction temperature was maintained at 25 °C. [a] was previously reported in [303].

Flavin reductases of two-component systems must transfer reduced flavin successfully to the monooxygenase enzymes for the insertion of single oxygen atom(s) into respective substrates to occur. Coupled assays were performed to evaluate the ability of the Y118 SsuE variants to support desulfonation. There was no measurable desulfonation activity observed in coupled assays (monitoring sulfite production) with the Y118A, Y118S SsuE, and ΔY118 SsuE variants (**Table 3.3**). However, desulfonation activity was observed with the Y118F SsuE variant with a k_{cat}/K_m value of 2.0 ± 0.5 μM^{-1} min^{-1} compared to the wild-type SsuE value of 2.2 ± 0.3 μM^{-1} min^{-1} (**Table 3.3**). The desulfonation activities with the Tyr118 SsuE variants correlated with the observed flavin reductase activities.

	k_{cat} (min^{-1})	K_m (μM)	k_{cat}/K_m ($\mu M^{-1}min^{-1}$)
Wild-type SsuE	93 ± 7	43 ± 6	2.2 ± 0.3
Y118A SsuE[a]	-	-	-
Y118S SsuE	-	-	-
Y118F SsuE	16 ± 4	8 ± 1	2.0 ± 0.5
ΔY118 SsuE	-	-	-

Table 3.3: Desulfonation activity of wild-type SsuD with the Y118 SsuE variants. Steady-state desulfonation kinetics coupling SsuE with SsuD in the presence of NADPH, FMN, oxygen, and octanesulfonate. The reaction mixture contained 0.2 μM of SsuD, 0.6 μM of SsuE, 2 μM FMN, and 0.5 mM NADPH with varying octanesulfonate (10 to 1000 μM). The desulfonation experiment was performed in 25 mM Tris (pH 7.5) and 0.1 M NaCl, at 25 °C. [a] was previously reported in [303].

3.3.3 Rapid Reaction Kinetics Studies on Y118 SsuE Variants

Rapid-reaction kinetic experiments were performed with the Y118 SsuE variants to further evaluate the functional roles of the π-helix in flavin reduction and transfer to SsuD. The reductive and oxidative half-reactions were monitored at 450 nm under single-turnover conditions. The reductive half-reaction catalyzed by wild-type SsuE was followed by a lag phase in the presence of SsuD (**Figure 3.1** and **Figure 3.2**). The lag phase was proposed to represent the transfer of reduced flavin from SsuE to SsuD which involves protein-protein interactions or conformational changes associated with the binding of reduced flavin by SsuD.

Following the lag phase, an increase in absorbance at 450 nm was observed due to oxidation of the reduced flavin. This lag phase between flavin reduction and oxidation was not observed with wild-type SsuE alone (when SsuD and octanesulfonate are not included in the reaction) because the oxidation of reduced flavin occurs immediately following the reduction phase. The oxidative half-reaction was non-enzymatic because SsuD and octanesulfonate were not included in the reaction. The kinetic traces for Y118A, Y118S and ΔY118 SsuE variants showed the reductive half-reaction, but there was no measurable $FMNH_2$ oxidation following the reductive half-reaction with these SsuE variants in the presence or absence of SsuD (**Figure 3.1** and **Figure 3.2**).

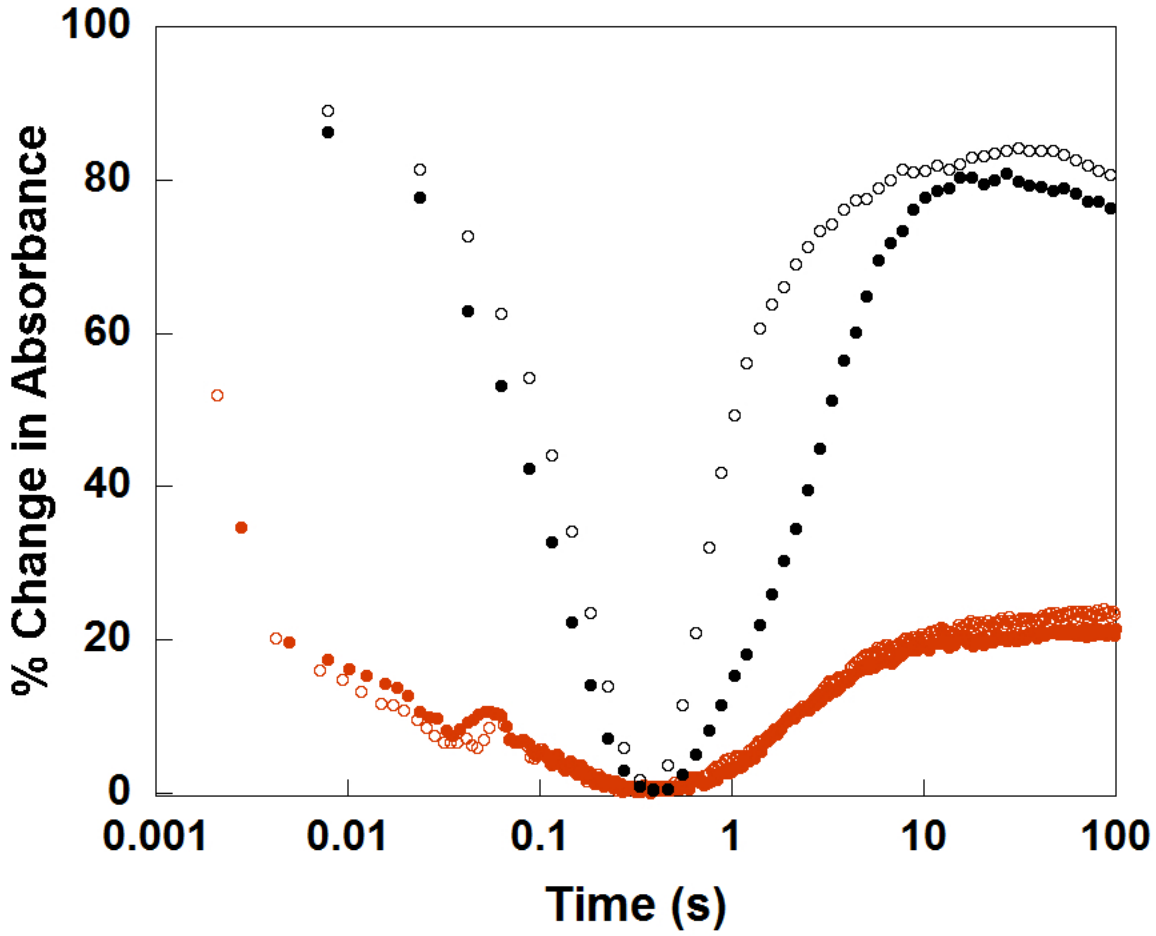

Figure 3.1: Rapid-reaction kinetics with Y118A SsuE. Stopped-flow kinetics monitoring flavin reduction and oxidation with Y118A SsuE in flavin reductase conditions only, or when coupled with SsuD for desulfonation. Kinetic traces of Y118A SsuE (○), and wild-type SsuE (○) when only FMN and NADPH are added; and for Y118A SsuE and SsuD (●), or wild-type SsuE and SsuD (●) when FMN, NADPH, and octanesulfonate was included in the reaction. The kinetic traces were monitored at 450 nm by mixing Y118A or wild-type SsuE (35 μM) with FMN (30 μM) and SsuD (35 μM when included), against NADPH (250 μM) and 50 μM octanesulfonate when SsuD was included. The experiments were performed in 25 mM potassium phosphate buffer, pH 7.5, at 4 °C.

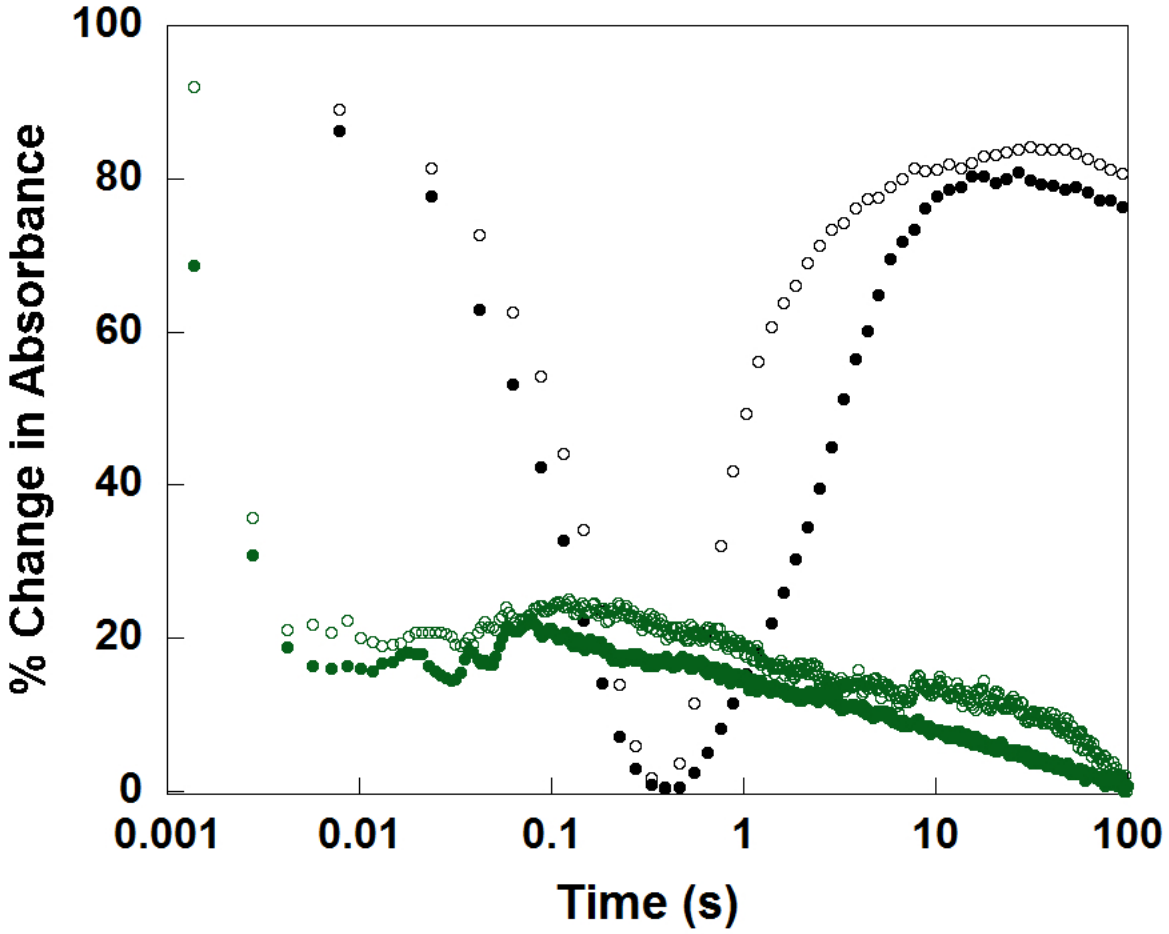

Figure 3.2: Rapid-reaction kinetic with ΔY118 SsuE. Rapid reaction kinetics of ΔY118 SsuE (compared to wild-type SsuE) in flavin reductase conditions and when coupled with SsuD for desulfonation in the presence of oxygen. Kinetic traces of ΔY118 SsuE (○), and wild-type SsuE (○) when only FMN and NADPH are added; and for ΔY118 SsuE and SsuD (●), or wild-type SsuE and SsuD (●) when FMN, NADPH, and octanesulfonate was included in the reaction. The traces were obtained as described in **Figure 3.1**.

3.3.4 Evaluation of the Oligomeric States of Y118 SsuE variants

The oligomeric states of the Y118 SsuE variants were evaluated to determine the effect of substituting or deleting Tyr118 in SsuE on the quaternary structure of SsuE. The Tyr118 in SsuE is within hydrogen bonding distance to Ala78 across the tetramer interface that may play a role in tetramer stabilization, regulation of FMN binding, and in regulating oligomeric state changes.[62, 308] The π-helix in SsuE could also play a role in flavin reduction and in the transfer of the reduced flavin to SsuD. The ΔY118 and Y118F SsuE variants were tetramers but the flavin-bound Y118A and Y118S SsuE were dimers (**Table 3.4**). Deflavination of Y118A and Y118S SsuE did not

	Molecular Weight, kDa	Oligomeric Structure
Wild-type SsuE	73.4 ± 5.3	Tetramer
Y118A SsuE	42.2 ± 1.4	Dimer
FF Y118A SsuE	39.1 ± 0.1	Dimer
Y118S SsuE	41.7 ± 1.3	Dimer
FF Y118S SsuE	39.5 ± 0.1	Dimer
Y118F SsuE	78.6 ± 5.9	Tetramer
ΔY118 SsuE	84.1 ± 11	Tetramer

Table 3.4: Evaluating the quaternary structure of the Y118 SsuE variants. The molecular weights of the Y118 SsuE variants (total concentration of 50 μM) were estimated using Agilent Bio SEC-3, 4.6 x 300 mm, 100 Å (0.1 - 100 kDa) column loaded into a 1260 Infinity GPC/SEC chromatograph and compared to monomeric weight of 21.3 kDa for the wild-type SsuE. The standard curve (Log of molecular weight versus retention time) was generated based on elution monitored at 280 nm.

convert the dimeric state of the variants into a tetramer implying the oligomeric states of Y118A and Y118S were independent of the presence of flavin (**Table 3.3**).

3.3.5 Protein-Protein Interaction Studies between the Variants of Tyr118 in SsuE and Wild-Type SsuD

Recent hydrogen-deuterium exchange mass spectrometry studies identified the protein-protein interaction sites in both SsuE and SsuD.[229] In the SsuE enzyme, the interacting regions include the π-helix located at the tetramer interface which is associated with a tyrosine residue (Tyr118) inserted at helix α4 resulting to a bulge at the point of insertion.[62] Fluorimetric titrations were performed to evaluate the effect of perturbing the π-helix in SsuE on protein-protein interactions with SsuD. The Y118A and Y118F SsuE variants interacted with SsuD giving K_d values of 0.0059 ± 0.0006 μM and 0.010 ± 0.001 μM respectively, compared to a K_d value of 0.018 ± 0.001 μM for wild-type SsuE. The ΔY118 SsuE variant showed no change in flavin-based fluorescence with the addition of SsuD suggesting that a residue at position 118 of SsuE was required for the interactions between SsuE and SsuD.

3.3.6 Evaluating the Mechanism of Reduced Flavin Transfer between SsuE and SsuD

Competitive assays are an excellent tool for determining if the transfer of ligands between two proteins occurs through diffusion or involves protein-protein interactions.[309] The desulfonation activity of SsuD was shown to be linearly-dependent on levels of wild-type SsuE which corresponded to an increase in protein-protein interactions and ultimately reduced flavin transfer to SsuD (**Figure 3.3**a). A desulfonation experiment was set up containing fixed amounts of SsuD and wild-type SsuE (in a 1:1 ratio), and with varying concentrations of Y118A SsuE.

a)

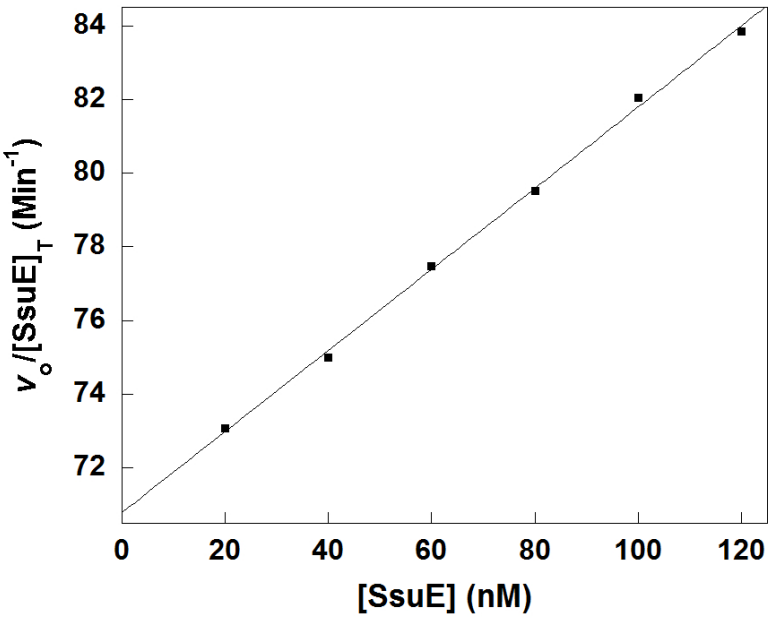

b)

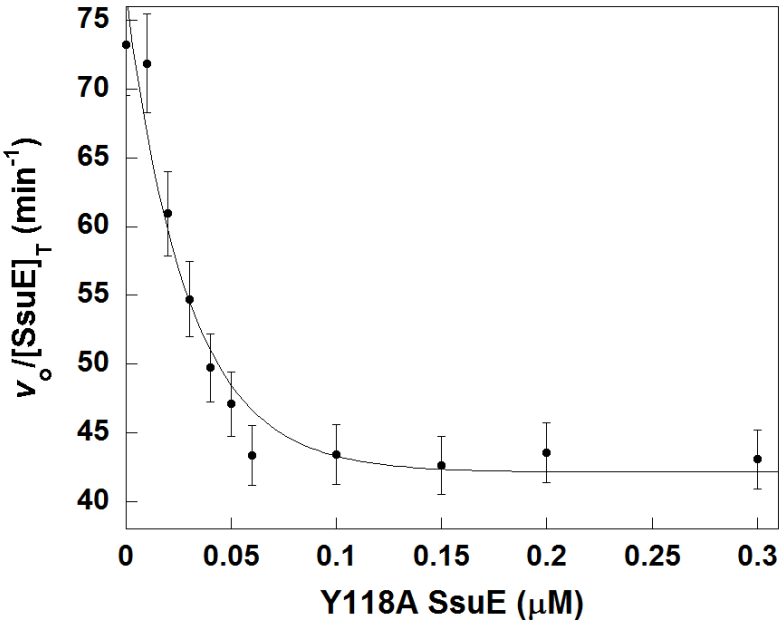

Figure 3.3: Competitive assay to evaluate the mechanism of reduced flavin transfer between SsuE and SsuD. a) Linear-dependence of desulfonation activity of SsuD on [SsuE], b) Y118A and wild-type SsuE competes for the interaction sites in SsuD.

Unlike the wild-type SsuE, the Y118A SsuE variant was unable to transfer reduced flavin to SsuD, and therefore could not support desulfonation activity.[308] Because both Y118A and wild-type SsuE enzymes can interact with SsuD, the two would compete for the interaction sites in SsuD resulting to a decline in catalytic activity when coupled together. The observed desulfonation activity would only be dependent on the SsuD interaction sites occupied by wild-type SsuE because the Y118A SsuE cannot transfer reduced flavin. If the transfer of reduced flavin occurs through diffusion, the catalytic activity would not change with the increase in amounts of Y118A SsuE because the reduced flavin would diffuse through the bulk solution to SsuD. There was an initial decrease in desulfonation activity observed with increasing concentrations of Y118A SsuE suggesting that the Y118A SsuE was competing with wild-type SsuE for the interaction sites in SsuD (**Figure 3.3**b). The decrease in desulfonation activity reached a plateau after 1 equiv of Y118A SsuE was added. The observed desulfonation activity by SsuD was only dependent on the interaction with wild-type SsuE because the Y118A SsuE cannot transfer reduced flavin to SsuD. The ability of wild-type SsuE and the Y118A SsuE variant to compete for the protein interaction sites in SsuD during desulfonation in steady-state conditions suggests that channeling mechanism was the mode of reduced flavin transfer between the alkanesulfonate monooxygenase system enzymes.

3.3.7 Determination of Three-Dimensional Structure of Y118A SsuE.

Previous studies showed that SsuE enzyme exists as a tetramer, is flavin-free as purified, and utilizes flavin as a substrate.[57] Flavin binding in SsuE triggers an oligomeric state shift from a tetramer to a dimer.[62] A π-helix resulting from a tyrosine residue (Tyr118) insertion created a bulge at the tetramer interface.[62] Three-dimensional structural studies of the FMN-bound and

Figure 3.4: Structural characterization of Y118A SsuE variant (apo) shows it exists as a dimer.

deflavinated Y118A SsuE were solved through X-ray crystallography (personal communication with our collaborator; Dr. Audrey Lamb). The holoY118A SsuE was obtained with a resolution 1.95 Å, existed as a dimer and had the flavin molecule exposed. Interestingly, the isoalloxazine ring of the FMN-bound to Y118A SsuE was drastically "flapping" over the active site. Upon reduction, the reduced Y118A SsuE (also a dimer obtained with a resolution of 1.9 Å) adopted a conformation different from that of the oxidized holo Y118A SsuE variant. Deflavination of Y118A SsuE was performed to establish the effect of the bound flavin in the oligomeric state of Y118A SsuE. The three-dimensional structure of the apoY118A SsuE was obtained with a resolution of 2.1 Å and space group of C2 existed as a dimer (**Figure 3.4**). Comparing the deflavinated Y118A SsuE structure to that of wild-type, the π-helix region in wild-type SsuE was now an α-helix in Y118A SsuE. The X-ray crystallography data obtained with the holo and apoY118A SsuE correlated with the results from size exclusion structural studies.

3.4 Discussion

Understanding the structural properties of enzymes is pivotal to comprehending their functionalities. Several factors are key for protein folding among them; random and selective polypeptide chain behavior, optimization of energetics, and favorable geometry.[310, 311] The chief secondary structures in protein architecture are α-helices and β-sheets.[208] Helical structures are the dominant secondary structures in the majority of proteins and are classified into α-helices, 3_{10}-helices, and π-helices based on the backbone hydrogen bonding pattern.[208] The α, 3_{10}, and π-helical protein structures are conventionally assigned based on hydrogen bonding trends between the carboxyl group of amino acid i and the amino group of amino acids $i + 3$, $i + 4$, and $i + 5$ respectively.[312] Protein evolution shapes the structural properties of proteins to optimize their functions, or adjust the functions based on environmental pressures.[313] The π-helices are characterized by a single-residue insertion into α-helices forcing a structural bulge as a result of five residues per turn. The π-helices are evolutionally designed to augment existing protein functions, or confer the enzymes with new catalytic roles.[207]

Structural studies on SsuE identified a π-helix located at the tetramer interface that evolved through a tyrosine residue insertion (Tyr118) in helix α4 of this flavodoxin-folded protein.[62] The π-helix is highly conserved at the tetramer interface in flavin reductases of two-component monooxygenase systems.[62] Only histidine appears to mimic the role of tyrosine in generating π-helices in flavin reductases of two-component monooxygenase systems. The hydroxyl group of Tyr118 in SsuE forms a hydrogen bond with the carboxyl group of Ala78 across the tetramer interface which may assist in stabilizing the tetrameric structure.[62] The amino group of Ala78 also docks FMN in the active site of SsuE through hydrogen bonding.[62] Substitution of Tyr118 in SsuE with Ala generated an FMN-bound Y118A SsuE variant which displayed kinetic properties

significantly different from wild-type SsuE enzyme.[303] The wild-type SsuE utilizes flavin as a substrate with a preference for FMN over FAD and hence, the Y118A SsuE variant retained the specificity for FMN.[57, 303] The flavin in Y118A SsuE was tightly bound and was not released following reduction. Interestingly, the Y118A SsuE variant did not support continuous turn-over in flavin reductase assays. In addition, there was no desulfonation activity in coupled assays with SsuD monitoring sulfite production. The rapid reaction kinetic traces for Y118A SsuE variant showed the reductive half-reaction, but no measurable $FMNH_2$ oxidation either in single enzyme assay, or when both SsuD and octanesulfonate were included. Although the reduced Y118A SsuE variant had slow NADPH oxidase activity, it supported the transfer of electrons to other electron acceptors.[303]

Additional variants of Tyr118 in SsuE were generated and experimental approaches implemented to further assess the catalytic and structural effect of mutating the π-helix in SsuE. Substitution of Tyr118 with serine generated an FMN-bound Y118S SsuE variant that displayed no measurable reductive or desulfonation kinetic activity as was previously observed with Y118A SsuE variant.[303] Substitution of Tyr118 with serine eliminated the aromatic group but maintained a hydroxyl group that could participate in hydrogen bond formation across the tetramer interface with Ala78. However, the serine residue is less bulky and has a shorter side chain compared to the tyrosine residue which could influence the architecture at the tetramer interface by forming a weak hydrogen bond with Ala78. The substitution of Tyr118 with Phe in Y118F SsuE eradicates the hydroxyl group in tyrosyl side chain which would prevent formation of the hydrogen bond with Ala78. The Y118F SsuE variant was flavin-free and had comparable flavin reductase and desulfonation activities as wild-type SsuE enzyme, suggesting the aromatic side chain of Tyr118 was required for catalysis. In addition, the binding affinity of Y118F SsuE for FMN was

comparable to that of wild-type SsuE. These kinetic similarities between Y118F and wild-type SsuE could be attributed to π-stacking interactions maintained at the tetramer interface by the phenyl groups of phenylalanine. Aromatic amino acids are often involved in π-π stacking interactions if the distance between them is < 7 Å.[314, 315] The phenyl rings of Tyr118 in SsuE are ~5.3 Å apart which confers the tetrameric core with both parallel-displaced and/or sandwich π-stacking interactions (**Figure 3.5**).[316] Therefore, multiple non-covalent interactions may play a role in stabilizing the tetrameric structure of SsuE and are requisite for catalytic activity. Our structural analysis on EmoB and 3k1y show that the π-stacking distances and hydrogen bond interactions are also maintained by the π-helical tyrosine in these flavin reductases of two-component monooxygenase systems.[172, 317]

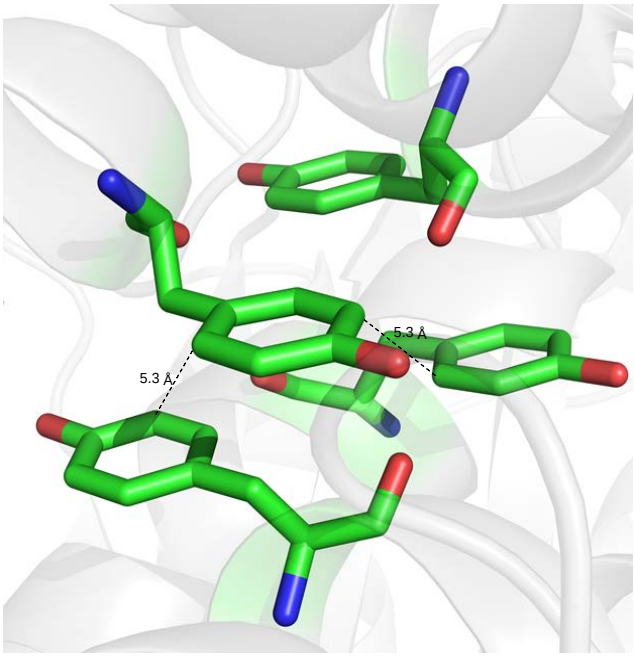

Figure 3.5: The Tyr118 in SsuE are within π-stacking distance which stabilize the quaternary structure of SsuE.

Since the π-helices in flavin reductases of two-component monooxygenase systems evolved through a tyrosine or histidine insertion, the Tyr118 residue was deleted (generating ΔY118 SsuE) to reverse the residue insertion in SsuE.[62] This deletion eliminated both the phenyl and hydroxyl groups of Tyr118 in SsuE. Further, the deletion should decrease the number of amino

acids per turn from five (π-helix in wild-type SsuE) to four (α-helix) in the ΔY118 SsuE variant. The ΔY118 SsuE variant had no measurable flavin reductase and desulfonation activity. Following the reductive half-reaction with Y118A SsuE variant there was no measurable $FMNH_2$ oxidation in rapid reaction kinetic traces in single enzyme assay, or when both SsuD and octanesulfonate were included. In addition, the ΔY118 SsuE variant had a 10-fold decrease in flavin affinity compared to the wild-type SsuE. Flavin binding in flavin reductases is dominated by serine/threonine-related hydrogen bonds of the flavin side chain and π-stacking interactions of the isoalloxazine ring with aromatic residues. The mutation of Tyr118 should not adversely affect the binding affinity of flavin because other flavin binding interactions were maintained. Although the creation of π-helices is unfavorable, the removal of a π-helix becomes even more energetically unfavorable after the π-helix has been developed and accommodated in a protein. The deletion of the insertion residue in the π-helix of a heat shock transcription factor created an α-helix but resulted into an unstable protein.[264] Deletion of the π-helix insertional conserved residue (Ser 456) in GABA transporters GAT-1 decreased activity by ~92%. This π-helix was reported to regulate gating and coupling electrogenic ion and substrate fluxes.[254] The deletion or substitutions of the π-helix insertion residue or nearby residues in GABA transporter proteins GAT-1 adversely affected gating and coupling of ions and substrates.[254]

Protein oligomerization (the interactome of tertiary structures resulting in formation of complex protein structures) enhances the effective concentration of active sites, stabilizes the protein's three-dimensional structures, and is an efficient method for regulating enzyme activity.[290, 291] The SsuE enzyme exists as a tetramer, but in the presence of the substrate FMN it shifts into a dimeric state.[62] Closer scrutiny of the SsuE tetramer shows that the active site is located near the tetramer interface suggesting the oligomeric switch exposes the active site of SsuE for

catalysis and facilitate reduced flavin transfer to SsuD. Although oligomerization may not be a requirement for activity, the active sites in several oligomeric enzymes are found in the oligomeric interfaces.[290, 291] The Tyr118 residue in SsuE is within hydrogen bonding distance to Ala78 across the tetramer interface and has been linked to tetramer stabilization, regulation of FMN binding, and oligomeric state changes in SsuE.[62, 308] Size exclusion chromatography studies on Tyr118 SsuE variants suggests the π-helix may regulate the observed oligomeric state shifts in SsuE. The Y118A and Y118S SsuE variants are FMN-bound as purified and exist as dimers which correspond with previous observations on flavin-bound SsuE. The dimeric structures were maintained even when the Y118A and Y118S SsuE enzymes were deflavinated. However, the Y118A and Y118S SsuE showed no flavin reductase or desulfonation activity when coupled with SsuD. The Y118F SsuE is flavin-free as purified and exists as a tetramer. Substitution of Tyr118 with phenylalanine (Y118F SsuE) eliminated the hydroxyl group of tyrosine, potentially leading to the disruption of the hydrogen bond network. However, the Y118F SsuE variant may be able to maintain π-stacking interactions at the tetramer interface that facilitates tetramer stabilization and catalytic activity. The ΔY118 SsuE variant was predominantly tetrameric even in the presence of flavin. The deletion of Tyr118 may have disrupted both π-stacking and hydrogen bonding interactions required for the regulation of oligomeric changes. Alternatively, the π-helix mutation may have created a disordered region that no longer supported relevant noncovalent interactions required for catalysis. Substitution of the residues involved in regulation of the oligomeric states of proteins often result in a loss of enzyme activity.[292] For instance, a single amino acid mutation destabilized the dimer of *Vibrio harveyi* flavin reductase.[318] In addition, substitution of the amino acid that regulates the quaternary structure of lactate dehydrogenase from dimer to tetramer stabilized the tetrameric structure.[319]

Oligomeric state changes are common structural phenomena manifested in various flavin reductases. The roles and regulations of these oligomeric changes have not been investigated. The existence of flavin reductases in different oligomeric states could be critical in the regulation of catalytic events and for preventing futile reactions. A monomer-dimer equilibrium was shown to exist with the NADPH:FMN reductase from *Vibrio harveyi* associated with the bacterial luciferase system in both apo and native enzymes.[293] Half-site activity was observed with LuxG, a dimeric flavin reductase associated with bacterial luciferase (LuxAB) system in *Photobacterium leiognathi (TH1).* This half-site activity was attributed to oligomeric state changes during catalysis.[294] A dimer-tetramer equilibrium that is dependent on enzyme concentration was observed with FerB, an NADPH:FMN reductase of *Paracoccus denitrificans*.[295] It was previously observed (in 2006 review) that the flavodoxin structures did not show obvious FMN binding sites and required major conformational changes to adopt a more open conformation.[320] That observation holds true today on several flavin reductases and the oligomeric state changes could be the answer. For instance, oligomeric state changes have not been reported with EmoB despite its structural similarity with SsuE. However, the flavin binding sites in EmoB are located near the dimer-dimer interface and would not be accessible for flavin binding, reduction and transfer in the tetrameric form.[171, 172]

The trafficking of reduced flavin in two-component flavin-dependent systems captures interest because of the unstable nature of free reduced flavin. If not successfully delivered to the intended oxygenase enzyme, reduced flavin could undergo non-enzymatic oxidation producing reactive oxygen intermediates. The mechanism of reduced flavin transfer in two-component flavin systems could occur through diffusion, direct channeling, or both. In free diffusion, the reduced flavin diffuses through the bulk solution from the flavin reductase to the monooxygenase enzyme.[157, 228, 229] The direct channeling mechanism involves protein-protein interactions between

the flavin reductase and the oxygenase.[161, 228] Protein-protein interactions were previously observed between SsuE and SsuD through affinity chromatography and fluorimetric studies indicating a channeling mechanism as the likely mechanism of reduced flavin transfer from SsuE to SsuD.[215] The protein-protein interaction sites between SsuE and SsuD were identified through hydrogen-deuterium exchange studies.[229] Perturbation of the interaction sites in SsuD through site-directed mutagenesis resulted in the loss of desulfonation activity implying that reduced flavin was not being transferred from SsuE to SsuD.[229]

Some of the residues which constitute the π-helix in SsuE including Tyr118 were implicated to be involved in protein-protein interaction with SsuD.[229] To evaluate the effect of perturbing the π-helix in SsuE on protein-protein interactions with SsuD, fluorimetric titrations of Y118 SsuE variants with SsuD were performed. All the Y118 SsuE variants (except ΔY118 SsuE variant) interacted with SsuD with comparable affinities to that of wild-type SsuE, suggesting the substitution of Tyr118 did not adversely affect protein-protein interactions with SsuD. However, the deletion of Tyr118 adversely affected the ability of SsuE to interact with SsuD suggesting that an amino acid residue at position 118 in SsuE was required for interaction with SsuD to occur.

A competition desulfonation assay was performed to further evaluate protein-protein interactions between SsuE and SsuD and to probe on the mechanism of reduced flavin transfer using the Y118A SsuE variant.[309] Unlike wild-type SsuE, the Y118A SsuE variant does not support reduced flavin transfer to SsuD because the reduced flavin remains tightly bound.[308] Consequently, the Y118A SsuE variant does not support desulfonation of alkanesulfonates by SsuD.[308] However, the Y118A SsuE variant is able to interact with SsuD. In a desulfonation reaction mixture coupling SsuD with both wild-type SsuE and Y118A SsuE variant, the SsuE enzymes should compete for the interaction sites on SsuD. As such, the desulfonation activity

observed with SsuD would only be dependent on wild-type SsuE and not on Y118A SsuE because only SsuE can provide SsuD with reduced flavin. There was an initial decrease in desulfonation activity as the concentrations of Y118A SsuE increased suggesting a competition existed between the SsuE enzymes for the interaction sites on SsuD. There was no significant change in desulfonation activity after 1 equiv of Y118A SsuE was added. If the transfer of reduced flavin between SsuE and SsuD occurs through diffusion, the catalytic activity would not decrease with increase in Y118A SsuE because the reduced flavin would diffuse through the bulk solution to SsuD. Protein-protein interactions bring the active sites of flavin reductase and monooxygenase enzymes in proximity facilitating direct transfer of reduced flavin and minimizing the crowding effect. In addition, the monooxygenase enzymes usually have characteristic high-affinity for reduced flavin which expedites the transfer and the binding of reduced flavin.[61] The interactions between SsuE and SsuD alters the kinetic mechanism of SsuE from sequential kinetic mechanism (during flavin reduction) to a rapid equilibrium-ordered mechanism during desulfonation (when SsuD and octanesulfonate are included).[2] Protein-protein interactions minimizes uncoupling of reduced flavin which would result in non-enzymatic oxidation generating reactive oxygen species. The channeling mechanism (as observed between SsuE and SsuD) also minimizes expenditure of NADH and NADPH for continued flavin reduction. Some two-component flavin systems have been shown to utilize both protein complexion and free diffusion under specified conditions.[201, 296, 321]

The perturbation of the π-helix in SsuE through generation of Y118A SsuE resulted into a canonical flavoprotein SsuE variant.[303] Three-dimensional structural studies of the FMN-bound and deflavinated Y118A SsuE were solved through X-ray crystallography (personal communication with our collaborator; Dr. Audrey Lamb). The deflavinated and flavin-bound

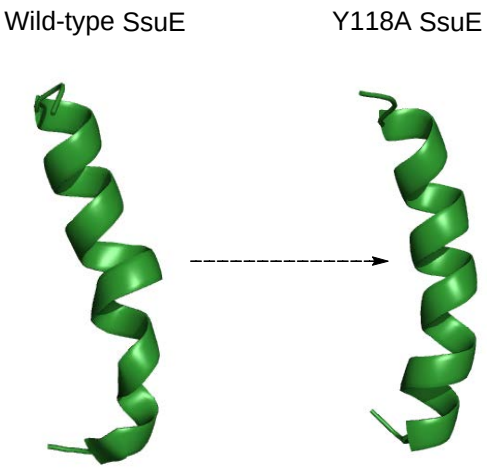

Figure 3.6: Comparison of the π-helix region of wild-type SsuE with the α-helix in Y118A SsuE variant.

Y118A SsuE were dimers in three-dimensional structures and through size exclusion chromatography, implying the π-helix perturbation impaired the tetramer formation. The structural effects of mutating Tyr118 in SsuE were not only manifested by the conversion of the tetramer SsuE enzyme to a dimer, but also in the conversion of the π-helix in wild-type SsuE to an α-helix in Y118A SsuE (**Figure 3.6**). The formation of π-helices requires an alignment of five amino acid residues to allow (i←i + 5) hydrogen bond which is energetically unfavorable and requires a large entropic energy.[236] Natural π-helices typically have seven residues that have two π-type hydrogen bonds.[208] The π-helix in wild-type SsuE contains two consecutive π-type hydrogen bonds (3.0 and 3.3 Å) characterized by five amino acids per turn. However, the generation of Y118A SsuE resulted in tighter hydrogen bonds (2.0 and 2.1 Å) in the same region with four amino acids per turn. This is characteristic of an α-helix and reveals that the π-helix in wild-type SsuE converted into an α-helix in the Y118A SsuE variant. This information coupled with previous secondary structural studies, suggests that circular dichroism spectroscopy was unable to distinguish between π-helix in wild-type SsuE and α-helix in the Y118A SsuE.[303] This shortcoming of circular dichroism spectroscopy has been previously observed with other systems.[252-254] Although wild-type SsuE undergoes flavin-induced oligomeric state changes to dimer, it was not clear how the tetramer dissociates.[62] The dissociation of the SsuE tetramer could generate dimers AB/CD, AC/

BD, or AD/BC (**Figure 3.7**). The three-dimensional dimeric structure of apo Y118A SsuE (**Figure 3.4**) corresponds to the AC/BD dimers of the wild-type SsuE (**Figure 3.7**).

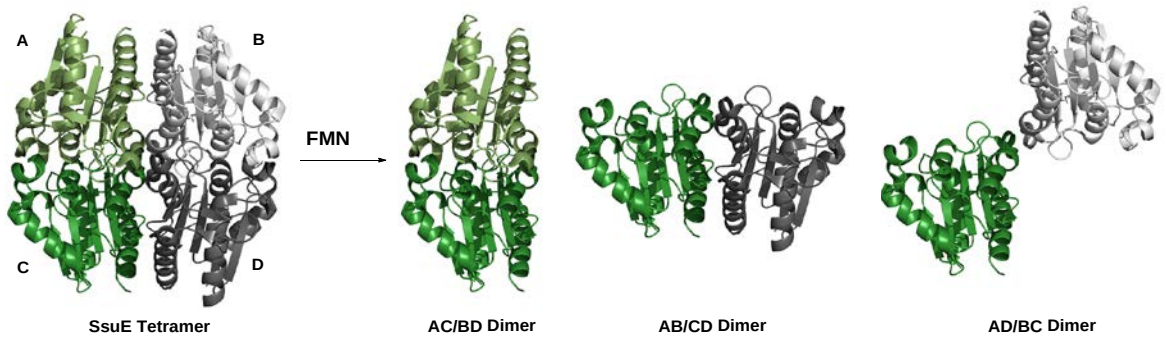

Figure 3.7: SsuE exists as a tetramer (85.2 kDa) but in the presence of flavin, the tetramer dissociates into dimer (42.6 kDa).

Upon reduction, the Y118 SsuE variants showed slow oxygen reactivity in both single-turnover and steady-state kinetic conditions.[303] Flavoproteins show diverse reactivities with dioxygen but there is no consensus into the structural features that facilitate activation of dioxygen by flavin reductases.[322] This oxygen-insensitivity by Y118 SsuE variants suggest the π-helix in SsuE may play a role in regulating oxygen reactivity with reduced flavin. In the three-dimensional structure of Y118A SsuE, the flavin molecule is exposed and highly mobile. The reduction of Y118A SsuE leads to conformational changes significantly different from that of oxidized Y118A SsuE (personal communication with our collaborator; Dr. Audrey Lamb). Despite the flavin molecule in Y118A SsuE variant being exposed which favors oxygen accessibility, the Y118A SsuE shows slow oxygen reactivity. For oxygen reactivity in flavoproteins, the active sites should favor oxygen accessibility to the flavin molecule and allow dioxygen reactivity with the reduced

flavin.[323] However, accessibility of the flavin bound on flavoproteins to oxygen does not always translate to oxygen reactivity. For instance, flavocytochrome b2 has a fully exposed flavin which is accessible to oxygen but it reacts slowly with oxygen.[160, 324] The difference in oxygen reactivities with flavoproteins continue to be fascinating and interesting field in understanding flavin-dependent chemistries.[322] Some nitroreductases are oxygen-insensitive and support flavin-dependent electron transfer to nitro compounds in the presence of oxygen. However, there is no consensus on the structural features that control oxygen reactivity in these flavin reductases.[325-327] These results on Y118 SsuE variants are novel and are fundamental in further assessment of oxygen reactivity and reduced flavin stabilization on SsuE and other NAD(P)H flavin reductases which has been difficult to assess due to the release reduced flavin.

In conclusion, the insertion of Tyr118 insertion crafts a π-helix at the tetramer interface essential for flavin binding, flavin reduction, protein-protein interactions, and flavin transfer. The π-helical structure is essential for regulation of oligomeric state changes and could be involved in regulating oxygen reactivity. Certain structural features and sequences mediate oligomerization and protein–protein interactions in two-component flavin-dependent oxygenase systems. A recent study uncovered enabling surface loops that mediated protein interactions while disabling surface loops prevented unwanted interactions.[328] The π-helix appear to be a key structural feature that augments oligomerization and protein–protein interactions in FMN reductases of two-component systems. These structural characterization and kinetic studies on variants of Tyr118 in SsuE are requisite in determining the evolutionary roles of π-helix in flavin reductases of two-component monooxygenase systems.

CHAPTER FOUR

4 Investigations on the Conformational Changes in SsuE and Role of the Loop Region in SsuD during Catalysis

4.1 Introduction

Enzymes are not static and often adopt different conformations which correlate to the functional state of the enzyme. Conformational changes have been investigated in the alkanesulfonate monooxygenase enzymes (SsuE and SsuD) through three-dimensional structural studies, kinetic experiments, and computational simulations. Understanding the conformational changes in the two-component flavin-dependent monooxygenase systems provide insights into the catalytic events leading to flavin reduction by the flavin reductases, the mechanism of reduced flavin transfer to the associated monooxygenase enzymes, and the insertion of oxygen atoms into corresponding substrates by the monooxygenase enzymes. The different conformational state changes reported with the alkanesulfonate monooxygenase system range from quaternary state changes in SsuE to flexible loop movement in SsuD, which have been shown to be critical for catalysis and in flavin transfer between the two enzymes.[62, 170, 215, 216, 218, 222, 303]

Flavin binding in the SsuE enzyme culminates into robust conformational changes resulting into quaternary structural changes from a tetramer into a dimer.[62] Oligomeric state changes are increasingly being identified in flavin reductases, but not much is known on how the quaternary structural changes influence catalysis and how they are regulated.[293-295] The SsuE enzyme supplies SsuD with reduced flavin for desulfonation of alkanesulfonates during sulfur limitation in bacteria.[57] It is not known how oligomeric state changes in SsuE are influenced by the presence of SsuD, and during reduced flavin transfer.[57] The channeling mechanism of reduced flavin transfer

from SsuE to SsuD involves protein-protein interaction which may promote structural changes in both enzymes.[171, 194, 215, 218, 229]

The SsuD enzyme is a monooxygenase enzyme and utilizes reduced flavin supplied by SsuE to activate molecular oxygen for the desulfonation reaction. The SsuD enzyme belongs to the bacterial luciferase family and has a TIM-barrel fold. Like most TIM-barrel proteins, SsuD enzyme has its active site positioned at the C-terminal end of the β-barrel.[209-212] The SsuD enzyme deviates from other TIM barrel proteins by having numerous insertion regions. One insertion region in SsuD is largely unresolved in the three-dimensional structure and is located at the putative active site. The insertion region in SsuD was shown to be highly flexible and characterized by major conformational changes.[211, 218] This unresolved region is conserved in SsuD homologs and has been proposed to close over the active site during catalysis.[61, 218] Partial deletions of the loop region in SsuD did not affect the secondary structure of SsuD, but the deletion variants were catalytically inactive.[218] Herein, we utilize site-directed spin labeling (SDSL) electron paramagnetic resonance (EPR) spectroscopy to probe potential oligomeric changes in SsuE in the presence of substrates and SsuD. We also utilize computational and experimental approaches to investigate the conformational changes in the loop region of SsuD.

4.2 Materials and methods

4.2.1 Materials

E. coli strains (XL-1 and BL21(DE3)) were purchased from Stratagene (La Jolla, CA). Plasmid vectors and pET21a were obtained from Novagen (Madison, WI). DNA primers were synthesized by Invitrogen (Carlsbad, CA). Ampicillin, streptomycin sulfate, ammonium sulfate, reduced nicotinamide adenine dinucleotide phosphate (NADPH), flavin adenine dinucleotide (FAD), flavin mononucleotide (FMN), glycine, lysozyme, potassium phosphate (monobasic anhydrous

and dibasic anhydrous), dimethyl sulfoxide (DMSO), 5,5-dithiobis-(2-nitrobenzoic acid) (DTNB), and urea were obtained from Sigma (St. Louis, MO). Isopropyl-β-D 1-thiogalactoside (IPTG), sodium chloride and glycerol were obtained from Macron Fine Chemicals (Center Valley, PA). 1-octanesulfonate was purchased from Fluka (Milwaukee, WI). MTSSL (1-oxyl-2,2,5,5-tetramethyl-3-pyrroline-3-methyl) was purchased from Toronto Research Chemicals.

4.2.2 Construction of SsuE and SsuD Variants.

Recombinant pET21a plasmid containing the *ssuE* and *ssuD* genes were separately used to construct the SsuE and SsuD variants. The GAA codon for Glu20 and the GAT codon for Asp111 were substituted with the Ala codon (GCG) in SsuD. For SsuE, the Trp36 codon (TGG) was substituted with the Cys codon (TGC) to generate W36C SsuE. Confirmation of the resultant *ssu* variants was performed through DNA sequence analysis. Confirmed variants were transformed into *E. coli* BL21(DE3) competent cells for protein expression, and glycerol stocks of wild-type SsuD and SsuE and their variants were stored at -80 °C. The variants were purified as previously reported.[2] The SsuD enzyme concentrations were determined spectrophotometrically using a molar absorption coefficient of 47900 M^{-1} cm^{-1} at 280 nm. The concentrations of wild-type SsuE and W36C SsuE enzymes were determined spectrophotometrically using a molar absorption coefficient of 20340 M^{-1} cm^{-1} and 15930 M^{-1} cm^{-1} respectively at 280 nm.[2]

4.2.3 SDSL EPR Spectroscopy Studies on SsuE

Following purification of W36C SsuE, covalent spin labeling of W36C SsuE with sulfhydryl-specific methanethiosulfonate spin label (MTSSL) was performed. The MTSSL (1-oxyl-2,2,5,5-tetramethyl-3-pyrroline-3-methyl) purchased from Toronto Research Chemicals contains a stable free radical. A 2 mM final concentration of MTSSL was added to 3 mL of 190 μM W36C SsuE and the mixture incubated at 4 °C overnight. Unreacted MTSSL was removed

through buffer exchange in an Amicon® Ultra-4 centrifugation filter (10 kDa MWCO). The mixture was washed with 25 mM potassium phosphate (pH 7.5), 0.1 M NaCl, and 10% glycerol five times through centrifugation (4424 x g) for 20 min at 4 °C. The concentration of spin-labeled W36C SsuE was 110 µM in 4 mL resulting in a 77% yield. The SL (spin-labeled) W36C SsuE variant was confirmed through mass spectrometry. Desulfonation assays were performed under steady-state kinetic conditions with both spin-labeled and unlabeled W36C SsuE, as previously outlined.[61]

Continuous wave EPR spectra were obtained at X-band (9 GHz) frequency on a Bruker EMX spectrometer (Bruker Biospin Corporation, Billerica, MA), fitted with the ER-4119-HS high sensitivity perpendicular-mode cavity. A temperature of 77 K was maintained by fitting the cavity with a liquid nitrogen finger Dewar. The spectra were recorded at a field modulation frequency of 100 kHz, a modulation amplitude of 0.1 mT, and a frequency of 9.413 GHz. All samples contained either unlabeled or SL W36C SsuE (60 µM) in 300 µL total volume and were prepared in 25 mM potassium phosphate (pH 7.5), 0.1 M NaCl, and 10% glycerol. Three separate solutions of NADPH-bound SL W36C SsuE, NADPH-bound SL W36C SsuE mixed with SsuD, and FMN were made anaerobic by alternate purging of high purity argon gas and evacuation for 20 min. Both NADPH-bound SL W36C SsuE and NADPH-bound SL W36C SsuE-SsuD samples were mixed with FMN and rapidly frozen quenched in an anaerobic chamber (summarized in **Table 4.1**). Unlabeled W36C SsuE, SL W36C SsuE, SL W36C SsuE with SsuD, FMN-bound SL W36C SsuE, FMN-bound SL W36C SsuE with SsuD, the MTS spin label alone, FMN mixed with the spin label, and FMN alone, were prepared under aerobic conditions (summarized in **Table 4.1**).

• Unlabeled W36C SsuE • SL W36C SsuE • SL W36C SsuE + SsuD • SL W36C SsuE + FMN • SL W36C SsuE + SsuD + FMN	• MTS spin label • FMN mixed with the spin label • FMN alone • SL W36C SsuE + FMN + NADPH • SL W36C SsuE + SsuD + FMN + NADPH

Table 4.1: Different conditions for SDSL EPR analysis of W36C SsuE enzyme. The samples that included both FMN and NADPH mixed with either SL W36C SsuE, or SL SsuE and SsuD were prepared anaerobically. The rest of sample mixtures highlighted were prepared in the presence of oxygen. The samples contained either unlabeled or SL W36C SsuE (60 μM in 300 μL total volume) and were prepared in 25 mM potassium phosphate (pH 7.5), 0.1 M NaCl, and 10% glycerol. The NADPH and FMN concentrations were 60 μM when included.

4.2.4 Computational and Experimental Studies on the Loop Region in SsuD

Computational simulation studies were performed to further investigate the loop movement in SsuD during catalysis.[329] The conformational changes were monitored using Amber (over a 1000 ns accelerated molecular dynamics simulation) comparing SsuD with no substrate bound, SsuD with both FMN and octanesulfonate (OCS) bound, and SsuD with reduced flavin and OCS bound.[329] The molecular dynamics simulation also identified the key residues on the loop region during catalysis. Site-directed mutagenesis studies and kinetic assays were performed on SsuD to experimentally evaluate the catalytic roles of the residues identified.

4.3 Results

4.3.1 Site-Directed Spin Labeling EPR Spectroscopy

SDSL-EPR spectroscopy involves the use of thiol reactive spin labeling compounds (**Figure 4.1**) to probe conformational changes and dynamics of thiolated proteins.[330] Because SsuE and SsuD enzymes are sulfur scavenging, SsuE contains no cysteine in its structure. A cysteine residue was introduced through site-directed mutagenesis (W36C SsuE) at a site away from the active site and the tetramer interface of SsuE (**Figure 4.2**). The SL W36C SsuE was purified as previously described, followed by covalent labeling with MTS. The W36C SsuE variant was purified in the presence and absence of DTT to ensure that the cysteine residue remained reduced. Both preparations effectively reacted with the MTS spin label. The SL W36C SsuE variant was confirmed through mass spectrometry giving a mass of 21352 Da which correlated with a mass of W36C SsuE (21170 Da) with covalently attached spin label (183 Da) (**Figure 4.3**).

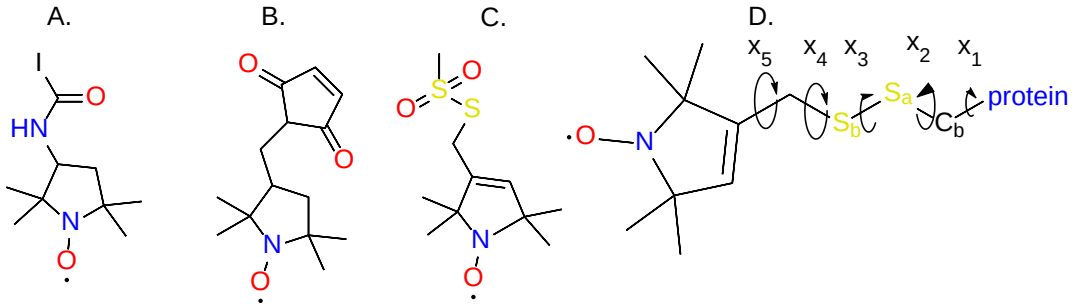

Figure 4.1: Commonly used nitroxide-based spin labels for SDSL EPR. A. Proxyl-iodoacetamide (IAP) B. Proxyl-maleimide (MLS) C. Proxy-methanethiosulfonate (MTSL) D. Reaction between cysteine residue and MTSL with dihedral angles labeled X_1 through X_5. (Adapted from [331]).

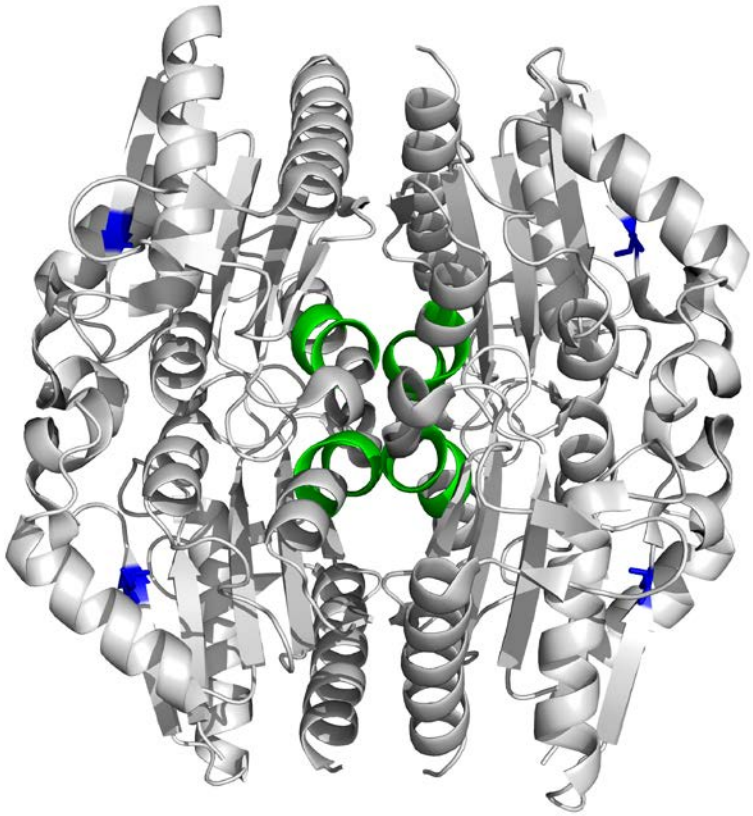

Figure 4.2: Spin labeling of SsuE for EPR studies. A cysteine was introduced at the blue-highlighted outer regions of SsuE (away from the active site and from the tetramer interface) resulting into the W36C SsuE variant. Methanethiosulfonate spin label was reacted with W36C SsuE generating SL W36C SsuE.

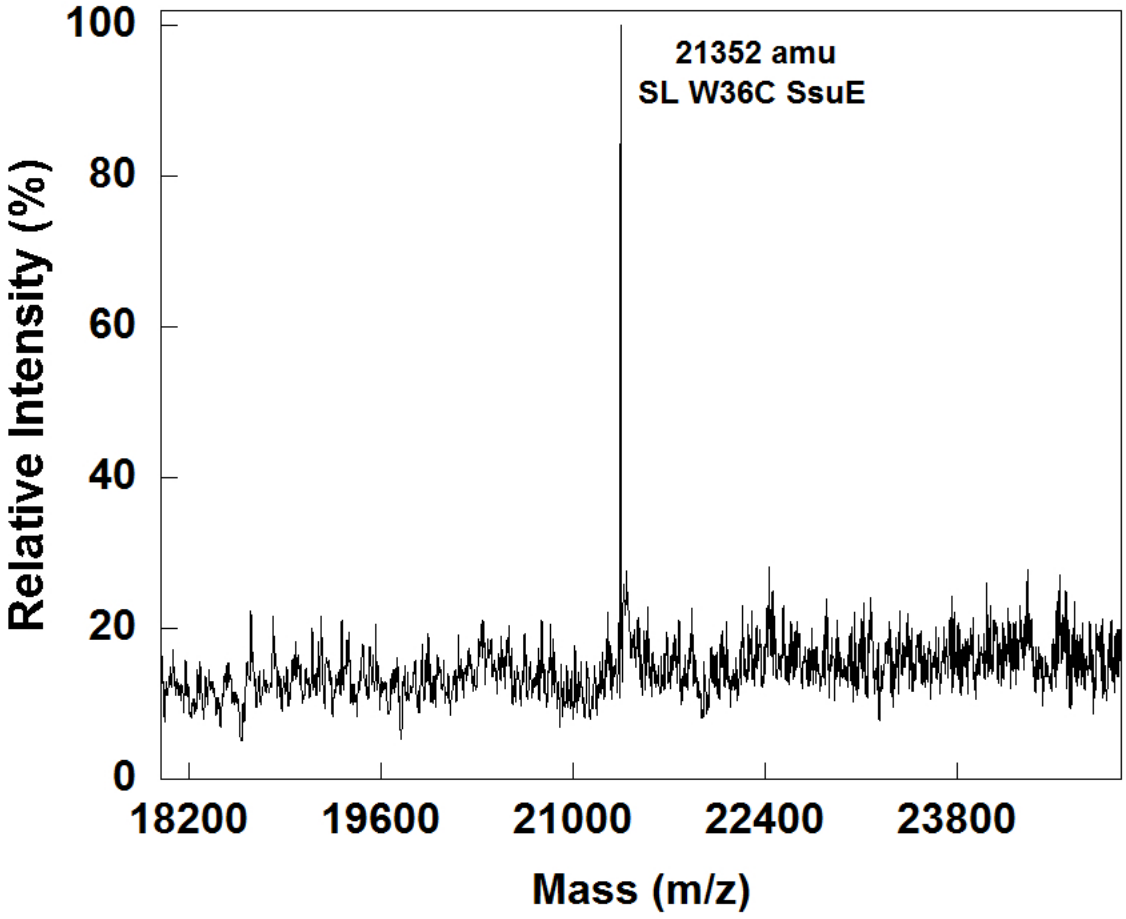

Figure 4.3: Mass spectrometric analysis of spin-labeled W36C SsuE. The SL W36C SsuE had a mass of 21352 Da compared to a mass of 21170 Da before spin labeling and 21253 Da for the wild-type SsuE enzyme.

Desulfonation assays were performed with W36C SsuE (before and following spin labeling) to determine if the mutation or labeling affected catalysis. The W36C SsuE enzyme gave a k_{cat}/K_m values of 2.6 ± 0.6 comparable to the wild-type SsuE (2.1 ± 0.1 $\mu M^{-1}min^{-1}$) suggesting the mutation did not affect activity. In addition, the spin-labeling of W36C SsuE enzyme did not

affect the enzymes ability to reduce flavin and the transfer it to SsuD and gave a k_{cat}/K_m value of 3.6 ± 1.2 $\mu M^{-1}min^{-1}$ (**Table 4.2**).

	k_{cat} (min^{-1})	K_m (μM)	k_{cat}/K_m ($\mu M^{-1}min^{-1}$)
Wild-type SsuE	50.8 ± 2.6	24.1 ± 1.6	2.1 ± 0.1
W36C SsuE	20.3 ± 0.7	7.8 ± 1.8	2.6 ± 0.6
SL W36C SsuE	16.7 ± 0.1	5.1 ± 1.7	3.6 ± 1.2

Table 4.2: Steady-state kinetic parameters of wild-type and W36C SsuE variant monitoring SsuD desulfonation.

EPR studies were performed to investigate spin labeled SsuE under various experimental conditions (**Table 4.1**). The unlabeled W36C SsuE was EPR silent because it lacked an unpaired electron (**Figure 4.4**). Spin labeling of W36C SsuE introduced a stable free radical enabling studies on SsuE through EPR. There were minor changes in the EPR signal with SL W36C SsuE when either NADPH, SsuD, or both NADPH and SsuD were added. Notably, the signal diminished significantly in the samples containing SL W36C SsuE mixed with FMN, or when SL W36C was mixed with both FMN and SsuD (**Figure 4.4** and **Figure 4.5**). However, when the sample mixture supported flavin reduction (SL W36C SsuE, FMN and NADPH, or SL W36C SsuE, SsuD, FMN and NADPH), the EPR signals were comparable to SL W36C SsuE alone (**Figure 4.4** and **Figure 4.5**). There was a slight increase in EPR signal when SL W36C SsuE was mixed with both FMN and SsuD compared to when the SL W36C SsuE mixed with FMN. Interestingly, there was a similar increase in the EPR signal when SL W36C SsuE was mixed with SsuD, FMN, and

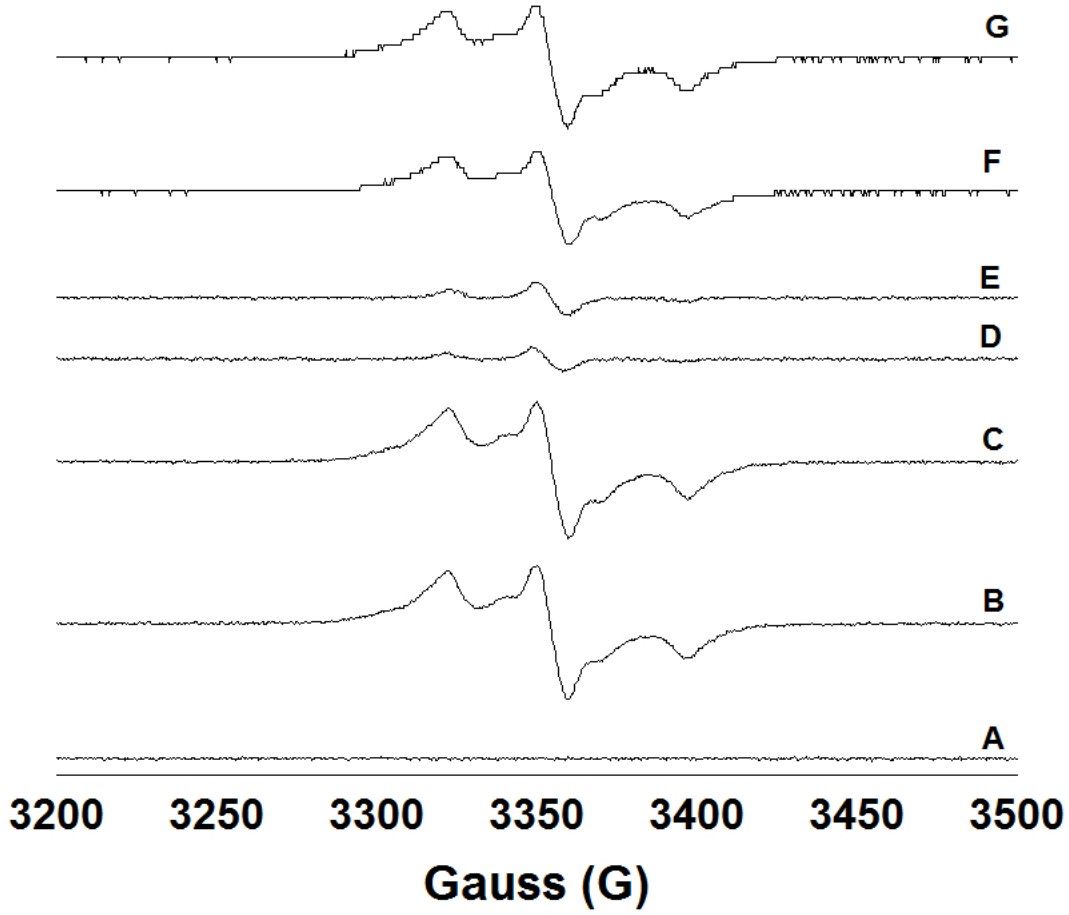

Figure 4.4: EPR spectra of SL W36C SsuE under different conditions. The signals correspond to various combinations of W36C SsuE. (A) W36C SsuE, (B) Spin-labeled SsuE, (C) SL W36C SsuE + SsuD, (D) SL W36C SsuE + FMN, (E) SL W36C SsuE + SsuD + FMN, (F) SL W36C SsuE + FMN + NADPH, and (G) SL W36C SsuE + SsuD + FMN + NADPH. Anaerobic conditions were maintained for (F) and (G). The experiments were performed in 25 mM potassium phosphate (pH 7.5), 0.1 M NaCl, and 10% glycerol. The concentration of the SL W36C SsuE and SsuD enzymes, of the substrate were 60 μM. EPR conditions: microwave frequency, 9.413 GHz; microwave power, 1.995 μW; temperature, 77 K; modulation amplitude, 0.1 mT.

NADPH compared to when the SL W36C SsuE was mixed with FMN and NADPH. In both cases, the slight increase could be attributed to protein-protein interactions between SL W36C SsuE and SsuD (**Figure 4.5**).

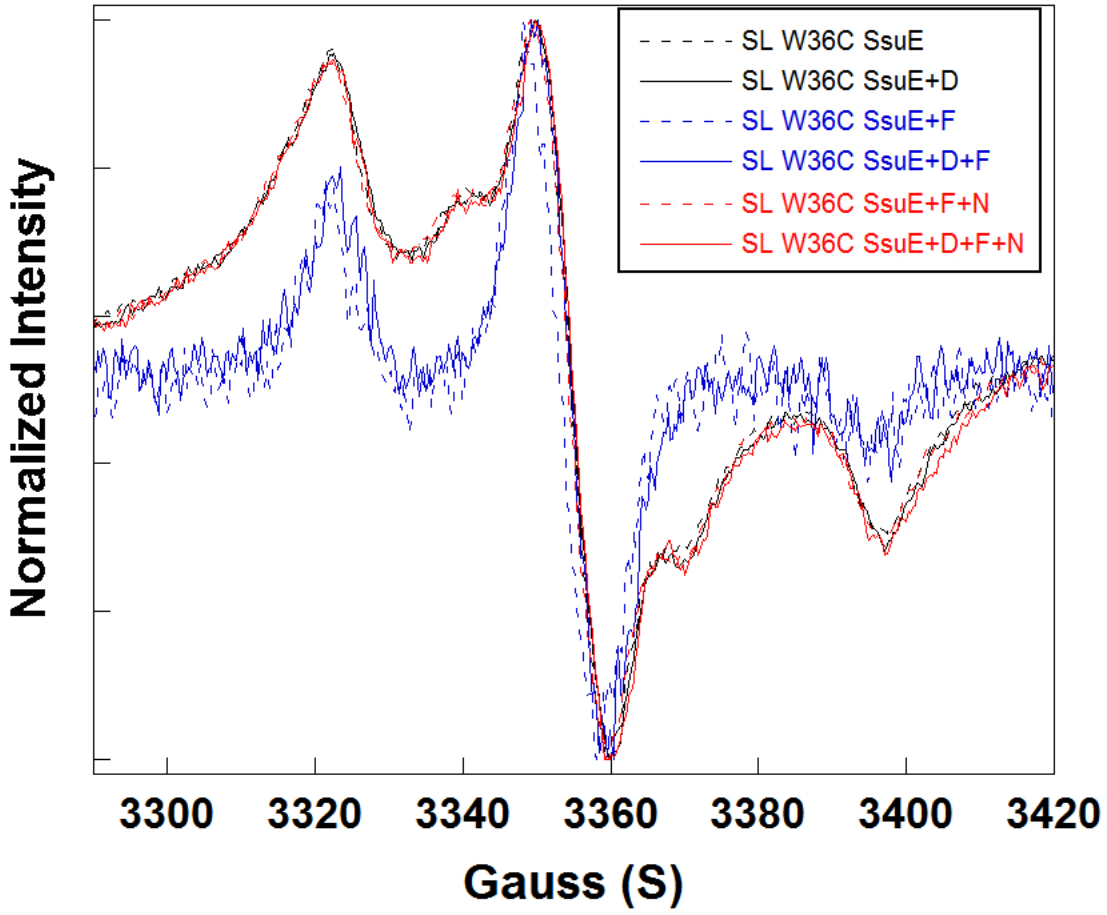

Figure 4.5: EPR spectra of SL W36C SsuE under different conditions. The experiments were performed in 25 mM potassium phosphate (pH 7.5), 10% glycerol, and 0.1 M NaCl. The concentrations of the SL W36C SsuE and SsuD enzymes, and of the substrates were 60 µM. EPR conditions: microwave frequency, 9.413 GHz; microwave power, 1.995 µW; temperature, 77 K; modulation amplitude, 0.1 mT. Inset initials; D (SsuD), F(FMN) and N (NADPH).

4.3.2 Computational and Experimental Studies Evaluating the Loop Region in SsuD

Computational studies suggested that Arg297 located in the flexible loop of SsuD formed salt-bridges over the active site of SsuD with Glu20 and Asp111 during catalysis (**Figure 4.6**).[332] The Arg297-Glu20 salt-bridge in SsuD resulting in the open conformation would allow the substrates to access the active site and/or permit product release. The Arg297-Asp111 salt-bridge forming a closed conformation in SsuD would lock substrates in the active site during

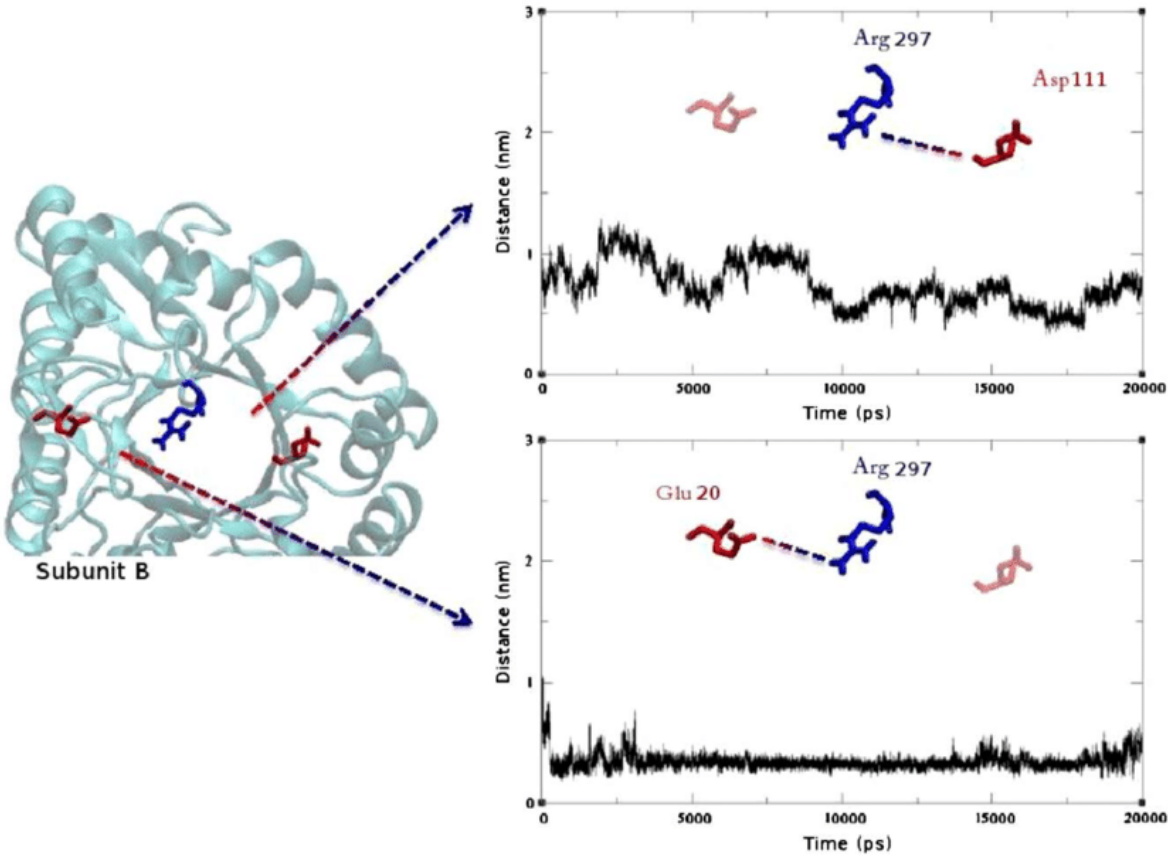

Figure 4.6: Molecular dynamics studies on the flexible loop region of SsuD. Computational studies proposed significant conformational changes over the active site of SsuD involving a switch from an Arg297−Asp111 salt bridge (closed conformation) to an Arg297−Glu20 salt bridge (open conformation). (Adapted with permission from [332]). Copyright © 2012 Taylor & Francis.

desulfonation.[332] Alanine variants of Glu20 and Asp111 were generated to evaluate the catalytic relevance of these residues through steady-state kinetic analyses. Steady-state kinetic parameters for E20A, D111A, and wild-type SsuD were obtained by monitoring the production of the TNB anion at 412 nm formed from the reaction of DTNB with the sulfite product. The k_{cat}/K_m values for the SsuD variants were comparable to the wild-type SsuD value of $1.4 \pm 0.2\ \mu M^{-1}\ min^{-1}$ (**Table 4.3**).

	k_{cat} (min^{-1})	K_m (μM)	k_{cat}/K_m ($\mu M^{-1}min^{-1}$)
Wild-type SsuD	43.3 ± 4.3	31.2 ± 2.0	1.4 ± 0.2
E20A SsuD	36.3 ± 3.7	32.2 ± 4.6	1.1 ± 0.2
D111A SsuD	40.5 ± 3.8	36.3 ± 3.5	1.1 ± 0.2
R297K SsuD[a]	1.5 ± 0.1	32.5 ± 4.6	0.04 ± 0.01
R297A SsuD[a]	ND	ND	ND

Table 4.3: Steady-state kinetic parameters of SsuD enzymes. Evaluation of the catalytic role(s) of Arg297−Asp111 and Arg297−Glu20 salt bridges in SsuD. (ND; not detected, [a]; Previously determined).[216, 235]

Recent computational simulation studies were performed to further elucidate the loop movement in SsuD following substrate binding and catalysis. The studies monitored conformational changes of SsuD with no substrate bound, SsuD with both FMN and octanesulfonate (OCS) bound, and SsuD with reduced flavin and OCS bound. The distance of ~22 Å observed with apo SsuD between the Phe261 located in the mobile loop and Pro112 decreased to ~20 Å when both FMN and octanesulfonate (OCS) were bound (**Figure 4.7**a). Interestingly, the distance decreased to ~5 Å when both reduced flavin and octanesulfonate were included in the simulations. The Phe261 approached Pro112 during desulfonation over the active site of SsuD

(**Figure 4.7**b). The Phe261 and Pro112 residues were proposed to interact during catalysis to stabilize the mobile loop. This ~17 Å decrease in distance between Phe261 and Pro112 accompanies the significant conformational changes in the loop region of SsuD (**Figure 4.7**).[329]

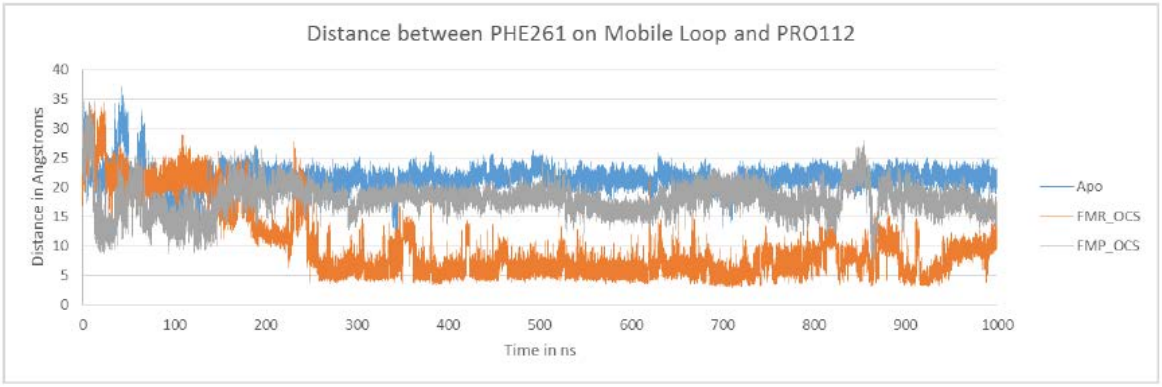

a) Monitoring changes in distance between Phe261 (in the flexible loop) and Pro112 in SsuD during catalysis.

SsuD | SsuD with both FMN and OCS bound | SsuD with both $FMNH_2$ and OCS bound

b) Substrate binding is accompanied by significant conformational changes over the active site of SsuD involving Phe261-Pro112 residue interactions.

Figure 4.7: Recent computational studies on the flexible loop region in SsuD. (Adapted with permission from [329]).

Site-directed mutagenesis and kinetic assays were performed experimentally on SsuD to evaluate the functional roles of Phe261 and Pro112 during desulfonation reaction. Both codons for Phe261 (TTC) and Pro112 (CCA) in SsuD were replaced with that of Ala (GCG), generating F261A and P112A SsuD variants respectively. The F261A and P112A SsuD variants were confirmed by DNA sequence analysis (Eurofins/Genomics, Louisville, KY). The SsuD variants were purified and desulfonation assays performed as previously outlined.[2, 222] Kinetic activity assays monitoring octanesulfonate desulfonation were performed on the F261A and P112A SsuD variants as previously described.[2, 222] The k_{cat}/K_m values for the F261A and P112A SsuD variants were 3.1 ± 0.5 $\mu M^{-1}min^{-1}$ and 2.2 ± 0.4 $\mu M^{-1}min^{-1}$, respectively, compared to a k_{cat}/K_m value of 2.2 ± 0.3 $\mu M^{-1}min^{-1}$ for the wild-type SsuD enzyme (**Table 4.4**), suggesting that the F261A-P112A interaction was not required for catalysis.

	k_{cat} (min^{-1})	K_m (μM)	k_{cat}/K_m ($\mu M^{-1}min^{-1}$)
Wild-type SsuD	93 ± 7	43 ± 6.0	2.2 ± 0.3
F261A SsuD	139 ± 10	45.0 ± 7.0	3.1 ± 0.5
P112A SsuD	72.0 ± 5.0	33.0 ± 6.0	2.2 ± 0.4

Table 4.4: Steady-state kinetic parameters of SsuD enzymes. Evaluation of the catalytic role(s) of the Phe261-Pro112 interactions in SsuD during desulfonation.

4.4 Discussion

Enzymes undergo structural and conformational changes which facilitate the execution of biochemical functions. These structural fluctuations are crucial for substrate recognition and binding, orientation of catalytic residues, product release, and protein–protein interactions.[333, 334] Different approaches can be utilized to investigate structural fluctuations in proteins during catalysis. SDSL-EPR spectroscopy is a useful tool to probe the local environment in enzymes, intramolecular conformational changes during catalysis, and protein-protein interactions.[330] Simulation and molecular modelling is rapidly growing in enzymology as it facilitates mechanistic, structural, and functional understanding which could contribute to protein design and engineering. Computational enzymology techniques, such as the combination of quantum mechanics and molecular mechanics (QM/MM), may provide reliable predictions on the functioning of enzymes, often complement experimental studies, and can be useful in the interpretation of experimental findings.[335, 336]

Various structural and conformational changes have been observed with the alkanesulfonate monooxygenase system enzymes. Flavin-free SsuE exists as a tetramer in solution, but changes to a dimer in the presence of flavin. These quaternary structural changes were not observed in three-dimensional studies of apo SsuE and when flavin bound.[62] The FMN-bound SsuE three-dimensional structure was obtained by soaking the preset SsuE crystals in an FMN solution. This could have forced the oligomeric state of FMN-bound SsuE to be a tetramer, contrary to the dimer observed in solution. Even then, conformational changes were observed upon reduction of the FMN-bound SsuE three-dimensional structure that were different from that of the FMN-bound SsuE.[62] Intriguingly, a π-helix exists at the tetramer interface of SsuE which helps stabilize the tetramer and has been proposed to regulate the flavin-induced oligomeric state

changes. The π-helical property is conserved in various flavin reductases of two-component systems and results from the insertional mutation of Tyr118 at the center of tetrameric interface. The π-helix in SsuE is located one residue away from the flavin binding site and could therefore be involved in the regulation of oligomeric state changes.[62] Mutation of the π-helix impairs the catalytic ability of SsuE to support continued turnover. Generation of Y118A SsuE variant resulted in flavin-bound SsuE variant which existed as a dimer.[303] The transfer of reduced flavin from the reductase to the monooxygenase enzymes is a crucial catalytic step in two-component flavin-dependent monoxygenase systems. The transfer of reduced flavin from SsuE to SsuD was shown to occur through a channeling mechanism which occurs through protein-protein interactions between the enzymes.[215, 229] Spin labeling EPR studies were performed to investigate conformational changes in SsuE during flavin binding, flavin reduction, and in the presence of SsuD. Spin labeling modification of proteins exploits the reactivity of the sulfhydryl group of cysteine residues engineered into proteins by site-directed mutagenesis. The cysteine residues are introduced at specific sites and should be the only cysteines in the enzyme. Any other cysteines are usually substituted with serine or alanine residues which may alter secondary structure and functional roles of the protein.[331] Fortunately, the SsuE enzyme contains no cysteine residues because it is expressed in bacteria during sulfur starvation conditions.

A cysteine residue was introduced through site-directed mutagenesis generating W36C SsuE and the variant was labeled with methanethiosulfonate spin label (MTS). The MTS is commonly used for spin labeling because it is sulfhydryl specific.[331] The W36C SsuE variant was purified in the presence and absence of DTT to evaluate if the Cys was oxidized during purification. There was no significant difference in spin labeling on both purifications suggesting the Cys residues in W36C SsuE were not oxidized. Desulfonation activity comparable to that of

wild-type SsuE was observed with both unlabeled and spin-labeled W36C SsuE implying that the mutation and spin labeling did not affect the ability to transfer reduced flavin to SsuD for desulfonation. The spin label reacted with W36C SsuE to form a disulfide bond with the protein. The linker between the nitroxide ring and the protein backbone is flexible, which minimizes changes in native fold and function.[331] The Trp36 residue in SsuE was an ideal site for site-directed spin labeling because it is positioned away from the active site of SsuE, away from the oligomeric interface, and away from the π-helix in SsuE. In addition, the Trp36 was not identified as part of the protein interaction regions with SsuD.[229] The MTSSL side chain is comparable to that of tryptophan and therefore the spin labeling may not significantly alter the protein function.[331]

SDSL-EPR spectroscopy can help probe structural and conformational changes in enzymes during catalysis.[330] It can be used to identify and quantify conformational changes and characterize the energetics involved in protein-protein, protein-ligand interactions, and protein allostery.[337] Continuous wave EPR spectra from nitroxide labeled proteins can give information on fast motions (0.1 to 100 ns time scale) through EPR spectra which may reflect secondary structure, backbone motions, and tertiary contacts involving the spin label.[338, 339] EPR studies were performed with labeled and unlabeled W36C SsuE in the presence of flavin, in the presence of SsuD, and under flavin reductase conditions. As expected, the non-spin labeled W36C SsuE showed no EPR signal since it lacks unpaired electrons (**Figure 4.4**). Covalent reaction between W36C SsuE and MTSSL introduced a stable free radical resulting into an EPR signal. There were minor changes in the EPR signal with SL W36C SsuE when NADPH, SsuD, or both NADPH and SsuD were Included. The EPR signal diminished when FMN was added to SsuE suggesting structural and conformational changes altering the spin-label environment. A similar decrease in signal intensity was observed when both FMN and SsuD were added to SL W36C SsuE. This decrease in EPR signal indicates

a shift in the magnetic field of SL W36C SsuE upon binding flavin suggesting a change in the spin label environment or quenching of the EPR signal.[272, 340] The EPR signal of SL W36C SsuE with either FMN and NADPH, or FMN, NADPH and SsuD, approaches in resemblance to that of SL W36C SsuE alone. Addition of NADPH and FMN would support flavin reduction and therefore, the SL W36C SsuE enzyme would probably be in $FMNH_2$-release mode. It was not possible to account for the changes in the EPR signal with SL W36C SsuE because the distance between the spin labels were ~27 Å which would impede spin-spin interactions. It would require pulse EPR techniques such as double electron–electron resonance (DEER) to monitor dipolar interactions between the spin labels in SL W36C SsuE. The pulse EPR techniques are able to yield distances and distance distributions between spin labels with distances up to 60 Å or more.[341] DEER, also known as pulse electron double resonance (PELDOR) can also facilitate the characterization of protein's conformational transitions and to determine oligomeric changes, and would therefore help study flavin-induced oligomeric changes in SsuE.[342-344]

The SDSL EPR experiments on SsuE were performed at 77 K which should have impeded tumbling, and therefore further studies will be necessary in non-frozen state (such as at room temperature) to allow the spin label to rapidly and/or randomly tumble.[345] Pulse EPR techniques are presently performed in frozen samples to unravel structural heterogeneity. Protein conformational changes which occur in millisecond time scale may alter the spin label environments triggering in the spin label to register different ns time scale motions. Therefore, conformational changes may result in two or more components of EPR spectrum which reflects the different motions of the nitroxide side chain. Because the quenching of EPR signal in SL W36C SsuE appear to be flavin-related, it would be important to repeat the experiments with different concentrations of FMN while monitoring the mobility of the spin label. In addition, the studies

could be performed with both SsuE and SsuD spin labeled. Overall, the structural and conformational changes on SsuE should depend on the distance distribution monitored by DEER coupled with motional components seen in EPR spectra, the equilibrium between protein conformers, and the rotameric states of the spin label.[337] The EPR studies on the SsuE-SsuD enzymes could also be supplemented by fluorescence spectroscopic studies.

Structural studies identified a π-helix located at the tetramer interface on SsuE which is highly conserved in flavin reductases of two-component monooxygenase systems.[62] The π-helix in SsuE is located near the flavin binding site and was suggested to regulate flavin-induced oligomeric state changes.[62] Generation of a Y118A SsuE variant resulted in FMN-bound Y118A SsuE variant which existed as a dimer. This π-helix mutation impaired the catalytic ability of SsuE to support continued flavin reductase activity.[303] Based on the EPR results with W36C SsuE, we have generated W36C, Y118A SsuE double variant which will facilitate further investigations on the kinetics and oxygen reactivity of Y118A SsuE through SDSL EPR studies.

The alkanesulfonate desulfonation enzyme SsuD has an insertion region that is largely unresolved in the three-dimensional structure and is located at the putative active site.[211, 218] Homology modeling was utilized to insert the unresolved loop region (residues 250−282). The loop region displayed tight interactions when both C(4a)-peroxyflavin ($FMNOO^-$) and octanesulfonate were bound to SsuD. The SsuD enzyme portrayed poor binding for alkanesulfonates in the absence of reduced flavin which correlates with previous experimental findings.[222] This highly flexible loop region has been proposed to close over the active site during catalysis.[61, 218] Partial deletions of the loop region in SsuD did not affect the binding affinity for reduced flavin or result in overall changes to the protein secondary structure.[218] However, the loop

region deletion SsuD variants were unable to desulfonate alkanesulfonates suggesting that a lid-gating conformational change could not be achieved with the deletion SsuD variants.[218]

Molecular dynamics simulation studies suggested conformational changes over the active site of SsuD involving a salt bridge switch from Arg297−Asp111 (closed conformation) to Arg297−Glu20 (open conformation) altered the accessibility of the SsuD active site.[332] Similar steady-state kinetic parameters were observed for the E20A and D111A SsuD variants as wild-type SsuD suggesting the Arg297-based salt bridges were not critical for the desulfonation reaction (**Table 4.3**). Therefore, the dynamic conformational changes to the proposed active form does not exist or is not initiated by a switch from the Arg297−Asp111 salt bridge to the Arg297−Glu20 salt bridge.[222] Generation of R297C and R297A SsuD variants showed no desulfonation activity, but the R297K SsuD had a ~4-fold decrease in the k_{cat}/K_m value compared to the wild type enzyme.[216] The Arg297 SsuD variants had no measurable accumulation of the C4a-(hydro)peroxyflavin intermediate, and lacked the ability to bind alkanesulfonates. The Arg297 SsuD was shown to stabilize the C4a-(hydro)peroxyflavin intermediate essential for the desulfonation reaction. The R297K and R297A SsuD variants exhibited proteolytic susceptibility in the presence of substrates unlike wild-type SsuD, suggesting the Arg297 protects the enzyme from proteolytic digestion upon binding of the reduced flavin.[216] The results from these studies suggest the Arg297 residue prevents the release of reactive intermediates during the desulfonation reaction in SsuD by facilitating a conformational change which actuates loop closure. In addition, it could be a catalytic base involved in orientation of alkanesulfonates in the active site of SsuD.[216]

Recent computational simulations monitoring the loop region showed a distinct decrease in distance between Phe261 and Pro112 when both $FMNH_2$ and OCS were included suggesting that the amino acids were interacting.[329] Proline and tryptophan residues are cyclic residues and

are both hydrophobic which favors their interaction. Aromatic side chains in proteins have negatively charged π faces while the proline ring has a partial positive charge. In addition, the proline residue is conformationally restricted which allows its interaction with aromatic amino acids with minimal entropic or steric hindrance.[346, 347] Experimental studies were performed on Phe261 and Pro112 in SsuD to evaluate the functional roles of these residues in the movement of the flexible loop of SsuD and in catalysis. There was no significant change in desulfonation activity with the F261A and P112 SsuD variants compared to wild-type SsuD suggesting that the F261A-P112A interaction was not vital for catalysis. However, the Phe261 and Pro112 residues may help keep solvent out of the active site in SsuD since they are both hydrophobic.[329] Such hydrophobicity prevents the rapid breakdown of labile flavin intermediates.[210] Enzymes with lid-gated active sites follow an induced fit mechanism for catalysis.[348] The unproductive oxidation of reduced flavin was observed with the SsuD deletion variants attributing the flexible loop to the protection of reduced flavin.[218] Flexible loops in TIM-barrel proteins contribute to the dynamics of the enzyme active site and in substrate binding. Loop closure over the active site protects the substrate and intermediates from bulk solvent during catalysis.[219-221] Beside lid-gating over the active during catalysis, the flexible loop in SsuD may facilitate the transfer of reduced flavin from SsuE to SsuD.[218]

CHAPTER FIVE

5 Evolutionary Studies on NAD(P)H:Flavin Reductases and Determination of Isofunctional Clusters

5.1 Introduction

Evolutionary-related enzymes may have a low sequence similarity and catalyze diverse reactions, but usually share conserved active sites architecture.[349-351] Knowing the chemistry catalyzed by members in a superfamily can facilitate functional predictions of unknown related members. Evolutionary analyses of enzymes give functional clues on sequenced genes that do not have experimental information. A better structural understanding on the conserved structural features typical to each superfamily serves as a guide for enzymatic experimental design.[352] Recent studies comparing the sequences and structures of the flavin reductases with known three-dimensional structures identified evolutionary differences in secondary structure and functions.[62] The analysis identified a subset of flavin reductases that possessed π-helices in their structures. These enzymes were flavin reductases of two-component monooxygenase systems. The π-helical structure was missing in the other flavin reductases that did not have an associated monooxygenase enzyme. π-Helices develop during protein evolution through mutational insertion of a single residue in an already established α-helix resulting in a gain or enhancement of a function.[62, 207, 208] π-Helices are conserved in functionally-related proteins, even when the proteins may have low sequence identity. For example, the chelatase family of proteins (with less than 12% overall sequence identity) that catalyzes the insertion of metals into various proteins have a π-helix at the active site.[208, 260-263] π-Helices in proteins tend to be less favored unless they confer a functional advantage. They augment functional sites in proteins and are highly conserved in sub-branches of protein superfamilies.[207, 239, 259]

The identified π-helices in a sub-branch of NADPH:flavin reductases are highly conserved, suggesting that they enable a common functionality.[62] These flavin reductases exhibit the conserved flavodoxin fingerprinting motif (T/S)XRXXSX(T/S).[62, 204] The flavin reductases bearing π-helices are members of two-component monooxygenase systems but the role the π-helices play in these enzymes is still under investigation.[62] The flavin reductases bearing π-helices exist as tetramers and have the π-helices centrally-located at the tetramer interface.[62] In addition, the active sites of the flavin reductases bearing π-helices are located near the oligomeric interfaces. Some of these flavin reductases undergo flavin-dependent oligomeric state changes during catalysis.[62] The π-helix in SsuE may assist in the regulation of quaternary structural changes, and may have developed to regulate structural changes required for catalysis. A challenge in identifying π-helices in flavin reductases is that only a few flavin reductases have been characterized or have their three-dimensional structures available. Evolutionary studies were utilized to further identify functional relationships in various flavin reductases based on the availability of three-dimensional structures and experimental characterization. In addition, Sequence Similarity Networks (SSN) were generated for SsuE through the Enzyme Function Initiative (EFI) to identify enzymes related to SsuE and to predict enzymatic functions on unknown SsuE-like enzymes.[353]

5.2 Experimental Approach and Results

5.2.1 Evolutionary Studies of SsuE and its Homologs

Three-dimensional structural homologs of SsuE were identified through Dali search and the extracted sequences utilized for the evolutionary studies.[354] The Dali server compares three-dimensional structures of proteins in the protein data bank for structural and sequence alignments.[354] The evolutionary studies on the extracted flavin reductases were performed using

the maximum-likelihood method based on the JTT matrix-based model.[355] The tree with the highest log likelihood (-6355.5383) is shown (**Figure 5.1**).

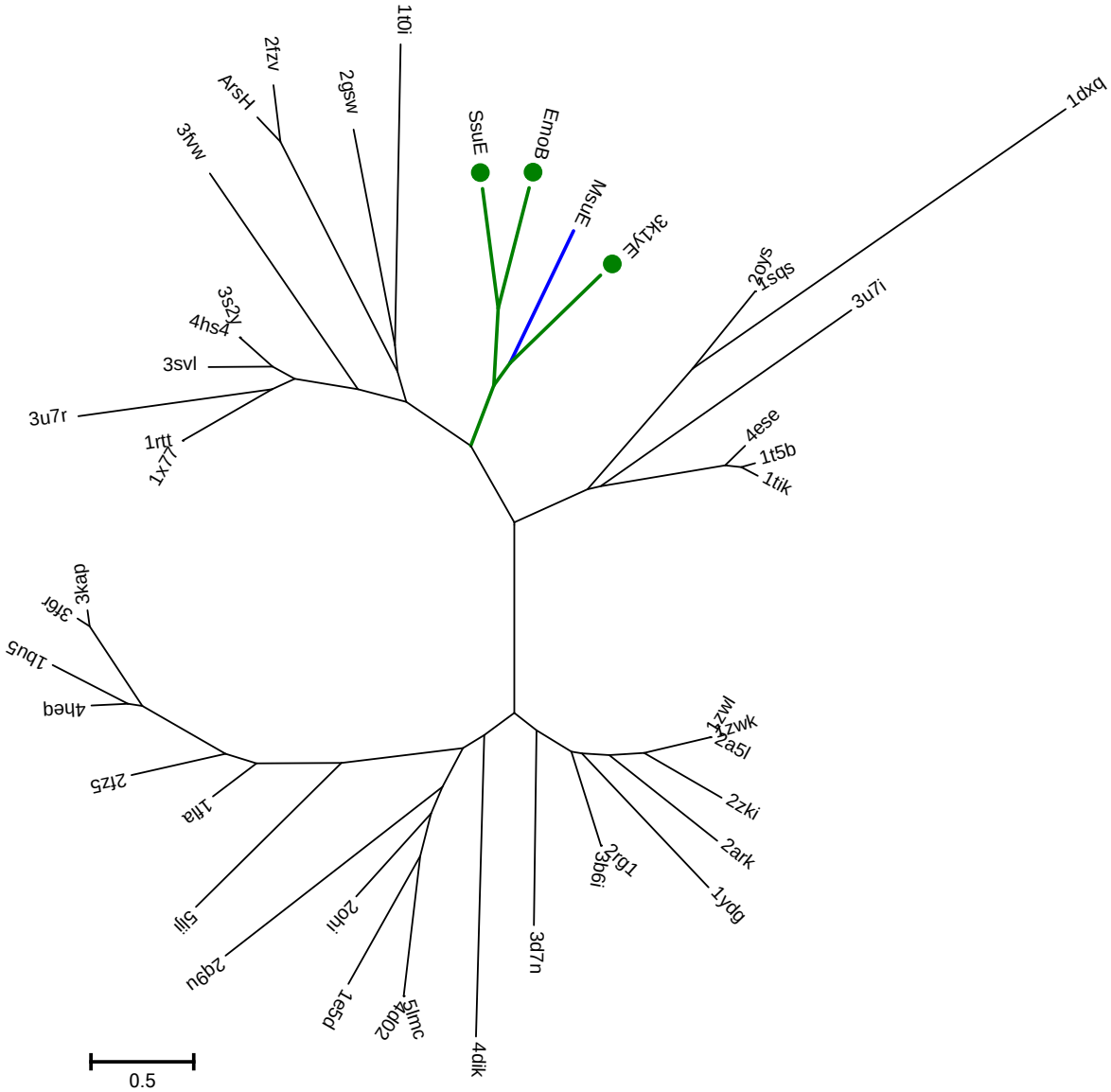

Figure 5.1: Evolutionary relationships of SsuE and its homologs. (●) are flavin reductases of two-component flavin systems and have a π-helix in their structures.

The initial trees for the heuristic search were obtained automatically by applying Neighbor-Join and BioNJ algorithms to a matrix of pairwise distances estimated using a JTT model, and then selecting the topology with superior log likelihood value. The tree is drawn to scale with branch

lengths measured in the number of substitutions per site. The analysis involved 44 amino acid sequences. All positions containing gaps and missing data were eliminated. There was a total of 79 positions in the final dataset. The evolutionary analyses were conducted in MEGA7.[356] The closely related homologs of SsuE were EMOB, MsuE, and 3k1y have 37, 32, and 29% respectively, in structural similarity compared to the SsuE enzyme. These flavin reductases are members of two-component flavin systems and have a π-helix in their structures. The other flavin reductases in the phylogenetic tree lacked the π-helical structure and do not have an associated monooxygenase enzyme (**Figure 5.1**).

5.2.2 Sequence Similarity Network on Flavin Reductases

The distribution of SsuE-like enzymes within bacterial phyla was computed using sequence similarity network (SSN) through the EFI-EST web tool.[353] The EFI network information was developed on SsuE using E-value 5 (BLAST Expect value) which gives a maximum blast sequences of 5000. An alignment score of 26 representing >35% sequence identity with SsuE extracted a total of 1092 sequences (**Figure 5.2**). The node networks shown herein are 80% representative networks. While the nodes show individual homologous sequences, the edges reflect statistically significant similarities among the flavin reductases obtained through pairwise alignments based on BLAST.[357]

Flavin reductases typically have a substrate preference for flavin (FAD and FMN), and for reduced pyridine nucleotides (NADH and NADPH).[358] SsuE has a substrate preference for FMN but can equally utilize NADPH and NADH as a source of reducing equivalents.[57, 303] Evolutionary studies show that 75% of flavoproteins are FAD-dependent.[359] In addition, the majority of flavin-dependent enzymes (90%) bind the flavin cofactor noncovalently. Whereas the FAD-dependent

proteins adopt a Rossmann fold (~ 50%), the FMN-containing flavoproteins predominantly adopt a TIM-barrel or a flavodoxin fold.[359]

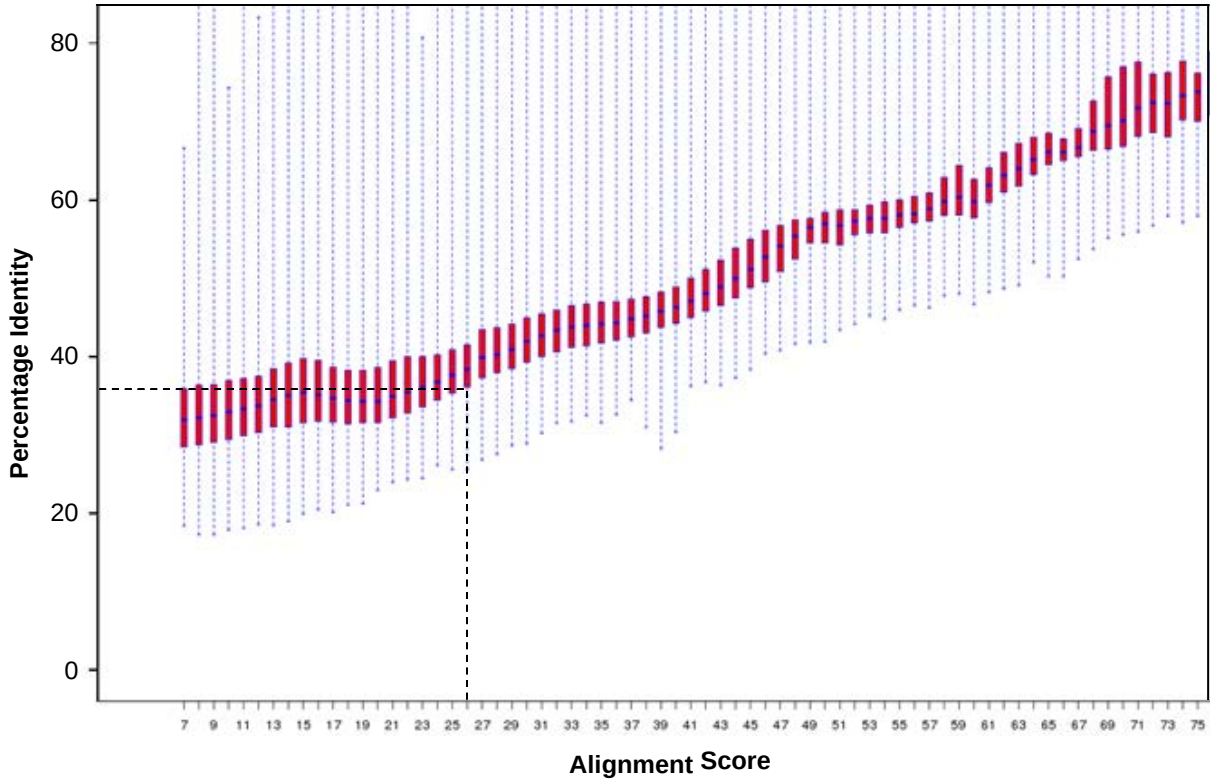

Figure 5.2: Percentage identity used in Sequence Similarity Network (SSN) on SsuE. The SSN studies were based on an alignment score of 26 which corresponds with ~35% sequence identity.

Although all the SsuE homologs extracted through EFI were FMN-dependent, the majority were denoted as having a substrate preference for NADPH over NADH (**Figure 5.3**). Flavin reductases utilize the functionally equivalent NADH or NADPH for electrons in the form of hydride groups. The phosphate group that distinguishes NADPH from NADH is spatially and covalently distant from the chemically active nicotinamide moiety, and therefore has no role in redox chemistry. This NAD(P)H substrate specificity allows cellular regulation of different

enzymatic pathways, minimizes unproductive reactions, and maintains chemical driving forces for different pathways by controlling the levels of NAD(P)H and NAD(P)$^+$.[162, 360]

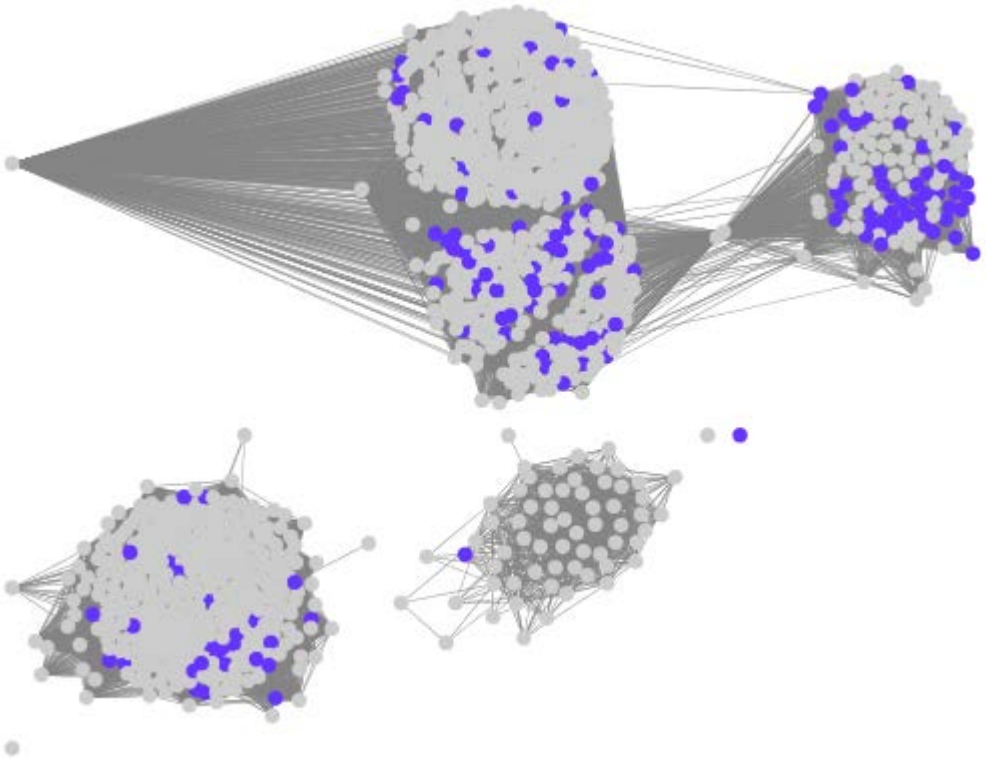

Figure 5.3: Substrate preferences demonstrated by FMN reductases as predicted by SSN studies. The NADPH-dependent FMN reductases (●) and NADH-dependent FMN reductases (●) were pooled using BLAST Expect value (E-value) of 5. The nodes show individual SsuE homologs and the edges reflect statistically significant similarities among the flavin reductases obtained through pairwise alignments.

Experimental, structural and theoretical information on enzymes in a superfamily can facilitate functional predictions of uncharacterized members in the superfamily. The functions of the SsuE-like enzymes (as predicted through the EFI-EST web tool) include FMN reductases associated with alkanesulfonate monooxygenases, methanesulfonate monooxygenases, EDTA degradation monooxygenases, luciferase-like monooxygenases, and hydroxymethylpyrimidine

transporter binding proteins (**Figure 5.4**). Most of the SsuE homologs are uncharacterized and the EFI-EST web tool could not predict their functions. Interestingly, the MsuE enzymes were distributed more in bacteria than SsuE enzymes although both are involved in sulfur scavenging during sulfur limiting conditions. The MsuE enzymes together with MsuD are involved in methanesulfonate desulfonation, while the SsuE enzymes support the desulfonation of diverse organosulfonates including C-2 to C-10 alkanesulfonates, 1,3-dioxo-2-isoindolineethanesulfonate,

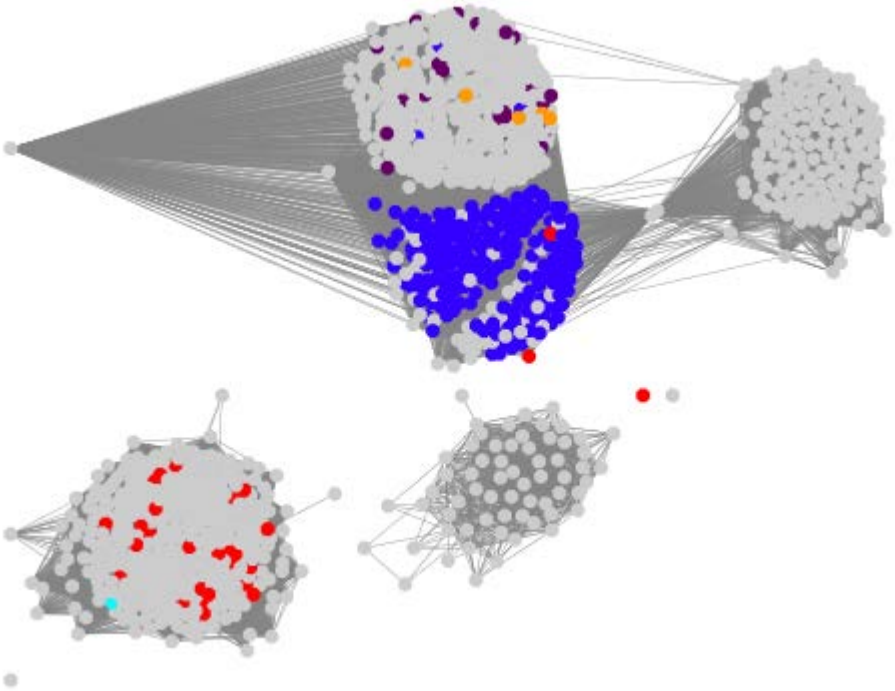

Figure 5.4: The function of SsuE homologs based on EFI-EST web tool analysis. The SsuE homologs identified were FMN reductases associated with alkanesulfonate monooxygenases (●), methanesulfonate monooxygenases (●) and EDTA degradation (●). Others included luciferase-like monooxygenase (LLM) partnered FMN reductases (●) and hydroxymethylpyrimidine ABC transporter binding protein (●). Majority of SsuE homologs are largely uncharacterized (●).

2-(4-pyridyl)ethanesulfonate, and sulfonated buffers by SsuD in various bacteria.[57, 62-64] Some SsuE-like proteins were predicted to be transporter proteins for hydroxymethylpyrimidine, a compound utilized in the biosynthesis of thiamine pyrophosphate (TPP) in prokaryotic cells. The hydroxymethylpyrimidine exists mainly as 4-amino-5-hydroxymethyl-2-methylpyrimidine pyrophosphate (HMP-PP)) and is coupled with 4-methyl-5-β-hydroxyethylthiazole phosphate to generate thiamine phosphate which is further phosphorylated to form TPP.[361]

Structural characterization is pivotal in assigning secondary structure to proteins. Out of the 1092 SsuE homologs extracted through EFI, only SsuE *(E. coli)*, EmoB, MsuE, and 3k1y have their three-dimensional structures solved (highlighted **Figure 5.5**). These flavin reductases are members of two-component monooxygenase systems and have a π-helix in their structure suggesting the π-helices enables a common functionality.[62] π-Helices develop during protein evolution through a single residue insertion in an already established α-helix generating a bulge at the point of insertion. The π-helices confer evolutionary functional advantages in proteins.[207, 208]

The insertional residues in the generation of π-helices are usually aromatic and large aliphatic amino acids (Ile, Leu, Tyr, Trp, Phe, His, and Asn).[208] Several of the flavin reductases, of two-component monooxygenase systems have a tyrosine inserted at the tetramer interface generating π-helices. The recently solved three-dimensional structure of MsuE from *Pseudomonas putida* KT2440 (protein data bank 4C76) shows it existed as a dimer.[362] However, our recent results from size exclusion studies gave molecular weight of 77 kDa for MsuE from *Pseudomonas aeruginosa* compared to a monomeric mass of 20 kDa suggesting the MsuE enzyme could be a tetrameric protein.

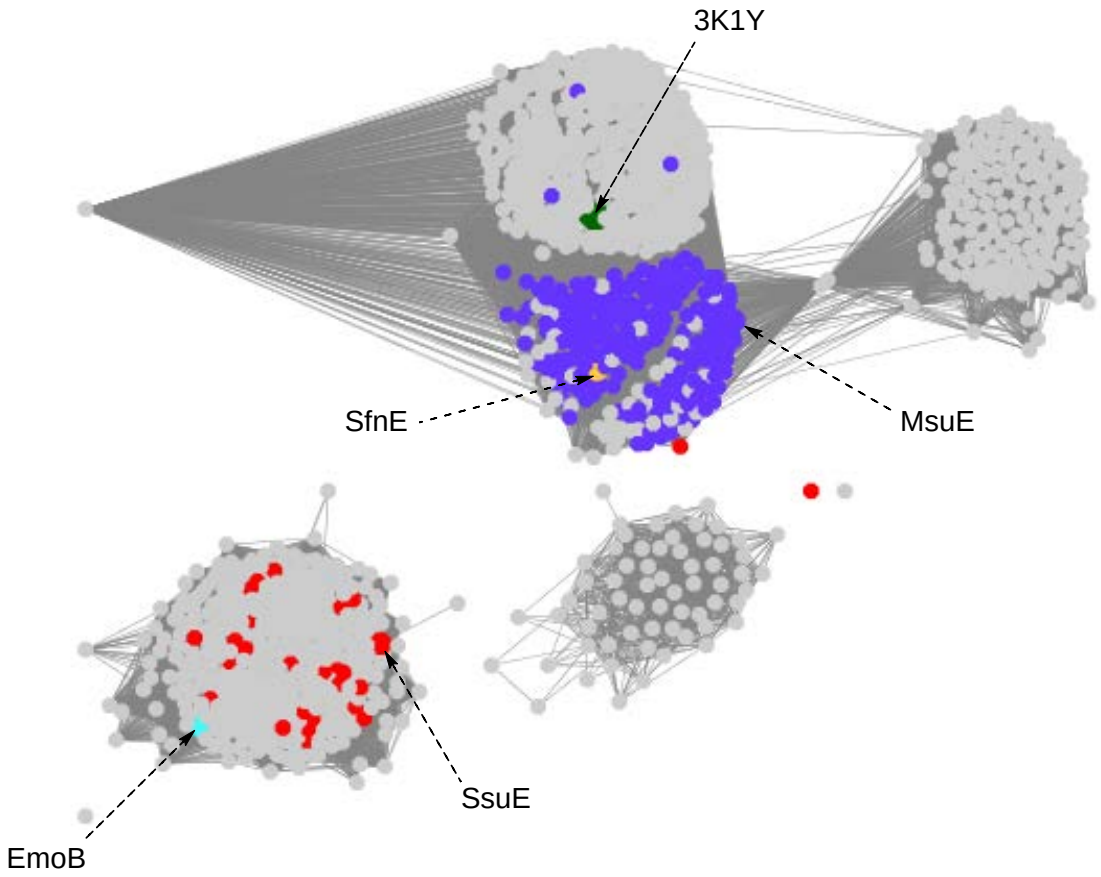

Figure 5.5: Sequence similarity network (SSN) of characterized SsuE homologs. The highlighted enzymes (except SfnE) are the only SsuE-like FMN reductases that have their three-dimensional structures solved.

Comparison of the three-dimensional structure of MsuE with those of the flavin reductases bearing π-helices shows a histidine residue located in the position of the π-helix tyrosine of SsuE (**Scheme 5.1**). Interestingly, another flavin reductase SfnE has a histidine in a similar position as the Tyr of SsuE (**Scheme 5.1**). Both MsuE and SfnE are flavin reductases of two-component monooxygenase systems that participate in scavenging for sulfur in bacteria. The SfnE enzyme supplies the associated monooxygenase SfnG with $FMNH_2$ for the C-S bond cleavage of $DMSO_2$

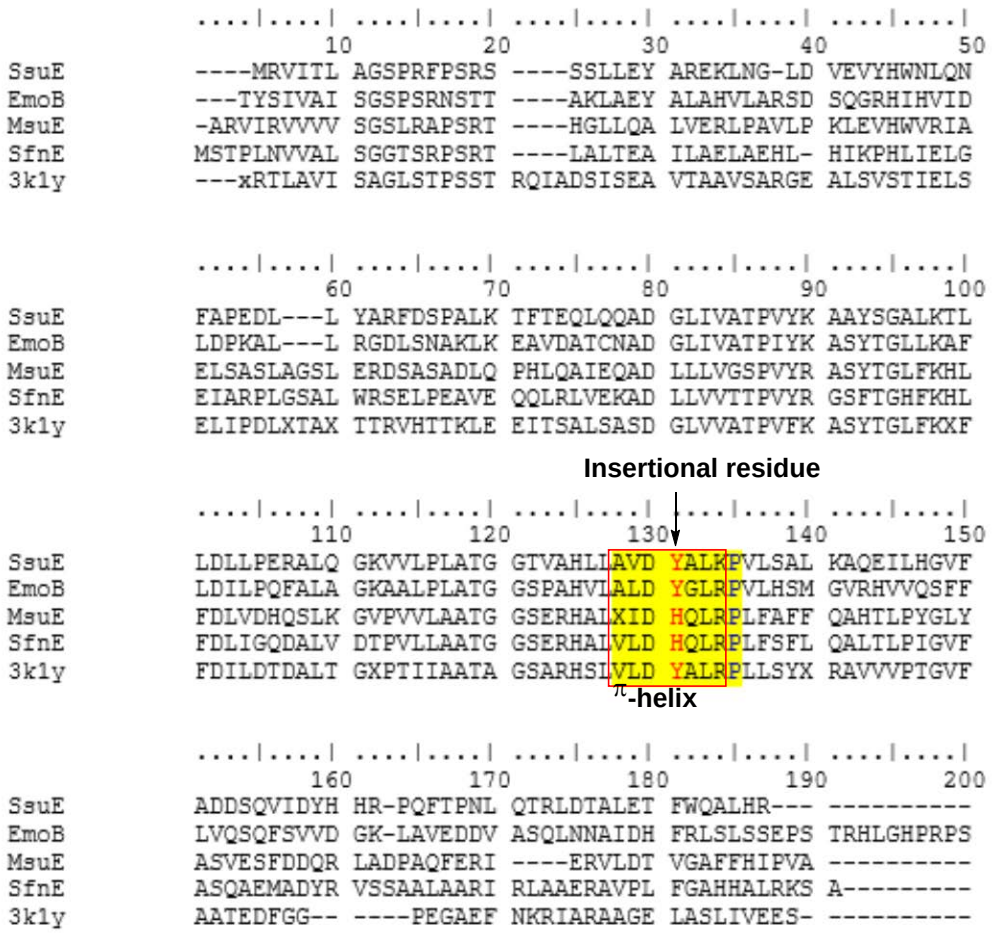

Scheme 5.1: Tyr and His insertions in flavin reductases of two-component monooxygenase systems generate π-helices.

to generate methanesulfinate and a molecule of formaldehyde. The MsuE enzyme supplies MsuC with $FMNH_2$ during the monooxygenation of methanesulfinate to methanesulfonate. In addition, the MsuE enzyme also supplies MsuD with $FMNH_2$ for the desulfonation of methanesulfonate generating sulfite and a molecule of formaldehyde.[163] The π-helical structure could be a norm in the flavin reductases associated with two-component monooxygenase systems indicative of a common evolutionary path and function.

Conclusions

A large number of flavoproteins have been characterized.[363, 364] Flavoproteins are diverse in nature and enhance various redox reactions including hydroxylation, halogenation, and monooxygenation of substrates, DNA repair, luminescence, and cellular signaling.[359] The chemistry catalyzed by flavoproteins differ from reaction to reaction making flavoproteins unique relative to other cofactor-dependent enzymes.[160] Flavoproteins exhibit remarkable selectivity, a virtue required for biocatalytic applications.[365] Two-component flavin-dependent oxygenase systems are increasingly being identified in which the reductive half-reaction and oxidative half-reactions are catalyzed by separate enzymes.[171]

Studies on the alkanesulfonate monooxygenase enzymes have assisted in elucidating the structural features that facilitate flavin reduction by SsuE, the transfer of the reduced flavin to SsuD, and desulfonation of various alkanesulfonates by SsuD. The reduction of flavin by flavin reductases and the transfer of reduced flavin to the monooxygenase enzymes are fundamental in the functioning of two-component flavin-dependent oxygenase systems.[171] Although diffusion has been reported as a mechanism of reduced flavin transfer from some flavin reductases to the associated oxygenase enzymes, the transfer of reduced flavin in vast majority of two-component systems occurs through a channeling mechanism which requires protein-protein interactions between the flavin reductases and the associated monooxygenase enzymes.[61, 201, 215, 229, 296, 321] This common flavin transfer mechanism utilized by the enzymes in FMN-dependent two-component systems suggests that analogous structural motifs are requisite to facilitate reduced flavin transfer. Competitive assays are an excellent tool for determining if the transfer of ligands between two proteins occurs through diffusion or involves protein-protein interactions.[309] The wild-type and the Y118A SsuE variant were able to compete for the protein interaction sites in SsuD during

desulfonation conditions affirming the channeling mechanism was the mode of reduced flavin transfer between the alkanesulfonate monooxygenase system enzymes. The studies on SsuE lay a foundation for the evaluation of common structural motifs requisite in protein-protein interactions in FMN-dependent two-component systems.

The transfer of reduced flavin from flavin reductases to the monooxygenase enzymes is followed by oxygen activation allowing the insertion of an oxygen atom into the corresponding substrates. Flavin monooxygenases react with molecular oxygen to form C4a-(hydro)peroxyflavin, which incorporates a single oxygen atom into organic substrates in hydroxylation and epoxidation reactions, and Baeyer–Villiger oxidation of various substrates. [366] Understanding the conformational changes in two-component flavin-dependent monooxygenase enzymes provide insights on how these structural changes promote varied catalytic functions. As such, different conformational changes have been reported with the alkanesulfonate monooxygenase enzymes ranging from quaternary structural changes in SsuE to loop movement in SsuD, which have been proposed to be critical for catalysis and in flavin transfer between the two enzymes.[62, 170, 215, 216, 218, 222, 303]

The flavin reductases of the two-component monooxygenase systems have a conserved π-helix located at the tetramer interface that originates from the insertion of a single amino acid residue usually histidine or tyrosine.[62, 303] Although π-helices provide an evolutionary gain or enhancement of an existing function, the defined role of these discrete secondary structures remains largely unexplored. The algorithms used to assign secondary structures in proteins often incorrectly annotate π-helices as α-helices.[207, 208] Using different algorithms in protein structural assignments often shows observable disagreement.[282] The π-helices are cryptic and tend to escape the angular restrictions and stringent H-bonding allocation standards of DSSP.[207] For precise

assignment of π-helices, modification of the existing helix identification algorithms is needed.[208] The use of modified π-helix definition algorithms shows that π-helices are more prevalent than initially reported.[208] Another challenge in assigning π-helices in flavin reductases of two-component flavin systems is that only a few three-dimensional structures have been solved. The π-helical structure enables SsuE to effectively utilize flavin as a substrate and transfer the reduced flavin to SsuD. This π-helix also promotes structural stability through a network of hydrogen bonds and π-stacking interactions at the tetramer interface of SsuE. The π-helical insertional residue Tyr118 in SsuE is required for flavin reduction and promotes the transfer of $FMNH_2$ from SsuE to SsuD through protein-protein interactions.

Oligomeric state changes are increasingly being identified in enzymes, but not much is known about how the quaternary structural changes influence catalysis and how these structural changes are regulated.[293-295] Oligomerization is requisite for the proper functioning of many proteins.[290, 291] Oligomeric interactions and the gross geometry of each monomer determines the stability and regulation of the quaternary structures. These factors are crucial in the regulation of cooperative conformational changes, and also influence the biochemical activity of the oligomers.[367] It is critical we uncover the structural features and sequence which mediate oligomerization and protein–protein interactions. Based on the studies on SsuE, the π-helices could be vital in regulating the oligomeric state changes in flavin reductases of two-component systems upon flavin binding and catalysis.

Flavin reduction by SsuE is followed by the transfer of reduced flavin to SsuD through a channeling mechanism which entails protein-protein interactions. The flexible loop over the active site of SsuD undergoes conformational changes which facilitate reduced flavin transfer, substrate binding, desulfonation reaction, and product release. The lid-gating conformation over the active

site of SsuD is accompanied by a decrease in distance between otherwise distant residues as was computationally manifested with Arg297 against Glu20 and Asp111, and Phe261 against Pro112. The evolutionary relationships between the flavin reductases homologous to SsuE predict that many of the SsuE homologs have not been characterized. Several flavin reductases extracted using EFI belong to two-component systems and are found in the cytosol. However, some of the flavin reductases homologous to SsuE were predicted to be membrane proteins involved in the transport of hydroxymethylpyrimidine, required in the biosynthesis of thiamine pyrophosphate (TPP) in prokaryotic cells.

Many two-component oxygenase systems utilize a channeling mechanism for reduced transfer as supported through kinetic studies and the identification of protein-protein interaction sites. Flavin reductases have been used as surrogate flavin reductases to supply unrelated oxygenase enzymes with reduced flavin which begs the questions; (1) Do these flavin reductases have fingerprint interaction motifs because they are structurally similar? (2) Is the efficiency of reduced flavin transfer maintained between different surrogate flavin reductases and unrelated oxygenase enzymes? (3) What other structural conformations promote protein-protein interactions in two-component flavin systems without compromising the active site architecture? Such structural factors would for example include the π-helices and substrate-induced oligomeric state changes in the flavin reductases, and the mobile loop regions in the monooxygenase enzymes. Exploration of these issues calls for a combination of spectroscopic studies, hydrogen-deuterium exchanges analysis, and quaternary structural studies. Finally, there is a need to probe the plausible ancestry and determinants of catalysis in two-component flavin systems through comparative analyses. This approach should compare enzymes in the NAD(P)H:FMN family to fully evaluate

how the π-helices confer evolutionary advantages that regulate flavin reduction and reduced flavin transfer while controlling oligomeric state changes.

REFERENCES

[1] Mandeville, C. W. (2010) Sulfur: A Ubiquitous and Useful Tracer in Earth and Planetary Sciences, *Elements 6*, 75-80.

[2] Gao, B., and Ellis, H. R. (2005) Altered mechanism of the alkanesulfonate FMN reductase with the monooxygenase enzyme, *Biochemical and biophysical research communications 331*, 1137-1145.

[3] Muyzer, G., and Stams, A. J. M. (2008) The ecology and biotechnology of sulphate-reducing bacteria, *Nat Rev Microbiol 6*, 441-454.

[4] Brosnan, J. T., and Brosnan, M. E. (2006) The sulfur-containing amino acids: an overview, *J Nutr 136*, 1636S-1640S.

[5] Hernandez, M. E., and Newman, D. K. (2001) Extracellular electron transfer, *Cellular and molecular life sciences : CMLS 58*, 1562-1571.

[6] Zheng, L. M., White, R. H., Cash, V. L., Jack, R. F., and Dean, D. R. (1993) Cysteine Desulfurase Activity Indicates a Role for Nifs in Metallocluster Biosynthesis, *Proceedings of the National Academy of Sciences of the United States of America 90*, 2754-2758.

[7] Johnson, D. C., Dean, D. R., Smith, A. D., and Johnson, M. K. (2005) Structure, function, and formation of biological iron-sulfur clusters, *Annual Review of Biochemistry 74*, 247-281.

[8] Wacey, D., Kilburn, M. R., Saunders, M., Cliff, J., and Brasier, M. D. (2011) Microfossils of sulphur-metabolizing cells in 3.4-billion-year-old rocks of Western Australia, *Nat Geosci 4*, 698-702.

[9] Shen, Y. A., Buick, R., and Canfield, D. E. (2001) Isotopic evidence for microbial sulphate reduction in the early Archaean era, *Nature 410*, 77-81.

[10] Philippot, P., Van Zuilen, M., Lepot, K., Thomazo, C., Farquhar, J., and Van Kranendonk, M. J. (2007) Early Archaean microorganisms preferred elemental sulfur, not sulfate, *Science 317*, 1534-1537.

[11] Ueno, Y., Ono, S., Rumble, D., and Maruyama, S. (2008) Quadruple sulfur isotope analysis of ca. 3.5 Ga Dresser Formation: New evidence for microbial sulfate reduction in the early Archean, *Geochim Cosmochim Ac 72*, 5675-5691.

[12] Shen, Y. N., Farquhar, J., Masterson, A., Kaufman, A. J., and Buick, R. (2009) Evaluating the role of microbial sulfate reduction in the early Archean using quadruple isotope systematics, *Earth Planet Sc Lett 279*, 383-391.

[13] Wacey, D., McLoughlin, N., Whitehouse, M. J., and Kilburn, M. R. (2010) Two coexisting sulfur metabolisms in a ca. 3400 Ma sandstone, *Geology 38*, 1115-1118.

[14] Autry, A. R., and Fitzgerald, J. W. (1990) Sulfonate-S - a Major Form of Forest Soil Organic Sulfur, *Biol Fert Soils 10*, 50-56.

[15] Lomans, B. P., van der Drift, C., Pol, A., and Op den Camp, H. J. M. (2002) Microbial cycling of volatile organic sulfur compounds, *Cellular and Molecular Life Sciences 59*, 575-588.

[16] Sugawara, M., Shah, G. R., Sadowsky, M. J., Paliy, O., Speck, J., Vail, A. W., and Gyaneshwar, P. (2011) Expression and Functional Roles of *Bradyrhizobium japonicum* Genes Involved in the Utilization of Inorganic and Organic Sulfur Compounds in Free-Living and Symbiotic Conditions, *Mol Plant Microbe In 24*, 451-457.

[17] Williams, S. J., Senaratne, R. H., Mougous, J. D., Riley, L. W., and Bertozzi, C. R. (2002) 5'-adenosinephosphosulfate lies at a metabolic branch point in mycobacteria, *The Journal of biological chemistry 277*, 32606-32615.

[18] Lomans, B. P., van der Drift, C., Pol, A., and Op den Camp, H. J. (2002) Microbial cycling of volatile organic sulfur compounds, *Cellular and molecular life sciences : CMLS 59*, 575-588.

[19] Sekowska, A., Kung, H. F., and Danchin, A. (2000) Sulfur metabolism in *Escherichia coli* and related bacteria: Facts and fiction, *Journal of molecular microbiology and biotechnology 2*, 145-177.

[20] Tai, C. H., Nalabolu, S. R., Jacobson, T. M., Minter, D. E., and Cook, P. F. (1993) Kinetic Mechanisms of the a-Isozyme and B-Isozyme of O-Acetylserine Sulfhydrylase from *Salmonella typhimurium* Lt-2 Using the Natural and Alternative Reactants, *Biochemistry 32*, 6433-6442.

[21] Hwang, C. C., Woehl, E. U., Minter, D. E., Dunn, M. F., and Cook, P. F. (1996) Kinetic isotope effects as a probe of the beta-elimination reaction catalyzed by O-acetylserine sulfhydrylase, *Biochemistry 35*, 6358-6365.

[22] Palde, P. B., Bhaskar, A., Rosa, L. E. P., Madoux, F., Chase, P., Gupta, V., Spicer, T., Scampavia, L., Singh, A., and Carroll, K. S. (2016) First-in-Class Inhibitors of Sulfur Metabolism with Bactericidal Activity against Non-Replicating *M. tuberculosis*, *Acs Chem Biol 11*, 172-184.

[23] Kopriva, S., Buchert, T., Fritz, G., Suter, M., Benda, R., Schunemann, V., Koprivova, A., Schurmann, P., Trautwein, A. X., Kroneck, P. M., and Brunold, C. (2002) The presence of an iron-sulfur cluster in adenosine 5'-phosphosulfate reductase separates organisms utilizing adenosine 5'-phosphosulfate and phosphoadenosine 5'-phosphosulfate for sulfate assimilation, *The Journal of biological chemistry 277*, 21786-21791.

[24] Bykowski, T., van der Ploeg, J. R., Iwanicka-Nowicka, R., and Hryniewicz, M. M. (2002) The switch from inorganic to organic sulphur assimilation in *Escherichia coli*: adenosine 5 '-phosphosulphate (APS) as a signalling molecule for sulphate excess, *Molecular microbiology 43*, 1347-1358.

[25] Mueller, E. G. (2006) Trafficking in persulfides: delivering sulfur in biosynthetic pathways, *Nature chemical biology 2*, 185-194.

[26] Miranda, K. M., and Wink, D. A. (2014) Persulfides and the cellular thiol landscape, *Proceedings of the National Academy of Sciences of the United States of America 111*, 7505-7506.

[27] Toohey, J. I. (1989) Sulfane Sulfur in Biological-Systems - a Possible Regulatory Role, *Biochemical Journal 264*, 625-632.

[28] Mihara, H., and Esaki, N. (2002) Bacterial cysteine desulfurases: their function and mechanisms, *Applied microbiology and biotechnology 60*, 12-23.

[29] Py, B., and Barras, F. (2010) Building Fe-S proteins: bacterial strategies, *Nat Rev Microbiol 8*, 436-446.

[30] Lill, R., and Muhlenhoff, U. (2005) Iron-sulfur-protein biogenesis in eukaryotes, *Trends in biochemical sciences 30*, 133-141.

[31] Fujii, T., Maeda, M., Mihara, H., Kurihara, T., Esaki, N., and Hata, Y. (2000) Structure of a NifS homologue: X-ray structure analysis of CsdB, an *Escherichia coli* counterpart of mammalian selenocysteine lyase, *Biochemistry 39*, 1263-1273.

[32] Lima, C. D. (2002) Analysis of the E. coli NifS CsdB protein at 2.0 A reveals the structural basis for perselenide and persulfide intermediate formation, *Journal of molecular biology 315*, 1199-1208.

[33] Goldsmith-Fischman, S., Kuzin, A., Edstrom, W. C., Benach, J., Shastry, R., Xiao, R., Acton, T. B., Honig, B., Montelione, G. T., and Hunt, J. F. (2004) The SufE sulfur-acceptor protein contains a conserved core structure that mediates interdomain interactions in a variety of redox protein complexes, *Journal of molecular biology 344*, 549-565.

[34] Black, K. A., and Dos Santos, P. C. (2015) Shared-intermediates in the biosynthesis of thio-cofactors: Mechanism and functions of cysteine desulfurases and sulfur acceptors, *Bba-Mol Cell Res 1853*, 1470-1480.

[35] Flint, D. H. (1996) *Escherichia coli* contains a protein that is homologous in function and N-terminal sequence to the protein encoded by the nifS gene of *Azotobacter vinelandii* and that can participate in the synthesis of the Fe-S cluster of dihydroxy-acid dehydratase, *The Journal of biological chemistry 271*, 16068-16074.

[36] Mihara, H., Kurihara, T., Yoshimura, T., Soda, K., and Esaki, N. (1997) Cysteine sulfinate desulfinase, a NIFS-like protein of *Escherichia coli* with selenocysteine lyase and cysteine desulfurase activities. Gene cloning, purification, and characterization of a novel pyridoxal enzyme, *The Journal of biological chemistry 272*, 22417-22424.

[37] Mihara, H., Maeda, M., Fujii, T., Kurihara, T., Hata, Y., and Esaki, N. (1999) A nifS-like gene, csdB, encodes an *Escherichia coli* counterpart of mammalian selenocysteine lyase. Gene cloning, purification, characterization and preliminary x-ray crystallographic studies, *The Journal of biological chemistry 274*, 14768-14772.

[38] Patzer, S. I., and Hantke, K. (1999) SufS is a NifS-like protein, and SufD is necessary for stability of the [2Fe-2S] FhuF protein in *Escherichia coli*, *Journal of Bacteriology 181*, 3307-3309.

[39] Sendra, M., Ollagnier de Choudens, S., Lascoux, D., Sanakis, Y., and Fontecave, M. (2007) The SUF iron-sulfur cluster biosynthetic machinery: sulfur transfer from the SUFS-SUFE complex to SUFA, *FEBS letters 581*, 1362-1368.

[40] Lauhon, C. T., and Kambampati, R. (2000) The *iscS* gene in *Escherichia coli* is required for the biosynthesis of 4-thiouridine, thiamin, and NAD, *The Journal of biological chemistry 275*, 20096-20103.

[41] Mihara, H., Kato, S., Lacourciere, G. M., Stadtman, T. C., Kennedy, R. A., Kurihara, T., Tokumoto, U., Takahashi, Y., and Esaki, N. (2002) The iscS gene is essential for the biosynthesis of 2-selenouridine in tRNA and the selenocysteine-containing formate dehydrogenase H, *Proceedings of the National Academy of Sciences of the United States of America 99*, 6679-6683.

[42] Papenbrock, J., Guretzki, S., and Henne, M. (2011) Latest news about the sulfurtransferase protein family of higher plants, *Amino acids 41*, 43-57.

[43] Cipollone, R., Ascenzi, P., and Visca, P. (2007) Common themes and variations in the rhodanese superfamily, *IUBMB life 59*, 51-59.

[44] Luque-Almagro, V. M., Huertas, M. J., Martinez-Luque, M., Moreno-Vivian, C., Roldan, M. D., Garcia-Gil, L. J., Castillo, F., and Blasco, R. (2005) Bacterial degradation of cyanide and its metal complexes under alkaline conditions, *Applied and environmental microbiology 71*, 940-947.

[45] Gallagher, L. A., and Manoil, C. (2001) *Pseudomonas aeruginosa* PAO1 kills *Caenorhabditis elegans* by cyanide poisoning, *Journal of Bacteriology 183*, 6207-6214.

[46] Shatalin, K., Shatalina, E., Mironov, A., and Nudler, E. (2011) H_2S: a universal defense against antibiotics in bacteria, *Science 334*, 986-990.

[47] Shen, J., Keithly, M. E., Armstrong, R. N., Higgins, K. A., Edmonds, K. A., and Giedroc, D. P. (2015) *Staphylococcus aureus* CstB Is a Novel Multidomain Persulfide Dioxygenase-Sulfurtransferase Involved in Hydrogen Sulfide Detoxification, *Biochemistry 54*, 4542-4554.

[48] Kluger, R., and Tittmann, K. (2008) Thiamin diphosphate catalysis: enzymic and nonenzymic covalent intermediates, *Chemical reviews 108*, 1797-1833.

[49] Hille, R., Retey, J., Bartlewski-Hof, U., and Reichenbecher, W. (1998) Mechanistic aspects of molybdenum-containing enzymes, *FEMS Microbiol Rev 22*, 489-501.

[50] Knowles, J. R. (1989) The mechanism of biotin-dependent enzymes, *Annu Rev Biochem 58*, 195-221.

[51] Attwood, P. V., and Wallace, J. C. (2002) Chemical and catalytic mechanisms of carboxyl transfer reactions in biotin-dependent enzymes, *Accounts of chemical research 35*, 113-120.

[52] Franke, J., and Hertweck, C. (2016) Biomimetic Thioesters as Probes for Enzymatic Assembly Lines: Synthesis, Applications, and Challenges, *Cell Chem Biol 23*, 1179-1192.

[53] Mercer, A. C., and Burkart, M. D. (2007) The ubiquitous carrier protein - a window to metabolite biosynthesis, *Natural product reports 24*, 750-773.

[54] Fontecave, M., Atta, M., and Mulliez, E. (2004) S-adenosylmethionine: nothing goes to waste, *Trends in biochemical sciences 29*, 243-249.

[55] Cook, A. M., Laue, H., and Junker, F. (1998) Microbial desulfonation, *FEMS Microbiol Rev 22*, 399-419.

[56] Kertesz, M. A. (2000) Riding the sulfur cycle--metabolism of sulfonates and sulfate esters in gram-negative bacteria, *FEMS Microbiol Rev 24*, 135-175.

[57] Eichhorn, E., van der Ploeg, J. R., and Leisinger, T. (1999) Characterization of a two-component alkanesulfonate monooxygenase from *Escherichia coli*, *The Journal of biological chemistry 274*, 26639-26646.

[58] van der Ploeg, J. R., Eichhorn, E., and Leisinger, T. (2001) Sulfonate-sulfur metabolism and its regulation in *Escherichia coli*, *Archives of microbiology 176*, 1-8.

[59] van der Ploeg, J. R., Weiss, M. A., Saller, E., Nashimoto, H., Saito, N., Kertesz, M. A., and Leisinger, T. (1996) Identification of sulfate starvation-regulated genes in *Escherichia coli*: a gene cluster involved in the utilization of taurine as a sulfur source, *Journal of Bacteriology 178*, 5438-5446.

[60] van Der Ploeg, J. R., Iwanicka-Nowicka, R., Bykowski, T., Hryniewicz, M. M., and Leisinger, T. (1999) The *Escherichia coli ssuEADCB* gene cluster is required for the utilization of sulfur from aliphatic sulfonates and is regulated by the transcriptional activator Cbl, *The Journal of biological chemistry 274*, 29358-29365.

[61] Zhan, X., Carpenter, R. A., and Ellis, H. R. (2008) Catalytic importance of the substrate binding order for the $FMNH_2$-dependent alkanesulfonate monooxygenase enzyme, *Biochemistry 47*, 2221-2230.

[62] Driggers, C. M., Dayal, P. V., Ellis, H. R., and Karplus, P. A. (2014) Crystal structure of *Escherichia coli* SsuE: defining a general catalytic cycle for FMN reductases of the flavodoxin-like superfamily, *Biochemistry 53*, 3509-3519.

[63] Endoh, T., Kasuga, K., Horinouchi, M., Yoshida, T., Habe, H., Nojiri, H., and Omori, T. (2003) Characterization and identification of genes essential for dimethyl sulfide utilization in *Pseudomonas putida* strain DS1, *Applied microbiology and biotechnology 62*, 83-91.

[64] Pereira, C. T., Moutran, A., Fessel, M., and Balan, A. (2015) The sulfur/sulfonates transport systems in *Xanthomonas citri pv. citri*, *BMC genomics 16*, 524.

[65] van der Ploeg, J. R., Barone, M., and Leisinger, T. (2001) Expression of the *Bacillus subtilis* sulphonate-sulphur utilization genes is regulated at the levels of transcription initiation and termination, *Molecular microbiology 39*, 1356-1365.

[66] Iwanicka-Nowicka, R., Zielak, A., Cook, A. M., Thomas, M. S., and Hryniewicz, M. M. (2007) Regulation of sulfur assimilation pathways in *Burkholderia cenocepacia*: identification of transcription factors CysB and SsuR and their role in control of target genes, *Journal of Bacteriology 189*, 1675-1688.

[67] Koch, D. J., Ruckert, C., Rey, D. A., Mix, A., Puhler, A., and Kalinowski, J. (2005) Role of the *ssu* and *seu* genes of *Corynebacterium glutamicum* ATCC 13032 in utilization of sulfonates and sulfonate esters as sulfur sources, *Applied and environmental microbiology 71*, 6104-6114.

[68] Kahnert, A., Vermeij, P., Wietek, C., James, P., Leisinger, T., and Kertesz, M. A. (2000) The ssu locus plays a key role in organosulfur metabolism in *Pseudomonas putida* S-313, *Journal of Bacteriology 182*, 2869-2878.

[69] van der Ploeg, J. R., Cummings, N. J., Leisinger, T., and Connerton, I. F. (1998) *Bacillus subtilis* genes for the utilization of sulfur from aliphatic sulfonates, *Microbiology 144 (Pt 9)*, 2555-2561.

[70] Louie, T. M., Xie, X. S., and Xun, L. (2003) Coordinated production and utilization of FADH2 by NAD(P)H-flavin oxidoreductase and 4-hydroxyphenylacetate 3-monooxygenase, *Biochemistry 42*, 7509-7517.

[71] Gisi, M. R., and Xun, L. (2003) Characterization of chlorophenol 4-monooxygenase (TftD) and NADH:flavin adenine dinucleotide oxidoreductase (TftC) of *Burkholderia cepacia* AC1100, *Journal of Bacteriology 185*, 2786-2792.

[72] Tofoli de Araujo, F., Bolanos-Garcia, V. M., Pereira, C. T., Sanches, M., Oshiro, E. E., Ferreira, R. C., Chigardze, D. Y., Barbosa, J. A., de Souza Ferreira, L. C., Benedetti, C. E., Blundell, T. L., and Balan, A. (2013) Structural and physiological analyses of the alkanesulphonate-binding protein (SsuA) of the citrus pathogen *Xanthomonas citri*, *PloS one 8*, e80083.

[73] Mao, F., Dam, P., Chou, J., Olman, V., and Xu, Y. (2009) DOOR: a database for prokaryotic operons, *Nucleic acids research 37*, D459-463.

[74] Hollenstein, K., Frei, D. C., and Locher, K. P. (2007) Structure of an ABC transporter in complex with its binding protein, *Nature 446*, 213-216.

[75] Neumann, J., Rose-Sperling, D., and Hellmich, U. A. (2016) Diverse relations between ABC transporters and lipids: An overview, *Biochimica et biophysica acta*.

[76] Subashchandrabose, S., Hazen, T. H., Brumbaugh, A. R., Himpsl, S. D., Smith, S. N., Ernst, R. D., Rasko, D. A., and Mobley, H. L. (2014) Host-specific induction of *Escherichia coli* fitness genes during human urinary tract infection, *Proceedings of the National Academy of Sciences of the United States of America 111*, 18327-18332.

[77] van der Ploeg, J. R., Iwanicka-Nowicka, R., Kertesz, M. A., Leisinger, T., and Hryniewicz, M. M. (1997) Involvement of CysB and Cbl regulatory proteins in expression of the tauABCD operon and other sulfate starvation-inducible genes in *Escherichia coli*, *Journal of Bacteriology 179*, 7671-7678.

[78] Iwanicka-Nowicka, R., and Hryniewicz, M. M. (1995) A new gene, *cbl*, encoding a member of the LysR family of transcriptional regulators belongs to *Escherichia coli cys* regulon, *Gene 166*, 11-17.

[79] Kredich, N. M. (2008) Biosynthesis of Cysteine, *EcoSal Plus 3*.

[80] Bykowski, T., van der Ploeg, J. R., Iwanicka-Nowicka, R., and Hryniewicz, M. M. (2002) The switch from inorganic to organic sulphur assimilation in Escherichia coli: adenosine 5'-phosphosulphate (APS) as a signalling molecule for sulphate excess, *Molecular microbiology 43*, 1347-1358.

[81] Martinez-Antonio, A., Janga, S. C., and Thieffry, D. (2008) Functional organisation of *Escherichia coli* transcriptional regulatory network, *Journal of molecular biology 381*, 238-247.

[82] Jervis, A. J., Crack, J. C., White, G., Artymiuk, P. J., Cheesman, M. R., Thomson, A. J., Le Brun, N. E., and Green, J. (2009) The O-2 sensitivity of the transcription factor FNR is controlled by Ser24 modulating the kinetics of [4Fe-4S] to [2Fe-2S] conversion, *Proceedings of the National Academy of Sciences of the United States of America 106*, 4659-4664.

[83] Dibden, D. P., and Green, J. (2005) In vivo cycling of the *Escherichia coli* transcription factor FNR between active and inactive states, *Microbiol-Sgm 151*, 4063-4070.

[84] Swinger, K. K., and Rice, P. A. (2004) IHF and HU: flexible architects of bent DNA, *Current opinion in structural biology 14*, 28-35.

[85] Dorman, C. J. (2009) Nucleoid-associated proteins and bacterial physiology, *Adv Appl Microbiol 67*, 47-64.

[86] Kertesz, M. A., and Mirleau, P. (2004) The role of soil microbes in plant sulphur nutrition, *Journal of experimental botany 55*, 1939-1945.

[87] Hummerjohann, J., Laudenbach, S., Retey, J., Leisinger, T., and Kertesz, M. A. (2000) The sulfur-regulated arylsulfatase gene cluster of *Pseudomonas aeruginosa*, a new member of the cys regulon, *Journal of Bacteriology 182*, 2055-2058.

[88] Hummerjohann, J., Kuttel, E., Quadroni, M., Ragaller, J., Leisinger, T., and Kertesz, M. A. (1998) Regulation of the sulfate starvation response in *Pseudomonas aeruginosa*: role of cysteine biosynthetic intermediates, *Microbiology 144 (Pt 5)*, 1375-1386.

[89] Nelson, K. E., Weinel, C., Paulsen, I. T., Dodson, R. J., Hilbert, H., Martins dos Santos, V. A., Fouts, D. E., Gill, S. R., Pop, M., Holmes, M., Brinkac, L., Beanan, M., DeBoy, R. T., Daugherty, S., Kolonay, J., Madupu, R., Nelson, W., White, O., Peterson, J., Khouri, H., Hance, I., Chris Lee, P., Holtzapple, E., Scanlan, D., Tran, K., Moazzez, A., Utterback, T., Rizzo, M., Lee, K., Kosack, D., Moestl, D., Wedler, H., Lauber, J., Stjepandic, D., Hoheisel, J., Straetz, M., Heim, S., Kiewitz, C., Eisen, J. A., Timmis, K. N., Dusterhoft, A., Tummler, B., and Fraser, C. M. (2002) Complete genome sequence and comparative analysis of the metabolically versatile *Pseudomonas putida* KT2440, *Environmental microbiology 4*, 799-808.

[90] Stover, C. K., Pham, X. Q., Erwin, A. L., Mizoguchi, S. D., Warrener, P., Hickey, M. J., Brinkman, F. S., Hufnagle, W. O., Kowalik, D. J., Lagrou, M., Garber, R. L., Goltry, L., Tolentino, E., Westbrock-Wadman, S., Yuan, Y., Brody, L. L., Coulter, S. N., Folger, K. R., Kas, A., Larbig, K., Lim, R., Smith, K., Spencer, D., Wong, G. K., Wu, Z., Paulsen, I. T., Reizer, J., Saier, M. H., Hancock, R. E., Lory, S., and Olson, M. V. (2000) Complete genome sequence of *Pseudomonas aeruginosa* PAO1, an opportunistic pathogen, *Nature 406*, 959-964.

[91] Endoh, T., Habe, H., Nojiri, H., Yamane, H., and Omori, T. (2005) The sigma54-dependent transcriptional activator SfnR regulates the expression of the *Pseudomonas putida* sfnFG operon responsible for dimethyl sulphone utilization, *Molecular microbiology 55*, 897-911.

[92] Kahnert, A., Mirleau, P., Wait, R., and Kertesz, M. A. (2002) The LysR-type regulator SftR is involved in soil survival and sulphate ester metabolism in *Pseudomonas putida*, *Environmental microbiology 4*, 225-237.

[93] Davison, J., Brunel, F., Phanopoulos, A., Prozzi, D., and Terpstra, P. (1992) Cloning and sequencing of Pseudomonas genes determining sodium dodecyl sulfate biodegradation, *Gene 114*, 19-24.

[94] Vermeij, P., Wietek, C., Kahnert, A., Wuest, T., and Kertesz, M. A. (1999) Genetic organization of sulphur-controlled aryl desulphonation in Pseudomonas putida S-313, *Molecular microbiology 32*, 913-926.

[95] Walsh, C. T., and Wencewicz, T. A. (2013) Flavoenzymes: versatile catalysts in biosynthetic pathways, *Natural product reports 30*, 175-200.

[96] Chaiyen, P., Fraaije, M. W., and Mattevi, A. (2012) The enigmatic reaction of flavins with oxygen, *Trends in biochemical sciences 37*, 373-380.

[97] Massey, V. (2000) The chemical and biological versatility of riboflavin, *Biochemical Society transactions 28*, 283-296.

[98] Pedrolli, D. B., and Mack, M. (2014) Bacterial flavin mononucleotide riboswitches as targets for flavin analogs, *Methods in molecular biology 1103*, 165-176.

[99] Mansjo, M., and Johansson, J. (2011) The riboflavin analog roseoflavin targets an FMN-riboswitch and blocks Listeria monocytogenes growth, but also stimulates virulence gene-expression and infection, *RNA biology 8*, 674-680.

[100] Powers, H. J. (2003) Riboflavin (vitamin B-2) and health, *The American journal of clinical nutrition 77*, 1352-1360.

[101] (1998) In *Dietary Reference Intakes for Thiamin, Riboflavin, Niacin, Vitamin B6, Folate, Vitamin B12, Pantothenic Acid, Biotin, and Choline*, Washington (DC).

[102] Sebrell, W. H., and Butler, R. E. (1939) Riboflavin Deficiency in Man (Ariboflavinosis), *Public health reports 54*, 2121-2131.

[103] Barile, M., Giancaspero, T. A., Brizio, C., Panebianco, C., Indiveri, C., Galluccio, M., Vergani, L., Eberini, I., and Gianazza, E. (2013) Biosynthesis of flavin cofactors in man: implications in health and disease, *Current pharmaceutical design 19*, 2649-2675.

[104] Joosten, V., and van Berkel, W. J. (2007) Flavoenzymes, *Current opinion in chemical biology 11*, 195-202.

[105] Ghisla, S., and Massey, V. (1989) Mechanisms of Flavoprotein-Catalyzed Reactions, *European Journal of Biochemistry 181*, 1-17.

[106] Bacher, A., Eberhardt, S., Fischer, M., Kis, K., and Richter, G. (2000) Biosynthesis of vitamin b2 (riboflavin), *Annu Rev Nutr 20*, 153-167.

[107] Fischer, M., and Bacher, A. (2008) Biosynthesis of vitamin B2: Structure and mechanism of riboflavin synthase, *Archives of biochemistry and biophysics 474*, 252-265.

[108] Eschenmoser, A., and Loewenthal, E. (1992) Chemistry of Potentially Prebiological Natural-Products, *Chem Soc Rev 21*, 1-16.

[109] Fischer, M., Schott, A. K., Romisch, W., Ramsperger, A., Augustin, M., Fidler, A., Bacher, A., Richter, G., Huber, R., and Eisenreich, W. (2004) Evolution of vitamin B2 biosynthesis. A novel class of riboflavin synthase in Archaea, *Journal of molecular biology 343*, 267-278.

[110] Chatwell, L., Krojer, T., Fidler, A., Romisch, W., Eisenreich, W., Bacher, A., Huber, R., and Fischer, M. (2006) Biosynthesis of riboflavin: structure and properties of 2,5-diamino-6-ribosylamino-4(3H)-pyrimidinone 5'-phosphate reductase of *Methanocaldococcus jannaschii*, *Journal of molecular biology 359*, 1334-1351.

[111] Graupner, M., Xu, H., and White, R. H. (2002) The pyrimidine nucleotide reductase step in riboflavin and F(420) biosynthesis in archaea proceeds by the eukaryotic route to riboflavin, *Journal of Bacteriology 184*, 1952-1957.

[112] Fischer, M., Romisch, W., Saller, S., Illarionov, B., Richter, G., Rohdich, F., Eisenreich, W., and Bacher, A. (2004) Evolution of vitamin B2 biosynthesis: structural and functional similarity between pyrimidine deaminases of eubacterial and plant origin, *The Journal of biological chemistry 279*, 36299-36308.

[113] Stenmark, P., Moche, M., Gurmu, D., and Nordlund, P. (2007) The crystal structure of the bifunctional deaminase/reductase RibD of the riboflavin biosynthetic pathway in *Escherichia coli*: implications for the reductive mechanism, *Journal of molecular biology 373*, 48-64.

[114] Chen, S. C., Chang, Y. C., Lin, C. H., Lin, C. H., and Liaw, S. H. (2006) Crystal structure of a bifunctional deaminase and reductase from *Bacillus subtilis* involved in riboflavin biosynthesis, *The Journal of biological chemistry 281*, 7605-7613.

[115] Richter, G., Fischer, M., Krieger, C., Eberhardt, S., Luttgen, H., Gerstenschlager, I., and Bacher, A. (1997) Biosynthesis of riboflavin: characterization of the bifunctional deaminase-reductase of *Escherichia coli* and *Bacillus subtilis*, *Journal of Bacteriology 179*, 2022-2028.

[116] Serrano, A., Sebastian, M., Arilla-Luna, S., Baquedano, S., Pallares, M. C., Lostao, A., Herguedas, B., Velazquez-Campoy, A., Martinez-Julvez, M., and Medina, M. (2015) Quaternary organization in a bifunctional prokaryotic FAD synthetase: Involvement of an arginine at its adenylyltransferase module on the riboflavin kinase activity, *Biochimica et biophysica acta 1854*, 897-906.

[117] Barile, M., Brizio, C., Valenti, D., De Virgilio, C., and Passarella, S. (2000) The riboflavin/FAD cycle in rat liver mitochondria, *European journal of biochemistry / FEBS 267*, 4888-4900.

[118] Brizio, C., Galluccio, M., Wait, R., Torchetti, E. M., Bafunno, V., Accardi, R., Gianazza, E., Indiveri, C., and Barile, M. (2006) Over-expression in *Escherichia coli* and characterization of two recombinant isoforms of human FAD synthetase, *Biochemical and biophysical research communications 344*, 1008-1016.

[119] Efimov, I., Kuusk, V., Zhang, X. P., and McIntire, W. S. (1998) Proposed steady-state kinetic mechanism for *Corynebacterium ammoniagenes* FAD synthetase produced by *Escherichia coli*, *Biochemistry 37*, 9716-9723.

[120] Manstein, D. J., and Pai, E. F. (1986) Purification and Characterization of FAD Synthetase from *Brevibacterium ammoniagenes*, *Journal of Biological Chemistry 261*, 6169-6173.

[121] Wu, M., Repetto, B., Glerum, D. M., and Tzagoloff, A. (1995) Cloning and Characterization of *Fad1*, the Structural Gene for Flavin Adenine-Dinucleotide Synthetase of *Saccharomyces cerevisiae*, *Molecular and cellular biology 15*, 264-271.

[122] Manstein, D. J., and Pai, E. F. (1986) Purification and characterization of FAD synthetase from *Brevibacterium ammoniagenes*, *The Journal of biological chemistry 261*, 16169-16173.

[123] Frago, S., Martinez-Julvez, M., Serrano, A., and Medina, M. (2008) Structural analysis of FAD synthetase from *Corynebacterium ammoniagenes*, *BMC microbiology 8*, 160.

[124] Massey, V., and Palmer, G. (1966) On Existence of Spectrally Distinct Classes of Flavoprotein Semiquinones . A New Method for Quantitative Production of Flavoprotein Semiquinones, *Biochemistry 5*, 3181-&.

[125] Murataliev, M. B. (1999) Application of electron spin resonance (ESR) for detection and characterization of flavoprotein semiquinones, *Methods in molecular biology 131*, 97-110.

[126] Fraaije, M. W., and Mattevi, A. (2000) Flavoenzymes: diverse catalysts with recurrent features, *Trends in biochemical sciences 25*, 126-132.

[127] Mansoorabadi, S. O., Thibodeaux, C. J., and Liu, H. W. (2007) The diverse roles of flavin coenzymes--nature's most versatile thespians, *The Journal of organic chemistry 72*, 6329-6342.

[128] Massey, V. (2000) The chemical and biological versatility of riboflavin, *Biochemical Society transactions 28*, 283-296.

[129] Crozier-Reabe, K., and Moran, G. R. (2012) Form follows function: structural and catalytic variation in the class a flavoprotein monooxygenases, *International journal of molecular sciences 13*, 15601-15639.

[130] Woo, J. C., and Silverman, R. B. (1994) Observation of two different chromophores in the resting state of monoamine oxidase B by fluorescence spectroscopy, *Biochemical and biophysical research communications 202*, 1574-1578.

[131] Ghisla, S., Massey, V., Lhoste, J. M., and Mayhew, S. G. (1974) Fluorescence and optical characteristics of reduced flavines and flavoproteins, *Biochemistry 13*, 589-597.

[132] Miura, R. (2001) Versatility and specificity in flavoenzymes: control mechanisms of flavin reactivity, *Chem Rec 1*, 183-194.

[133] Kuhn, R., Reinemund, K., and Weygand, F. (1934) Synthesis of lumi-lactoflavin., *Ber Dtsch Chem Ges 67*, 1460-1462.

[134] Karrer, P., Schopp, K., and Benz, F. (1935) Syntheses of flavins IV, *Helv Chim Acta 18*, 426-429.

[135] Blyth, A. W. (1879) Blyth on the Composition of Cows' Milk in Health and Disease *Journal of Chemical Society, Transaction 35*, 530-539.

[136] Thompson, C. W. (1877) Voyage of the Challenger, *Macmillan & Co., London 2*, 85.

[137] Vaz, A. D. N., Chakraborty, S., and Massey, V. (1995) Old Yellow Enzyme - Aromatization of Cyclic Enones and the Mechanism of a Novel Dismutation Reaction, *Biochemistry 34*, 4246-4256.

[138] Job, V., Marcone, G. L., Pilone, M. S., and Pollegioni, L. (2002) Glycine oxidase from *Bacillus subtilis*. Characterization of a new flavoprotein, *The Journal of biological chemistry 277*, 6985-6993.

[139] Swoboda, B. E., and Massey, V. (1965) Purification and Properties of the Glucose Oxidase from *Aspergillus niger*, *The Journal of biological chemistry 240*, 2209-2215.

[140] Nishiya, Y., and Imanaka, T. (1998) Purification and characterization of a novel glycine oxidase from *Bacillus subtilis*, *FEBS letters 438*, 263-266.

[141] Binda, C., Mattevi, A., and Edmondson, D. E. (2002) Structure-function relationships in flavoenzyme-dependent amine oxidations: a comparison of polyamine oxidase and monoamine oxidase, *The Journal of biological chemistry 277*, 23973-23976.

[142] Entsch, B., Ballou, D. P., and Massey, V. (1976) Flavin-oxygen derivatives involved in hydroxylation by p-hydroxybenzoate hydroxylase, *The Journal of biological chemistry 251*, 2550-2563.

[143] Duane, W., and Hastings, J. W. (1975) Flavin Mononucleotide Reductase of Luminous Bacteria, *Mol Cell Biochem 6*, 53-64.

[144] Macheroux, P., Ghisla, S., and Hastings, J. W. (1993) Spectral Detection of an Intermediate Preceding the Excited-State in the Bacterial Luciferase Reaction, *Biochemistry 32*, 14183-14186.

[145] Ryerson, C. C., Ballou, D. P., and Walsh, C. (1982) Mechanistic Studies on Cyclohexanone Oxygenase, *Biochemistry 21*, 2644-2655.

[146] Muller, F. (1987) Flavin radicals: chemistry and biochemistry, *Free radical biology & medicine 3*, 215-230.

[147] Fischer, D. W., Kerton, R. R., and Muller, F. G. (1973) Contribution to Development of an Environmental Economy, *Jahrb Sozialwissensc 24*, 28-37.

[148] Gibson, Q. H., and Hastings, J. W. (1962) Oxidation of Reduced Flavin Mononucleotide by Molecular Oxygen, *Biochemical Journal 83*, 368-&.

[149] Iyanagi, T., Makino, N., and Mason, H. S. (1974) Redox properties of the reduced nicotinamide adenine dinucleotide phosphate-cytochrome P-450 and reduced nicotinamide adenine dinucleotide-cytochrome b5 reductases, *Biochemistry 13*, 1701-1710.

[150] Thorpe, C., and Kim, J. J. P. (1995) Flavoprotein Structure and Mechanism .3. Structure and Mechanism of Action of the Acyl-Coa Dehydrogenases, *Faseb Journal 9*, 718-725.

[151] Venkataram, U. V., and Bruice, T. C. (1984) On the Mechanism of Flavin-Catalyzed Dehydrogenation Alpha,Beta to an Acyl Function - the Mechanism of 1,5-Dihydroflavin Reduction of Maleimides, *Journal of the American Chemical Society 106*, 5703-5709.

[152] Jablonski, E., and DeLuca, M. (1977) Purification and properties of the NADH and NADPH specific FMN oxidoreductases from *Beneckea harveyi*, *Biochemistry 16*, 2932-2936.

[153] Hemmerich, P. (1973) Flavin-O_2 interaction mechanisms and the function of flavin in hydroxylation reactions, *Annals of the New York Academy of Sciences 212*, 13-26.

[154] Gibson, Q. H., and Hastings, J. W. (1962) The oxidation of reduced flavin mononucleotide by molecular oxygen, *The Biochemical journal 83*, 368-377.

[155] Mewies, M., McIntire, W. S., and Scrutton, N. S. (1998) Covalent attachment of flavin adenine dinucleotide (FAD) and flavin mononucleotide (FMN) to enzymes: the current state of affairs, *Protein science : a publication of the Protein Society 7*, 7-20.

[156] Chaiyen, P., Fraaije, M. W., and Mattevi, A. (2012) The enigmatic reaction of flavins with oxygen, *Trends in biochemical sciences 37*, 373-380.

[157] Massey, V. (1994) Activation of Molecular-Oxygen by Flavins and Flavoproteins, *Journal of Biological Chemistry 269*, 22459-22462.

[158] Palfey, B. A., and McDonald, C. A. (2010) Control of catalysis in flavin-dependent monooxygenases, *Archives of biochemistry and biophysics 493*, 26-36.

[159] Xiang, L., Kalaitzis, J. A., and Moore, B. S. (2004) EncM, a versatile enterocin biosynthetic enzyme involved in Favorskii oxidative rearrangement, aldol condensation, and heterocycle-forming reactions, *Proceedings of the National Academy of Sciences of the United States of America 101*, 15609-15614.

[160] Mattevi, A. (2006) To be or not to be an oxidase: challenging the oxygen reactivity of flavoenzymes, *Trends in biochemical sciences 31*, 276-283.

[161] Massey, V. (1994) Activation of molecular oxygen by flavins and flavoproteins, *The Journal of biological chemistry 269*, 22459-22462.

[162] Knaus, T., Paul, C. E., Levy, C. W., de Vries, S., Mutti, F. G., Hollmann, F., and Scrutton, N. S. (2016) Better than Nature: Nicotinamide Biomimetics That Outperform Natural Coenzymes, *Journal of the American Chemical Society 138*, 1033-1039.

[163] Habe, H., Kouzuma, A., Endoh, T., Omori, T., Yamane, H., and Nojiri, H. (2007) Transcriptional regulation of the sulfate-starvation-induced gene sfnA by a sigma54-dependent activator of *Pseudomonas putida*, *Microbiology 153*, 3091-3098.

[164] Torres Pazmino, D. E., Dudek, H. M., and Fraaije, M. W. (2010) Baeyer-Villiger monooxygenases: recent advances and future challenges, *Current opinion in chemical biology 14*, 138-144.

[165] Montersino, S., Tischler, D., Gassner, G. T., and van Berkel, W. J. H. (2011) Catalytic and Structural Features of Flavoprotein Hydroxylases and Epoxidases, *Adv Synth Catal 353*, 2301-2319.

[166] Pazmino, D. E. T., Winkler, M., Glieder, A., and Fraaije, M. W. (2010) Monooxygenases as biocatalysts: Classification, mechanistic aspects and biotechnological applications, *Journal of biotechnology 146*, 9-24.

[167] Carpenter, R. A., Zhan, X., and Ellis, H. R. (2010) Catalytic role of a conserved cysteine residue in the desulfonation reaction by the alkanesulfonate monooxygenase enzyme, *Biochimica et biophysica acta 1804*, 97-105.

[168] Abu-Soud, H. M., Clark, A. C., Francisco, W. A., Baldwin, T. O., and Raushel, F. M. (1993) Kinetic destabilization of the hydroperoxy flavin intermediate by site-directed modification of the reactive thiol in bacterial luciferase, *The Journal of biological chemistry 268*, 7699-7706.

[169] Paquatte, O., and Tu, S. C. (1989) Chemical Modification and Characterization of the Alpha Cysteine-106 at the *Vibrio harveyi* Luciferase Active-Center, *Photochemistry and photobiology 50*, 817-825.

[170] Robbins, J. M., and Ellis, H. R. (2012) Identification of critical steps governing the two-component alkanesulfonate monooxygenase catalytic mechanism, *Biochemistry 51*, 6378-6387.

[171] Ellis, H. R. (2010) The FMN-dependent two-component monooxygenase systems, *Archives of biochemistry and biophysics 497*, 1-12.

[172] Nissen, M. S., Youn, B., Knowles, B. D., Ballinger, J. W., Jun, S. Y., Belchik, S. M., Xun, L., and Kang, C. (2008) Crystal structures of NADH:FMN oxidoreductase (EmoB) at different stages of catalysis, *The Journal of biological chemistry 283*, 28710-28720.

[173] Hastings, J. W., and Gibson, Q. H. (1963) Intermediates in the bioluminescent oxidation of reduced flavin mononucleotide, *The Journal of biological chemistry 238*, 2537-2554.

[174] Gunsalus-Miguel, A., Meighen, E. A., Nicoli, M. Z., Nealson, K. H., and Hastings, J. W. (1972) Purification and properties of bacterial luciferases, *The Journal of biological chemistry 247*, 398-404.

[175] Hastings, J. W. (1996) Chemistries and colors of bioluminescent reactions: a review, *Gene 173*, 5-11.

[176] Suadee, C., Nijvipakul, S., Svasti, J., Entsch, B., Ballou, D. P., and Chaiyen, P. (2007) Luciferase from *Vibrio campbellii* is more thermostable and binds reduced FMN better than its homologues, *Journal of biochemistry 142*, 539-552.

[177] Tinikul, R., Thotsaporn, K., Thaveekarn, W., Jitrapakdee, S., and Chaiyen, P. (2012) The fusion *Vibrio campbellii* luciferase as a eukaryotic gene reporter, *Journal of biotechnology 162*, 346-353.

[178] Westerlund-Karlsson, A., Saviranta, P., and Karp, M. (2002) Generation of thermostable monomeric luciferases from *Photorhabdus luminescens*, *Biochemical and biophysical research communications 296*, 1072-1076.

[179] Xu, Y., Mortimer, M. W., Fisher, T. S., Kahn, M. L., Brockman, F. J., and Xun, L. (1997) Cloning, sequencing, and analysis of a gene cluster from *Chelatobacter heintzii* ATCC 29600 encoding nitrilotriacetate monooxygenase and NADH:flavin mononucleotide oxidoreductase, *Journal of Bacteriology 179*, 1112-1116.

[180] Firestone, M. K., and Tiedje, J. M. (1978) Pathway of degradation of nitrilotriacetate by a *Pseudomonas* species, *Applied and environmental microbiology 35*, 955-961.

[181] Payne, J. W., Bolton, H., Jr., Campbell, J. A., and Xun, L. (1998) Purification and characterization of EDTA monooxygenase from the EDTA-degrading bacterium BNC1, *Journal of Bacteriology 180*, 3823-3827.

[182] Bohuslavek, J., Payne, J. W., Liu, Y., Bolton, H., Jr., and Xun, L. (2001) Cloning, sequencing, and characterization of a gene cluster involved in EDTA degradation from the bacterium BNC1, *Applied and environmental microbiology 67*, 688-695.

[183] Nakayama, N., Matsubara, T., Ohshiro, T., Moroto, Y., Kawata, Y., Koizumi, K., Hirakawa, Y., Suzuki, M., Maruhashi, K., Izumi, Y., and Kurane, R. (2002) A novel enzyme, 2'-hydroxybiphenyl-2-sulfinate desulfinase (DszB), from a dibenzothiophene-desulfurizing bacterium *Rhodococcus erythropolis* KA2-5-1: gene overexpression and enzyme characterization, *Biochimica et biophysica acta 1598*, 122-130.

[184] Oldfield, C., Pogrebinsky, O., Simmonds, J., Olson, E. S., and Kulpa, C. F. (1997) Elucidation of the metabolic pathway for dibenzothiophene desulphurization by *Rhodococcus sp.* strain IGTS8 (ATCC 53968), *Microbiology 143 (Pt 9)*, 2961-2973.

[185] Gray, K. A., Pogrebinsky, O. S., Mrachko, G. T., Xi, L., Monticello, D. J., and Squires, C. H. (1996) Molecular mechanisms of biocatalytic desulfurization of fossil fuels, *Nat Biotechnol 14*, 1705-1709.

[186] Abin-Fuentes, A., Mohamed Mel, S., Wang, D. I., and Prather, K. L. (2013) Exploring the mechanism of biocatalyst inhibition in microbial desulfurization, *Applied and environmental microbiology 79*, 7807-7817.

[187] Sousa, S. F., Sousa, J. F., Barbosa, A. C., Ferreira, C. E., Neves, R. P., Ribeiro, A. J., Fernandes, P. A., and Ramos, M. J. (2016) Improving the Biodesulfurization of Crude Oil and Derivatives: A QM/MM Investigation of the Catalytic Mechanism of NADH-FMN Oxidoreductase (DszD), *The journal of physical chemistry. A 120*, 5300-5306.

[188] Schulz, H., Bohringer, W., Waller, P., and Ousmanov, F. (1999) Gas oil deep hydrodesulfurization: refractory compounds and retarded kinetics, *Catal Today 49*, 87-97.

[189] Wicht, D. K. (2016) The reduced flavin-dependent monooxygenase SfnG converts dimethylsulfone to methanesulfinate, *Archives of biochemistry and biophysics 604*, 159-166.

[190] Tu, S. C. (2001) Reduced flavin: donor and acceptor enzymes and mechanisms of channeling, *Antioxid Redox Signal 3*, 881-897.

[191] Ye, Q., Hu, Y., and Jin, C. (2014) Conformational Dynamics of *Escherichia coli* Flavodoxins in Apo- and Holo-States by Solution NMR Spectroscopy, *PloS one 9*, e103936.

[192] Lei, B. F., and Tu, S. C. (1998) Mechanism of reduced flavin transfer from *Vibrio harveyi* NADPH-FMN oxidoreductase to luciferase, *Biochemistry 37*, 14623-14629.

[193] Filisetti, L., Fontecave, M., and Niviere, V. (2003) Mechanism and substrate specificity of the flavin reductase ActVB from *Streptomyces coelicolor*, *The Journal of biological chemistry 278*, 296-303.

[194] Ellis, H. R. (2011) Mechanism for sulfur acquisition by the alkanesulfonate monooxygenase system, *Bioorganic chemistry 39*, 178-184.

[195] Batie, C. J., and Kamin, H. (1984) Electron transfer by ferredoxin:$NADP^+$ reductase. Rapid-reaction evidence for participation of a ternary complex, *The Journal of biological chemistry 259*, 11976-11985.

[196] Batie, C. J., and Kamin, H. (1984) Ferredoxin:$NADP^+$ oxidoreductase. Equilibria in binary and ternary complexes with $NADP^+$ and ferredoxin, *The Journal of biological chemistry 259*, 8832-8839.

[197] Gassner, G., Wang, L., Batie, C., and Ballou, D. P. (1994) Reaction of phthalate dioxygenase reductase with NADH and NAD: kinetic and spectral characterization of intermediates, *Biochemistry 33*, 12184-12193.

[198] Gassner, G. T., and Ballou, D. P. (1995) Preparation and characterization of a truncated form of phthalate dioxygenase reductase that lacks an iron-sulfur domain, *Biochemistry 34*, 13460-13471.

[199] Niviere, V., Vanoni, M. A., Zanetti, G., and Fontecave, M. (1998) Reaction of the NAD(P)H:flavin oxidoreductase from *Escherichia coli* with NADPH and riboflavin: identification of intermediates, *Biochemistry 37*, 11879-11887.

[200] Gao, B., and Ellis, H. R. (2007) Mechanism of flavin reduction in the alkanesulfonate monooxygenase system, *Biochimica et biophysica acta 1774*, 359-367.

[201] Jun, S. Y., Lewis, K. M., Youn, B., Xun, L., and Kang, C. (2016) Structural and biochemical characterization of EDTA monooxygenase and its physical interaction with a partner flavin reductase, *Molecular microbiology 100*, 989-1003.

[202] Meighen, E. A. (1979) Biosynthesis of aliphatic aldehydes for the bacterial bioluminescent reaction: stimulation by ATP and NADPH, *Biochemical and biophysical research communications 87*, 1080-1086.

[203] Kunjapur, A. M., and Prather, K. L. (2015) Microbial engineering for aldehyde synthesis, *Applied and environmental microbiology 81*, 1892-1901.

[204] Vorontsov, II, Minasov, G., Brunzelle, J. S., Shuvalova, L., Kiryukhina, O., Collart, F. R., and Anderson, W. F. (2007) Crystal structure of an apo form of *Shigella flexneri* ArsH protein with an NADPH-dependent FMN reductase activity, *Protein science : a publication of the Protein Society 16*, 2483-2490.

[205] Agarwal, R., Bonanno, J. B., Burley, S. K., and Swaminathan, S. (2006) Structure determination of an FMN reductase from *Pseudomonas aeruginosa* PA01 using sulfur anomalous signal, *Acta crystallographica. Section D, Biological crystallography 62*, 383-391.

[206] Farias-Rico, J. A., Schmidt, S., and Hocker, B. (2014) Evolutionary relationship of two ancient protein superfolds, *Nature chemical biology 10*, 710-715.

[207] Cooley, R. B., Arp, D. J., and Karplus, P. A. (2010) Evolutionary origin of a secondary structure: pi-helices as cryptic but widespread insertional variations of alpha-helices that enhance protein functionality, *Journal of molecular biology 404*, 232-246.

[208] Fodje, M. N., and Al-Karadaghi, S. (2002) Occurrence, conformational features and amino acid propensities for the pi-helix, *Protein engineering 15*, 353-358.

[209] Campbell, Z. T., Weichsel, A., Montfort, W. R., and Baldwin, T. O. (2009) Crystal structure of the bacterial luciferase/flavin complex provides insight into the function of the beta subunit, *Biochemistry 48*, 6085-6094.

[210] Li, L., Liu, X., Yang, W., Xu, F., Wang, W., Feng, L., Bartlam, M., Wang, L., and Rao, Z. (2008) Crystal structure of long-chain alkane monooxygenase (LadA) in complex with coenzyme FMN: unveiling the long-chain alkane hydroxylase, *Journal of molecular biology 376*, 453-465.

[211] Eichhorn, E., Davey, C. A., Sargent, D. F., Leisinger, T., and Richmond, T. J. (2002) Crystal structure of *Escherichia coli* alkanesulfonate monooxygenase SsuD, *Journal of molecular biology 324*, 457-468.

[212] Fisher, A. J., Raushel, F. M., Baldwin, T. O., and Rayment, I. (1995) 3-Dimensional Structure of Bacterial Luciferase from *Vibrio harveyi* at 2.4 Angstrom Resolution, *Biochemistry 34*, 6581-6586.

[213] Nagano, N., Orengo, C. A., and Thornton, J. M. (2002) One fold with many functions: The evolutionary relationships between TIM barrel families based on their sequences, structures and functions, *Journal of molecular biology 321*, 741-765.

[214] Sparks, J. M., and Baldwin, T. O. (2001) Functional implications of the unstructured loop in the (beta/alpha)(8) barrel structure of the bacterial luciferase alpha subunit, *Biochemistry 40*, 15436-15443.

[215] Abdurachim, K., and Ellis, H. R. (2006) Detection of protein-protein interactions in the alkanesulfonate monooxygenase system from *Escherichia coli*, *Journal of Bacteriology 188*, 8153-8159.

[216] Carpenter, R. A., Xiong, J., Robbins, J. M., and Ellis, H. R. (2011) Functional role of a conserved arginine residue located on a mobile loop of alkanesulfonate monooxygenase, *Biochemistry 50*, 6469-6477.

[217] Robbins, J. M., and Ellis, H. R. (2014) Steady-state kinetic isotope effects support a complex role of Arg226 in the proposed desulfonation mechanism of alkanesulfonate monooxygenase, *Biochemistry 53*, 161-168.

[218] Xiong, J., and Ellis, H. R. (2012) Deletional studies to investigate the functional role of a dynamic loop region of alkanesulfonate monooxygenase, *Biochimica et biophysica acta 1824*, 898-906.

[219] Farber, G. K., and Petsko, G. A. (1990) The evolution of alpha/beta barrel enzymes, *Trends in biochemical sciences 15*, 228-234.

[220] Malabanan, M. M., Amyes, T. L., and Richard, J. P. (2010) A role for flexible loops in enzyme catalysis, *Current opinion in structural biology 20*, 702-710.

[221] Miller, B. G., Hassell, A. M., Wolfenden, R., Milburn, M. V., and Short, S. A. (2000) Anatomy of a proficient enzyme: the structure of orotidine 5'-monophosphate decarboxylase in the presence and absence of a potential transition state analog, *Proceedings of the National Academy of Sciences of the United States of America 97*, 2011-2016.

[222] Armacost, K., Musila, J., Gathiaka, S., Ellis, H. R., and Acevedo, O. (2014) Exploring the catalytic mechanism of alkanesulfonate monooxygenase using molecular dynamics, *Biochemistry 53*, 3308-3317.

[223] Fisher, A. J., Thompson, T. B., Thoden, J. B., Baldwin, T. O., and Rayment, I. (1996) The 1.5-angstrom resolution crystal structure of bacterial luciferase in low salt conditions, *Journal of Biological Chemistry 271*, 21956-21968.

[224] Xin, X., Xi, L., and Tu, S. C. (1991) Functional Consequences of Site-Directed Mutation of Conserved Histidyl Residues of the Bacterial Luciferase Alpha-Subunit, *Biochemistry 30*, 11255-11262.

[225] Huang, S. Q., and Tu, S. C. (1998) Identification and characterization of a catalytic base in bacterial luciferase by chemical rescue of a dark mutant (vol 36, pg 14609, 1997), *Biochemistry 37*, 8614-8614.

[226] Baldwin, T. O., Chen, L. H., Chlumsky, L. J., Devine, J. H., and Ziegler, M. M. (1989) Site-Directed Mutagenesis of Bacterial Luciferase - Analysis of the Essential Thiol, *J Biolum Chemilum 4*, 40-48.

[227] Nicoli, M. Z., Meighen, E. A., and Hastings, J. W. (1974) Bacterial luciferase. Chemistry of the reactive sulfhydryl, *The Journal of biological chemistry 249*, 2385-2392.

[228] Gibson, Q. H., Massey, V., and Atherton, N. M. (1962) The nature of compounds present in mixtures of oxidized and reduced flavin mononucleotides, *The Biochemical journal 85*, 369-383.

[229] Dayal, P. V., Singh, H., Busenlehner, L. S., and Ellis, H. R. (2015) Exposing the Alkanesulfonate Monooxygenase Protein-Protein Interaction Sites, *Biochemistry 54*, 7531-7538.

[230] Kumar, P., and Bansal, M. (2015) Identification of local variations within secondary structures of proteins, *Acta Crystallogr D 71*, 1077-1086.

[231] Baker, E. N., and Hubbard, R. E. (1984) Hydrogen bonding in globular proteins, *Progress in biophysics and molecular biology 44*, 97-179.

[232] Barlow, D. J., and Thornton, J. M. (1988) Helix geometry in proteins, *Journal of molecular biology 201*, 601-619.

[233] Ren, Z., Ren, P. X., Balusu, R., and Yang, X. J. (2016) Transmembrane Helices Tilt, Bend, Slide, Torque, and Unwind between Functional States of Rhodopsin, *Scientific reports 6*.

[234] Low, B. W., and Baybutt, R. B. (1952) The Pi-Helix - a Hydrogen Bonded Configuration of the Polypeptide Chain, *Journal of the American Chemical Society 74*, 5806-5807.

[235] Lin, Z. X., Liu, H. Y., Riniker, S., and van Gunsteren, W. F. (2011) On the Use of Enveloping Distribution Sampling (EDS) to Compute Free Enthalpy Differences between Different Conformational States of Molecules: Application to 3(10-), alpha-, and pi-Helices, *J Chem Theory Comput 7*, 3884-3897.

[236] Rohl, C. A., and Doig, A. J. (1996) Models for the 3(10)-helix/coil, pi-helix/coil, and alpha-helix/3(10)-helix/coil transitions in isolated peptides, *Protein science : a publication of the Protein Society 5*, 1687-1696.

[237] Ramachandran, G. N., and Sasisekharan, V. (1968) Conformation of polypeptides and proteins, *Advances in protein chemistry 23*, 283-438.

[238] Kumar, P., and Bansal, M. (2015) Dissecting pi-helices: sequence, structure and function, *Febs Journal 282*, 4415-4432.

[239] Weaver, T. M. (2000) The pi-helix translates structure into function, *Protein Science 9*, 201-206.

[240] Yamashita, A., Singh, S. K., Kawate, T., Jin, Y., and Gouaux, E. (2005) Crystal structure of a bacterial homologue of Na+/Cl--dependent neurotransmitter transporters, *Nature 437*, 215-223.

[241] Hollingsworth, S. A., Berkholz, D. S., and Karplus, P. A. (2009) On the occurrence of linear groups in proteins, *Protein science : a publication of the Protein Society 18*, 1321-1325.

[242] Armen, R., Alonso, D. O., and Daggett, V. (2003) The role of alpha-, 3(10)-, and pi-helix in helix-->coil transitions, *Protein science : a publication of the Protein Society 12*, 1145-1157.

[243] Mahadevan, J., Lee, K. H., and Kuczera, K. (2001) Conformational free energy surfaces of Ala(10) and Aib(10) peptide helices in solution, *Journal of Physical Chemistry B 105*, 1863-1876.

[244] Lee, K. H., Benson, D. R., and Kuczera, K. (2000) Transitions from alpha to pi helix observed in molecular dynamics simulations of synthetic peptides, *Biochemistry 39*, 13737-13747.

[245] Feig, M., MacKerell, A. D., and Brooks, C. L. (2003) Force field influence on the observation of pi-helical protein structures in molecular dynamics simulations, *Journal of Physical Chemistry B 107*, 2831-2836.

[246] Shirley, W. A., and Brooks, C. L., 3rd. (1997) Curious structure in "canonical" alanine-based peptides, *Proteins 28*, 59-71.

[247] Gibbs, N., Sessions, R. B., Williams, P. B., and Dempsey, C. E. (1997) Helix bending in alamethicin: molecular dynamics simulations and amide hydrogen exchange in methanol, *Biophysical journal 72*, 2490-2495.

[248] Kovacs, H., Mark, A. E., Johansson, J., and van Gunsteren, W. F. (1995) The effect of environment on the stability of an integral membrane helix: molecular dynamics simulations of surfactant protein C in chloroform, methanol and water, *Journal of molecular biology 247*, 808-822.

[249] Lee, K. H., Benson, D. R., and Kuczera, K. (2000) Transitions from alpha to pi helix observed in molecular dynamics simulations of synthetic peptides, *Biochemistry 39*, 13737-13747.

[250] Duneau, J. P., Genest, D., and Genest, M. (1996) Detailed description of an alpha helix-->pi bulge transition detected by molecular dynamics simulations of the p185c-erbB2 V659G transmembrane domain, *Journal of biomolecular structure & dynamics 13*, 753-769.

[251] Liu, L. S., Sahu, I. D., McCarrick, R. M., and Lorigan, G. A. (2016) Probing the Secondary Structure of Membrane Peptides Using H-2-Labeled d(10)-Leucine via Site-Directed Spin-Labeling and Electron Spin Echo Envelope Modulation Spectroscopy, *Journal of Physical Chemistry B 120*, 633-640.

[252] Amos, S. T., Vermeer, L. S., Ferguson, P. M., Kozlowska, J., Davy, M., Bui, T. T., Drake, A. F., Lorenz, C. D., and Mason, A. J. (2016) Antimicrobial Peptide Potency is Facilitated by Greater Conformational Flexibility when Binding to Gram-negative Bacterial Inner Membranes, *Scientific reports 6*, 37639.

[253] Micsonai, A., Wien, F., Kernya, L., Lee, Y. H., Goto, Y., Refregiers, M., and Kardos, J. (2015) Accurate secondary structure prediction and fold recognition for circular dichroism spectroscopy, *Proceedings of the National Academy of Sciences of the United States of America 112*, E3095-3103.

[254] Dayan, O., Nagarajan, A., Shah, R., Ben-Yona, A., Forrest, L. R., and Kanner, B. I. (2017) An extra amino acid residue in transmembrane domain 10 of the GABA transporter GAT-1 is required for efficient ion-coupled transport, *The Journal of biological chemistry*.

[255] Bloom, J. D., and Arnold, F. H. (2009) In the light of directed evolution: pathways of adaptive protein evolution, *Proceedings of the National Academy of Sciences of the United States of America 106 Suppl 1*, 9995-10000.

[256] Dean, A. M., and Thornton, J. W. (2007) Mechanistic approaches to the study of evolution: the functional synthesis, *Nature reviews. Genetics 8*, 675-688.

[257] Worth, C. L., Gong, S., and Blundell, T. L. (2009) Structural and functional constraints in the evolution of protein families, *Nature reviews. Molecular cell biology 10*, 709-720.

[258] Jacob, F. (1977) Evolution and tinkering, *Science 196*, 1161-1166.

[259] Cartailler, J. P., and Luecke, H. (2004) Structural and functional characterization of pi bulges and other short intrahelical deformations, *Structure 12*, 133-144.

[260] Al-Karadaghi, S., Hansson, M., Nikonov, S., Jonsson, B., and Hederstedt, L. (1997) Crystal structure of ferrochelatase: the terminal enzyme in heme biosynthesis, *Structure 5*, 1501-1510.

[261] Lecerof, D., Fodje, M., Hansson, A., Hansson, M., and Al-Karadaghi, S. (2000) Structural and mechanistic basis of porphyrin metallation by ferrochelatase, *Journal of molecular biology 297*, 221-232.

[262] Schubert, H. L., Raux, E., Wilson, K. S., and Warren, M. J. (1999) Common chelatase design in the branched tetrapyrrole pathways of heme and anaerobic cobalamin synthesis, *Biochemistry 38*, 10660-10669.

[263] Wu, C. K., Dailey, H. A., Rose, J. P., Burden, A., Sellers, V. M., and Wang, B. C. (2001) The 2.0 angstrom structure of human ferrochelatase, the terminal enzyme of heme biosynthesis, *Nature structural biology 8*, 156-160.

[264] Hardy, J. A., Walsh, S. T., and Nelson, H. C. (2000) Role of an alpha-helical bulge in the yeast heat shock transcription factor, *Journal of molecular biology 295*, 393-409.

[265] Gibson, R. P., Turkenburg, J. P., Charnock, S. J., Lloyd, R., and Davies, G. J. (2002) Insights into trehalose synthesis provided by the structure of the retaining glucosyltransferase OtsA, *Chemistry & biology 9*, 1337-1346.

[266] Rennex, D., Cummings, R. T., Pickett, M., Walsh, C. T., and Bradley, M. (1993) Role of tyrosine residues in Hg(II) detoxification by mercuric reductase from *Bacillus sp.* strain RC607, *Biochemistry 32*, 7475-7478.

[267] Sarma, G. N., Nickel, C., Rahlfs, S., Fischer, M., Becker, K., and Karplus, P. A. (2005) Crystal structure of a novel *Plasmodium falciparum* 1-Cys peroxiredoxin, *Journal of molecular biology 346*, 1021-1034.

[268] Luecke, H., Schobert, B., Richter, H. T., Cartailler, J. P., and Lanyi, J. K. (1999) Structure of bacteriorhodopsin at 1.55 A resolution, *Journal of molecular biology 291*, 899-911.

[269] Kolbe, M., Besir, H., Essen, L. O., and Oesterhelt, D. (2000) Structure of the light-driven chloride pump halorhodopsin at 1.8 A resolution, *Science 288*, 1390-1396.

[270] Purohit, P., Chakraborty, S., and Auerbach, A. (2015) Function of the M1 pi-helix in endplate receptor activation and desensitization, *J Physiol-London 593*, 2851-2866.

[271] Soderberg, C., Gillam, M. E., Ahlgren, E. C., Hunter, G. A., Gakh, O., Isaya, G., Ferreira, G. C., and Al-Karadaghi, S. (2016) The Structure of the Complex between Yeast Frataxin and Ferrochelatase: CHARACTERIZATION AND PRE-STEADY STATE REACTION OF FERROUS IRON DELIVERY AND HEME SYNTHESIS, *The Journal of biological chemistry 291*, 11887-11898.

[272] Bradshaw, M. D., and Gaffney, B. J. (2014) Fluctuations of an exposed pi-helix involved in lipoxygenase substrate recognition, *Biochemistry 53*, 5102-5110.

[273] Shelar, A., and Bansal, M. (2016) Helix perturbations in membrane proteins assist in inter-helical interactions and optimal helix positioning in the bilayer, *Biochimica et biophysica acta 1858*, 2804-2817.

[274] Sazinsky, M. H., and Lippard, S. J. (2005) Product bound structures of the soluble methane monooxygenase hydroxylase from *Methylococcus capsulatus* (Bath): protein motion in the alpha-subunit, *Journal of the American Chemical Society 127*, 5814-5825.

[275] Bailey, L. J., McCoy, J. G., Phillips, G. N., Jr., and Fox, B. G. (2008) Structural consequences of effector protein complex formation in a diiron hydroxylase, *Proceedings of the National Academy of Sciences of the United States of America 105*, 19194-19198.

[276] Cooley, R. B., Dubbels, B. L., Sayavedra-Soto, L. A., Bottomley, P. J., and Arp, D. J. (2009) Kinetic characterization of the soluble butane monooxygenase from *Thauera butanivorans*, formerly '*Pseudomonas butanovora*', *Microbiology 155*, 2086-2096.

[277] Kumar, S., and Bansal, M. (1998) Dissecting alpha-helices: position-specific analysis of alpha-helices in globular proteins, *Proteins 31*, 460-476.

[278] Richardson, J. S., and Richardson, D. C. (1988) Amino acid preferences for specific locations at the ends of alpha helices, *Science 240*, 1648-1652.

[279] Rajashankar, K. R., and Ramakumar, S. (1996) Pi-turns in proteins and peptides: Classification, conformation, occurrence, hydration and sequence, *Protein science : a publication of the Protein Society 5*, 932-946.

[280] Low, B. W., and Grenville-Wells, H. J. (1953) Generalized Mathematical Relationships for Polypeptide Chain Helices: The Coordinates of the II Helix, *Proceedings of the National Academy of Sciences of the United States of America 39*, 785-801.

[281] Guex, N., and Peitsch, M. C. (1997) SWISS-MODEL and the Swiss-PdbViewer: an environment for comparative protein modeling, *Electrophoresis 18*, 2714-2723.

[282] Cao, C., Wang, G. S., Liu, A., Xu, S. T., Wang, L. C., and Zou, S. X. (2016) A New Secondary Structure Assignment Algorithm Using C-alpha Backbone Fragments, *International journal of molecular sciences 17*.

[283] Kabsch, W., and Sander, C. (1983) How good are predictions of protein secondary structure?, *FEBS letters 155*, 179-182.

[284] Frishman, D., and Argos, P. (1995) Knowledge-based protein secondary structure assignment, *Proteins 23*, 566-579.

[285] Labesse, G., Colloc'h, N., Pothier, J., and Mornon, J. P. (1997) P-SEA: a new efficient assignment of secondary structure from C alpha trace of proteins, *Computer applications in the biosciences : CABIOS 13*, 291-295.

[286] Richards, F. M., and Kundrot, C. E. (1988) Identification of structural motifs from protein coordinate data: secondary structure and first-level supersecondary structure, *Proteins 3*, 71-84.

[287] Yan, R., Wang, X., Huang, L., Yan, F., Xue, X., and Cai, W. (2015) Prediction of structural features and application to outer membrane protein identification, *Scientific reports 5*, 11586.

[288] Kabsch, W., and Sander, C. (1983) Dictionary of protein secondary structure: pattern recognition of hydrogen-bonded and geometrical features, *Biopolymers 22*, 2577-2637.

[289] Al-Karadaghi, S., Cedergren-Zeppezauer, E. S., and Hovmoller, S. (1994) Refined crystal structure of liver alcohol dehydrogenase-NADH complex at 1.8 A resolution, *Acta crystallographica. Section D, Biological crystallography 50*, 793-807.

[290] Ali, M. H., and Imperiali, B. (2005) Protein oligomerization: How and why, *Bioorganic & medicinal chemistry 13*, 5013-5020.

[291] Marianayagam, N. J., Sunde, M., and Matthews, J. M. (2004) The power of two: protein dimerization in biology, *Trends in biochemical sciences 29*, 618-625.

[292] Andrews, F. H., Rogers, M. P., Paul, L. N., and McLeish, M. J. (2014) Perturbation of the monomer-monomer interfaces of the benzoylformate decarboxylase tetramer, *Biochemistry 53*, 4358-4367.

[293] Liu, M. Y., Lei, B. F., Ding, Z. H., Lee, J. C., and Tu, S. C. (1997) *Vibrio harveyi* NADPH:FMN oxidoreductase: Preparation and characterization of the apoenzyme and monomer-dimer equilibrium, *Archives of biochemistry and biophysics 337*, 89-95.

[294] Nijvipakul, S., Ballou, D. P., and Chaiyen, P. (2010) Reduction kinetics of a flavin oxidoreductase LuxG from *Photobacterium leiognathi* (TH1): half-sites reactivity, *Biochemistry 49*, 9241-9248.

[295] Sedlacek, V., Klumpler, T., Marek, J., and Kucera, I. (2014) The structural and functional basis of catalysis mediated by NAD(P)H:acceptor Oxidoreductase (FerB) of *Paracoccus denitrificans*, *PloS one 9*, e96262.

[296] Sucharitakul, J., Tinikul, R., and Chaiyen, P. (2014) Mechanisms of reduced flavin transfer in the two-component flavin-dependent monooxygenases, *Archives of biochemistry and biophysics 555-556*, 33-46.

[297] Riek, R. P., and Graham, R. M. (2011) The elusive pi-helix, *Journal of structural biology 173*, 153-160.

[298] Weaver, T. M. (2000) The pi-helix translates structure into function, *Protein science : a publication of the Protein Society 9*, 201-206.

[299] Strittmatter, P. (1961) The Nature of the Flavin Binding in Microsomal Cytochrome b5 Reductase, *Journal of Biological Chemistry 236*, 2329-2335.

[300] Whitby, L. G. (1953) A new method for preparing flavin-adenine dinucleotide, *The Biochemical journal 54*, 437-442.

[301] Sazinsky, M. H., and Lippard, S. J. (2006) Correlating structure with function in bacterial multicomponent monooxygenases and related diiron proteins, *Accounts of chemical research 39*, 558-566.

[302] Ferrario, V., Braiuca, P., Tessaro, P., Knapic, L., Gruber, C., Pleiss, J., Ebert, C., Eichhorn, E., and Gardossi, L. (2012) Elucidating the structural and conformational factors responsible for the activity and substrate specificity of alkanesulfonate monooxygenase, *Journal of biomolecular structure & dynamics 30*, 74-88.

[303] Musila, J. M., and Ellis, H. R. (2016) Transformation of a Flavin-Free FMN Reductase to a Canonical Flavoprotein through Modification of the pi-Helix, *Biochemistry 55*, 6389-6394.

[304] Kabsch, W. (2010) Integration, scaling, space-group assignment and post-refinement, *Acta crystallographica. Section D, Biological crystallography 66*, 133-144.

[305] Adams, P. D., Afonine, P. V., Bunkoczi, G., Chen, V. B., Davis, I. W., Echols, N., Headd, J. J., Hung, L. W., Kapral, G. J., Grosse-Kunstleve, R. W., McCoy, A. J., Moriarty, N. W., Oeffner, R., Read, R. J., Richardson, D. C., Richardson, J. S., Terwilliger, T. C., and Zwart, P. H. (2010) PHENIX: a comprehensive Python-based system for macromolecular structure solution, *Acta crystallographica. Section D, Biological crystallography 66*, 213-221.

[306] Emsley, P., and Cowtan, K. (2004) Coot: model-building tools for molecular graphics, *Acta crystallographica. Section D, Biological crystallography 60*, 2126-2132.

[307] Chen, V. B., Arendall, W. B., 3rd, Headd, J. J., Keedy, D. A., Immormino, R. M., Kapral, G. J., Murray, L. W., Richardson, J. S., and Richardson, D. C. (2010) MolProbity: all-atom structure validation for macromolecular crystallography, *Acta crystallographica. Section D, Biological crystallography 66*, 12-21.

[308] Musila, J., and Ellis, H. R. (2016) Transformation of a flavin-free FMN reductase to a canonical flavoprotein through modification of the pi-helix, *Biochemistry*.

[309] Geck, M. K., and Kirsch, J. F. (1999) A novel, definitive test for substrate channeling illustrated with the aspartate aminotransferase/malate dehydrogenase system, *Biochemistry 38*, 8032-8037.

[310] Trinh, X. H., Trovato, A., Seno, F., Banavar, J. R., and Maritan, A. (2005) Geometrical model for the native-state folds of proteins, *Biophysical chemistry 115*, 289-294.

[311] Miyashita, O., Wolynes, P. G., and Onuchic, J. N. (2005) Simple energy landscape model for the kinetics of functional transitions in proteins, *The journal of physical chemistry. B 109*, 1959-1969.

[312] Cao, C., Xu, S., and Wang, L. (2015) An Algorithm for Protein Helix Assignment Using Helix Geometry, *PloS one 10*, e0129674.

[313] Deb, D., Vishveshwara, S., and Vishveshwara, S. (2009) Understanding protein structure from a percolation perspective, *Biophysical journal 97*, 1787-1794.

[314] Burley, S. K., and Petsko, G. A. (1985) Aromatic-Aromatic Interaction - a Mechanism of Protein-Structure Stabilization, *Science 229*, 23-28.

[315] McGaughey, G. B., Gagne, M., and Rappe, A. K. (1998) pi-stacking interactions - Alive and well in proteins, *Journal of Biological Chemistry 273*, 15458-15463.

[316] Mignon, P., Loverix, S., Steyaert, J., and Geerlings, P. (2005) Influence of the pi-pi interaction on the hydrogen bonding capacity of stacked DNA/RNA bases, *Nucleic acids research 33*, 1779-1789.

[317] Northeast Structural Genomics Consortium Target CdR100D, *To be published*.

[318] Jawanda, N., Ebalunode, J., Gribenko, A., Briggs, J., Lee, J. C., and Tu, S. C. (2008) A single-residue mutation destabilizes *Vibrio harveyi* flavin reductase FRP dimer, *Archives of biochemistry and biophysics 472*, 51-57.

[319] Clarke, A. R., Wigley, D. B., Barstow, D. A., Chia, W. N., Atkinson, T., and Holbrook, J. J. (1987) A single amino acid substitution deregulates a bacterial lactate dehydrogenase and stabilizes its tetrameric structure, *Biochimica et biophysica acta 913*, 72-80.

[320] Sancho, J. (2006) Flavodoxins: sequence, folding, binding, function and beyond, *Cellular and molecular life sciences : CMLS 63*, 855-864.

[321] Morrison, E., Kantz, A., Gassner, G. T., and Sazinsky, M. H. (2013) Structure and Mechanism of Styrene Monooxygenase Reductase: New Insight into the FAD-Transfer Reaction, *Biochemistry 52*, 6063-6075.

[322] Leferink, N. G. H., Fraaije, M. W., Joosten, H. J., Schaap, P. J., Mattevi, A., and van Berkel, W. J. H. (2009) Identification of a Gatekeeper Residue That Prevents Dehydrogenases from Acting as Oxidases, *Journal of Biological Chemistry 284*, 4392-4397.

[323] Baron, R., Riley, C., Chenprakhon, P., Thotsaporn, K., Winter, R. T., Alfieri, A., Forneris, F., van Berkel, W. J. H., Chaiyen, P., Fraaije, M. W., Mattevi, A., and McCammon, J. A. (2009) Multiple pathways guide oxygen diffusion into flavoenzyme active sites, *Proceedings of the National Academy of Sciences of the United States of America 106*, 10603-10608.

[324] Boubacar, A. K., Pethe, S., Mahy, J. P., and Lederer, F. (2007) Flavocytochrome b2: reactivity of its flavin with molecular oxygen, *Biochemistry 46*, 13080-13088.

[325] Peterson, F. J., Mason, R. P., Hovsepian, J., and Holtzman, J. L. (1979) Oxygen-sensitive and -insensitive nitroreduction by *Escherichia coli* and rat hepatic microsomes, *The Journal of biological chemistry 254*, 4009-4014.

[326] Rau, J., and Stolz, A. (2003) Oxygen-insensitive nitroreductases NfsA and NfsB of *Escherichia coli* function under anaerobic conditions as lawsone-dependent Azo reductases, *Applied and environmental microbiology 69*, 3448-3455.

[327] Whiteway, J., Koziarz, P., Veall, J., Sandhu, N., Kumar, P., Hoecher, B., and Lambert, I. B. (1998) Oxygen-insensitive nitroreductases: analysis of the roles of nfsA and nfsB in development of resistance to 5-nitrofuran derivatives in *Escherichia coli*, *Journal of Bacteriology 180*, 5529-5539.

[328] Akiva, E., Itzhaki, Z., and Margalit, H. (2008) Built-in loops allow versatility in domain-domain interactions: lessons from self-interacting domains, *Proceedings of the National Academy of Sciences of the United States of America 105*, 13292-13297.

[329] Cronin, N. I. (2015) Using Molecular Dynamics to Examine the Effect of a Novel L505H Mutation on Drug-Resistant B-Raf-V600E and to Understanding the Mechanistic Role of

the Mobile Loop Region in Alkanesulfonate Monooxygenase In *Thesis*, Auburn University.

[330] Klug, C. S., and Feix, J. B. (2008) Methods and applications of site-directed spin Labeling EPR Spectroscopy, *Method Cell Biol 84*, 617-658.

[331] Czogalla, A., Pieciul, A., Jezierski, A., and Sikorski, A. F. (2007) Attaching a spin to a protein -- site-directed spin labeling in structural biology, *Acta biochimica Polonica 54*, 235-244.

[332] Ferrario, V., Braiuca, P., Tessaro, P., Knapic, L., Gruber, C., Pleiss, J., Ebert, C., Eichhorn, E., and Gardossi, L. (2012) Elucidating the structural and conformational factors responsible for the activity and substrate specificity of alkanesulfonate monooxygenase, *Journal of biomolecular structure & dynamics 30*, 74-88.

[333] Hammes, G. G. (2002) Multiple conformational changes in enzyme catalysis, *Biochemistry 41*, 8221-8228.

[334] Koshland, D. E. (1994) The Key-Lock Theory and the Induced Fit Theory, *Angew Chem Int Edit 33*, 2375-2378.

[335] van der Kamp, M. W., and Mulholland, A. J. (2008) Computational enzymology: insight into biological catalysts from modelling, *Natural product reports 25*, 1001-1014.

[336] Mulholland, A. J. (2008) Computational enzymology: modelling the mechanisms of biological catalysts, *Biochemical Society transactions 36*, 22-26.

[337] Cafiso, D. S. (2014) Identifying and quantitating conformational exchange in membrane proteins using site-directed spin labeling, *Accounts of chemical research 47*, 3102-3109.

[338] McHaourab, H. S., Lietzow, M. A., Hideg, K., and Hubbell, W. L. (1996) Motion of spin-labeled side chains in T4 lysozyme. Correlation with protein structure and dynamics, *Biochemistry 35*, 7692-7704.

[339] Columbus, L., and Hubbell, W. L. (2004) Mapping backbone dynamics in solution with site-directed spin labeling: GCN4-58 bZip free and bound to DNA, *Biochemistry 43*, 7273-7287.

[340] Gu, L., Liu, C., and Guo, Z. F. (2013) Structural Insights into A beta 42 Oligomers Using Site-directed Spin Labeling, *Journal of Biological Chemistry 288*, 18673-18683.

[341] Jeschke, G. (2012) DEER distance measurements on proteins, *Annu Rev Phys Chem 63*, 419-446.

[342] Altenbach, C., Kusnetzow, A. K., Ernst, O. P., Hofmann, K. P., and Hubbell, W. L. (2008) High-resolution distance mapping in rhodopsin reveals the pattern of helix movement due to activation, *Proceedings of the National Academy of Sciences of the United States of America 105*, 7439-7444.

[343] Masureel, M., Martens, C., Stein, R. A., Mishra, S., Ruysschaert, J. M., McHaourab, H. S., and Govaerts, C. (2014) Protonation drives the conformational switch in the multidrug transporter LmrP, *Nature chemical biology 10*, 149-155.

[344] Boura, E., Rozycki, B., Herrick, D. Z., Chung, H. S., Vecer, J., Eaton, W. A., Cafiso, D. S., Hummer, G., and Hurley, J. H. (2011) Solution structure of the ESCRT-I complex by small-angle X-ray scattering, EPR, and FRET spectroscopy, *Proceedings of the National Academy of Sciences of the United States of America 108*, 9437-9442.

[345] Guzzi, R., and Bartucci, R. (2015) Electron spin resonance of spin-labeled lipid assemblies and proteins, *Archives of biochemistry and biophysics 580*, 102-111.

[346] Biedermannova, L., K, E. R., Berka, K., Hobza, P., and Vondrasek, J. (2008) Another role of proline: stabilization interactions in proteins and protein complexes concerning proline and tryptophane, *Physical chemistry chemical physics : PCCP 10*, 6350-6359.

[347] Zondlo, N. J. (2013) Aromatic-Proline Interactions: Electronically Tunable CH/pi Interactions, *Accounts of chemical research 46*, 1039-1049.

[348] Sullivan, S. M., and Holyoak, T. (2008) Enzymes with lid-gated active sites must operate by an induced fit mechanism instead of conformational selection, *Proceedings of the National Academy of Sciences of the United States of America 105*, 13829-13834.

[349] Babbitt, P. C., and Gerlt, J. A. (1997) Understanding enzyme superfamilies. Chemistry As the fundamental determinant in the evolution of new catalytic activities, *The Journal of biological chemistry 272*, 30591-30594.

[350] Gerlt, J. A., and Babbitt, P. C. (2001) Divergent evolution of enzymatic function: mechanistically diverse superfamilies and functionally distinct suprafamilies, *Annu Rev Biochem 70*, 209-246.

[351] Glasner, M. E., Gerlt, J. A., and Babbitt, P. C. (2006) Evolution of enzyme superfamilies, *Current opinion in chemical biology 10*, 492-497.

[352] Brown, S. D., and Babbitt, P. C. (2014) New Insights about Enzyme Evolution from Large Scale Studies of Sequence and Structure Relationships, *Journal of Biological Chemistry 289*, 30221-30228.

[353] Gerlt, J. A., Bouvier, J. T., Davidson, D. B., Imker, H. J., Sadkhin, B., Slater, D. R., and Whalen, K. L. (2015) Enzyme Function Initiative-Enzyme Similarity Tool (EFI-EST): A web tool for generating protein sequence similarity networks, *Biochimica et biophysica acta 1854*, 1019-1037.

[354] Holm, L., and Rosenstrom, P. (2010) Dali server: conservation mapping in 3D, *Nucleic acids research 38*, W545-549.

[355] Jones, D. T., Taylor, W. R., and Thornton, J. M. (1992) The rapid generation of mutation data matrices from protein sequences, *Computer applications in the biosciences : CABIOS 8*, 275-282.

[356] Kumar, S., Stecher, G., and Tamura, K. (2016) MEGA7: Molecular Evolutionary Genetics Analysis Version 7.0 for Bigger Datasets, *Molecular biology and evolution 33*, 1870-1874.

[357] Altschul, S. F., Madden, T. L., Schaffer, A. A., Zhang, J., Zhang, Z., Miller, W., and Lipman, D. J. (1997) Gapped BLAST and PSI-BLAST: a new generation of protein database search programs, *Nucleic acids research 25*, 3389-3402.

[358] Niviere, V., Fieschi, F., Decout, J. L., and Fontecave, M. (1999) The NAD(P)H:flavin oxidoreductase from *Escherichia coli*. Evidence for a new mode of binding for reduced pyridine nucleotides, *The Journal of biological chemistry 274*, 18252-18260.

[359] Macheroux, P., Kappes, B., and Ealick, S. E. (2011) Flavogenomics - a genomic and structural view of flavin-dependent proteins, *Febs Journal 278*, 2625-2634.

[360] Cahn, J. K., Werlang, C. A., Baumschlager, A., Brinkmann-Chen, S., Mayo, S. L., and Arnold, F. H. (2017) A General Tool for Engineering the NAD/NADP Cofactor Preference of Oxidoreductases, *ACS synthetic biology 6*, 326-333.

[361] Begley, T. P., Downs, D. M., Ealick, S. E., McLafferty, F. W., Van Loon, A. P., Taylor, S., Campobasso, N., Chiu, H. J., Kinsland, C., Reddick, J. J., and Xi, J. (1999) Thiamin biosynthesis in prokaryotes, *Archives of microbiology 171*, 293-300.

[362] Gibson, R. P., Isupov, M., Littlechild, J.A. (2014) Crystal Structure of the FMN-Reductase Msue from *Pseudomonas Putida* Kt2440, *To be published*.

[363] Riebel, A., Dudek, H. M., de Gonzalo, G., Stepniak, P., Rychlewski, L., and Fraaije, M. W. (2012) Expanding the set of rhodococcal Baeyer-Villiger monooxygenases by high-throughput cloning, expression and substrate screening, *Applied microbiology and biotechnology 95*, 1479-1489.

[364] Mascotti, M. L., Juri Ayub, M., Dudek, H., Sanz, M. K., and Fraaije, M. W. (2013) Cloning, overexpression and biocatalytic exploration of a novel Baeyer-Villiger monooxygenase from *Aspergillus fumigatus* Af293, *AMB Express 3*, 33.

[365] Balke, K., Kadow, M., Mallin, H., Sass, S., and Bornscheuer, U. T. (2012) Discovery, application and protein engineering of Baeyer-Villiger monooxygenases for organic synthesis, *Organic & biomolecular chemistry 10*, 6249-6265.

[366] Ceccoli, R. D., Bianchi, D. A., and Rial, D. V. (2014) Flavoprotein monooxygenases for oxidative biocatalysis: recombinant expression in microbial hosts and applications, *Front Microbiol 5*, 25.

[367] Marcos, E., Crehuet, R., and Bahar, I. (2011) Changes in Dynamics upon Oligomerization Regulate Substrate Binding and Allostery in Amino Acid Kinase Family Members, *PLoS computational biology 7*.